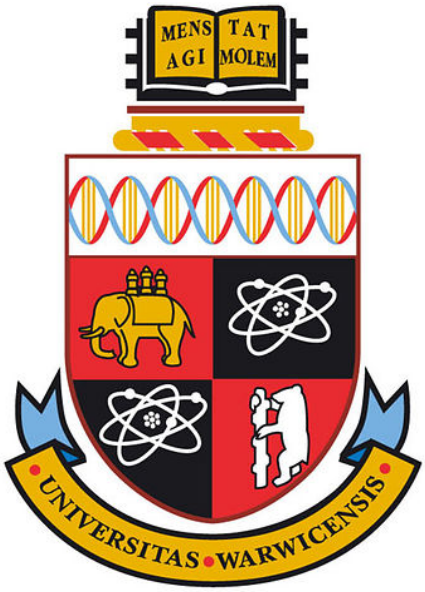

HAG5, a MYST Histone Acetyltransferase, modulates plant growth, defence and drought responses

by

Anna González Gil

Thesis

Submitted to The University of Warwick

For the degree of

Doctor of Philosophy

School of Life Sciences

September 2019

I dedicate this work to my family, for their unconditional support throughout my scientific journey across the world

Table of Contents

List of Figures

List of Tables

Acknowledgments

This PhD journey has been, without a doubt, one of the most challenging and enriching experiences of my life. I made it through alive due to the support of the great people I encountered along this path. I want to express my sincere gratitude to my supervisor, who encouraged me to apply for this PhD programme in spite of my eccentric scientific background. I thank him for challenging me as a scientist and trusting me to develop this project throughout the past 3 years. Undoubtedly, his guidance has helped me develop into a better scientist and grow into a better human, and for that I will be eternally grateful.

I would like to extend my gratitude to everyone that has helped me in moments of scientific need. Jose Guiterrez and Richard Napier for their help, expertise and scientific input. Sophie Piquerez, for instructing me when I first joined the lab. Arsheed, for sharing his protein wisdom and Alonso for addressing my every doubt with immense patience and thorough detail. In addition, I infinitely thank the post-docs in our group: Ana, for her guidance and for sharing her never-ending knowledge, Daniela, for her brilliant and innovative input to this project and Vesi, for her hard work and massive input towards figuring out HAG5. I feel truly lucky to have been surrounded by such brilliant scientists.

I have been fortunate enough to collaborate with a lot of people within this project. I thank Selena, my second supervisor, for all her help, endless energy and encouragement. Moussa Benhamed, for hosting me in his research group. David Latrasse, for teaching me the secrets of ChIP and Lorenzo Concia for working his magic with our sequencing data. Finally, I would like to thank Olivier Loudet for believing in my project and squeezing us in the amazing phenoscope.

I infinitely thank my best friends and forever-special people, Dan, Rory, Natassa, and Edu, for their support, wisdom and hilarity in and outside the lab.

I would also like to thank all the people from C30 that have been part of my daily life over the last four years, for their help in the lab, the shared coffees and beers and the great times had. Overall, it has been quite a ride.

Authors Declarations

This thesis is submitted to the University of Warwick in support for my application for the degree of Doctor of Philosophy. No part of the work submitted here has also been submitted in any previous application for any degree. The work presented in this thesis was undertaken by myself except when otherwise stated.

Due to the multidisciplinary approaches used throughout this thesis, several collaborations have been established, and previous work has been performed by past members of the Ntoukakis group.

The initial screening of the histone acetyltransferase Arabidopsis mutants with Pseudomonas was performed by Dr. Sophie Piquerez and Dr. Chrysa Sergaki, as well as the floral dipping to generate the complemented lines. In addition, microarray sample preparation was performed by Dr. Sophie Piquerez. The Yeast-2-Hybrid screening of transcription factors for HAG4 interactors was performed by Alexia Tornesaki, as well as the dehydration assays in PEG plates. This project is based on the previous phenotyping of *hag5* mutants performed by Dr. Stephanie Kancy. In collaboration with Dr. Veselina Uzunova, she was responsible for the generation of the homology model of HAG5 and the *in silico* screening of inhibitors. In addition, Dr. Veselina Uzunova has developed the homology model of HAG4, and optimised protein purification protocols for i*n vitro* assays of HAG4 and HAG5 activity. Pathogenesis assays with Verticillium were done by Dr. Danai Gkizi from Sotiris Tjamos laboratory at the Agricultural University of Athens.

A collaboration was stablished with Moussa Benhamed's research group to sequence and analyse ChIP-seq libraries, and data analysis was performed by Dr. Lorenzo Concia. Furthermore, the drought tolerance assay using the phenoscope was done by Dr. Olivier Loudet and Elodie Gilbaout form the INRA in Versailles.

Sample preparation for measuring ABA content was performed by Dr. Selena Gimenez-Ibanez, and hormone content was done by Angel Zamarreño and Jose Maria García-Mina from Universidad de Navarra. Finally, CRISPR/Ca9 edited Brassica lines were generated by Tom Lawrenson and Penny Hundleby from the John Innes Centre.

Abstract

Climate change, unstable environmental conditions, rapid increase in human population and scarcity of resources are creating food insecurity. Climate change affects pathogen spread and water availability, challenging crop production globally. This could be the cause of severe food shortage in developing countries. Indeed, plant diseases and water scarcity are the main causes of crop losses, annually exceeding $220 billion worldwide (FAO, 2018). A sustainable strategy to prevent such losses is to create plants with enhanced tolerance to biotic and abiotic stresses. Unfortunately, enhanced stress tolerance often comes with severe developmental penalties such as reduced growth and yield.

In this thesis, I have identified that the histone acetyltransferase HAG5 acts as a major regulatory hub controlling plant homeostasis in a manner that simultaneously regulates stress responses and growth. The *Arabidopsis thaliana* mutant of this enzyme (*hag5*) has enhanced leaf area, longer roots and increased resistance to bacterial pathogens. In addition, the mutant is more tolerant to drought and less sensitive to abscisic acid (ABA), a phytohormone known to regulate plant growth and stress responses. We explored the molecular mechanisms underlying HAG5 activity and discovered that this enzyme interacts with an ABA responsive transcription factor and positively regulates ABA signalling. Through transcriptomic analysis, we unveiled that HAG5 is responsible for the transcriptional regulation of genes involved in cellular detox processes through reactive oxygen species (ROS) scavenging. By modulating ROS accumulation at the transcriptional level, HAG5 can potentially regulate the timing of plant commitment to senescence upon stress. Hence, supressing HAG5 activity results in delayed senescence and increased drought recovery.

We exploited the high level of conservation of *HAG5* across plant lineages in an effort to engineer high-performing plants with enhanced disease resistance and drought tolerance, yet minimal impact upon growth. Here we describe two main lines of research; gene editing of *HAG5* using CRISPR technology in *Brassica oleracea* and developing chemical inhibitors of the enzyme for foliar applications. Altogether, these strategies hold the potential to minimise crop losses, improving performance and stress responses by targeting HAG5 activity in crop plants.

Abbreviations

35S	Cauliflower Mosaic Virus promoter
ABA	Abscisic Acid
ABF	ABRE Binding Factor
ABI	Abscisic Acid Insensitive
ABRE	Abscisic acid Response Element
AD	Activation domain
AREB	Abscisic acid Response Elemen Binding Proteinst
ARM	Armadillo
A. thaliana	*Arabidopsis thaliana*
AT	Amino 1,2,4, Triazole
AUDPC	Area Under Disease Progress Curve
B. oleracea	*Brassica oleracea*
BGI	Beijing Genome Institute
bp	base pair
BRACT	Biotechnology Resources for Arable Crop Transformation
BRM	BRAHMA
BR	Brassinosteroid
CBB	Coomassie Brilliant Blue
cDNA	Complementary deoxyribonucleic acid
CDPK	Calcium Dependent Protein Kinase
CFU	Colony Forming Units
ChIP	Chromatin Immunoprecipitation
SEQ	Sequencing
DA	Drought Avoidance
DB	Deoxyribonucleic Acid Binding
DE	Drought Escape
DEG	Differentially Expressed Gene
DMSO	dimethyl sulfoxide
DNA	Deoxyribonucleic Acid
DPI	Days Post Inoculation
DRE	Drought Response Element

DSB	Double Stranded Break
DT	Drought Tolerance
DW	Dry Weight
DZ	Differentiation Zone
ERF	Ethylene Response Factor
ET	Ethylene
ETI	Effector Triggered Immunity
ETS	Effector Triggered Susceptibility
EV	Empty Vector
EZ	Elongation Zone
FAO	Food and Agriculture Organisation
FLC	*FLOWERING LOCUS C*
FRAP	Fluorescence Recovery After Photobleaching
FW	Fresh Weigth
GA	Gibberellic Acid
GO	Gene Ontology
HAT	Histone Acetyl Transferase
HDAC	Histone Deacetylase
HIS3	Histidine
HPLC	High-Performance Liquid Chromatography
HR	Hyper Sensitive Response
IDT	Integrated DNA Technologies
IP	Immunoprecipitation
IPCC	Intergovernmental Panel on Climate Change
IQR	Inter Quartile Range
JA	Jasmonic Acid
KB	King's B
LEA	*LATE EMBRYOGENESIS ABUNDANT*
lncRNA	Long non-coding RNA
LUC	Luciferase
MAMP	Microbe-Associated Molecular Pattern
MAPK	Mitogen-Activated Protein Kinase
MS	Murashige and Skoog

MTI	MAMP-Triggered Immunity
MZ	Meristem Zone
NAM	No Apical Meristem
NASC	Nottingham Arabidopsis Stock Centre
NBS-LRR	Nucleotide-Binding Site Leucine-Rich Repeat
NE	Nuclear Extract
NECGs	Nuclear Encoded Chloroplast Targeted
NRL	Nucleosomal Repeat Length
OD	Optical Density
OE	Overexpressor
PA	Phaseic acid
PCR	Polymerase Chain Reaction
P. syringae	*Pseudomonas syringae*
PRA	Projected Rosette Area
PC	Principal Component
PDC	Programmed Cell Death
PP2C	Protein Phosphatase Type 2c
PR	Pathogenesis Related
PRR	Pathogen Recognition Receptor
PTI	Pathogen-Triggered Immunity
PTM	Post-Translational Modification
PW	*POWERDRESS*
PYR	PYRABACTIN-RESISTANCE LIKE RECEPTORS
QC	Quiescent Center
qPCR	quantitative Polymerase Chain Reaction
R	Resistance
RNA	Ribonucleic acid
RNAi	RNA interference
RNAPII	RNA Polymerase II
ROS	Reactive Oxygen Species
RT-PCR	Reverse-Transcription PCR
SA	Salicylic Acid
SD	Standard Deviation

sgRNA	single-guide RNA
SWC	Soil water content
TALENS	Transcription Activator Like Effector Nucleases
TEF	Transcription Elongator Factor
TSS	Transcription Start Site
Ub	Ubiquitin
V. dhaliae	*Verticillum dahliae*
Y2H	Yeast-2-Hybrid
YFP	Yellow Fluorescent Protein

Chapter 1 Introduction

1.1. Motivation: improving crops to adapt to the changing environmental conditions

Climate change stands as the biggest threat for the environment, calling for changes in production and consumption habits worldwide. Earth's climate has undergone changes throughout history due to very small variations in Earth's orbit. However, human activity since the beginning of the industrial revolution in the middle of the 20th century is the major cause of this phenomena (IPCC, 1990). The effects of climate change have been assessed periodically since the creation in 1988 of the Intergovernmental Panel on Climate Change (IPCC), by the United Nation General Assembly (Resolution 543/53,1988). According to the scientific reports gathered by the IPCC over the years, the main cause of climate change is the increase of certain gases, such as water vapour, nitrous oxide, carbon dioxide and methane, in the atmosphere (IPCC, 1990). These gases are known to block heat by affecting the transfer of infrared energy through the atmosphere. As a consequence, their accumulation results in the increase of global temperature, a phenomenon known as global warming. Indeed, over the last 100 years, the global average temperature has increased by 0.74ºC (Oreskes, 2004). As seen in Figure 1.1, the amount of solar energy received by the Earth has followed the Sun's natural 11-year cycle of small ups and downs, with no net increase since the 1950s. Over the same period, global temperature has risen markedly, evidencing that the increment in global temperature is not caused by solar radiation received, and is indeed the effect of an anthropogenic climate change (Oreskes, 2004). These data correlates with the levels of atmospheric carbon dioxide, which have increased from 280 parts per million to 400 parts per million in the last 150 years (Field, 2014, Ekwurzel et al., 2017). Two thirds of these CO_2 and CH_4 emissions are produced by 90 major industrial carbon producers (Ekwurzel et al., 2017), whilst other human activities such as deforestation, land use changes, fossil fuel combustion and intensive farming also contribute to CO_2 accumulation.

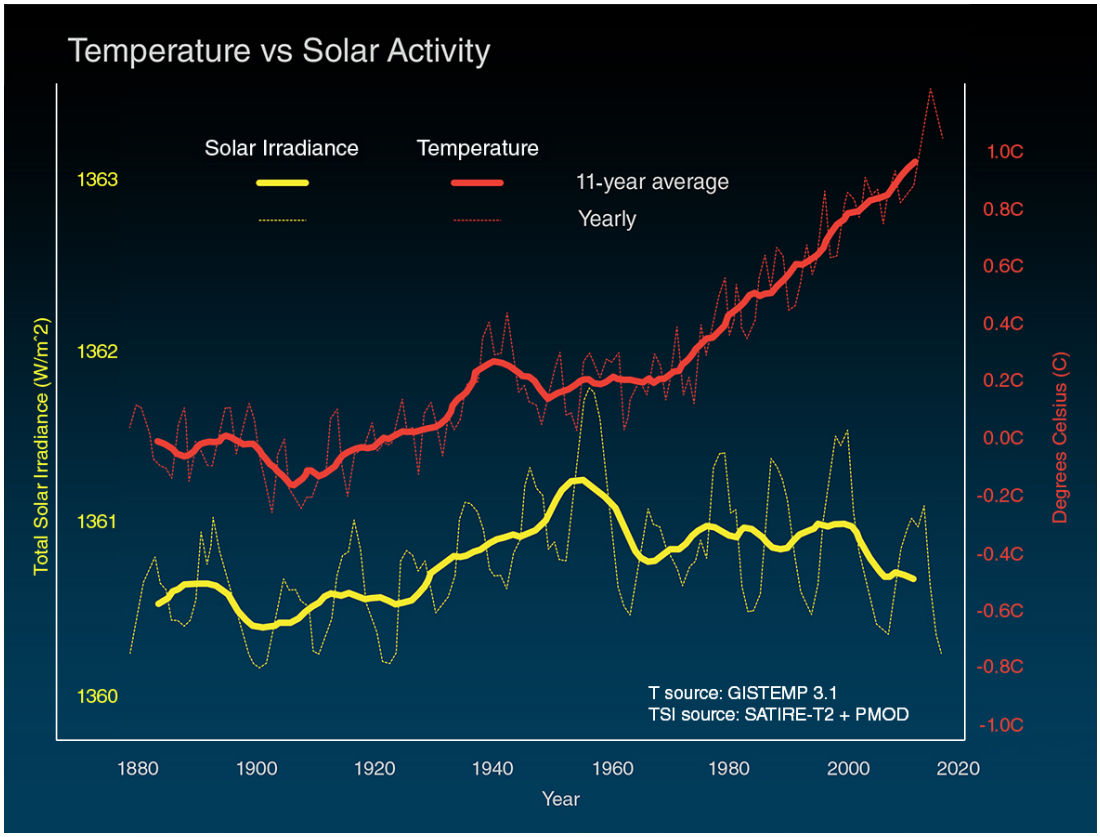

Figure 1.1. Changes in global temperature vs solar activity since 1880. Global surface temperature changes (red line) and the Sun's energy received by the Earth (yellow line) are represented in watts (units of energy) per square meter. The thinner lines show the yearly levels while the thicker lines show the 11-year average trends. Eleven-year averages are used to reduce the year-to-year natural noise in the data, making the underlying trends more obvious. Credit: NASA/JPL-Caltech.

The effects of global warming comprise rising sea levels, increased temperature of the oceans, decreased snow and ice surface coverage, as well as climatological anomalies such as heat and cold waves, floods, drought, fires or wind storms (Field, 2014). Climate change represents a fundamental challenge for humanity as it will deeply and permanently affect life on Earth (M. Pasqui, 2019). These environmental changes are coupled with an increase in human population. At the current growth rate, the United Nations have predicted that the world population will exceed 9 billion by 2050 (FAO, 2018), threatening food security worldwide. Food security, as defined by the Food and Agriculture Organisation of the United Nations (FAO), is “a situation that exists when all people, at all times, have physical, social and economic access to sufficient, safe and nutritious food that meets their dietary needs and food preferences for an active and healthy life” (FAO, 2002). Currently, more than 1 billion people

around the world do not have adequate access to food, whilst 30 to 50% of food grown worldwide is either lost (post-harvest) or wasted. The effects of increasing affluence, urbanisation and climate change will add pressure to food supplies, and the FAO predicts that demand for food will grow by over 40% by 2030 and 70% by 2050 (FAO, 2018). Whilst some crops may respond favourably to the increase of CO_2, higher temperatures and fluctuating climate patterns will affect the areas where crops grow best and alter plant natural communities, challenging crop production and food security worldwide.

1.1.1. Climate change and its effects on agriculture

Arable crops are mainly monoculture systems. The reduction of genetic diversity results in constant yields, but if the cultivar is susceptible to a particular stress, the entire harvest is threatened. This event is known as genetic erosion, and it consists of the loss of variation in crops, an event that has been perpetuated since the modernization of agriculture. In fact, from the more than 50,000 edible plants in the world, just 15 of them provide 90% of the worlds calorific intake, with cereals alone supplying 50% of such intake (FAO). Monocultures have led to the genetic uniformity of crops and an increased vulnerability to pests, adverse weather conditions and diseases, which will influence how arable crops respond to the currently changing natural environments (Mark van de et al., 2016).

The natural environment is the entire platform upon which life is based. For crops, the state of the environment directly influences soil water and nutrient availability, pollinators and the abundance of certain pests, pathogens, insects and weeds (Nelleman, 2009). Ecological disruptions caused by climate change can favour the emergence of plant pathogens and pests that were not autochthonous (Bebber et al., 2013), which can be particularly detrimental in the case of monocultures. This is expected to impact agricultural yield and reduce the quantity of food produced, which will have major impacts in food security globally (Springmann et al., 2016).

A particularly concerning situation is the one regarding cereal crop production, due to their contribution to the global calorific intake. Nowadays, 25% of the world's cereal production takes place in Asia. Climate change is already promoting the melting of portions of the Himalayan glaciers and influencing the monsoon patterns and floods

and drought affluency in these regions. If these phenomena aggravate, it will lead to an increased uncertainty over the availability of water for irrigation, affecting lives and livelihoods, and ultimately challenging the world's cereal production.

Climate change alone is not the major cause of crop losses and food shortage. Land degradation, expansion of urban areas and conversion of crops and crop lands for non-food production purposes (such as cotton or biofuels) is decreasing food production and arable land. These factors are projected to decrease cropping area worldwide between 8-20% by 2050 (Nelleman, 2009). However, the major factor reducing arable land is linked to livestock consumption. In fact, one third of the total arable land is destined to produce animal feed (Foley et al., 2011). Moreover, livestock grazing is a key factor of deforestation, with 70% of the previously forested land in the Amazon being turned into pasture land (Nelleman, 2009). This is a controversial topic, since the very recent fires in the Amazonian rainforest have resulted in 906,000 hectares burnt as an effort to deforest land for agriculture and pasture. The livestock sector has a negative effect in agriculture but also in climate change, being responsible for 18% of the greenhouse gas emission (FAO, 2006b). With consumer habits being far from adopting sustainability, meat consumption is projected to increase to over 52 kg/person/year (FAO,2006), which will divert over half of the produced cereals to animal feed by 2050 (Nelleman, 2009).

Besides land degradation, water scarcity is another major limiting factor for crop production and is being influenced by the increase in global temperatures and decreased precipitations due to global warming. Water scarcity and the subsequent drought stress have been a major contributor to severe food shortages and famines throughout history. In the period between 1983 and 2009, approximately three-fourths of the global harvested areas (454 million hectares) experienced yield losses due to drought, which resulted in estimated losses of 166 billion U.S. dollars (Kim et al., 2019). With the increase in temperature and drought seasons due to global warming, this situation will be further aggravated. As well as weather conditions and precipitations, crop production relies in fresh water through irrigation. Nowadays, approximately nearly 70% of the world water reservoir is used for agriculture, and 40% of the world food is produced in irrigated soils (Chaves and Oliveira, 2004). With the increasing world population, is estimated that water withdrawals will escalate by

at least 15% as a result of incrementing agricultural production (FAO, AQUASTAT data 2017).

All the above facts combined evidence the urgent need for changing agricultural practices and resources usage in order to fulfil the increasing demand for food whilst minimising the detrimental environmental effects associated with extensive agriculture.

1.1.2. Impact of biotic stresses on agriculture

In the context of climate change, plant pests and diseases, combined with increased susceptibility, could potentially deprive humanity of up to 50% of major crop production (Oerke, 2006). If we combined this data with losses that happen after harvesting, the overall losses in food production become critical, especially for resource-poor regions. Pest and disease management has played its role in doubling food production in the last 40 years, but pathogens still claim 30% of the global harvest, (Scott and Peter, 2005) (Chakraborty and Newton, 2011). A study documenting losses in rice yield in the period between 2001 and 2003, attributed 15.1% of total losses to pests, 10.8% to pathogens and 1.4% to viruses, with the remaining 10.2% accounted for by weeds (Oerke, 2006). In financial terms, disease losses cost approximately US $220 billion yearly. Consequently, minimising crop losses due to plant diseases is a sustainable method for increasing current crop production.

The past century of disease-resistance breeding was largely limited to germplasm from sexually compatible wild species that remained more resistant to infection (Staskawicz et al., 2013). However, this strategy is slow and its field efficacy is often shortened. Therefore, one of the milestones of plant biologists is to achieve increased resistance against economically important pathogens, whilst maintaining at the same time complex agronomic traits such as yield, shape and flavour. Despite our advances in understanding the molecular mechanisms regulating plant growth and immunity, there are not enough sustainable strategies derived from this knowledge that are currently applicable. The starting point for developing such strategies is the model pathosystem between *Arabidopsis thaliana* and *Pseudomonas syringae,* which comprises a valuable tool for researchers worldwide to decipher the mechanisms of

plant defence. In the following sections we will review this system and the advances in understanding plant homeostasis and immune responses that derived from it.

1.2. *Arabidopsis* and *Pseudomonas* as a model pathosystem

During the last thirty years, there have been intensive efforts addressed at understanding the nature of plant-pathogen interactions as well as the mechanisms underlying plant immunity. The model pathosystem *Arabidopsis thaliana* and *Pseudomonas syringae* has been extensively used in order to elucidate the virulence strategies of the pathogen as well as the defence responses of the plant host. *Arabidopsis thaliana* was consensually established as a model plant system by the scientific community due to its small size, rapid generation time, prolific seed production through self-pollination and usefulness for genetic experiments (Koornneef and Meinke, 2010). Nowadays, there is a vast library of mutants created through EMS mutagenesis or T-DNA insertion which include mutants for almost all of the ~27,000 *A. thalian*a genes. These available resources comprise a valuable tool-box for analysing gene function using a reverse genetics approach. Furthermore, the wide geographical distribution of accessions, known as natural variation (Hoffmann, 2002), together with the vast diversity of molecular resources and biochemical protocols available, provides an opportunity to study important features of evolutionary ecology at the molecular level. In the context of immunity, Arabidopsis is susceptible to a wide number of pathogens, including viruses such as the cucumber mosaic virus (CMV), bacteria (*Pseudomonas syringae*), fungi (*Golovinomyces orontii*), oomycetes (*Hyaloperonospora arabidopsidis*), nematodes (*Heterodera glycines*) and insect pests (*Acyrthosiphon pisum*), having a similar pathogen response than other higher plant species (Andargie and Li, 2016).

In the early nineties, plant-pathogenic Pseudomonas bacteria was established as an economically important agricultural pest, since it is the cause of the bacterial spec in tomato (Y. Bashan, 1978). *Pseudomonas syringae* pv. *tomato* DC3000, also known as *P. syringae* DC3000, carries a large repertoire of virulence factors, effector proteins secreted through the Type III secretion system and coronatine, which structurally mimics the plant hormone jasmonate (JA-Ile) (Zhao et al., 2003). Molecular-level studies of *Pseudomonas syringae* have provided knowledge of toxin production, the

hrp genes that control bacterial virulence and avirulence through production of a type III secretion system, and the first pathogen avirulence (*avr*) genes ever to be cloned and molecularly characterized (Dangl, 1996, Alfano et al., 1997). Indeed, the genes *avrRpt2* and *avrRpm1* were cloned and characterised, establishing pathogen strains and attributing the resulting elicited resistance in Arabidopsis to a single pathogen *avr* gene (Whalen et al., 1991, Debener et al., 1991). Study of *P. syringae* DC3000 pathogenesis has not only provided several conceptual advances in understanding how a bacterial pathogen employs type III effectors to suppress plant immune responses and promote disease susceptibility but has also facilitated the discovery of the immune function of stomata and key components of JA signaling in plants.

1.3. Immune responses in Arabidopsis

As sessile organisms, plants have developed sophisticated mechanisms for responding to environmental stimuli, modulating homeostasis to overcome different types of stresses and ensure reproduction. In the context of plant immunity, plants have evolved several layers of defence mechanisms to recognise and respond to the invasion of microbial pathogens (Jones and Dangl, 2006).

Plant defence relies on the recognition of pathogens, which takes place by receptors located in the plasma membrane (Figure 1.2). These receptors detect conserved pathogen elicitors called microbe associated molecular patterns (MAMPs). After epitope recognition, microbe-associated molecular pattern immunity (MTI) gets activated (Figure 1.2, 1), which restricts the growth of the vast majority of potential pathogens encountered by plants (Boller and Felix, 2009). As part of MTI, signal from the activated plasma membrane receptors gets translocated into the nucleus via intracellular kinase cascades. Subsequently, the nuclear transcriptional machinery gets activated and through the coordinated action of transcription factors, there is a selective activation of immune related genes (Chinchilla et al., 2007).

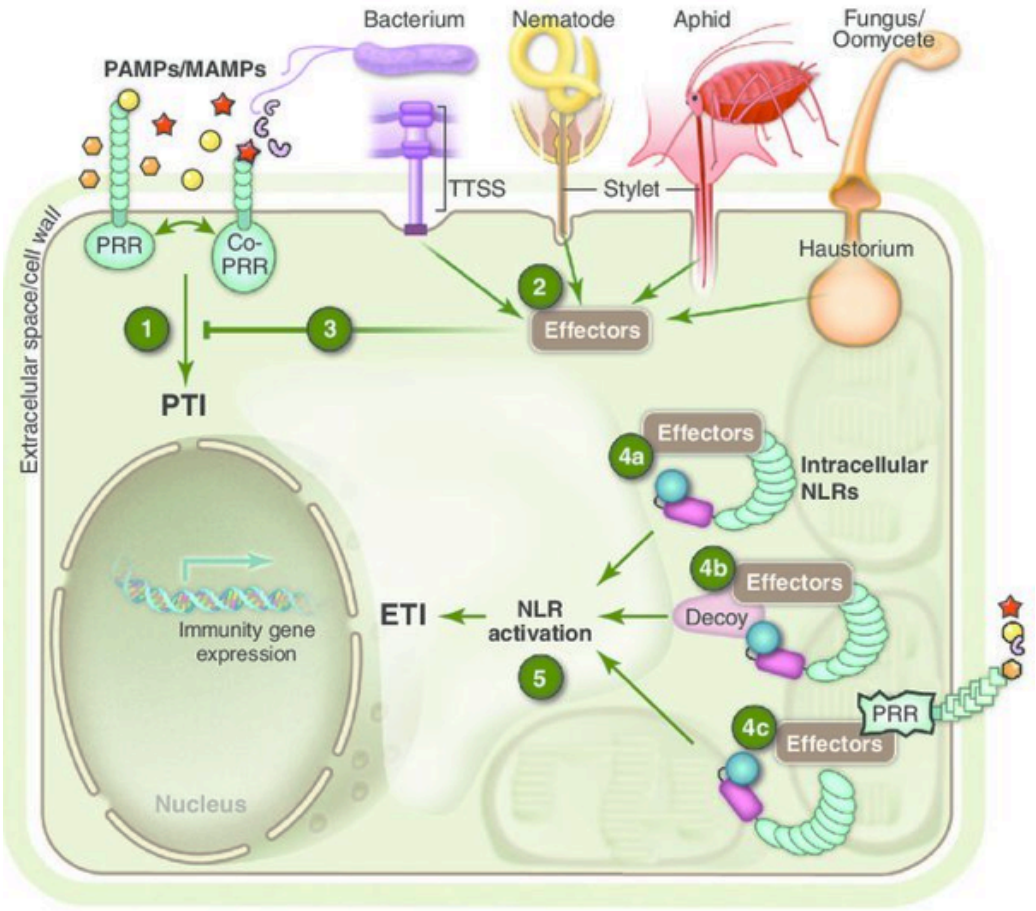

Figure 1.2. Schematic representation of the plant immune system. Pathogens expressing PAMPs/MAMPs get recognized by extracellular plant PRRs receptors and initiate PTI (1). Pathogens deliver virulence effectors to the plant cell to block plant immune responses (2). These effectors are addressed to specific subcellular locations where they can suppress PTI and facilitate virulence (3). Plant intracellular NLR receptors can sense effectors through direct interaction (4a); through the effector activity modifying decoy protein (4b) or by sensing the alteration of a host virulence target by the effector (4c). This results in NLR-dependent activation of effector-triggered immunity (ETI), a stronger defence response to limit pathogen spread (5). (Staskawicz et al., 2013).

Pathogens have evolved a parallel mechanism based on the secretion of small proteins to change the hosts cellular environment and promote pathogenesis (Jones and Dangl, 2006). These proteins are known as effectors, and in the case of *P. syringae*, are secreted through the type III secretion system (T3SS). T3SS is a needle-like structure through which the effectors get delivered to the cytoplasm of hosts cells. The 28 *P. syringae* type III effectors are classified as Hop (Hrp outer proteins) or Avr (Avirulence) proteins (Lindeberg et al., 2012). Avr effectors are recognised by plant

immune receptors known as resistance (*R*) genes (Dangl and Jones, 2001). The role of the effectors repertoire is to suppresses MAMP-triggered immunity (MTI) while evading internal surveillance by plant resistance (R) proteins that activate a stronger defence response known as effector-triggered immunity (ETI) (Jones and Dangl, 2006). This layer of defence is often associated with localized programmed cell death (PCD), known as the hypersensitive response (HR), a common plant strategy to limit pathogen spread (Greenberg, 2003). In general, MTI establishes basal resistance to diverse adapted and non-adapted microbes, whereas ETI plays a central role in defending against host-adapted pathogens (Spoel and Dong, 2012).

R proteins are plant resistance proteins, typically nucleotide-binding site leucine-rich repeat (NB-LRR) proteins that perceive type III effectors and initiate ETI and often, a localized programmed cell death known as the hypersensitive response (HR) to stop pathogen spread. NB-LRR proteins can directly or indirectly interact with a particular effector. In case of indirect recognition, the interacting protein can be a guardee or decoy (Kourelis and Van Der Hoorn, 2018, Dangl and Jones, 2006). In this case, a plant protein targeted by an effector acts as a bait (or guardee), triggering defence signaling by a second NRL upon effector binding (Cesari et al., 2014).

Even though single NLR proteins are sufficient for both effector recognition and signaling activation, NLRs also work through oligomerisation. A recent study combining crystallography and pathogenesis assays has described the so called "resistosome". This protein complex consists of an ATP-dependent pentamer responsible for activating the hypersensitive cell death response, conferring resistance to *Xanthomonas campestris pv. campestris* (Xcc) in Arabidopsis (Wang et al., 2019a).

Overall, the plant defence mechanisms upon pathogen recognition include the synthesis of plant-derived antimicrobial peptides (phytoalexins) and other compounds to suppress pathogenicity by direct detoxification or through inhibition of the activity of virulence factors (Ahuja et al., 2012). Both MTI and ETI induce systemic acquired resistance (SAR) through generation of mobile signals, accumulation of salicylic acid, and secretion of the antimicrobial PR (pathogenesis-related) proteins that result in increased protection in the case of a secondary infection. SAR can even be passed on to progeny through epigenetic marks created post-infection (Fu and Dong, 2013).

Recent studies evidenced that plants also use RNA interference (RNAi) to detect invading viral pathogens and target the viral RNA for cleavage (Rosas-Diaz et al., 2018).

1.3.1. Defence-growth trade-off

Plant hormones are small organic molecules that regulate growth, development, reproduction and response to biotic and abiotic stress. Environmental cues trigger changes in the quantity of these signal molecules, activating different plant responses. Salicylic acid (SA), jasmonic acid (JA) and ethylene (ET) are considered the major plant defence hormones. SA signalling is induced upon biotrophic pathogens, whilst JA is mostly involved in defence against insect herbivores and in coordination with ET, against necrotrophic pathogens (Glazebrook, 2005). JA synthesis and signalling induced by *P. syringae* are repressed by SA accumulation (Spoel et al., 2003), evidencing that SA and JA signaling pathways act antagonistically. Abscisic acid (ABA) is also involved in pathogen resistance, since *P. syringae* reduces the biosynthesis of ABA, which in turn controls stomata closure and promotes callose deposition to prevent pathogen invasion (De Torres-Zabala et al., 2007). On the other hand, hormones such as auxin, brassinosteroids (BRs) and gibberellins (GAs) regulate various growth processes in a sometimes synergistic fashion, suggesting physiological redundancy and crosstalk between the different pathways (Depuydt and Hardtke, 2011). These growth and reproduction promoting hormones are also implicated in the growth-defence trade-off.

Whilst defence mechanisms are crucial for plant survival, they come at the expense of plant growth. These is thought to be due to a limited amount of resources that have to be directed either for defence or growth/reproduction (Huot et al., 2014b). As a consequence, fine-tuning the amplitude and duration of the defence response to successfully overcome the infection without a severe developmental cost is crucial for plant survival. Fine-tuning of these growth-defence responses occurs mainly through hormonal crosstalk. The best characterised trade-off is the one between defence mediated by triggered MTI, salicylic acid (SA), and jasmonate (JA) versus growth mediated by auxin, brassinosteroids (BRs), and gibberellins (GAs) (Figure 1.3).

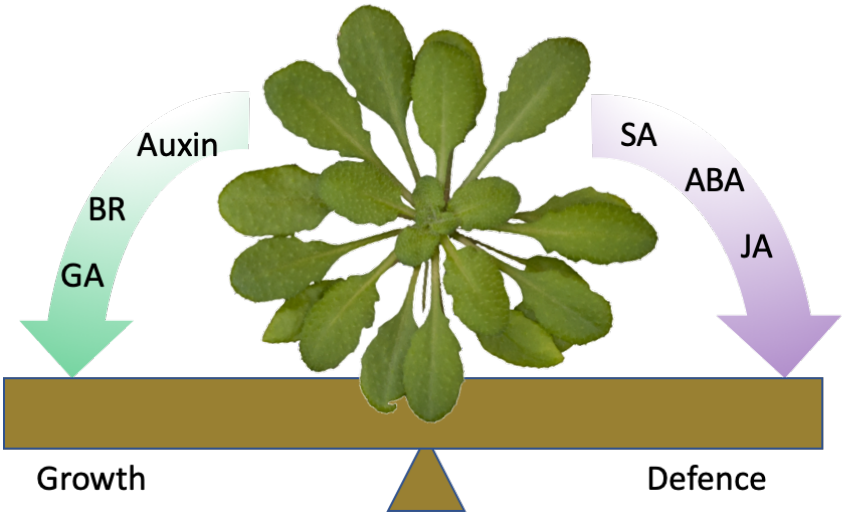

Figure 1.3. Diagram of defence and growth trade-offs. Plants resources are allocated towards growth or defence, depending on the presence or absence of specific stresses. This process is facilitated by hormone cross-talk. BR, brassinosteroid; GA, gibberellin; SA, salicylic acid; ABA, abscisic acid; JA, jasmonates. Adapted from (Huot et al., 2014a).

Up to date, the trade-off between growth and immunity has been successfully uncoupled in different studies (Spoel et al., 2007, Campos et al., 2016). However, it is questionable whether the uncoupling of this coregulation would benefit plant fitness overall. The evolutionary conservation across land plant species of the SA and JA antagonism and the tight coregulation of both phytohormones, suggests that this trade-off is important for fitness (Thaler et al., 2012). Furthermore, increased growth is not equivalent to enhanced fitness, but rather the plants' ability to successfully regulate homeostasis to respond to different environmental cues minimising the negative developmental effects.

1.4. Drought stress in Arabidopsis

1.4.1. Mechanisms of drought response

In plants, the water deficit caused by drought results in a reduction of growth and development, decreased leaf water potential and turgor loss, closure of stomata, and decrease in cell enlargement and growth (Verslues et al., 2006). It also leads to a

decrease in photosynthetic activity, senescence and, ultimately, death (Chaves et al., 2003).

Drought resistance is a trait that allows plants to cope with water shortage and its derived negative effects. There are different types of drought stress, arising from extended periods of gradual water scarcity (days, weeks, or months, for example) to short periods of significant dehydration (hours or days). Consequently, the response of the plant as a whole to drought stress involves the development of a series of changes at different levels, including molecular, physiological, and morphological modifications that help plants coping with this stress. Depending on those factors, there are three main strategies to achieve drought resistance (Figure 1.4).

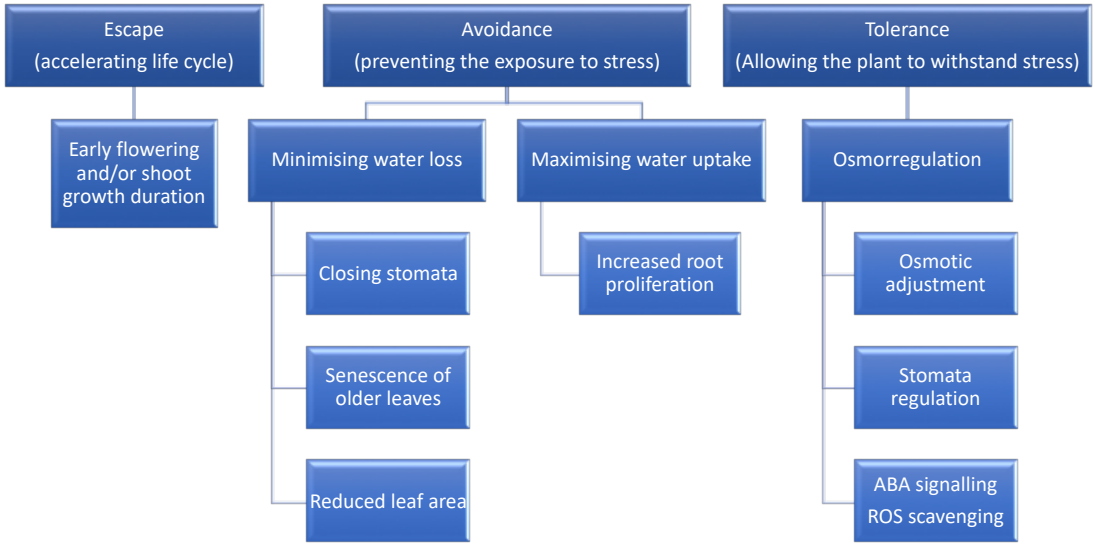

Figure 1.4. Schematic map of drought response strategies. Drought escape, avoidance or tolerance are three different mechanisms by which the plant modulates homeostasis, resulting in accelerated reproduction, reduced metabolism and growth or decreased water loss, respectively. Adapted from (Anna De Leonardis, 2012).

The first one is known as drought escape (DE), and relies on the ability of plants to complete their life cycle during sufficient water supply and before the onset of drought stress. This strategy is characteristic of desert plants, annual crops and pasture plants, which have early flowering phenotypes, short life cycles and certain developmental plasticity to produce seeds before experiencing water scarcity (Chaves et al., 2003, Fang and Xiong, 2015). The second strategy is known as drought avoidance (DA), and it is based on the ability of plants to minimise water loss,

maintaining turgor and therefore preventing or delaying the negative impact of the drought stress (Kumar et al., 2012). Hydration maintenance is achieved by increasing water intake and reducing water loss. The increased water intake is related to traits such as increased root growth rate, root depth and root dry weight. The reduced water loss is achieved through the regulation of stomata closure, storage in plant cells, reduced plant growth and plant senescence, among others (Chaves et al., 2003). The third strategy is known as drought tolerance (DT), or drought recovery, and is classified as the ability of plants to function while at low water potential, maintaining a certain level of physiological activity even under severe drought stress conditions or whilst desiccated (Tardieu and Tuberosa, 2010, Fang and Xiong, 2015). In the third mechanism of plant resistance to drought (DT), plants can tolerate drought by promoting antioxidant defence mechanisms, production of dehydrins and late embryogenesis abundant (LEA) proteins, coordinating the abscisic acid (ABA) response and maximising water-use efficiency (Kumar et al., 2012). However, the overall adaptation and response to drought is a result of combining all three strategies. The drought tolerance mechanism involves a rapid regulation of genes and metabolic pathways associated with repair or reduction of damage due to stress. Such genes aim not only to protect the plant from the stress through the production of metabolic proteins, such as compatible solutes, water channel proteins, and membrane transporters, but also to participate in the regulation of the downstream signal transduction in response to drought (Seki et al., 2007). In the following section we will describe the molecular mechanisms that take part during drought response.

1.4.2. ABA perception and signalling pathway

Plants recognise water deficit conditions at their roots, triggering changes in plant homeostasis, stress damage control, repair mechanisms and growth control through the production of growth inhibiting hormones, such as abscisic acid (ABA) (Zhu, 2002). Under drought stress, ABA elicits two distinct responses: rapid and gradual. The earliest and most rapid plant reaction, regulated mainly by ABA, is stomatal closure, which minimizes the water loss in the aerial plants of the plant through transpiration. This is achieved via changes in ion fluxes within the guard cell, that ultimately decrease their volume and close across the airway pore. The gradual

ABA-mediated drought response consists of an increase in hydraulic conductivity as well as cell elongation in the root, enabling the plant to recover after water-deficit stress. Furthermore, ABA induces the accumulation of osmotically active compounds, also known as osmoprotectants, which reduce cellular damage.

Active levels of ABA in response to stress result from the precise coordination between ABA biosynthesis, catabolism, conjugation, compartmentation and transport (Finkelstein, 2013). The ABA biosynthesis pathway has been elucidated through the combined effort of characterising ABA deficient mutants and profiling ABA biosynthetic intermediates. Bioinformatic and reverse genetic studies have provided information about key regulatory steps being catalysed by differentially expressed gene families conserved among plants, while others are controlled by single enzymes (Finkelstein, 2013). Furthermore, ABA metabolism is subjected to feedback regulation, since some genes involved in ABA biosynthesis and catabolism are directly regulated by ABA. Some of these metabolic enzymes are regulated by environmental signals such as drought, salinity, temperature, and light, as well as by other hormones, intrinsic developmental programs, and circadian rhythms (Finkelstein, 2013).

The first steps of ABA biosynthesis take place in the plastids, starting with the MEP pathway and the production of carotenoids. Phytoene is the first committed carotenoid, and it is synthesized through sequential condensation reactions of isopentenyl diphosphate (C5) in which geranyl geranyl diphosphate synthase (GGPPS) adds one isoprene unit progressively to generate C10, C15 and C20 molecules (Figure 1.5). Condensation of two geranyl geranyl diphosphate (GGP) molecules by phytoene synthase results in the C40 structure known as phytoene (reviewed by (Finkelstein, 2013)). Phytoene turns into β-carotenes, which are converted to zeaxanthin, and subsequently, to violaxanthin by a two-step epoxidation catalysed by the zeaxanthin epoxidase (ZEP) (Figure 1.5). Violaxanthin produces neoxanthin (9-cis-epoxycarotenoid), which undergoes oxidative cleavage to produce xanthoxin, which is catalysed by 9-cis-epoxycarotenoid dioxygenase (NCED) in a rate-limiting step (Figure 1.5). Xanthoxin is then transported to the cytosol, where is converted to ABA by a two-step reaction. First, xanthoxin is converted to abscisic aldehyde by an enzyme encoded by the *Arabidopsis ABA2* gene, and then aldehyde oxidase (AO) isoforms catalyse the oxidation of abscisic aldehyde to produce ABA.

Even though there are three genes in Arabidopsis encoding for aldehyde oxidases, AAO3 seems to be the major enzyme responsible for this step, since only the *aao3* mutants show decreased ABA levels (Seo et al., 2000).

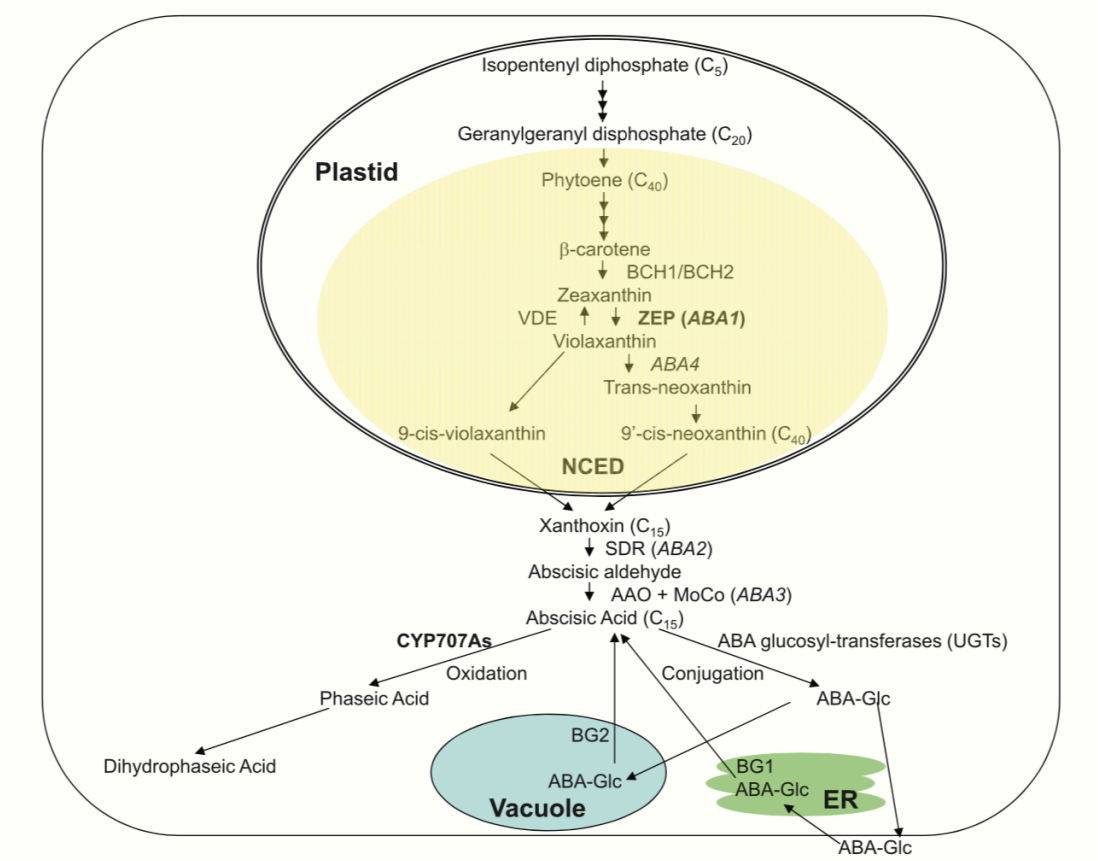

Figure 1.5. ABA metabolic pathways. The various steps of ABA biosynthesis, degradation and conjugation are displayed in the different cellular compartments in which these events take place. Key enzymes involved in different regulatory steps are shown in bold, and their coding gene, in italics. From (Finkelstein et al 2013).

ABA levels are also regulated by its catabolism, which takes place through either hydroxylation or esterification (reviewed by Finkelstein et al 2013). ABA hydroxylation is performed by the ABA-8‘-hydroxylases encoded by the CYP707A family of hydrolases. This reaction gives an unstable intermediate (8’-OH-ABA) which is isomerized into phaseic acid (PA). On the other hand, esterification of ABA to ABA-glucose ester (ABA-GE) results in an storage or transport form of inactive ABA. In fact, ABA-GE accumulates in vacuoles and the apoplast, to then be re-located into the ER upon dehydration stress (Figure 1.5).

The core ABA signalling pathway consists of ABA receptors (RCAR/PYL/PYRs) and GPCR type G-proteins (GPCRs), protein phosphatases (PP2Cs), kinases (SnRK2s), transcription factors and ion channel proteins. ABA is recognised by receptors known as PYR1 (PYRABACTIN-RESISTANCE LIKE receptors). In Arabidopsis, there are 14 homologues of these PYL-like receptors that bind ABA (Park et al., 2009). When activated through ABA binding, these membrane receptors bind to and inhibit the activity of a family of key negative regulators of the ABA signalling pathway, Protein phosphatases type 2C (PP2Cs) (Ma-Lauer et al., 2009). PP2Cs consists of a protein family of 80 members in Arabidopsis (Fuchs et al., 2013). Group A PP2Cs constitutively interact with and repress the protein kinases SnRK2s, inactivating them via dephosphorylation of multiple Ser/Thr residues within the activation loop (Umezawa et al., 2009).

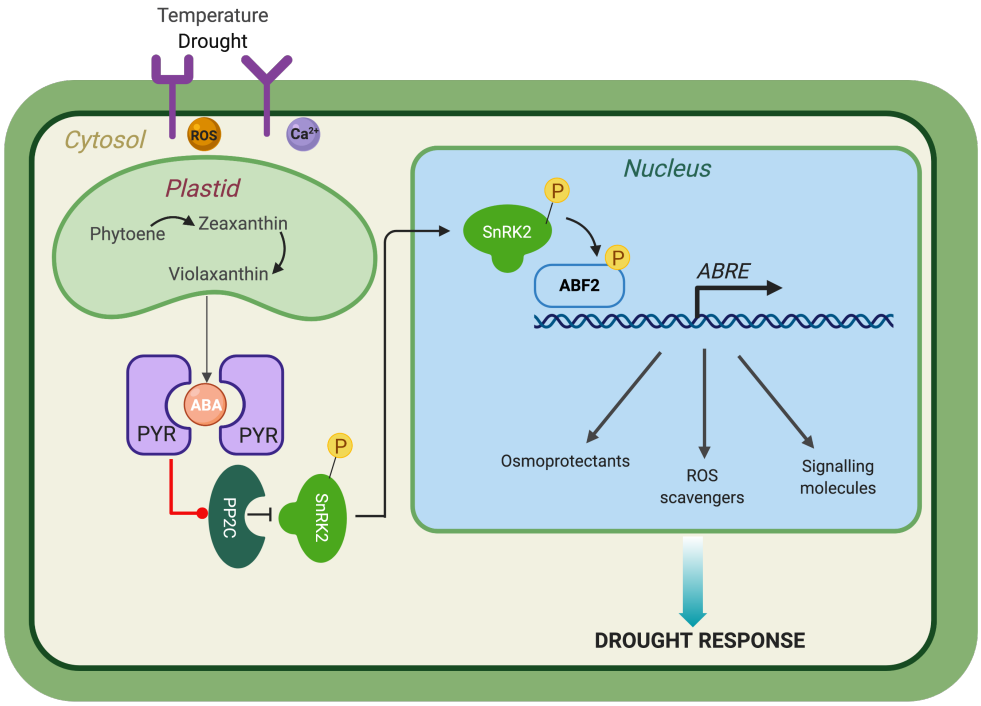

Figure 1.6. Illustration of drought-induced ABA biosynthesis and signal transduction. Abiotic stresses such as drought, recognised through sensors, activate ABA biosynthesis through Ca^{2+} or ROS-dependent phosphorylation cascades. ABA biosynthesis is initially catalysed in the plastids, until an ABA precursor is translocated into the cytoplasm where the final form of ABA gets synthesized. Cytoplasmic ABA is recognised by the PYR receptors, which results in the inhibition of PP2C phosphorylase and subsequent activation of SnRK2 kinases. Active SnRK2 translocate into the nucleus to phosphorylate

ABA responsive transcription factors (such as ABF2), which proceed to the activation of ABA responsive genes under the control of DRE/ABRE elements.

Following inactivation of PP2Cs by the PYL-like active receptors, SnRK2 kinases are released to directly auto-phosphorylate and trans-phosphorylate downstream targets such as S-type anion channels or transcription factors required for the expression of ABA response genes (Figure 1.6) (Kulik et al., 2011).

In addition to SnRK2 kinases, MAPK (mitogen activated protein kinase) cascades have also been shown to be implicated in ABA signaling. Many previous studies indicate the participation of MAPK cascades in ABA-mediated responses, including antioxidant defence, guard cell signaling and seed germination (reviewed by (Danquah et al., 2014)). MAPKs constitute the most known signalling mechanism in plants, playing an essential role translating the perception of a stimuli into a cellular response. A MAPK cascade consists of at least three sequentially acting serine/threonine kinases, a MAP kinase kinase kinase (MAPKKK), a MAP kinase kinase (MAPKK) and finally, the MAP kinase (MAPK) itself, with each phosphorylating, and hence activating, the next kinase in the cascade (Colcombet and Hirt, 2008). ABA induces the transcriptional regulation, protein accumulation, stability and kinase activity of several components of distinct MAPK signalling cascades, which suggests the involvement of MAPK pathways in ABA signalling (Fujita et al., 2006, Li et al., 2017a, Li et al., 2017c). For instance, MPK3 is activated by both H_2O_2 and ABA in Arabidopsis seedlings, and its over-expression increases ABA sensitivity in ABA-induced growth arrest assays (Lu et al., 2002). MPK9 and MPK12 are preferentially expressed in guard cells, get activated by ABA and mediate ABA guard cell signalling (Xing et al., 2008). A more recent study showed that the complete MAP3K17/18-MKK3-MPK1/2/7/14 module is under the transcriptional and post-translational control of the ABA core signalling pathway (Danquah et al., 2015). However, despite the evidence of MAPK being regulated by ABA at different levels, the direct roles of most of them in ABA signalling have not been characterized.

Transcription factors that regulate ABA responsive genes include AREBs (ABA-responsive element binding proteins)/ABFs (ABRE binding factors), ABI5 (ABA insensitive 5), MYB (myeloblastosis), MYC (myelocytomatosis), NAM (no apical meristem) and ERF (ethylene response factor) (Sah et al., 2016). Molecular analysis of promoters of ABA-responsive genes led to the identification of a conserved

cis-acting element, designated ABRE (ABA-responsive element) (Fujita et al., 2011). ABREs can be recognized by ABRE-binding proteins (AREBs) or ABRE-binding factors (ABFs), which belong to group A of the basic leucine zipper (bZIP) TFs. ABA-dependent phosphorylation of bZIP transcription factors in multiple RXXS/T sites by SnRK2 kinases is necessary for their activation (Kagaya et al., 2002). About 75 members of the bZIP TFs family have been identified in Arabidopsis, divided into more than 10 different groups. Many of the well-studied group A bZIP TFs play a central role in ABA signaling and are upregulated by drought stress. In fact, transcriptomic studies with multiple *areb* mutants and *snkr2* mutants concluded that AREB1, AREB2, and ABF3 and ABF1 are the major transcription factors downstream of the ABA-activated SnRK2s in ABA signal transduction during vegetative growth (Yoshida et al., 2015).

Upon phosphorylation, AREB/ABFs are activated and bind to the ABA-responsive cis-element (ABRE; PyACGTGG/TC), enriched in the promoter regions of drought-inducible genes. AREB/ABFs function as master transcriptional activators regulating ABRE-dependent gene expression in ABA signalling under drought stress conditions. In addition to SnRK2 and MAPK signal transduction, drought stress signaling can be triggered by accumulation of calcium-dependent protein kinase (CDPK). CDPKs sense perturbations in cytosolic calcium ion (Ca^{2+}) levels, which are altered in plant cells in response to drought (Harper et al., 2004). When CDPKs get activated, transduce the signal into phosphorylation cascades, leading to the activation of drought-responsive gene transcription.

Recent studies have added an extra level of complexity to the ABA signaling pathway. A study by Wang et al., showed that ABFs directly bind to the promoter of group A PP2C genes (*ABI1* and *ABI2*), mediating their rapid induction upon exogenous ABA treatment, and therefore playing a role in the negative feedback regulation of ABA signalling (Figure 1.7).

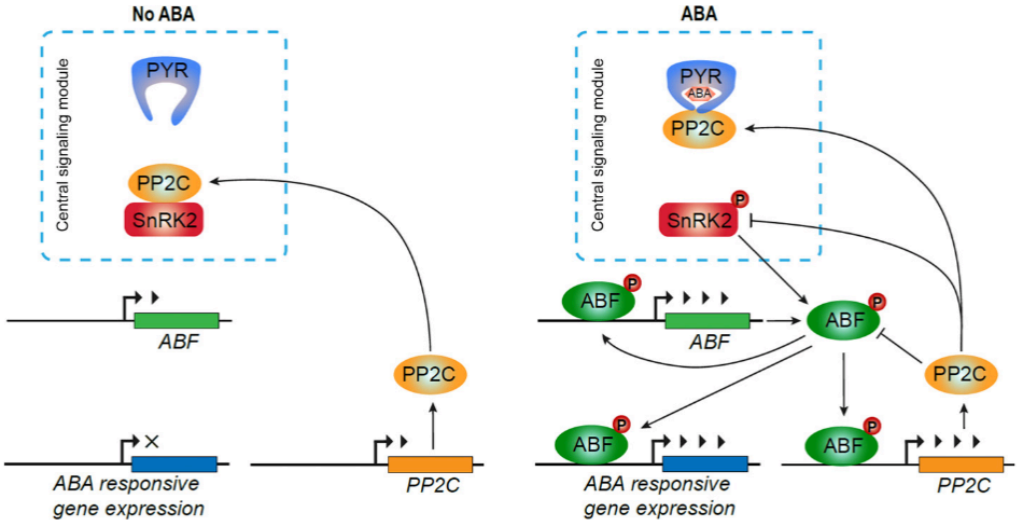

Figure 1.7. ABRE-binding factor (ABF) transcription factors play a role in the feedback regulation of abscisic acid (ABA) signaling. This transcription factors activate the expression of group A PP2C genes, which are negative regulators of ABA signalling. In the absence of ABA, the PP2Cs are active and repress SnRK2 activity, and both ABF and group A PP2C genes maintain basal levels of expression. Upon ABA, ABA-bound PYR/PYL/RCAR receptor proteins inhibit PP2Cs activity, which results in SnRK2s activation and phosphorylation of ABF proteins. ABA induces ABF gene expression (regulated by ABFs themselves) and protein accumulation. Active ABFs induce the expression of group A PP2Cs and other ABA-responsive genes. PP2Cs can dephosphorylate and inactivate ABFs, forming a regulatory loop to tightly control ABA signalling homeostasis (Wang et al., 2019b).

The authors hypothesize that ABA negatively regulates its own signalling pathway as part of a desensitization mechanism to adjust ABA signaling after a dramatic increase in ABA levels upon stress, in order to increase the root:shoot biomass ratio (Wang et al., 2019b). Another exciting finding from this research is that ABFs (bZIP transcription factors) are involved in their own induction upon ABA, since ABA-mediated expression of *ABF2* is mediated by ABF1, ABF3 and ABF4 (Wang et al., 2019b).

1.4.3. Transcriptional responses to ABA

ABA signalling in response to drought results in changes in gene expression to reprogram metabolism. Indeed, almost 10% of the Arabidopsis protein coding genes are regulated by ABA (Nemhauser et al., 2006). As a result of using transcriptomic approaches to understand the transcriptional response to different abiotic stresses, 245 ABA-inducible genes were identified in Arabidopsis. Among the ABA-inducible genes, 63% (155 genes) were induced by drought, 54% (133 genes) by high salinity and 10% (25 genes) by cold treatment (Seki et al., 2002). Amongst these genes, there are functional proteins to reduce the negative impacts of drought (such as osmolytes, heat shock proteins, antioxidant enzymes, and dehydrins), as well as regulatory proteins such as transcription factors (Fujita et al., 2011).

There are three different groups of drought stress responsive genes depending on their protein products. The first group includes proteins involved in protection of macromolecules and cellular structures such as LATE EMBRIOGENESIS ABUNTANT (LEA) proteins as well as enzymes that synthesise osmolytes (Seki et al., 2007). This group also includes free radical scavengers, whose role is to protect from the damage produced by reactive oxygen species (ROS). Furthermore, there are molecular chaperones and proteinase to remove denatured proteins (Zhu, 2002).

The second group of drought-regulated genes includes membrane transporters and ion channels involved in water and ion uptake, such as aquaporins and ion transporters. The third group of drought stress responsive genes are those involved in the regulation of signal transduction, such as MAP kinases and phosphatases, as well as transcription factors (Campo et al., 2014). In addition to transcriptional changes, plants undergo posttranscriptional and posttranslational mechanisms as additional layers of regulation of adaptation to drought (Campo et al., 2014).

Posttranscriptional and posttranslational modifications contribute to the fine-tuning of plant homeostasis and response to drought stress. Posttranscriptional modifications such as alternative splicing and RNA-mediated silencing also play a role in the amount of specific transcripts, whilst posttranslational modifications are involved in the activity, subcellular localisation and half-life of proteins. Post-translational modifications, including dephosphorylation, phosphorylation and ubiquitination, play important roles in regulating ABA signalling (reviewed by (Yang

et al., 2017)). The most notorious post-translational modification involved in ABA responses are the de-phosphorylation of SnRK2s kinases by PP2C and the phosphorylation of bZIP transcription factors through active SnRK2s kinases. In addition, poly ubiquitination mediated by E3 ubiquitin (Ub) ligases has been found to be important in ABA perception, ABA signal transduction and the induction of ABA responses, since ABA receptors (PYR/PRLs), PP2Cs, PP2As, TFs and ABA-responsive proteins are targeted for E3 Ub ligase-mediated polyubiquitination and degraded by the 26S proteasome.

1.4.4. ABA-independent drought responses

In addition to the ABA-dependent drought responses, the drought-stress signal is also mediated by an ABA-independent pathway, also known as the osmotic stress signal. This pathway regulates the expression of drought-inducible genes, which are under the control of the dehydration-responsive cis-element/C-repeat (DRE/CRT), a conserved DNA sequence (A/GCCGAC) that gets recognised by DREB1 and DREB2 transcription factors. *DREB* transcription factors are highly induced by drought, high salinity, and heat stress. A recent transcriptomic and network analysis study identified 211 ABA-dependent genes and 1,118 ABA-independent genes involved in drought stress response through RNA-seq. Using GO term enrichment, the authors showed that ABA-dependent differentially expressed genes (DEGs) were significantly enriched in expected biological processes such as drought and ABA stimulus, while ABA-independent DEGs were preferentially enriched in response to jasmonic acid (JA), salicylic acid (SA) and gibberellin (GA) stimuli, evidencing the hormonal cross-talk regulating drought stress responses (Shiwei Liu, 2018). Furthermore, the authors characterised 94 genes acting as core interacting components of the ABA-dependent and independent drought responses, suggesting crosstalk between elements of both pathways. Consistent with these findings, full activation of *RD29A* and *RD29B* transcription, key drought responsive genes encoding dehydrins, depends upon the combined regulation of the DRE and ABRE elements (Virlouvet et al., 2014). The *RD29A* promoter contains both ABRE and DRE elements (Narusaka et al., 2003). In contrast, the *RD29B* promoter has two adjacent ABRE elements regulated by the ABF TF family members ABF2, ABF3, and ABF4 (Fujita et al., 2005).

Besides the expression and activation of specific transcription factors downstream of a signalling pathway, gene expression is dependent on epigenetic mechanisms that modulate the level of compaction of the chromatin, which will be reviewed in the following sections.

1.5. Chromatin remodelling and gene expression

1.5.1. Regulation of transcription

Gene transcription occurs when the RNA polymerase synthetises mRNA from DNA, which following the central dogma of molecular biology, is used as a template to produce a functional protein through translation (Crick, 1970). In Eukaryotes, RNA polymerase II (RNAPII) recruits a number of transcription factors to initiate transcription. Traditionally, the initiation of transcription is considered the crucial step controlling transcript synthesis. However, in recent years, it has become apparent that the elongation phase of RNAPII transcription is also dynamic and highly regulated. In fact, a variety of so-called transcript elongation factors (TEFs) have been identified, which regulate the process of transcript elongation. TEFs facilitate efficient mRNA synthesis in the chromatin context either acting as histone chaperones, modifying histones within transcribed regions, or modulating the catalytic activity of RNAPII (Grasser and Grasser, 2018). The RNA polymerase complex targets loci through its association with transcription factors (TFs) which contain DNA-binding domains and often recognise sequence-specific motifs (such as the ABRE elements recognised by the ABF transcription factors (Fujita et al., 2005)). Overall the regulation of transcription is a highly dynamic and complex process that depends on the recruitment of several components that participate in the RNAPII complex, as well as chromatin modifiers that control the accessibility of the transcriptional machinery (Nightingale et al., 1998).

1.5.2. Chromatin organisation

Gene expression in eukaryotes involves a complex interplay among transcription factors and chromatin proteins that pack chromosomal DNA into the nucleus (Kadonaga, 1998). Nuclear DNA is packaged into nucleosomes, each of which consists of a histone octamer. Each octamer is composed by two molecules of each of the core histones (H2A, H2B, H3, and H4), around which approximately 146–147 bp of DNA are wrapped (Kornberg and Lorch, 1999). The linker histone H1 binds to the entry/exit sites of DNA on the surface of the nucleosome, influencing the nucleosomal repeat length (NRL) and establishing higher-order chromatin structures such as the so-called 30-nm fibre (Woodcock, 2005) (Figure 1.8). The dynamic nature of chromatin in eukaryotes plays a crucial role in regulating gene expression without causing changes in the nucleotide sequence.

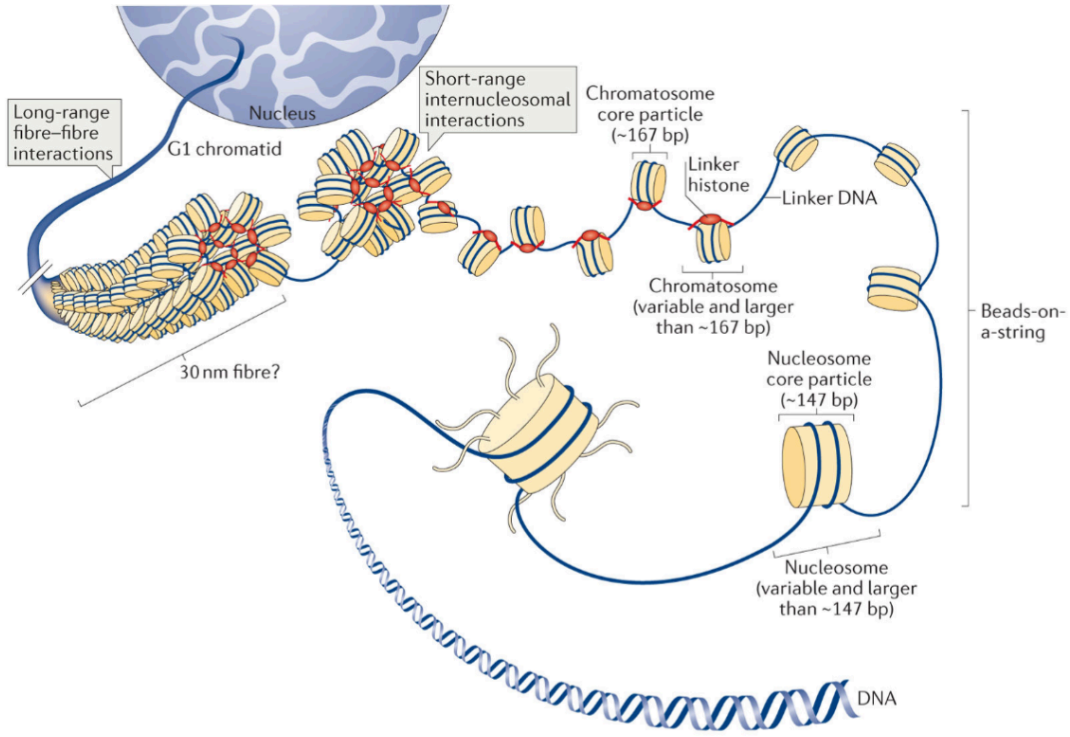

Figure 1.8. Representation of different levels of chromatin organisation. The multiple levels of chromatin occur via interactions between DNA and histones. These levels include the formation of the nucleosome core particle, strings of nucleosomes (bead-on-a-string arrangement), the chromatosome core particle, the 30 nm fibres and the association of individual fibres, which results in tertiary structures (Fyodorov et al., 2018).

The genomic regions with lower levels of folding are known as euchromatin, whilst those with higher folding are known as heterochromatin. In addition, there are regions whose topology is variable (facultative heterochromatin) due to histone modifications in N-terminal tails and DNA modifications such as DNA methylation (Jenuwein, 2001). Due to the association between DNA and histones, DNA undergoes topological alterations which reflect permissive or inhibiting sates regarding the access of specific loci to transcription factors, effector proteins and RNA pol II.

The lysine-rich N-terminus domain of histones can undergo a variety of post-translational modifications, such as acetylation, methylation, phosphorylation, ubiquitination or ADP-ribosylation (Strahl and Allis, 2000) (Figure 1.9). These modifications affect chromatin structure by directly changing the physical association between DNA and histones within the nucleosome, or indirectly by recruiting histone-modifying complexes (Kouzarides, 2007). The figure below represents all the known covalent modifications of the core histones that conform the nucleosome, also known as the "histone code". These modifications get recognized by other proteins, resulting in downstream events.

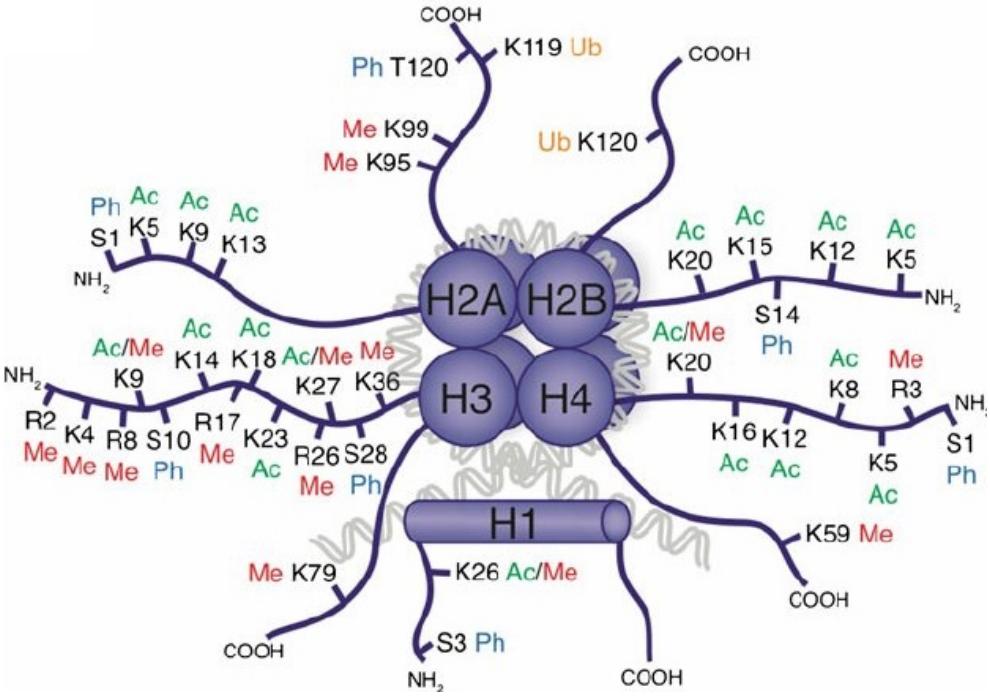

Figure 1.9. Histone post-translational modifications. Representation of currently known covalent histone post-translational modifications (PTMs) on the N- and C- terminal tails of each histone. Me = methylation; Ac = acetylation; Ub = ubiquitination; Ph = phosphorylation. Green represents active marks, red corresponds to silencing marks, blue to DNA-damage associated marks and yellow to protein degradation marks. Adapted from (Zhao et al., 2013).

Chromatin structure can also be affected by ATP-dependent remodelling complexes. In Arabidopsis, a well characterized ATP-dependent remodelling complex is the SWI/SNF chromatin remodeller, which modulates core histone protein polypeptides, incorporates histone variants and modifies nucleotides in DNA strands within the nucleosome (Jerzmanowski, 2007).

Direct DNA cytosine methylation is another mechanism that alters chromatin structure (Figure 1.10). In plants, methylation of cytosines in target genes or promoter sequences is associated with transcriptional repression (Alvarez et al., 2010). Both histone acetylation and DNA methylation marks can be inherited from one generation to the next, altering gene expression without sequence mutations. This phenomenon is referred to as "transgenerational epigenetics" (Hauser et al., 2011), and it has gained interest over the past decade as an alternative for increasing plant resistance to stress without altering the genome sequence. Indeed, environmental stresses can cause changes in the epigenome (Boyko et al., 2007), however, inherited epigenetic marks tend to be erased in early developmental stages, during the resetting of the epigenetic state in the germline, getting lost over generations (Heard and Robert, 2014). As a consequence, whether transgenerational epigenetics is a mechanism of genetic imprinting in plants in response to changing environments or just the result of the failure to reinforce or reset the epigenome is an issue that remains controversial.

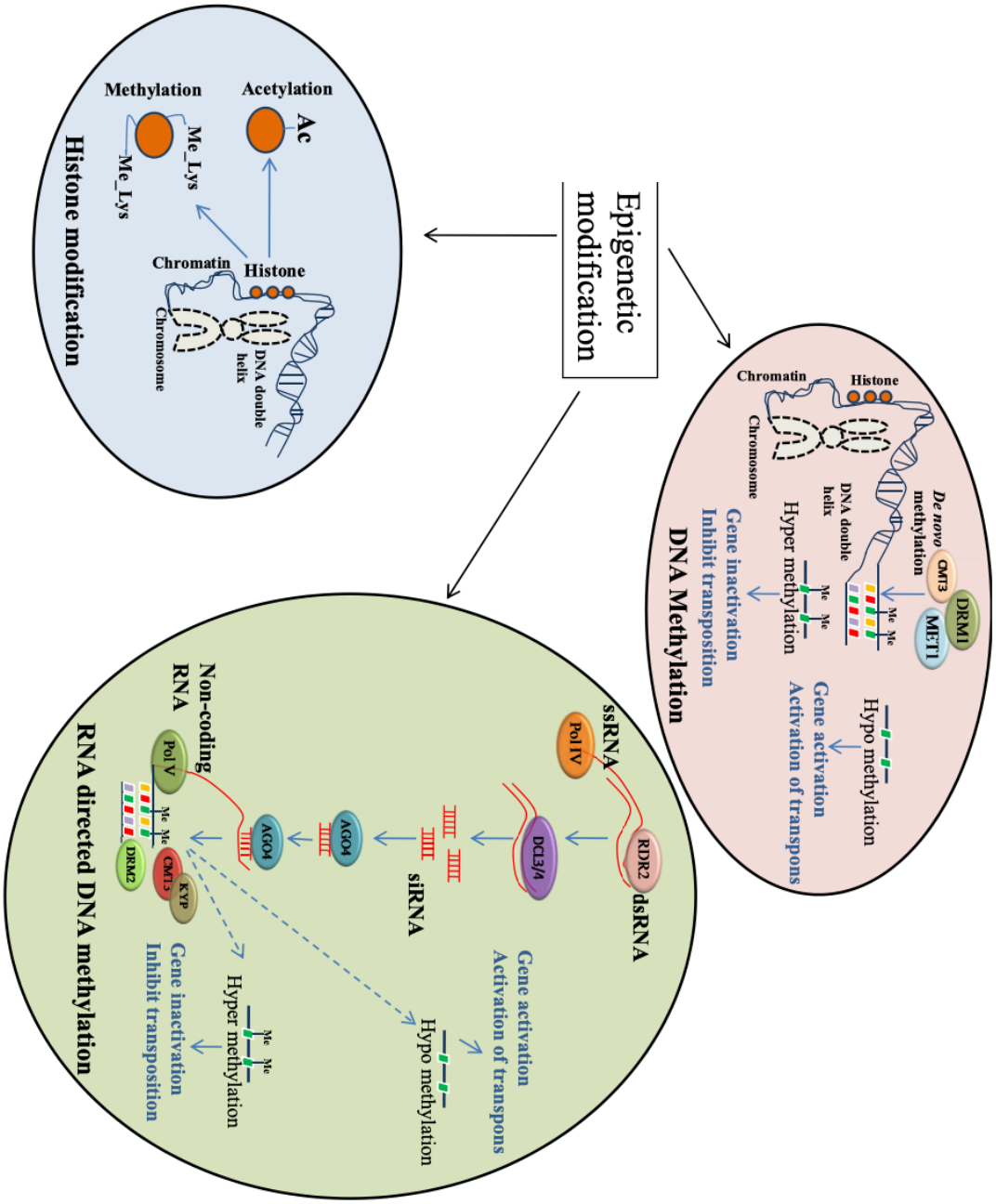

Figure 1.10. Schematic diagram of the epigenetic mechanisms in plants. These epigenetic mechanisms are DNA methylation, RNA directed DNA methylation and histone modifications. DNA methylation results in gene silencing and inactivation of transposable elements. Histone modifications such as methylation and acetylation also regulate gene expression. Small non-coding RNAs mediate DNA methylation by recruiting methylase complexes. CMT3: Chromomethylase; DCL3: Dicer-like 3; DRM: domain rearrangement methyltransferase; MET1: methyltransferase; Pol IV/V: DNA-dependent RNA polymerase; RDR2: RNA-dependent RNA polymerase. Adapted from (Pandey et al., 2016).

Besides histone modifications and DNA methylation, small non-coding RNAs also play a role in heterochromatin regulation. Recent studies show their involvement in recruiting heterochromatin-related proteins influencing their association with chromatin or their enzymatic activity (Figure 1.10) (reviewed by (Johnson and Straight, 2017)).

Finally, canonical histones can be replaced by histones with different physical proteins, known as histone variants, or released in order to allow gene expression, DNA repair or replication (Kouzarides, 2007). Histone variants are isoforms of core histones with similar properties and functions acquired through convergent evolution (Talbert et al., 2012). H3 variants such as H3.1 and H3.3 are replication-dependent, and differ from each other by four amino acid residues (Stroud et al 2012). These variants localise in different regions of the genome. For instance, H3.3 is more abundant over gene bodies and actively transcribed regions of the genome whilst H3.1 is essential for the H3K27me1 and epigenetic memory associated with H3K27me3 through cell division (Stroud et al 2012). Different histone variants are incorporated in a replication dependent or independent manner by different histone chaperon complexes.

Overall, cellular processes involving DNA (DNA-repair, replication and transcription) are influenced by chromatin structure, and one of the central milestones of this thesis is to characterise the effects of histone modifications, particularly histone acetylation, in regulating plant responses to stress by determining DNA accessibility.

1.5.3. Histone modifications

The conformational changes of the DNA around histones due to post-translational modifications of histone tails result in gene activation or repression. Histone modifications are catalysed by a variety of histone-modifying enzymes, which are recruited to specific genomic regions by transcription factors (Kouzarides, 2007). Gene expression is directly associated with chromatin accessibility by transcription factors and RNA polymerase II recruitment. For instance, histone acetylation adds a negative charge to lysine residues at the N-terminal histone tail. Because of the amino group, lysine is normally a positively charged amino acid, which strongly binds to the negatively charged DNA. The acetyl group neutralizes this positive charge, reducing

the binding between histones and DNA and facilitating the access of the transcriptional machinery to the loci associated to acetylated histone marks (Roth et al., 2001). As a consequence, histone acetylation often associates with active transcription, where active genes are preferentially associated with highly acetylated histones, whereas inactive genes are associated with hypoacetylated histones (Hebbes et al., 1988).

The consensus in plants is that transcriptional silencing is associated with H3 lysine 27 (H3K27) methylation, H3 and H4 hypoacetylation and hypermethylated DNA, whereas actively transcribed regions associate with H3 and H4 hyperacetylation, H3K4 trimethylation and DNA hypomethylation (Roudier et al., 2011). However, overall, the active or inactive state of the chromatin depends on the number and accumulation of epigenetic marks associated to a particular genomic region, which ultimately defines how tightly the DNA is wrapped around histones and thus, how accessible to transcription factors and the transcriptional machinery.

1.5.4. Histone Acetyl Transferases in Arabidopsis

Histone acetyltransferases (HATs) catalyse the covalent transfer of an acetyl group from a molecule of acetyl-CoA to the amino (–NH2) group of lysine at the N-terminal tail of histones. The antagonistic reaction is carried out by histone deacetylases (HDAC), which catalyse the hydrolysis of the acetyl group. There are 16 HDACs and 12 HATs encoded in the Arabidopsis genome, and their antagonistic activity regulates gene expression through transcriptional activation.

A phylogenetic study classified the 12 HATs in 4 different subfamilies based on comparative sequence analysis: GNAT (HAG1, HAG2, HAG3), MYST (HAG4 and HAG5) , p300/CBP (HAC1, HAC2, HAC4, HAC5, HAC12), and TAFII250 (HAF1 and HAF2) (Ritu Pandey, 2002) (Figure 11a). These enzymes are involved in the regulation of different processes such as plant development, response to abiotic stress (Earley et al., 2007, Xu et al., 2013), responses to light, regulation of flowering time (Xiaoa et al., 2013) and hormonal pathways. The different domain predictions for each HAT, along with their target specificity are presented in Figure 1.11a. This figure illustrates that each family possess a specific HAT domain (highlighted in red), which are responsible for the domain specific acetylation of different histone residues (Figure 1.12b).

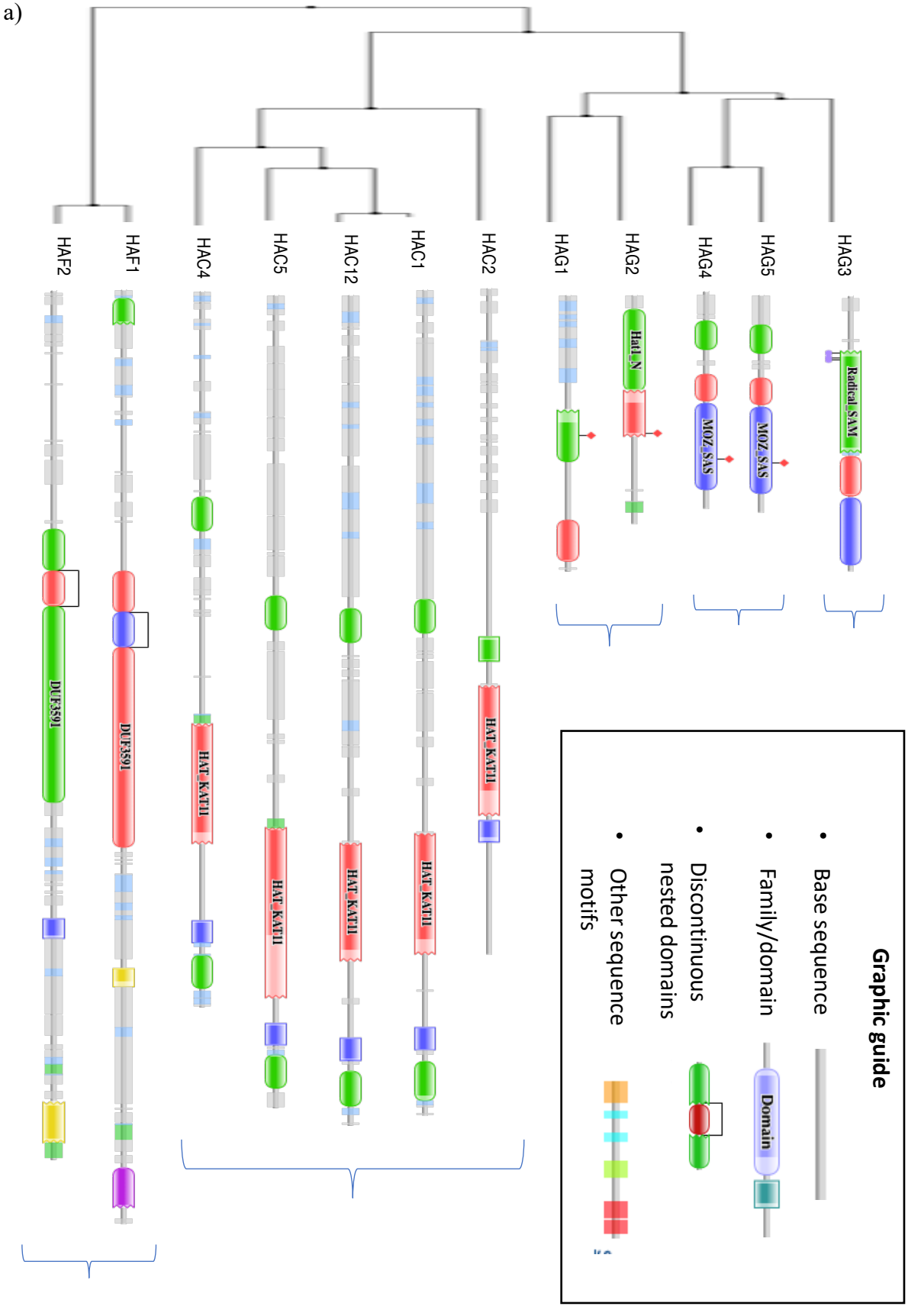
a)
HAG3
HAG5
HAG4
HAG2
HAG1
HAC2
HAC1
HAC12
HAC5
HAC4
HAF1
HAF2
Radical_SAM
MOZ_SAS
MOZ_SAS
Hat1_N
HAT_KAT11
HAT_KAT11
HAT_KAT11
HAT_KAT11
HAT_KAT11
DUF359
DUF359
Graphic guide
Base sequence
Family/domain
Domain
Discontinuous nested domains
Other sequence motifs

b)

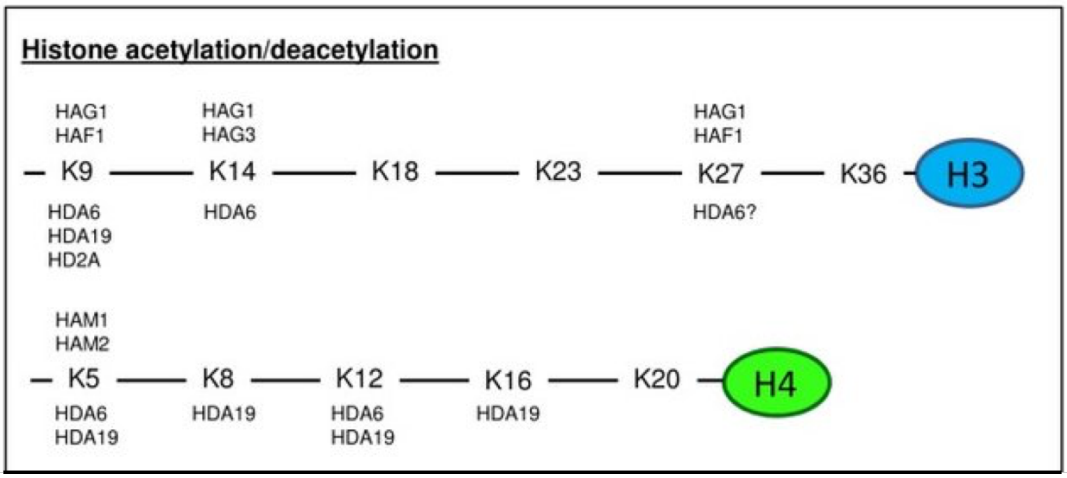

Figure 1.11. Phylogenetic tree, domain architecture and substrates of Arabidopsis HATs. **a)** Neighbour-Joining phylogenetic tree was constructed based on protein alignments of Arabidopsis HATs proteins using ClustalX2. The schematic diagrams show the domain organization of these proteins according to analysis of PFAM searches. Different domains are indicated by the use of different colours. **b)** Histone modifications on specific residues of H3 and H4 histone tails by different histone modifiers. Lysine amino acids (K) are targeted for histone acetylation/deacetylation by histone acetyltransferases (HAG, HAF, HAM) and histone deacetylases (HDAC). Adapted from (Liew et al., 2013).

This study focuses on the GNAT/MYST superfamily of HAT and their roles in regulating plant biotic and abiotic stress responses. In the GNAT/MYST superfamily of HAT proteins, GNAT proteins are defined by the presence of a HAT domain which is comprised of four motifs, A-D, whereas MYST proteins possess only the A motif of the HAT domain (Ritu Pandey, 2002). The GNAT family is comprised of four subfamilies: GCN5, ELP3, HAT1 and HPA2. In the Arabidopsis genome, HAG1, HAG3 and HAG2, are homologous of the GCN5, ELP3, HAT1 subfamilies, respectively (Ritu Pandey, 2002). HAG1 plays an essential role in many plant developmental processes, such as meristem function, cell differentiation, leaf and floral organogenesis and responses to environmental conditions such as light and cold (Servet et al., 2010), whereas HAG2 and HAG3 are positive regulators of aliphatic glucosinolate biosynthesis (Gigolashvili et al., 2008).

In mammals, the MYST family proteins are involved in a wide range of cell functions ranging from transcriptional activation and silencing, apoptosis, cell cycle progression, DNA replication or DNA repair linked to pathological disorders such as

cancer (Delarue et al., 2008). In Arabidopsis, two MYST histone acetyltransferases HAG4 and HAG5 (also referred to as HAM1 and HAM2), are assumed to work redundantly acetylating Histone 4 at lysine 5 (H4K5Ac) *in vitro* (Earley et al., 2007). Several studies have characterized the processes that are affected by HAG4 and HAG5 histone acetylation. Delarue et al. discovered that HAG4 and HAG5 work redundantly to regulate gametophyte development, being the double mutant *ham1/ham2* lethal, which emphasizes the critical role such enzymes play in development (Delarue et al., 2008). Furthermore, HAG4 and HAG5 are involved in the regulation of flowering time through epigenetic modification of the H4K5Ac status within the chromatin of *FLC* and *MADS- box*, affecting flowering genes 3/4 (*MAF3/4*) (Xiaoa et al., 2013). Arabidopsis mutants *ham1* and *ham2* also showed increased DNA damage after UV-B, suggesting that the role of these proteins in DNA damage repair has been conserved through evolution (Casati et al., 2008, Campi et al., 2012).

Even though *HAG4* and *HAG5* have been thought to be complete homologues and have redundant functions, this study focuses on understanding the evolutionary divergence between the two enzymes, which have acquired specific and distinct functions through their exclusive interacting partners. The phenotypic characterisation of *hag4* and *hag5* loss-of function mutants is carried out across Chapters 3 and 4 of this thesis.

1.6. Epigenetic regulation of drought responses

Histone acetyltransferases and deacetylates play important roles in regulating the transcriptional responses to ABA and drought, ultimately modulating plant survival upon abiotic stress. Histone modifications and nucleosome occupancy in the promoters and ORFs of the drought inducible genes are responsible for their upregulation upon drought (To and Kim, 2014). A ChIP-seq study by Kim et al. looked at the levels of histone marks on the regions of four drought stress-inducible genes (*RD29A*, *RD29B*, *RD20* and *RAP2.4*) after drought treatment. The authors found enrichment of H3K4me3 and H3K9ac in correlation with gene activation and RNAPII occupancy after drought in all four genes. Furthermore, enrichment of H3K23ac and H3K27ac marks occurred in coding regions of all genes except *RD29A* (Kim et al., 2008a), suggesting these marks occur in a gene-specific manner upon drought stress.

H3K4me3 has been associated with stress memory, since the levels of this mark as well as RNAPII occupancy remain relatively high after stress recover. A study by Ding et al. looking at stress memory after recovery showed that *RD29B* and *RAB18* genes displayed induced transcript levels after recovery when re-exposed to drought stress (trained plants). However, this increased induction was lost after 7 days of recovery form the first stress, suggesting that dehydration stress-induced transcriptional memory persist for few days but its lost after 7 days under watered conditions. The enhanced transcript levels in the "trained" plants correlated with H3K4me3 levels and Ser-5P (phosphorylation at serine 5) of Pol II C-terminal domain (CTD levels. This suggests that enrichment of H3K4me3 and Ser-5P Pol II positively regulates drought-inducible gens, providing a degree of transcriptional memory by keeping enriched levels after a first time stress exposure (Ding et al., 2012). Interestingly, the bZIP transcription factors AREB1, AREB2 and AREB3, which induce the expression of the previously mentioned drought-responsive genes, are not required for the stress-memory induction of these genes, suggesting that drought responsive genes are under different mechanisms of regulation (Ding et al., 2012).

Besides the histone marks associated to drought-responsive genes, there are many studies investigating the role of various chromatin remodellers in drought stress (Table 1-1).

Table 1-1. Summary of epigenetic components involved in drought responses. Modified from (Luo et al., 2017).

Epigenetic regulators	Functions	Relation with stress tolerance	References
ATX1	Histone methyltransferase	Positive	Ding et al. (2011)
MAI1	Silencer	Negative	Henning et al. (2005)
MYST, ELP3, GCN5	Histone acetyltransferase	Positive	Papaefthimioi et al. (2010)
AtDH2C	Histone deacetylase	Positive	Sridha and Wu (2006)
CHR12	Chromatin remodeller	Negative	Mlynarova et al. (2007)
BRM	Chromatin remodeller	Positive	Han et al. (2012)
HDA6	Histone deacetylase	Negative	Chen et al. (2010)
HDA9	Histone deacetylase	Negative	Chen et al. (2016)
HDA19	Histone deacetylase	Negative	Song et al. (2005)
HD2A-D	Histone deacetylase	Negative	Luo et al. (2012)

HDA6 is involved in drought stress tolerance by regulating the expression of genes involved in acetate biosynthesis and stimulating JA signalling pathway under the control of H4 acetylation (Kim et al., 2017). HDA9 also acts as a negative regulator

of drought since the loss-of function mutant displayed increase tolerance to dehydration and upregulation of drought responsive genes. HDA9 forms a histone deacetylase complex with POWERDRESS (PW) and SANT (SWI3/DAD2/N-CoR/TFIII-B) targeting H3K9 and H3K14 acetylation (Kim et al., 2016). The role of HDA19 in ABA and drought responses has been extensively characterised, since it forms various repressive complexes to fine-tune different components of ABA and drought signalling pathways. Song et al. were the first scientist reporting HDA19 forming a repressive complex with the transcription factor ERF7 and Sin3 to silence stress response genes upon ABA and drought treatments (Song et al., 2005). A similar study reported HDA19 as part of a repressive complex with SNL1 and SNL2 negatively regulating ABA biosynthesis through histone deacetylation at H3K9/18 and H3K14 (Wang et al., 2013d). In addition, *ABI3* expression is repressed by HDA19 -BES1-TPL in response to brassinosteroids, affecting ABA signalling (Ryu et al., 2014). A more recent study reports that HD19 interacts with MSI1 and SIN3-like protein to modulate the expression of ABA receptor and responsive genes through H3K9 acetylation. (Mehdi et al., 2015). Finally, HDA19 forms a complex with HDA6 and HDC1 required for deacetylating H3K9K14 during abiotic stress responses (Perrella et al., 2013). HD2-type histone deacetylases are also involved in drought responses. The expression of these proteins (*HD2A, HD2B, HD2C AND HD2D)* is downregulated upon ABA and salt treatments and overexpression of some members of the family, like *HD2D* and *HD2C* results in increase drought tolerance (Han et al., 2016, Sridha and Wu, 2006). Furthermore, HD2C interacts with HDA6 to modulate H3K9K14 acetylation and H3K9 dimethylation upon ABA treatment (Luo et al., 2012).

Even though histone deacetylation has been very well characterised in the context of drought responses, very little is known about the role of histone acetyltransferases in this context, since it has been historically assumed that their roles are purely antagonistic to HDACs. However, the complex interplay between HDACs and other proteins evidences that the epigenetic regulation of drought responses is a highly complicated process besides the catalytic activity of HDAs. Indeed, gene expression is modulated by chromatin accessibility in a very specific and complex-dependent manner. A recent study in *Populus trichocarpa* found that AREB1/ABF2 forms an activating complex with ADA2b and GCN5 to enhance H3K9ac and enrich

RNA polymerase II recruitment at the ABRE motifs in the promoters of three drought-responsive genes (Li et al., 2019). As a consequence, it is very possible that HATs also play important roles in regulating the transcriptional response to abiotic stress, forming complexes with other transcription factors and DNA-binding proteins to fine-tune plant stress responses.

1.7. Aims of this study

Gene expression regulated through chromatin remodelling affects a variety of downstream processes, since the transcriptomic landscape depends on the accessibility of the chromatin. As described above, histone acetyltransferases regulate various biological processes through histone acetylation, and in most cases, are considered to be positive regulators of gene expression (Roudier et al., 2011). As a consequence, we selected histone acetyltransferases (HATs) as candidates for our research, due to their potential on regulating plant homeostasis and responses to stress in a genomic scale. The aim of this study is to characterise HATs involved in the regulation of plant biotic or abiotic stress responses in order to understand the molecular mechanisms that govern fine-tuning of plant responses to stress. Given the challenges that climate change will bring upon food security, understanding how plants respond to pathogens and extreme environmental conditions, such as drought, is crucial for developing technologies for improving crop performance.

To this end, this study began with a reverse genetics approach using Arabidopsis HATs T-DNA insertion lines investigating the immunity phenotypes resulting from down-regulating or knocking out particular HATs (Chapter 3). This screening revealed that *hag5* knock-down mutant was more tolerant to infection with *Pto* DC3000, highlighting HAG5, a member of the MYST family of HATs, as a negative regulator of plant immunity. Interestingly, *hag5* mutants did not suffer from the developmental trade-off that results from enhanced immunity phenotypes and displayed increased leaf area and fresh weight. As a consequence, there are beneficial associated to the suppression of *HAG5* expression in plan performance. Further characterisation of *hag5* mutant phenotypes can be found on Chapter 3 of this thesis, where the developmental effects of mutating HAG5, as well as the response to pathogens, will be further developed.

HAG5 resulted from a duplication event in Brassica, and it has been previously described as redundant to its paralogue *HAG4* (Delarue et al., 2008). As a consequence, *hag4* T-DNA insertion mutants are carried along this research in order to investigate the level of redundancy between both enzymes.

Chapter 4 is dedicated to the understanding of the molecular mechanisms by which HAG5 regulates plant growth and immunity. The first step described on this chapter consists of a yeast-two hybrid (Y2H) screening using a library of Arabidopsis transcription factors (TFs) to identify interacting candidates. The positive interactors revealed that HAG5 is involved in ABA signalling. As a consequence, Chapter 4 of this thesis follows various strategies such as hormone sensitivity assays, drought tolerance phenotyping and transcriptomic approaches to identify the level at which HAG5 modulates ABA responses (ABA biosynthesis, perception, signalling or response). Nonetheless, the ultimate goal of our research is to increase plant performance and response to drought and pathogens without compromising development and growth. Therefore, Chapter 5 describes the screening and characterisation of potential inhibitors of HAG5 catalytic activity obtained using *in silico* modelling. These inhibitors are designed to mimic the effects of the loss-of function mutant in wild type plants, in an effort to design agrochemicals for foliar applications. An alternative approach to implement our findings is using CRISPR/Cas9 *Brassica oleracea* lines targeting the homologue of *HAG5*. Exploring the effects of gene editing in *B. oleracea* will not only translate our research to other plant crops, but also help investigate the conservation of *HAG5* as a regulatory hub controlling growth, development and responses to stress across plant lineages.

Chapter 2 Materials and methods

2.1. Plant lines

2.1.1. *Arabidopsis thaliana*

The wild type ecotype used in this work was *Arabidopsis thaliana* ecotype Columbia (Col-0). *Arabidopsis* seeds were sown on *Arabidopsis* mix with Intercept and stratified at 4°C for 2 days in dark conditions. For physiological assays, seeds were germinated and grown in an Aralab growth chamber set at a short photoperiod of 10h light, 21°C, 60%humidity. Two weeks after germination, seedlings were carefully transferred to individual pots. When necessary, 3 to 4 weeks old plants were transferred to a growth chamber with 16h light photoperiod in order to obtain seeds.

For *in vitro* work, Arabidopsis seeds were surface-sterilised by chlorine gas exposure. Seeds in a seed storage (glassine) bag were incubated with chlorine gas for 4h inside a sealed desiccator. The chlorine gas was produced by adding 3mL of hydrochloric acid 37% to a beaker containing 100mL of 10% sodium hypochlorite. Seedlings were grown in sterile half (2.15g/L) Murashige and Skoog medium (1/2 MS, Duchefa Biochemie), with 1% sucrose if indicated, pH adjusted with KOH 1 M at 5.80 ± 0.02 and 0.5% Phytagel (Sigma). Nystatin 25µg/mL, was added, if required, once the medium was autoclaved and cooled below 65°C. All plating procedures were carried out under sterile conditions using a Class II cabinet. Seedlings were stratified in darkness for 2 days at 4ºC and then transferred to a Sanyo cabinet set to 10h light, 21°C and 60% humidity.

The Arabidopsis T-DNA insertion SALK (Alonso et al., 2003) and GABI-kat lines (Kleinboelting et al. 2012) were purchased from the Nottingham Arabidopsis Stock Centre (NASC), and can be found in Table 2-1.

Table 2-1. Arabidopsis T-DNA insertion lines used in this study.

Arabidopsis line	AGI number	T-DNA insertion line	Used in
hag1-6	At3g54610	SALK 150784	Chap. 3
hag2-1	At5g56740	SALK 051832	Chap. 3
hag4-1	At5g64610	SALK 103726	Chap. 3, 4
hag4-2	At5g64610	SALK 027726	Chap. 3, 4
hag5-1	At5g09740	SALK 012086	Chap. 3, 4, 5
hag5-2	At5g09740	SALK 106046	Chap. 3, 4, 5
hac1-1	At1g79000	SALK 070277	Chap. 3
hac2-84	At1g67220	SALK 049434	Chap. 3
hac4-1	At1g55970	SALK 051750	Chap. 3
hac5-1	At3g12980	SALK 024278	Chap. 3
hac12-1	At1g16710	SALK 071102	Chap. 3
haf2-1	At3g19040	SALK 110029	Chap. 3
fls2	At5g46330	SALK 062054	Chap. 3
brm-3	At2g46020	SALK 088462	Chap. 4
snrk2.2/2.3	At3g50500, At5g66880	GABI-Kat 807G04, SALK 107315	Chap. 4

2.1.2. *Brassica oleracea*

B. oleracea DH1012 seeds were sown in FP7 pots containing F1 compost. Seeds were sown to twice the depth of the size of the seed, and grown in an Aralab growth chamber set at a short photoperiod of 10h light, 21°C and 60% humidity.

2.1.3. *Nicothiana benthamiana*

N. benthamiana seeds were sown on FP7 pots filled with humid F2 soil and grown in an Aralab growth chamber set at a short photoperiod of 10h light, 21°C and 60% humidity. During the germination stage, pots were wrapped with film to preserve humidity. Two weeks after germination, seedlings were carefully transferred to FP9 individual pots with M2 compost and grown until ready for infiltration.

2.2. Bacterial strains

Bacteria stocks were in 20% glycerol at -80°C. *Escherichia coli* strains and *Agrobacterium tumefaciens* (*Rhizobium radiobacter*) were grown on Luria Broth (LB) medium (1% tryptone, 0.5% yeast extract, 1% NaCl liquid, or solid, with the addition of 1.5% agar) (Bertani, 1951). The antibiotics used for selection were added to the medium after autoclaving, when it cooled below 65°C. *P. syringae* strains were grown in King's Broth medium (20g/L proteose peptone, 8.6mM K_2HPO_4, 163mM glycerol, pH adjusted to 7.0 with HCl before autoclaving); liquid, or solid, with the addition of 1.5% agar (King et al., 1954) adding the required antibiotics for selection (Table 2-2), after the medium was autoclaved and cooled below 65°C. For single colony isolation, stocks were streaked onto solid plates and incubated over-night prior to inoculation in liquid medium. *E. coli* strains were grown at 37°C. *A. tumefaciens* and *P. syringae* strains were grown at 28°C. Liquid cultures were grown in an incubator with shaking at 220 rpm.

Table 2-2. Bacterial strains and antibiotic resistance used in this study.

Species	Strain	Open Reading Frame	Vector	Selection	Citation
E.coli	TOP10	-	-	-	Thermo Fisher (C404010)
E.coli	BL21 Rosetta (DE3)	-	-	-	Sigma Aldrich (70954)
A. tumefaciens	GV3101	-	-	Ampicillin 1 μg/mL Chloramphenicol 10 μg/mL	(Holsters et al., 1980)
P. syringae	*pv tomato* DC3000	-	pVSP61	Rifampicin 100 μg/mL Gentamycin 100 μg/mL	(Cuppels, 1986)
P. syringae	*pv tomato* DC3000	AvrRpt2	pVSP61	Rifampicin 100 μg/mL Gentamycin 100 μg/mL	(Cuppels, 1986)

2.3. Generation of Arabidopsis transgenic lines

Transformation of female gametes was accomplished by dipping developing Arabidopsis inflorescences for a few seconds into a 5% sucrose solution containing 0.01-0.05% (vol/vol) Silwet L-77 and resuspended Agrobacterium cells carrying the genes to be transferred. We used *Agrobacterium tumefaciens* GV3101 expressing the WT *HAG5* genomic DNA and promoter in a pEG302 vector (complemented lines) or

HAG5 cDNA in a pEG202 vector (overexpressor lines) to transform T0 female gametes of h*ag5-2* plants. Treated plants were allowed to set seed (T1), which were then sown on selective media to screen for transformants. The selective media used was ½ MS 1% Sucrose with 10µg/mL of BASTA (glufosinate-ammonium, Sigma 77182). The positive transformants were then potted in soil, genotyped to confirm the presence of the insert and kept for seed production (T2). To check for homozygous plants, seeds from T2 lines (T3) were sown into selective media to check for 100% survival rate.

2.4. Plant development assays

2.4.1. Leaf surface area measurements

Arabidopsis plants were grown in soil as described in section 2.1.1. Photographs were taken 4 to 5 weeks after germination, using a ruler for setting the scale. Leaf surface area was calculated using ImageJ (Schneider et al., 2012). 24 plants were measured per genotype, and the average leaf surface area was used to represent the size of each genotype.

2.4.2. Primary root length measurements

Arabidopsis seedlings were grown in plates as described in section 2.1.1. 15 days after germination, plates were scanned using a HP PSC 2500 scanner, with a resolution of 1200 DPI and including a ruler to set the scale. Root length was measured with ImageJ (Schneider et al., 2012), using the free-hand tool. At least 40 seedlings were used per genotype and condition.

2.4.3. Root meristem measurements

Seedlings were grown in plates as described in section 2.1.1. 4 to 10 days post-germination, root tips were sliced using a scalpel, and mounted on a glass slide with 100µL of 10µg/µL of Propidium Iodide (Sigma P-4170) diluted in water. The stained

root tips were imaged using the confocal microscope Leica TSC SP5. At least 10 roots were imaged per genotype and condition. Meristem size was quantified as the number of dividing cells from the quiescent centre until the first expanding cortical cell.

2.4.4. Stomatal density measurements

Leaves 7, 8 or 9 from 5 weeks-old Arabidopsis plants grown in soil were harvested and fixed in 70% EtOH overnight. Then, 5 washes with 75% EtOH were performed, and leaves were incubated in the same solution for 2h. Samples where then transferred into Hoyer's solution (Chloralhydrate/water/glycerol, 8:3:1 v/v) and incubated until the leaves were translucent. Sections of the central part of the leaf were dissected with a scalpel and mounted on a glass slide using Hoyer's solution. 14 leaves and two sections/leaf were imaged per genotype. Images of an area of 0.0768mm^2 were taken using the Zeiss™ Axiovert – A1 microscope (Zeiss).

2.5. Biotic stress assays

2.5.1. Bacterial growth

Infiltration

A single bacterial colony of *P. syringae* was inoculated in 15mL of liquid (KB) with the corresponding antibiotics and grown overnight at 28°C, shaking at 215 rpm. Cells were then harvested by centrifugation (3000g for 10 min), washed and re-suspended in sterile 10mM $MgCl_2$. For spraying assays, bacterial suspensions of OD_{600} 0.01 (equivalent to $2x10^5$ colony-forming units/mL) were prepared in 10mM $MgCl_2$. The optical density was measured with a Biochrom WPA CO8000 cell density meter (Biochrom Ltd., UK) at 600 nm (OD_{600}). Three leaves of 4-5 week old Arabidopsis plants (leaves 7, 8 and 9) were infiltrated using a needleless 1mL syringe. Bacterial populations in infected leaves were quantified three days post-inoculation.

Spraying

P. syringae strains were inoculated in 15mL liquid cultures and incubated overnight at 28°C, shaking at 215 rpm. The cultures were harvested by centrifugation (3000g for 10 min), washed and re-suspended in sterile 10mM $MgCl_2$ for spraying assays, bacterial suspension of OD_{600} 0.1 (equivalent to $2x10^7$ colony-forming units/mL) was prepared in 10mM $MgCl_2$, 0.04% Silwet L-77 (Lehle Seeds, USA). The optical density was measured with a Biochrom WPA CO8000 cell density meter (Biochrom Ltd., UK) at 600 nm (OD_{600}). Six 5 week-old plants per line were inoculated, and plants from different lines were randomised in trays before spraying to avoid position effects. Plants were preferably infected before midday to consider stomata openings (~11 am). Spray inoculation was performed with a Sparmax TC-620X spray paintbrush (The Airbrush Company, UK), at a pressure of 1 bar until the whole leaf surface was completely wet. Infected plants were then sealed in the infection tray and kept for the required infection time (0 to 3 days-post inoculation) in the Aralab growth chamber.

For sample collection, 0.5 cm^2 leaf discs from leaves number 6 and 7, were collected with a disc borer. Two leaf discs were collected per plant, resulting in a total of 12 leaf disks per genotype and condition. 2 leaf discs (corresponding to a leaf surface area of 1 cm^2) were added to 2mL tubes containing two metallic beads (3 mm diameter) and 200µL of 10mM $MgCl_2$. To grind the plant tissue, two pulses of 28hz for 30 seconds were applied with a mixer mill (Tissue Lyser MM300, Retsch). The plant and bacterial suspension was then diluted up to 1mL with 800µL of 10mM, $MgCl_2$ and serial dilutions were plated on KB plates containing the selective antibiotics. After incubating the plates over-night at 28°C, bacterial colonies were counted at each dilution and the log of colony forming units (CFU) was calculated for each line. Each experiment, as described, was repeated 3 times on different days, or otherwise as stated.

2.5.2. *Verticillium dahliae* assay

V. dahliae isolated from Raphanus sativus L. (provided by E. Ligoxygakis, National Agricultural Research Institute, Crete, Greece), with known pathogenicity

against *A. thaliana* plants (Tjamos et al., 2005), was used in the experiments. The fungal strain was cryopreserved by freezing a conidial suspension in 25% aqueous glycerol at 80ºC. Prior to being used, the fungus was transferred to potato dextrose agar (Merck) at 24ºC for 5 days. For the bioassays, 107 conidia per mL suspended in distilled water were prepared from a culture grown for 5 days at 24ºC in sucrose sodium nitrate liquid medium. Three weeks old plants were inoculated with *V. dahliae* by root drenching with 10mL of a suspension of 1×10^7 conidia/mL of sterile distilled water (Tjamos et al., 2005). Control plants were mock-inoculated with 10mL of sterile distilled water. Disease severity at each observation was calculated from the number of leaves that showed wilting as a percentage of the total number of leaves of each plant, and was periodically recorded for 25 days after inoculation. Disease ratings were plotted over time to generate disease progression curves. AUDPC was calculated by the trapezoidal integration method (Campbell and Madden 1990). Disease was expressed as a percentage of the maximum possible area for the whole period of the experiment, which is referred to as the relative AUDPC. For this experiment, 30 plants were used per treatment and plant genotype.

2.6. Abiotic stress assays

2.6.1. Drought tolerance in soil

Drought tolerance assays were performed as described by (Sakamoto et al., 2004) with minor modifications. 24 plants per genotype were grown in an Aralab growth chamber set at a short photoperiod of 10h light, 21°C and 60%humidity. When the plants were 3 weeks-old, drought stress was imposed by withholding water for 14 days. After the stress, plants were re-watered and the trays were covered with a plastic cap for recovery for 2 days. 14 days after regular re-watering, pictures of plants were taken and the percentage of recovery was calculate as the number of plants that had recovered/total number of plants x 100.

2.6.2. Drought tolerance using the Phenoscope

The experiments on the Phenoscope were performed according to (Tisne et al., 2013). Arabidopsis seeds were stratified in a 0.1% agar solution for 3 days at 4°C in the dark, and sown on plugs maintained at saturation (100% SWC) in plastic trays. After germination, one individual seedling was kept per plug, with as much synchronous germination as possible across plugs. For each genotype, more plugs (+30%) were sown than the number needed for the experiment, allowing selection (essentially based on the size of the cotyledons to control for homogeneous early development) among 1-week-old seedlings of the same genotype or group of genotypes. These plugs were then installed on the robot (8 days after sowing).

Before starting the experiment, empty pots were individually weighed to define the tare. Then the selected seedlings were installed in the Phenoscope pots, one by one in a pre-determined order to weigh the seedling promptly at 100% SWC. This weight was used to define the target weight for each pot individually, according to the watering instructions, which differed between treatments, from day to day and from pot to pot. From sowing to the end of the experiment, seedlings were watered with specific nutrient solution (derived from that described previously by (Loudet et al., 2003) but with 5mM nitrate). The photoperiod in the growth room was set to short days (8h light/16h dark) to avoid interaction with early flowering and to optimize the study of vegetative shoot growth and the response to treatment during the exponential growth phase. Light was provided by 177 cool-white daylight fluorescent tubes to an intensity of 230lmol m^2 sec^1. The air temperature was set to 21°C during the day and 17°C at night, with a constant relative humidity of 65%. Relative humidity and air temperature were measured every 5 sec using a Rotronich C2–S probe (www.rotronic.com). They were then averaged every 5 min and stored in the Phenoscope DB. For the drought stress, 2 watering conditions were used: 60% SWC for non-limiting conditions (called 'WW' for well-watered) and 30% SWC for mildly growth-limiting watering conditions (called “WD” for water deficit). A picture of each individual plant was taken every day at the same day-time and a semi-automatic segmentation process was performed to extract leaf pixels. Several traits were calculated from these data: Projected Rosette Area (PRA), circle radius, convex hull area, average red, green and blue components (leaf pixels, RGB colour scale), and

derived phenotypic traits such as the compactness (ratio PRA / convex hull area) and the Relative Expansion Rate (RER) over specific time windows, as previously described by (Tisne et al., 2013).

All statistical analyses were performed as described by (Tisne et al., 2013). In brief, phenotypic data were first processed to identify potential outlier plants amongst replicates. Statistical differences between genotypes and conditions were tested by ANOVA and Tukey test using the Tukey HDS() function in R software (R Development Core Team, 2007; http://www.r-project.org/). ll statistical analyses were performed using R software (R Development Core Team, 2007; http://www.r-project.org/). Statistical differences between accessions were tested by ANOVA, and Tukey test was performed using the Tukey HSD() function.

2.6.3. Drought tolerance in plates

½ MS plates were prepared as described in section 2.1.1., but using exactly 50mL of ½ MS media per plate. 15 seeds per row and 2 rows per plate were sown for each genotype. Plants were grown vertically in a Sanyo cabinet set to 10h light, 21°C and 60%humidity. Pictures of plates were taken when phenotypical differences in leaf turgor were observed (approximately 4 weeks after sowing the seeds).

2.6.4. Drought tolerance with reduced water potential

Seeds were stratified at 4ºC for 2 days and germinated for 5-7 days in ½ MS media without sucrose. Then, seedlings were transferred under sterile conditions into PEG-infused plates and grown vertically for 7 days, when pictures of the plates were taken. MS plates and PEG-infused plates were prepared as described by (Kumar et al., 2015). Root length was quantified from pictures of plates taken 7 days post-transfer, using ImageJ as described in section 2.4.2.

2.6.5. Analysis of water relations

Water loss and final water content were measured as described by (Yoshida et al., 2002, Fujita et al., 2005), with minor modifications. Rosettes from 5-week-old

soil-grown plants were excised and weighed for fresh weight over time. Detached aerial parts were then dried to determine dry weight. Water content was standardised as a percentage relative to the initial water content of aerial parts of the plant. Water content was calculated as [(FWi – DW)/(FW0 – DW)] * 100, where FWi and FW0 are fresh weight for any given interval and original fresh weight, respectively, and DW is dry weight. Final water content was determined at 20h post-detachment.

2.7. Abscisic Acid assays

2.7.1. Germination

Seedlings were germinated *in vitro* as described in section 2.1.1, in ½ MS, 1% sucrose plates supplemented with 0, 0.25, 0.5 or 0.75µM of ABA. 20 to 50 seeds per genotype were sown in each plate, and the mutant lines were germinated along Col-0 lines in the same plate, as control. After stratification, plates were monitored for radicle emergence (3-4 days after stratification) and for cotyledon greening (7-10 days after stratification). Pictures of the plates were taken at each significant time point and the percentage of germination or cotyledon greening was calculated for each genotype and condition.

2.7.2. Root elongation assay

Seeds were germinated *in vitro* as described in section 2.1.1. 6 days after germination, seedlings were transferred to plates with ½ MS, 1% sucrose supplemented with 0, 2, 5, 10 or 30µM of ABA. 20 seedlings of Col-0 and 20 seedlings of the mutant lines were transferred to each plate and grown vertically for 12 days after germination. Pictures of plates were taken every day after transferring the seedlings into the plates with ABA, and root elongation was measured for each genotype, condition and time point using ImageJ as described in section 2.4.2. The growth rate in the treatment plates was calculated as a percentage of the root growth that took place in the control plates (no ABA).

2.7.3. Expression of ABA marker genes

Seedlings were grown for 10 days *in vitro* as described in section 2.1.1. On the 10th day, 10 seedlings per genotype were transferred to ½ MS 1% Sucrose plates (control) and ½ MS 1% Sucrose supplemented with 50μM of ABA (treatment). After 7h of incubation in the growth cabinet (Aralab, 10h light, 21°C and 60% humidity), 3 seedlings per genotype and condition were frozen in liquid nitrogen for further RNA extraction. Three replicates per sample were collected as technical replicates. RNA extraction and qPCR were performed as described in section 2.9.

2.7.4. Measuring ABA content

ABA content was analysed in plant extracts using high-performance liquid chromatography and electrospray-mass spectrometry (HPLC-ESI-MS/MS). The extraction and purification of ABA was carried out using the method described by (Bacaicoa et al., 2011). Hormones were quantified by HPLC-ESI-MS/MS using a HPLC device (2795 Alliance HT; Waters Co., Milford, MA) coupled to a 3200 Q TRAP LC/MS/MS System (Applied Biosystems/MDS Sciex, Ontario, Canada), equipped with an electrospray interface. A reverse-phase column (Synergi 4mm Hydro-RP 80A, 150x2 mm; Phenomenex, Torrance, CA) was used. The detection and quantification of ABA was carried out using multiple reaction monitoring (MRM) in the negative-ion mode, employing multilevel calibration curves with deuterated hormones as internal standards as described in (Bacaicoa et al., 2011). Data samples were processed using Analyst 1.4.2 Software from Applied Biosystems/MDS (Sciex, Ontario, Canada). Two T-DNA insertion mutants displaying ABA insensitivity were used as controls: *brm-3* (SALK_088462, (Farrona et al., 2007)) and *snrk2.2/2.3* mutants (Fujii et al., 2007). Plants were grown by Dr. Selena Gimenez-Ibanez and experimental procedures were carried out by Jose Maria García Mina and Dr. Ángel María Zamarreño.

2.8. Molecular Biology methods

2.8.1. Plant DNA extraction for genotyping

DNA from *Arabidopsis* was extracted from leaf issue (an amount of tissue equivalent to 0.5cm^2) with 100µL of 5% Chelex (Biorad). The samples were ground manually at room temperature. Samples were further mixed through vortex and then incubated at 95°C for five minutes in a thermocycler. To remove the tissue debris, the samples were spun at maximum speed on a benchtop centrifuge for five minutes. 30µL of the supernatant were collected and stored at 4°C for further DNA testing. 1µL of extracted DNA was used for PCR reactions.

2.8.2. Gateway cloning

For *in planta* expression of *HAG5,* the destination gateway vectors pEG202 (N-ter FLAG, 35S promoter) and pEG302 (C-ter FLAG, native promoter cloned with gene) were chosen (Earley et al., 2007). Both the *HAG5* genomic sequence with a native promoter and *HAG5* cDNA were cloned from plant genomic DNA and cDNA libraries, respectively. *HAG5 g*enomic DNA and cDNA were cloned in pDONR-Zeo® by Chrysa Sergaki, prior amplification using the primers from Table 2-3 and high fidelity Q5 DNA polymerase (NEB) to avoid PCR-induced mutations. A BP reaction was performed using pDONR-Zeo® as the target vector and BP clonase 2 enzyme mix (Invitrogen). Proteinase K treatment at 37ºC was used to eliminate protein from the sample before transforming pDONR-Zeo-*HAG5* into TOP10 *E. coli* cells, which were then selected in Zeocin. Positive clones were checked by colony PCR. After extracting plasmid DNA from positive clones, LR reactions were performed using 150ng of pEarleyGate® vectors 202 (for cDNA) and 302 (for gDNA), 150ng of pDONR-Zeo-*HAG5* vector and Gateway™ LR clonase™ II enzyme mix (Invitrogen, 11791020). Proteinase K treatment, transformation and colony PCR were performed as before with the difference that selection was made in Kanamycin (100µg/mL). Positive clones were sent for sequencing. pEG202-*HAG5* was used to transform *A. tumefaciens* GV3101.

For in plant expression of *ARIA* we selected the expression vector pEG104 (N-ter YFP, 35S promoter). *ARIA* in pDEST-DB was extracted from the transcription factor library in *E. coli*. A BP reaction was performed using pDONR-Zeo® as the target vector and Gateway™ BP clonase™ II enzyme mix (Invitrogen, 11789100). The resulting reaction was transformed into *E. coli* TOP10 competent cells and selected with Zeocin. Colony PCR (using primers VN943 and VN944) and plasmid miniprep isolation was performed from colonies expressing *ARIA*. A LR reaction was performed using Gateway™ LR clonase™ II enzyme mix, 150ng of pEarleyGate104 and 150ng of pDONR/zeo-*ARIA*. Proteinase K treatment, transformation and colony PCR (using primers VN943 and VN944) were performed as before using Kanamycin (100µg/mL) for selection. Plasmid was extracted, sequenced, and transformed into *A. tumefaciens* GV3101.

Table 2-3. Primers used for cloning and sequencing *HAG5* and *ARIA*. *attB1 and attB2* sites are in bold.

Code	Name	Sequence	Modification
VN340	PromHAG5-F	**AAAAAGCAGGCTCCACC**ACAAGATGACATTTCCATTAG	attB1
VN341	HAG5-FO	**AAAAAGCAGGCTCCACC**GGATCGTCAGCGAATACAG	attB1
VN342	HAG5-RC	**AGAAAGCTGGGTC**TTAACTCTGGTCCTTGTAAG	attB2
VN343	HAG5-RO	**AGAAAGCTGGGTC**ACTCTGGTCCTTGTAAGG	attB2
VN344	HAG5-R1	TTTCCCGTCTCTCCACC	-
VN345	HAG5-F1	AATGTATGTACTTCACACC	-
VN346	HAG5-F2	GACCTTGATTCAGTAGAG	-
VN347	HAG5-F3	GAAGTGTGACCTGAAGC	-
VN348	HAG5-F4	CTTACTAAGCTACAGAGG	-
VN943	ARIA_ex1_F	TTGCTGCTCAAGTCTCGGTA	-
VN944	ARIA_ex1_R	CGCTTCCCTTCTCAACTTCG	-

2.8.3. *E. coli* transformation

Electrocompetent TOP10 *E. coli* cells (Invitrogen, C66455) were thawed on ice for 30 mins. 2.5µL of plasmid was added to 50µL of thawed cells and incubated for 5 min on ice. The cells were transferred to an electroporation cuvette and electroporated using the Eco1 program (1800V, capacity 25µF and 200 Ω resistance) in a Micro Pulser Electroporator (Bio-Rad). Cells were re-suspended in 500µL of liquid LB, transferred to an Eppendorf tube and incubated for 1h at 37ºC shaking at 215 rpm. Cells were collected through centrifugation (5 min, 3200 rpm) using a microcentrifuge and re-suspended in 50µL of liquid LB. This volume of cells was then plated on LBA plates with the corresponding antibiotics and incubated overnight at 37ºC.

For chemically competent TOP10 *E. coli* cells, 50µL of thawed cells + 2.5µL of plasmid were subjected to heat shock by incubating for 30 seconds at 42ºC in a water bath, and placed on ice immediately after. The following steps are as described above after the electroporation step.

2.8.4. *A. tumefaciens* transformation

A. tumefaciens GV3101 competent cells were thawed, mixed with 1µg of plasmid and incubated on ice for 30 minutes. Cells were heat-shocked in liquid nitrogen for 5 minutes followed by an incubation at 37ºC for 5 minutes. Cells were incubated on ice for 5 minutes and subsequently resuspended in 1mL of LB. For recovery, the resuspended cells were incubated for 2.5h at 28ºC with shaking at 210 rpm. Colonies were plated on LBA plates with the appropriate antibiotics.

2.8.5. *A. tumefaciens* for *N. benthamiana* transient expression

Cells form overnight cultures were harvested by centrifugation at 3500 rpm and washed twice in Agro-infiltration buffer (10mM MES pH 5.6, 10mM $MgCl_2$). OD_{600} was adjusted to 0.4 for single or double construct infiltration. *N. benthamiana* leaves were infiltrated with the bacterial cultures using a 2mL syringe. Harvesting of leaf tissue occurred 3 days post-infiltration.

2.8.6. *E. coli* and *P. syringae* plasmid extraction

Overnight liquid cultures were harvested by centrifugation (10 min at 3000g). Plasmid purification was carried out using QIAprep® Spin Miniprep kit (Quiagen, 27104), according to manufacturer's instructions.

2.8.7. Colony PCR

Bacterial colonies were picked using a sterile pipette tip and diluted in 50µL of sterile H_2O, following a 95ºC incubation for 10 min to disrupt the bacterial cells. 1µL of the bacterial solution was added per PCR and procedures were carried out as described in section 2.8.8.

2.8.8. Polymerase chain reaction

DNA fragments from bacteria or plant material were amplified using the KAPA Taq PCR Kit (Sigma Aldrich, KK1014). The following components were added to the PCR reaction mixture: DNA template, 1x buffer, 100µM dNTPs, 500nM Forward primer (F), 500 nm reverse primer (R) and 0.05% KAPA Taq Polymerase) to a final volume of 20µl. Thermocycler programs were modified for specific primers from the version in Table 2-4, and PCR products were analysed by agarose gel electrophoresis as described in section 2.8.10.

2.8.9. Polymerase chain reaction for genotyping

Two PCR reactions were used per sample to amplify DNA fragments from T-DNA insertion lines. LP – RP primers, flanking the T-DNA insertion, in wild type plants produced a PCR fragment of 1000 ± 200 base pairs. LBb1.3 – RP primers in homozygous lines produced a band of an expected size of 500 ± 200 base pairs. Heterozygous lines produced bands in both PCR reactions. The primer sequences were obtained the primer design tool provided by the Salk institute, (http://signal.salk.edu/tdnaprimers.2.html). Primers were synthesised by IDT

Integrated DNA Technologies, Inc. (IDT), and can be found in Table 2-5. Conditions of the PCR reaction can be seen in Table 2-4.

Table 2-4. Thermocycler conditions of the polymerase chain reaction for genotyping.

Step	Temperature (ºC)	Time	Cycles
Initial denaturation	98	30 sec	1
Denaturation	98	10 sec	30
Annealing	55	20 sec	
Elongation	72	30 sec	
Final elongation	72	4 min	1
Cooling	4	Hold	

Table 2-5. Primers used for genotyping SALK lines.

Code	Name	Sequence	Amplicon size	Description
VN41	LBb1.3	ATTTTGCCGATTTCGGAAC	500 bp	Genotyping SALK lines
VN49	N655396-LP	ATGGTGTGCGAATCTATGACC	1062 bp	Genotyping *hag4-2* mutants
VN50	N655396-RP	ACGGAGAGGAAAGCTCAAGAC		Genotyping *hag4-2* mutants
VN51	N681550-LP	AGAATCAGCCACTTCAACACG	1127 bp	Genotyping *hag4-1* mutants
VN52	N681550-RP	GATTCTGAATTCGTGAGAGCG		Genotypig *hag4-1* mutants
VN53	N660075-LP	GTCGAAGAAGAGGAAAATGGG	1051 bp	Genotyping *hag5-2* mutants
VN54	N660075-RP	CATATGCCTTTGAAGCTGCTC		Genotyping *hag5-2* mutants
VN55	N659671-LP	CCAATTCCAATGATCCAATTG	1029 bp	Genotyping *hag5-1* mutants
VN56	N659671-RP	TTCACTCATGGATACTTCCGC		Genotyping *hag5-1* mutants

2.8.10. Gel electrophoresis

PCR products were separated by size through electrophoresis on 1-2% agarose (Sigma, A4718), 1 x TAE buffer (40mM Tris base, 1mM EDTA, 20mM acetic acid, pH 8.0) gels, with 1 x GelRed® (Biotium, 41001). The agarose gel was run between 10 to 40 min at 100 V, 500 A and imaged using a UV transilluminator (Gel Doc 1000, Bio-Rad).

2.9. RNA methods

2.9.1. RNA extraction using Trizol®

Plant tissue for RNA extraction was frozen in liquid nitrogen immediately after harvesting and kept at -80°C until processing. Plant tissue was ground in liquid nitrogen with a drill borer fitting a 2mL micro-centrifuge tube. Immediately after, 1mL of TRIzol® Reagent (Thermo Fisher Scientific, 15596026) was added to the powder, mixed well by vortexing, and incubated at room temperature for 5 min. 200µL of chloroform was added to the sample, mixed gently and incubated for another further 5 minutes at room temperature. Samples were spun at 12500g for 20 minutes at 4°C. The aqueous supernatant was carefully transferred to RNase-free microcentrifuge tubes (ThermoFisher, AM12400) avoiding carrying over contamination from the aqueous/organic interface. RNA was precipitated adding an equal volume of isopropanol, mixing gently and incubating for 3h at -20°C. Samples were spun at 16800g for 20 minutes at 4°C. The supernatant was removed and the RNA pellet was rinsed twice with 1mL 70% ethanol in DEPC water. Dried RNA pellets were re-suspended in 50µL nuclease-free water by incubating at 65°C for 5 minutes.

2.9.2. RNeasy® Mini kit for RNA extraction

Arabidopsis seedlings were stored in RNAse free tubes (3 seedlings per sample) and flash-frozen in liquid nitrogen. Samples were ground using a drill borer fitting a 2mL micro-centrifuge tube. RNA extraction was performed using RNeasy® Mini kit (Quiagen, 74104), following manufacturer instructions. RNA samples were treated with DNAse I as described in the following section. For quality control, RNA concentration was quantified using a NanoDrop ND-1000 (Thermo Fisher Scientific). Samples were then run in an Agilent 2100 Bioanalyzer System (Agilent Technologies) to check RNA purity and integrity.

2.9.3. DNAse treatment and RNA quality assessment

RNA samples were treated with TURBO™ DNase (Thermo Fisher, AM2238) following manufacturer's instructions. 5µL of buffer and 1µL of DNase enzyme were added to each RNA sample and incubated at 37°C for 30 minutes. Then, 5µL of the Inactivation Reagent were added, incubated at room temperature for 5 minutes and gently mixed by hand. After precipitating the inactivating resin by centrifugation at 10000g for 1.5 minutes, 35µL of clean RNA were transferred to a RNase-free tube. RNA quality was determined on a 1% agarose gel electrophoresis, and the concentration and purity were measured with a NanoDrop ND-1000 (Thermo Fisher Scientific). RNAs were stored at -20°C for short-term use and at -80°C for long-term storage.

2.9.4. Complementary DNA (cDNA) synthesis

For cDNA synthesis 2µg of RNA were reverse-transcribed with the SuperScript™ II Reverse Transcriptase (Thermo Fisher Scientific, 18064), following manufacturer's specifications and using a primer for polyA tails. Final cDNAs were diluted with 40µL nuclease-free water for a final volume of 60µL. cDNAs were stored at -20°C.

2.9.5. Quantitative PCR (qPCR) conditions

qPCR was performed with SYBR®green JumpStart™ Taq ReadyMix™ (Sigma, S4438), following manufacturer's recommendations. The mix conditions are specified in Table 2-6, and PCR conditions can be found in Table 2-7. The list of primers used for RT-PCR is displayed in Table 2-8, and the qPCR primers, in Table 2-9. Three technical replicates were used per sample. The thermocyclers used were the 384-well plate CFX384 Touch™ Real-Time PCR Detection System (Bio-Rad Laboratories), and a 96-well plate Mx3005P qPCR System (Agilent Technologies).

Table 2-6. Components used for qPCR with SYBR® Green JumpStart™ polymerase.

Component	Volume per triplicate	
	66 mL (96-well)	**30 mL (384-well)**
2 x JumpStart Taq ReadyMix	33 μL	15 μL
10 mM Forward primer	2.96 μL	1.35 μL
10 mLM Reverse primer	2.96 μL	1.35 μL
Template DNA	5 μL	2.3 μL
Water	22.66 μL	10 μL

Table 2-7. Thermocycling conditions used in qPCR reactions with SYBR® green JumpStart™ polymerase.

Step	Temperature	Time	Cycles
Initial denaturation	94 °C	2 minutes	1
Denaturation	94 °C	1 seconds	40
Annealing, elongation and fluorescence reading	60/62 °C	60 seconds	
Dissociation curve	40-98 °C	10 seconds/0.5 °C	1

Table 2-8. Primers used for RT-PCR in *hag5* mutants.

Code	Name	Sequence	Description
VN356	HAG5-P4-F	CCTTTAACTCCTGATCAAGCTAT	Forward RT-PCR primer for HAG5 to check *hag5* mutants (published as P4 by Latrasse et al. 2008. BMC Plant Biol)
VN357	HAG5-P5-R	CTACAGCGCACTCTACTGAATC	Reverse RT-PCR primer for HAG5 to check *hag5* mutants (published as P5 by Latrasse et al. 2008. BMC Plant Biol)
VN358	HAG5-P6-R	GACAGCCCGCTTTACTTACACA	Reverse RT-PCR primer for HAG5 to check *hag5* mutants (published as P6 by Latrasse et al. 2008. BMC Plant Biol) in 3'UTR

Table 2-9. Primers used for qPCR testing the expression of ABA marker genes.

Gene	name	Gene ID	Sequence
RAB18	RAB18 F	At5g66400	GGAACCGGGACCGGGACTGA
	RAB18 R		CCAGATCCGGAGCGGTGAAGC
RD29A	RD29A F	At5g52310	CCGGAATCTGACGGCCGTTTA
	RD29A R		CCGTCGGCACATTC TGTCGAT
RD29B	RD29B F	At5g52300	GCAAGCAGAAGAACCAATCA
	RD29B R		CTTTGGATGCTCCCTTCTCA
CYP707A2	CYP707A2 F	At2g29090	TCGGGGACAAAGAGGAGCCCA
	CYP707A2 R		GCCCGGTAGGTCGAGAGGCA
HAG5	HAG5-F	At5g09740	GTGATGTGTCGGTGGAGAGA
	HAG5-R		GCTTGTTACCTTGTCTTCCAC

Table 2-10.Primers used for testing expression levels of *HAG4* and *HAG5*

Code	Name	Sequence	Description
VN354	qHAG5-F	GTGATGTGTCGGTGGAGAGA	Forward qPCR primer for *HAG5* (published by Xiao et al. 2013. Journal Plant Physiol)
VN355	qHAG5-R	GCTTGTTACCTTGTCTTCCAC	Reverse qPCR primer for *HAG5* (published by Xiao et al. 2013. Journal Plant Physiol)
VN370	qHAG4-F	CCAGAATACAATGACTGCGTG	Forward qPCR primer for *HAG4* (published by Xiao et al. 2013. Journal Plant Physiol)
VN371	qHAG4-R	TCTTCTTGCCATCCACCTCA	Reverse qPCR primer for *HAG4* (published by Xiao et al. 2013. Journal Plant Physiol)
VN707	qaTUB_F	TACACCAACCTCAACCGCCT	Forward qPCR primer for *α-tubulin*
VN708	qaTUB_R	TGGGGCATAGGAGGAAAGCA	Reverse qPCR primer for *α-tubulin*

2.9.6. qPCR analysis

qPCR data was extracted for C_T values (theoretical cycle to overcome a threshold) accepting automatically calculated thresholds and imported into an excel file. Data was analysed with the $\Delta\Delta C_T$ method (Livak and Schmittgen, 2001). As controls, several genes with highly consistent expression levels at the studied conditions were used as a reference for the total messenger RNA concentration. *a-TUBULIN* (a-*TUB*) was used as housekeeping gene (Table 2-10). All qPCR primers

were tested for efficiency on a standard curve with at least 6 template concentrations diluted 10-fold, accepting only efficiencies between 90 and 100%.

2.10. Agilent microarray

flg22 elicitation, RNA extraction, amplification, labelling and hybridisation were performed by Dr. Sophie Piquerez, and will not be described in detail in this section. The microarray used was the Agilent Arabidopsis (V4) Gene Expression Microarrays (4x44K, G2519F-021169). The arrays were scanned using the NimbleGen MS200 scanner (NimbleGen, Roche) at 532 nm (Cy3). To align the array template to scanned images and to extract per probe intensity values, Agilent Feature Extraction Software (Agilent) was used.

2.10.1. Data normalisation and differential expression

Normalisation and pre-processing of the microarray data were carried out using the Bioconductor LIMMA (Linear Models for Microarray Data) software package (Ritchie et al., 2015) within the statistical and programming environment R (R Core Team, 2013). Microarray images were imported and background correction applied using the method "normexp". Normalisation was then carried out between arrays to correct for sampling differences and array performance. Filtering of the data was then carried out to remove probes lacking signal and overexposed probes, against predetermined spike-in controls. Samples were then assigned to groups and intra-group sample correlation checked as a quality control measure. Samples displaying unacceptable probe expression correlation with other group members were removed from further analysis (threshold of Correlation Coefficient ≤ 0.8). Groups were then fit with the linear model "lmFit" using a design of "~0+factor(groups)". Differential expression testing of contrasts between conditions was then carried out. Empirical Bayes statistical moderation ("eBayes") of gene expression test values was employed to improve accuracy of differential expression calling. A false discovery rate (FDR) corrected p-value threshold of 0.05 was used when determining the cut-off for gene differential expression along with a log2 fold-change value of 1 (corresponding to a two-fold up- or down-regulation). LIMMA analysis was carried out using standard parameters for all functions unless explicitly stated.

2.10.2. Venn diagrams, GO term enrichment and heatmap

Venn diagrams were produced using the R package "VennDiagram" (Chen and Boutros, 2011), using the lists of DEGs generated as described in the previous section. To identify over-represented Gene Ontology terms in the data, the topGO package v2.32.0 (Alexa and Rahnenfuhrer, 2007), using the "classic" algorithm and Fisher's exact test for enrichment scoring against the ontology "org.At.tair.db". Multiple-testing correction was carried out using Benjamini-Hochberg correction, and GO-terms were considered significant at a corrected p-value ≤ 0.01. Enrichment for a GOterm within the list of DEGs was calculated as the fold-change of the number of significant genes annotated to each term/number of significant genes annotated to GO term if the transcriptome was randomly sampled with the same number of genes.

The heatmap was generated pre-selecting the genes form the Abscisic acid signalling pathway GO term (GO:0009738) from the list of DEGs. The heatmap was generated using the function "pheatmap".

Unless explicitly stated, default parameters were used for all tools, and scripts used for these analyses can be provided upon request.

2.11. Chromatin immuno-precipitation (ChIP-seq)

Plant tissue (at least 100 seedlings per sample) untreated or treated with ABA (as described in section 2.7.3) was cross-linked and processed for chromatin immuno-precipitation (ChIP). Plant tissue was cross-linked by adding 25mL of cross-linking buffer (40mM sucrose, 1mM PMSF, 10mM Tris/HCl pH 8.00, 1mM EDTA and 1% formaldehyde) and vacuum-infiltrated for three rounds of 10 minutes under a fume hood. Excess of formaldehyde was quenched by the addition of 1mL of 2M glycine solution (freshly prepared) and vacuum-infiltrated for 5 more minutes. Cross-linked tissue was rinsed twice in sterile water and dried before freezing it in liquid nitrogen. Frozen tissue was stored at -80°C.

2.11.1. Nuclei extraction and chromatin sonication

Cross-linked tissue was thoroughly ground to fine powder in liquid nitrogen using a chilled pestle and mortar. Approximately 2g worth of powder were used for chromatin extraction. Nuclei extraction was performed in 20mL of Extraction buffer 1 (0.4 M sucrose, 210mM Tris-HCL pH.8, 10mM $MgCl_2$, 5mM β-mercaptoethanol, 0.2% Plant Protease Inhibitors (Serva)). Homogenised tissue was filtered through two layers of miracloth (Millipore), and nuclei were concentrated by centrifugation at 1500g for 15 minutes at 4°C. Iterative washes with Extraction buffer 2 (0.25 M sucrose, 10mM Tris-HCL pH. 8, 10mM $MgCl_2$, 1% Triton X-100, 5mM β-mercaptoethanol, and 0.2% Plant Protease Inhibitors (Serva)), and nuclei precipitation (spinning at 1500g for 10 minutes at 4°C) ensured chloroplast depletion. The pellet (nuclei) were resuspended in 1mL of Extraction buffer 3 (1.7 M Sucrose, 10mM Tris-HCL pH.8, 2mM $MgCl_2$, 0.15 % Triton X-100, 5mM β-mercaptoethanol, 0.2% Plant Protease Inhibitors (Serva)), and centrifuged (16000g, 4°C, 1h).

2.11.2. Covaris sonication

The pellets were resuspended in 1mL of Nuclei Lysis Buffer (50mM Tris-HCL pH.8, 10mM EDTA, 0.1% SDS, 0.2% Plant Protease Inhibitors (Serva)), transferred into a glass vial and sonicated (Peak power: 174 V, Duty factor 20, Cycles/Burst 200) for 17s at 4°C under vacuum conditions. Samples were transferred to 1.5 mL tubes and centrifuged for 5 min at 14000 rpm and 4°C.

2.11.3. Chromatin IP

10µL of sonicated chromatin per sample were kept as input. 100µL of sonicated samples were diluted with 900µL of cold ChIP dilution buffer (1.1% Triton X-100, 1.2mM EDTA, 16.7 M Tris-HCL pH 8.0, 16.7mM NaCl, 0.2% Plant Protease Inhibitors (Serva)). Antibodies were added to each sample (Table 2-11) and left rotating over night at 4°C. Dynabeads™ Protein A beads (ThermoFisher Scientific, 10002D) were added to each sample and incubated for 2h in the rotating wheel at 4°C. Beads were precipitated by centrifugation and separated using a magnetic rack. Beads

were washed two times with 1mL of Low Salt Wash Buffer (150mM NaCl, 0.1% SDS, 1% Triton X-100, 2mM EDTA, 20mM Tris-HCl pH8), 2 times with high Salt Wash Buffer (500mM NaCl, 0.1% SDS, 1% Triton X-100, 2mM EDTA, 20mM Tris-HCl pH8), 2 times with LiCl Wash Buffer (0,25M LiCl, 1% NP40 (Igepal, CA-630), 1mM EDTA, 10mM Tris-HCl pH8) and 2 times with TE buffer (1mM EDTA, 10mM Tris-HCL pH.8). Beads were eluted in 200µL of Elution Buffer (1% SDS, 0.1 M NaHCO3), vortexed and incubated 15 min at 65°C. This last step was performed twice until the eluted volume reached 400µL. Input samples were diluted 1:4 with Elution Buffer and treated in parallel.

Table 2-11. Antibodies used for ChIP-qPCR and ChIP-seq.

Target	Reference	V used for IP
Rabbit polyclonal to Histone H3	ab1791 Abcam	1 µL
Rabbit polyclonal to Histone H4K5ac	07-237 Sigma	2 µL

2.11.4. Chromatin purification

IP and input samples were reverse cross-linked with 5M NaCl at 65°C overnight and treated with RNaseA (Ambion cocktail, AM2271) for 20 min at 37°C. Proteinase K treatment was performed for 3h at 50°C. Phenol/Chloroform/IAA (pH8) was added to each sample prior centrifugation (1300rpm, 10 min at room temperature). Supernatant was removed and mixed with 3M NaAc pH5.5, 1µL of GlycoBlue™ (Invitrogen 15mg/ml, LSAM9515) and 100% EtOH for overnight precipitation at -20°C. Precipitated chromatin was washed with 70% EtOH and resuspended in 20µL of sterile water. Qubit™ 4 fluorometer (Invitrogen) and Qubit™ 4 IQ Assay Kit (Invitrogen) were used to quantify immunoprecipitated chromatin.

2.11.5. Library preparation

cDNA library preparation was performed using 10ng of DNA per sample and using NEBNext® Ultra DNA library prep Kit (NEB, E7370S), following instructions from manufacturer. Samples were then run in an Agilent 2100 Bioanalyzer System (Agilent Technologies) to check sample quality.

2.11.6. ChIP-seq data analysis

The bioinformatic analysis were performed by Dr. Lorenzo Concia. Raw FASTQ files were preprocessed with Trimmomatic v0.36 (Bolger et al., 2014) to remove Illumina sequencing adapters. 5′ and 3′ ends with quality score below 5 (Phred+33) were trimmed and reads shorter than 30 bp after trimming were discarded. The command line used is "trimmomatic-0.36 PE -phred33 ILLUMINACLIP:TruSeq3-SE.fa:2:30:10 LEADING:5 TRAILING:5 MINLEN:30". Trimmed FASTQ files were aligned to TAIR10 genome assembly with Bowtie2 v.2.3.3 (Langmead et al. 2012) with "--very-sensitive" pre-setting.

Differential peaks between the ABA-treated mutant and the ABA-treated wild-type were identified with diffReps (Shen et al. 2013) using the relevant untreated sample as background control. Furthermore, differential peaks between ABA-treated and untreated mutants were identified with diffReps (Shen et al. 2013) using the untreated and ABA-treated wild-type as background controls, respectively.

The genes overlapping with differential peaks were identified and bedtools v2.27.1 intersect (Quinlan et al. 2010) and Araport11 genome annotation. Normalized average values of the read densities were computed over 10 bp non-overlapping genomic bins with the tool bamCoverage v3.1.0 from the suite DeepTools2 (Ramírez et al. 2016). Spearman correlation between samples was calculated using the tool multiBigwigSummary and plotted as heatmap and scatter plots with the tool plotCorrelation from the same suite.

2.12. Biochemistry methods

2.12.1. Protein immunoprecipitation with nuclear enrichment

To extract nuclear proteins a nuclear enrichment protocol was followed. First, plant tissue was flash-frozen in liquid nitrogen and pulverised into a fine powder. Approximately 5g of infiltrated *N. benthamiana* leaves were used per sample. Grounded samples were resuspended in cold Honda Buffer containing 1.25% Ficoll (GE healthcare), 2.5% Dextran T40 (Sigma), 440mM sucrose, 0.5% TritonX-100 at a ratio 2:1, and filtered through two layers of Miracloth (Merck Millipore). Samples

were incubated in a rotating wheel at 4 ºC for 15 min. Samples were centrifugated at 3000g using a high-speed centrifuge for 30 min at 4˚C. Precipitated nuclei were resuspended in 1mL of Honda Buffer and transferred with a cut 1mL pipette tip to a low-protein binding tube (Thermo-Fisher). Samples were centrifuged at 1500g for 15 min at 4ºC in an Eppendorf bench-top centrifuge. This step was repeated until the nuclei were no longer green. Nuclei were burst using lysis buffer containing 1% TritonX-100, 10mM EDTA, 50mM Tris-HCl and sonicated (High power, 3x30sec ON, 60 sec OFF) to break the chromatin. Samples were centrifuged in a bench-top centrifuge at max speed for 30 min at 4ºC to break the nuclei. A small aliquot of the supernatant (10% of the sample) was kept as an input before the IP. Immunoprecipitation was performed on the lysate (supernatant) diluted 2 times in IP buffer (16.7mM Tris-HCl, 1.2mM EDTA, 167mM NaCl, 1.1% TritonX-100) for 4h at 4ºC in a rotating wheel after the addition of GFP-Trap agarose beads (ChromoTek) or FLAG beads (Merck) pre-washed with washing buffer (20mM Tris-CHL pH 8.0, 150mM NaCl, 2mM EDTA pH 8.0, 1mM PMSF). Beads were washed thoroughly with beads-washing buffer containing 1.1% TritonX-100 to remove non-specific binding. For anti-FLAG pull-down, proteins were eluted from beads using FLAG peptide (0.25mg/ml) The eluted protein sample was concentrated using Strataclean resin (Agilent, 400714). Input and IP samples (beads/resin) were resuspended in 1x SDS+DTT and incubated at 90ºC for 10 minutes. Samples were loaded on a 10% SDS-PAGE gel (120V, 40 min), transferred onto a PVDF membrane (30V over night at 4ºC) and blotted with the corresponding antibodies (Table 2-12). ICL™ Kit (Thermo Scientific) was used as a chemiluminescent method to visualise the western blot in an ImageQuant™ LAS 4000 biomolecular imager (GE Analytical Instruments).

Table 2-12. Antibodies used in this study.

Target	Antigen	Source	Concentration
Primary antibody			
α-GFP-HRP	GFP/YFP tag	Santa Cruz Biotechnology	1:10000
α-FLAG (Mouse)	FLAG tag	Merck	1:2000
Secondary antibody			
α-mouse-HRP	Mouse IgG	Merck	1:10000
Affinity matrix			
GFP trap	GFP/YFP tag	ChromoTek	
FLAG beads	FLAG tag	Merck	

2.13. Histone acetyltransferase activity assay

6xHis-Tagged *HAG5* and *ARIA* cDNA were transiently expressed in *E. coli* Rosetta cells, and purified by Dr. Veselina Uzunova (methodology not described). A fluorescence-based HAT activity kit was purchased from Active Motif (81158). Controls without substrate and Acetyl-CoA were included to account for background activity. The reaction was performed at room temperature for 20 min in the dark. The reaction was stopped by addition of STOP solution, followed by developed solution. The resulting fluorescence was measured at an excitation wavelength of 360nm and emission at 465nm using a plate reader (TECAN) after preparing each reaction in triplicate wells in a 96-well plate.

2.14. Yeast Two-Hybrid assay

2.14.1. Yeast transformation

This experiment required *S. cerevisiae* strain Y8930 transformed with *HAG4* and *HAG5* (sub-cloned in yeast 2-hybrid vector pDEST-DB). Transformation was performed by first suspending pelleted yeast culture (3mL grown overnight at 28°C with shaking) in 0.1M LiAc in a 1.5mL Eppendorf tube, spinning at 2500rpm for 5 min at room temperature and then resuspending again in 20mL of 0.1M LiAc. To this, was added 30mL 1M LiAc, 40mL 2mg/ml ssDNA, 10mL sterile ddH_2O and ~200ng of miniprepped *HAG4* or *HAG5* plasmids. The tube contents were inverted following

addition of 200mL of PEG 4000 (fresh and filter sterilised) then incubated for 1hour at 42°C in a water bath.

2.15. Y2H screening of interactors

The yeast two-hybrid (Y2H) assay was performed to test protein interactions using the pDEST-DB/pDEST-AD Y2H system (Dreze et al., 2010), where prey constructs *HAG4* and *HAG5* and empty vector control pDEST-DB were transformed into strain Y8930, with the transcription factor library having previously been cloned into strain Y8800 as bait constructs. Prey constructs were +Leucine, while bait constructs were +Tryptophan, with interactions permitting the synthesis of histidine, such that successfully mated yeast with both a bait and prey construct might grow on -LeuTrp but would only grow on -LeuTrpHis if the proteins encoded by bait and prey constructs interacted in yeast. The competitive inhibitor of the HIS3 enzyme 3-amino 1,2,4 triazole (3AT) was also used as a supplement to test the strength of positive interactions. All yeast cultures were grown in Synthetic Complete (SC) media (6.8g Yeast Nitrogen Base, 20g ammonium sulphate, 40g glucose, 5.2 amino acid drop out mix, ddH_2O to 1L, adjusted to pH 5.9 with 1M NaOH) lacking the appropriate amino acids to select for constructs of interest at 28°C for 2 days with shaking. Matted strains with both the bait and prey interaction pair to be tested were grown in -Leu-Trp and then spotted onto selective solid media plates using 1mL inoculation loops.

2.16. Screening of HAG5 inhibitors

2.16.1. Root meristem inhibition assays

Arabidopsis seedlings were grown vertically *in vitro* as described in section 1.1.1. 5 days after stratification, the seedlings were transferred to ½ MS 1% sucrose plates supplemented with DMSO (10mg/mL) or 2µM of inhibitor (see Table 2-13). The seedlings were then incubated vertically overnight and the root tips imaged as described in section 2.4.3.

Table 2-13. HAG5 inhibitor candidates from the ChemBridge library used in this study.

Name	Compound name
A	N-(4-{[5-(3-nitrophenyl)-2-furoyl]amino}phenyl)-1-benzofuran-2-carboxamide
B	3-(butyrylamino)-N-[1-(3-hydroxybenzyl)piperidin-3-yl]benzamide
C	2-[4-allyl-5-({2-[(4-methyl-3-nitrophenyl)amino]-2-oxoethyl}thio)-4H-1,2,4-triazol-3-yl]-N-(2-methylphenyl)acetamide
D	N-(2-methoxyethyl)-1-[1-(3-phenylpropanoyl)-4-piperidinyl]-1H-1,2,3-triazole-4-carboxamide
E	N,N'-(1,4-piperazinediyldi-3,1-propanediyl)bis(3-methylbenzamide)
F	2-[({5-[1-(5-methoxy-2-furoyl)piperidin-4-yl]-4-methyl-4H-1,2,4-triazol-3-yl}methyl)(methyl)amino]ethanol
G	N-{3-[4-({[3-(3,5-Dimethyl-1H-pyrazol-1-yl)propanoyl]amino}methyl)-5-methyl-1,3-oxazol-2-yl]phenyl}-2,5-dimethyl-3-furamide

Chapter 3 HAG5 is a negative regulator of growth and immunity

3.1. Context of this chapter

3.1.1. Transcriptional regulation of PTI in plants

A major common part of the immune response is the reprogramming of gene expression. Both PTI and ETI significantly alter the expression of approximately 10% of the plant genome, enabling the activation of several cellular responses (Zipfel et al., 2004). Early responses are highly coordinated between different elicitors, but later transcriptional changes tend to diverge and be more specialised (Denoux et al., 2008). These common and early changes in transcription are mainly directed to the production of antimicrobial compounds.

Upon pathogen perception through microbe-associated molecular pattern (MAMPs) recognition, two signalling modules get activated: mitogen-activated protein kinases (MAPKs) and calcium-dependent protein kinases (CDPKs) (Figure 3.1). MAPKs and CDPKs transduce early MTI signals into the subsequent intracellular transcriptional reprogramming machinery (Tena et al., 2011). Figure 3.1 illustrates plant MTI signalling and its outputs, regulated by transcription (Li et al., 2016b). MTI activation results in callose deposition, stomatal closure as well as production of ethylene (ET) and antimicrobial compounds (Macho and Zipfel, 2014). All of these events constitute the plant coordinated effort to restrict pathogen growth and fight infection.

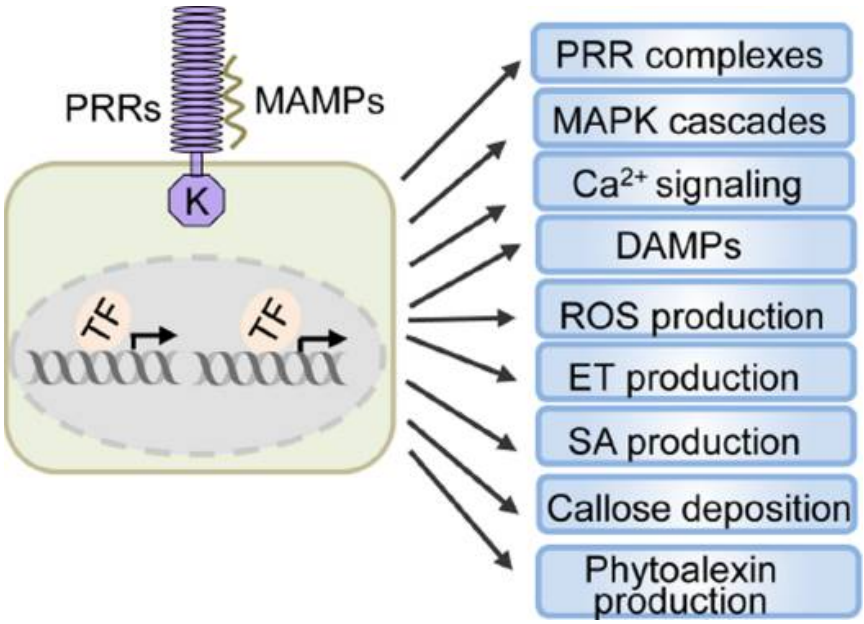

Figure 3.1. Perception of different MAMPs by PRRs controls various PTI responses via transcriptional regulation. TF: transcription factor. Figure from (Li et al., 2016a).

In recent years, and due to the affordability and advancing of sequencing techniques, there has been an increase in the generation and publishing of transcriptomic data. This phenomenon has allowed the combination of multiple microarray and RNA-seq data to generate comprehensive studies looking at the common and distinct transcriptional changes in *Arabidopsis thaliana* at different developmental stages and under an array of pathogen and elicitor treatments. One example of this integrative studies is the one published by Lewis et al., in which the authors characterised the transcriptional changes over the infection course with *Pseudomonas syringae* DC3000. One of their findings is that the genes induced within the first two hours of infection are related to salicylic acid (SA) biosynthesis and the transient production of ROS, whereas the expression of nuclear encoded chloroplast-targeted genes (NECGs), associated with photosynthesis-related processes, are significantly suppressed. These results suggest that plants might reduce their photosynthetic activity to restrict the resources needed by the pathogens as an additional defence mechanism (Lewis et al., 2015). Another interesting finding of this study is that genes associated with chromatin remodelling were down-regulated in the presence of effector proteins, implying that pathogens attack the epigenetic machinery to increase their virulence. Upon activation of immunity, there are complex networks

that consist of positive and negative feedback loops that result in signal amplification and tight regulation of defence responses. Gene transcription and its regulation are tightly controlled in order to maintain homeostasis, and undergo changes after stress. In the following section we will revise the epigenetic regulation of gene expression in the context of plant immunity.

3.1.2. Histone acetylation in defence responses

As sessile organisms, plants rely on this highly dynamic mechanism to fine-tune gene expression under certain environmental or developmental conditions. Previous studies have focused on the epigenetic regulation of defence-related genes, and the organisation and initiation of a fast and appropriate immune response. For instance, Ding et al., showed that mutating genes involved in histone modifications and chromatin remodelling in Arabidopsis and rice lines results in altered resistance levels to diverse microbial pathogens (Ding and Wang, 2015). From all the different histone modifications, this chapter will be focused particularly on the study of histone acetylation and its role in maintaining plant homeostasis and regulating plant immunity.

All core histones can be acetylated and deacetylated in different positions, normally in Lysine residues located primarily on N-terminal tails, resulting in 26 putative acetylation sites per nucleosome (Lusser et al., 2001). In general, acetylation results in a looser chromatin state, allowing the transcriptional machinery to access the DNA, whilst de-acetylation results in tighter chromatin, less likely to undergo active transcription (Berger, 2007). Histone lysine acetylation is regulated by histone acetyltransferases (HATs) and histone deacetylases (HDACs). The antagonistic activity of these enzymes is responsible for the acetylation state of the chromatin throughout the genome. Each eukaryotic genome encodes several of these enzymes, and their expression dynamics and specificity vary significantly.

There are several studies describing the role of HATs and HDACs in plant immunity. One of the most studied histone modifiers is HDA19, which is involved in the defence response against the necrotrophic pathogen *Alternaria brassicicola* by regulating the expression of jasmonic acid (JA) and ethylene signalling pathways (Zhou et al., 2005). In addition, HDA19 interacts with two WRKY transcription

factors (WRKY38 and WRKY62), involved in resistance to *Pseudomonas syringae* (Kim et al., 2008b). These transcription factors are induced by salicylic acid (SA) in a NPR1 (Nonexpressor of PR Gene 1) dependent way, or by virulent *Pseudomonas syringae*, and are negative regulators of plant basal defence (Kim et al., 2008b). HDA19 negatively regulates de expression of both TFs, conferring increased resistance to the pathogen and fine-tuning defence responses. Moreover, HDA19 has been reported to modulate H3 acetylation at *PR1* and *PR2* loci in salicylic acid (SA) mediated defence responses (Choi et al., 2012).

Similar to *HDA19*, *HDA6* expression is induced by JA and ACC (1-aminocyclopropane-1-carboxylic acid), and is important for the repression of defence genes involved in the SA pathway (Wu et al., 2008). In fact, HDA6 is involved in the JA-pathway, and *hda6* mutants display increased resistance to *Pto* DC3000. Another negative regulator of immunity is the Arabidopsis orthologue of the yeast *Sir2* (silent information regulator 2) deacetylase, *SRT2*. Sir2 proteins are NAD^+-dependent histone deacetylases, which can deacetylate histone and non-histone substrates. Arabidopsis *srt2* mutants are more resistant to *Pto* DC3000 and overexpress genes involved in the SA-defence pathway, such as *pathogenesis-related gene 1* (*PR1*) (Wang et al., 2010). By contrast, HD2B, which gets activated by MAPKs, is a positive regulator of Arabidopsis innate immunity through reprogramming of defence gene expression upon pathogen detection (Latrasse et al., 2017). Contrary to the described HDACs, the Arabidopsis histone acetyltransferase HAC1 is a positive regulator of plant responses to stress. In wild type plants, priming with *Pto* DC3000 *hrcC* treatment results in an enrichment of histone marks associated with activation of transcription (H3K9ac, H3K14ac, H3K4me2 and H3K4me3), but *hac-1* mutants do not undergo the enrichment of such marks after priming (Singh et al., 2014). These results show that HAC1, even though is not directly involved in response to biotic stress, is required for the priming of PTI-responsive genes.

All these studies evidence that the regulation of histone acetylation plays a key role in modulating plant responses to pathogens. Nonetheless, it remains to be fully elucidated how HAT and HDACs are targeted to the proper loci to allow genome-wide changes in a specific manner. Consequently, one of the milestones of this thesis is to further investigate the role of histone acetyltransferases and the molecular mechanisms by which they regulate plant immunity.

3.1.3. Screening of Arabidopsis HAT mutants for immunity phenotypes

Histone acetyltransferases (HATs) are involved in various biological processes through transcriptional regulation of numerous genes. In mammals, CREB-binding (CBP)/p300 proteins intervene in several physiological events including cell proliferation, differentiation and apoptosis (Goodman and Smolik, 2000). In plants, histone acetyltransferases influence responses to environmental conditions and gene interactions (Boycheva et al., 2014).

The Arabidopsis genome encodes 12 HATs (Figure 3.2a) classified in different subfamilies (Ritu Pandey, 2002).

In order to identify candidates that regulate responses to pathogens amongst the HATs, previous members of the Ntoukakis lab followed a reverse genetics approach to investigate the response of *Arabidopsis hat* mutant lines to the hemibiotrophic pathogen *P. syringae* DC3000, which has been defined as a model pathogen in section 1.2 of Chapter 1. Nine homozygous T-DNA insertion lines from the 12 *Arabidopsis* HATs were obtained from the Nottingham Arabidopsis Stock Centre (NASC) (Alonso et al., 2003) and tested for their immunity phenotypes.

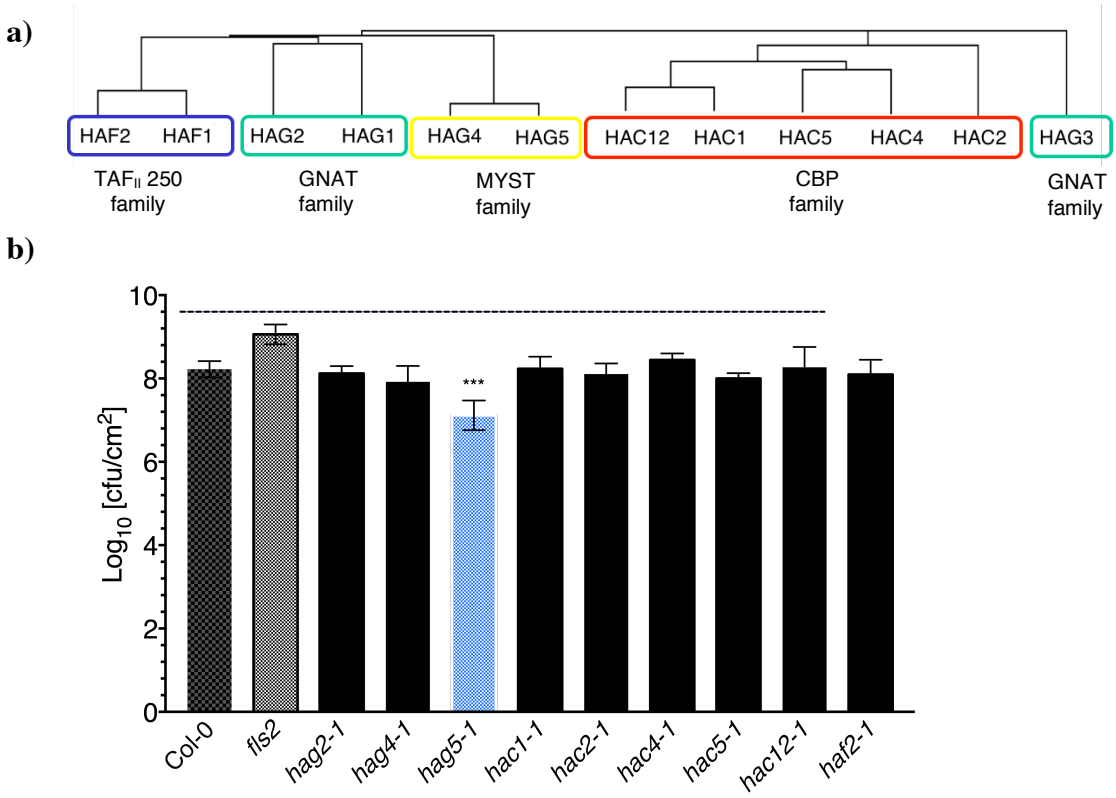

Figure 3.2. Screening of histone acetyltransferases for immunity phenotypes. **a)** Phylogenetic classification of Arabidopsis histone acetyltransferases. The phylogenetic tree was constructed after multiple sequence alignment of all HAT amino acid sequences using Clustal Omega (Sievers et al., 2011) with neighbour joining clustering. **b)** *hag5-1* mutants are more tolerant to Pto DC3000. *fls2* was included as a susceptible control. 5-week-old plants were sprayed inoculated with *Pseudomonas syringae pv. tomato* DC3000 (OD_{600} = 0.01). Samples were collected 3 days post-inoculation. Statistical significance versus Col-0 was determined by two-tailed t-test, n = 6, *** $P \leq 0.001$. Error bars indicate standard error. Genotyping for homozygosity was performed by Ntiana Mamafidou (an Erasmus student) and the bacterial growth assay was performed by Sophie Piquerez (a post-doctoral research assistant) and Dr. Stephanie Kancy (a previous PhD student).

These lines were spray-inoculated with *P. syringae* DC3000 and the bacterial growth was assessed three days post-inoculation (dpi) (Figure 3.2b). The *fls2* mutant was included as an experimental control, since it has been previously reported that the lack of the FLS2 receptor results in increased susceptibility (Zipfel et al., 2004). The bacterial growth is quantified as the colony forming units (CFU) of bacteria per cm^2 of leaf. When challenged with *P. syringae* DC3000, 8 out of the 9 mutants had a very similar response to Col-0, with a bacterial growth of $\log_{10}(CFU/cm^2) = 8$. However, this assay revealed that *hag5-1* is more tolerant to the bacterial pathogen, with a

decreased bacterial growth after three dpi. These results highlight HAG5 as an interesting HAT with a potential role in plant defence.

Activation of immunity often comes with a severe developmental trade-off assumed to be necessary in order to prioritize defence over growth-related cellular functions (Huot et al., 2014a). Throughout this chapter the different phenotypes of *hag5* mutants will be investigated in order to elucidate the mechanisms that are regulated or affected by HAG5, hoping to achieve a better understanding of how HATs modulate stress responses and plant development.

3.1.4. HAG5 is a MYST histone acetyltransferase

HAG5 belongs to the MYST family of HATs (Ritu Pandey, 2002), and shares 87.9% identity to its paralogue *HAG4* (Delarue et al., 2008) (Figure 3.3). According to Wolfe data (http://wolfe.gen.tcd.ie/), *HAG4* (At5g64610) and *HAG5* (At5g09740) occurred from a duplication event that took place during polyploidization on its Brassicaceae ancestor. Hence, they are believed to have redundant functions in Arabidopsis, since mutating both genes results in a lethal phenotype due to defects in gametophyte formation (Delarue et al., 2008). Furthermore, HAG4 and HAG5 are thought to work redundantly acetylating Histone 4 lysine 5 (H4K5Ac) *in vitro* (Earley et al., 2007). Previous studies have shown that HAG4 and HAG5 are involved in the regulation of flowering time through epigenetic modification of the H4K5Ac status within the chromatin of *FLC* and *MADS*- box genes, affecting flowering genes 3/4 (*MAF3/4*) (Xiaoa et al., 2013). Moreover, HAG4 and HAG5 are also involved in DNA damage repair, since the single *hag4* and *hag5* mutants showed increased DNA damage after Ultraviolet-B radiation stress (Casati et al., 2008, Campi et al., 2012).

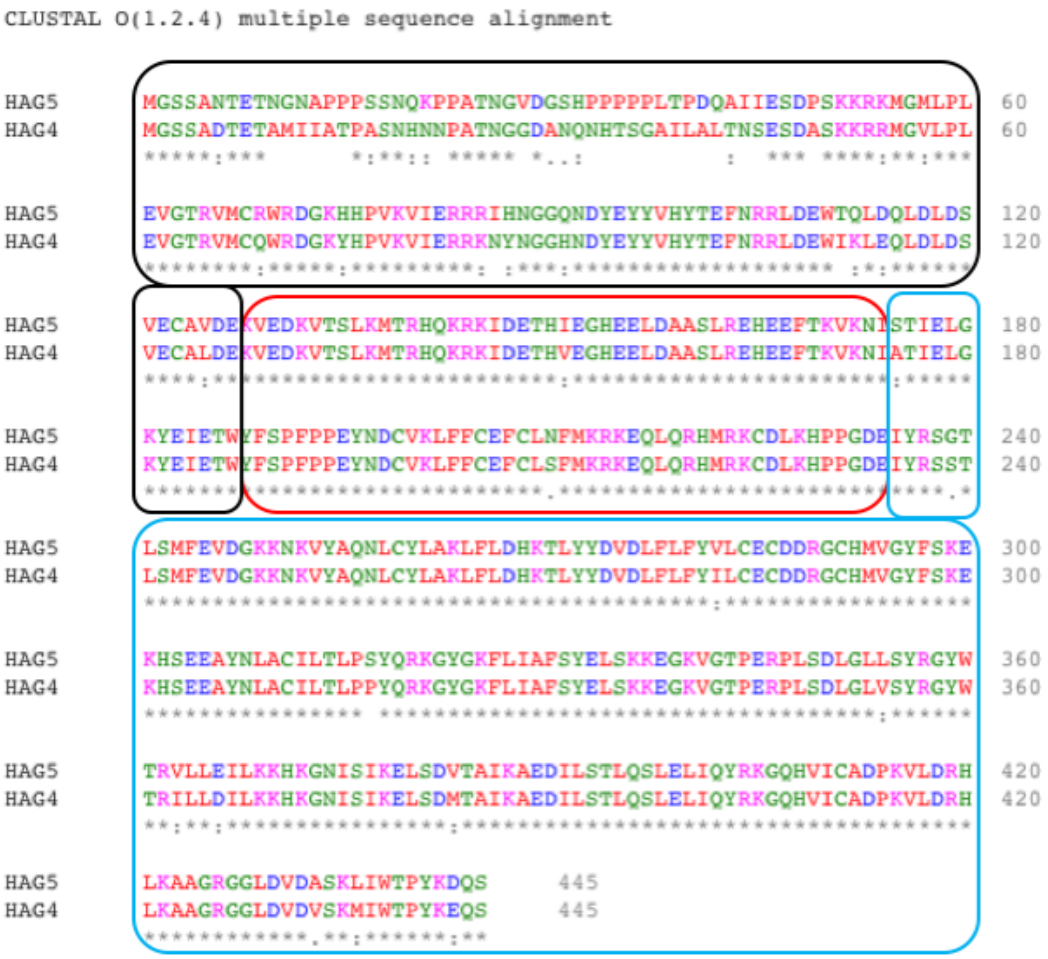

Figure 3.3. Protein sequence alignment of Arabidopsis HAG4 and HAG5 using Clustal Omega (version 1.2.4). The same colouring for aligned residues indicates conservation of amino acid chemical properties. (ClustalX colouring, blue: hydrophobic, red: positively charged, magenta: negative charged, green: polar, cyan: aromatic, pink: cysteine, yellow: proline, orange: glycine).The black box represents the Chromodomain/TUDOR domain, the red box the linker domain and the blue box, the acetyltransferase catalytic domain.

Recent findings show that HAG4 and HAG5 are part of the PEAT complex, composed of PWWP domain-containing proteins, EPCR (Enhancer of polycomb related) proteins, ARID (AT-rich interaction domain-containing) proteins, and TRB (telomere repeat binding) proteins, as well as HDA6 and HDA9 histone deacetylases. This repressor complex is recruited to individual loci, and is involved in heterochromatin formation and gene repression through modulation of siRNAs and DNA methylation. It is hypothesised that the PEAT complex also has a locus-specific

activating role, possibly related to the histone acetyltransferase activity of HAG4 and HAG5 (Lian-Mei Tan et al., 2018).

In yeast and animals, the MYST-type histone acetyltransferases act as catalytic subunits of conserved NuA4/Tip60-type histone acetyltransferase complexes (Doyon and Cote, 2004), known to primarily acetylate H4 and H2A N-terminal tails. In mammals, this highly conserved complex is involved in a wide range of cellular functions, such as transcriptional activation and silencing, apoptosis, cell cycle progression, DNA replication or DNA repair linked to pathological disorders like cancer (Squatrito et al., 2006). Tip60 (*KAT5*) and hMOF (*KAT8*), orthologues of the *Arabidopsis HAG5*, directly acetylate the transcription factor p53 at lysine 120 (K120), within its DNA binding domain. p53 is a transcription factor that regulates gene expression to induce cell cycle arrest and apoptosis (Vousden and Lane, 2007). The acetylation of p53 by Tip60 modulates its activity, triggering apoptosis induced by severe DNA damage (Wang et al., 2018). This fact is crucial, since we will further speculate with the idea that HAG5 might acetylate transcription factors *in vivo* in order to regulate their activity.

3.2. HAG5 is a negative regulator of growth

In order to understand the role of HAG5 in plant growth and immunity, T-DNA insertion mutants from the SALK institute (NASC, http://arabidopsis.org.uk/) were selected for further characterisation. These lines have a sequence of T-DNA (transfer DNA) from *Agrobacterium tumefaciens* disrupting a genomic region of interest, as displayed in (Figure 3.4). These disruptions often cause changes in gene expression when located in regulatory or intergenic regions (reference). We considered that having two allelic mutants was necessary in order to discard any observed phenotypes being a product of the T-DNA insertion itself.

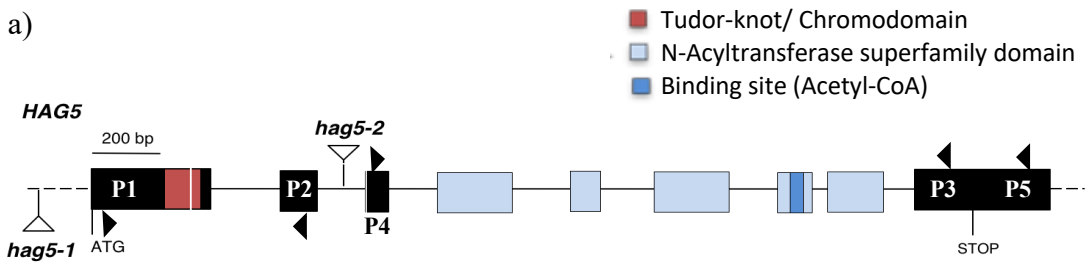

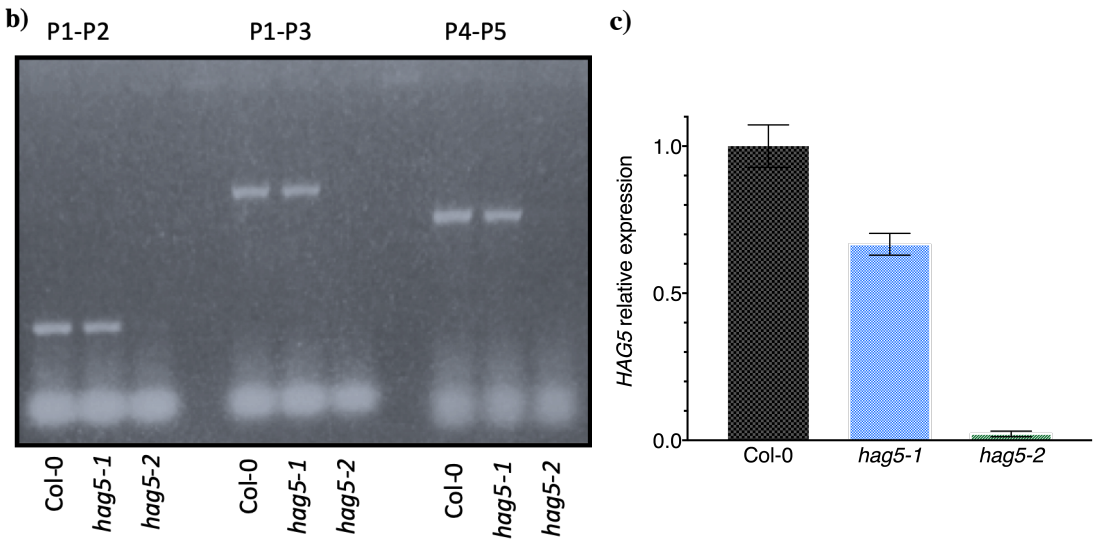

Figure 3.3. Schematic representation of *hag5* mutants**. a)** Diagram of *HAG5* genomic DNA showing T-DNA insertion positions of both SALK lines. Boxes indicate position of exons, lines indicate introns and untranslated regions. Triangles represent primers used in section b. **b)** PCR electrophoresis showing amplicons of three different regions of *HAG5* cDNA in Col-0, *hag5-1* and *hag5-2* mutants. cDNA was reverse-transcribed from RNA extracted form 14 day old seedlings (n = 3 seedlings per genotype). **c)** Relative expression of *HAG5* in Col-0, *hag5-1* and *hag5-2* in 4-weeks-old plants in basal conditions was determined by qPCR using gene-specific primers. Gene expression was normalised against the housekeeping gene *TIP41*. Error bars represent SD between technical replicates (n = 3).

The mutant line named as *hag5-1* (SALK_012086C) has an insertion in the promoter region, and the *hag5-2* line (SALK_106046C), within the gene body (Figure 3.4a). As determined by qPCR assays, the expression of *HAG5* is downregulated in the *hag5-1* mutant, which indeed displays 75% of the *HAG5* expression level found in Col-0. The *hag5-2* mutant is a knock out, since *HAG5* mRNA levels were not detected by qPCR (Figure 3.4c). When checking the presence of different *HAG5* cDNA fragments through PCR, *hag5-2* mutants did not show amplification of any of the different gene fragments, suggesting that the T-DNA insertion might have cause a truncation that results in no mRNA synthesis of *HAG5* (Figure 3.4b).

Since *HAG5* is a paralogue of *HAG4*, two T-DNA insertion lines for this gene were acquired in order to investigate the redundancy or specialisation between both genes. *hag4-1* (SALK_103726) is a knock-down T-DNA insertion mutant with the insertion in the promoter, whilst *hag4-2* (SALK_027726) is a loss-of-function mutant with a T-DNA insertion in the first exon (Figure 3.5a).

The expression level of *HAG4* in *hag4-1* is 60% of the HAG4 expression level found in Col-0 whilst the expression of *hag4-2* is less than 10% (Figure 3.5b)

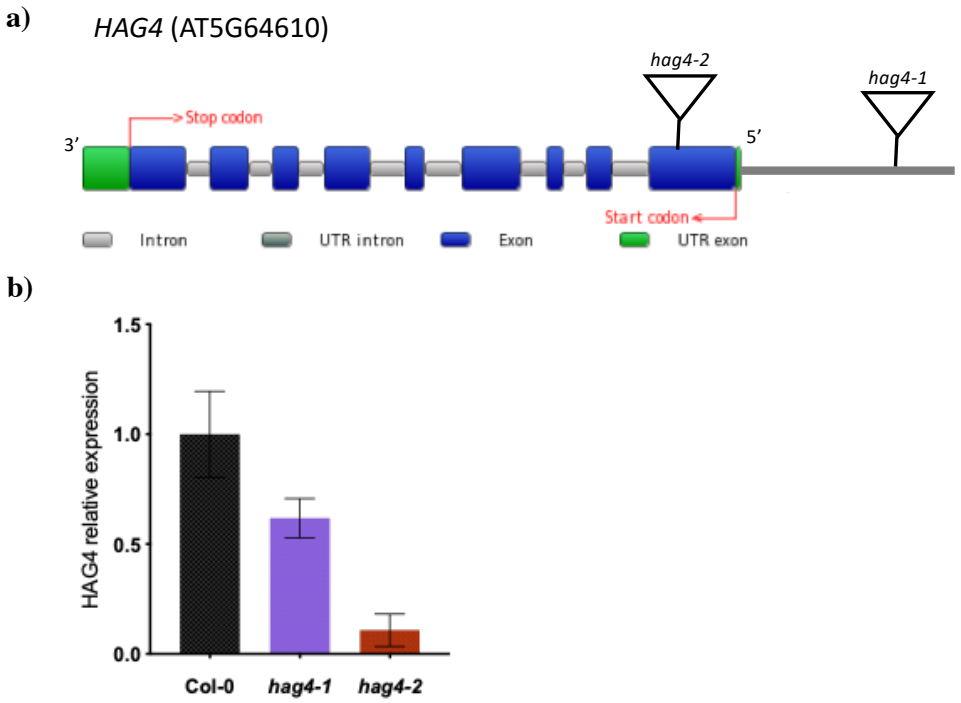

Figure 3.4. Schematic representations of *hag4* mutants. **a)** Diagram of the location of the T-DNA insertions in *hag4-1* (SALK_103726C) and *hag4-2* (SALK_027726C) mutants. **b)** Expression of *HAG4* in Col-0, *hag4-1* and *hag4-2* seedlings in basal conditions (14 day old seedlings grown in ½ MS plates). The primers used can be found in section 2.8.9 of Chapter 2. Gene expression was normalised against the housekeeping gene α*Tubulin*. Error bars correspond to SD (n = 3).

Even though *hag5* mutants were previously reported to have no obvious phenotypes when compared to Col-0 (Delarue et al., 2008), developmental differences were found in seedlings (10-15 day old) and adult plants (5-weeks-old) grown under short-day photoperiod (Figure 3.6a). As seen in Figure 3.6a, b, *hag5* mutants have increased leaf surface area. This data was obtained by taking pictures of 24 5-weeks old rosettes of each genotype and measuring the leaf area using ImageJ (https://imagej.nih.gov/ij/). In addition, we characterised the phenotype of Col-0 and *hag5-2* seedlings. To determine if there were phenotypic differences, seedlings were grown vertically in ½ MS plates for 14 days and root length was measured using ImageJ. The results in Figure 3.6c, d show that *hag5-2* mutants have longer primary roots when compared to Col-0.

The architecture of Arabidopsis primary root consists of cell files arranged as concentric circles, with the quiescent centre (QC) located at the inner site of the root apex. The primary root is divided into three developmental zones along its longitudinal axis. In the zone closest to the QC, known as the meristem (MZ), cells divide prior to expansion. In the next developmental zone, the elongation zone (EZ), cells elongate and gradually differentiate without further cell division. The third zone, the differentiation zone (DZ), consists of mature, terminally differentiated, cells that no longer elongate (Dolan et al., 1993). As a consequence, an increase in root length like the one displayed by *hag5-2* mutants can be due to the expansion of cells in the elongation zone (EZ), or the increase in number of dividing cells in the cortical meristem (MZ) (Beemster and Baskin, 1998). To investigate if the root phenotype of *hag5* mutants was due to any of these phenomena, we imaged the root tips of 4 to 6 day old seedlings using confocal microscopy and propidium iodide to stain the cell walls. As seen in Figure 3.6d-e, both *hag5* lines have an increased number of dividing cortical cells in the root meristem, arising from the quiescent centre. From these results it can be hypothesized that HAG5 has a role in plant development and acts as a negative regulator of leaf area and root growth, which highlights this enzyme as a promising candidate for improving crop performance.

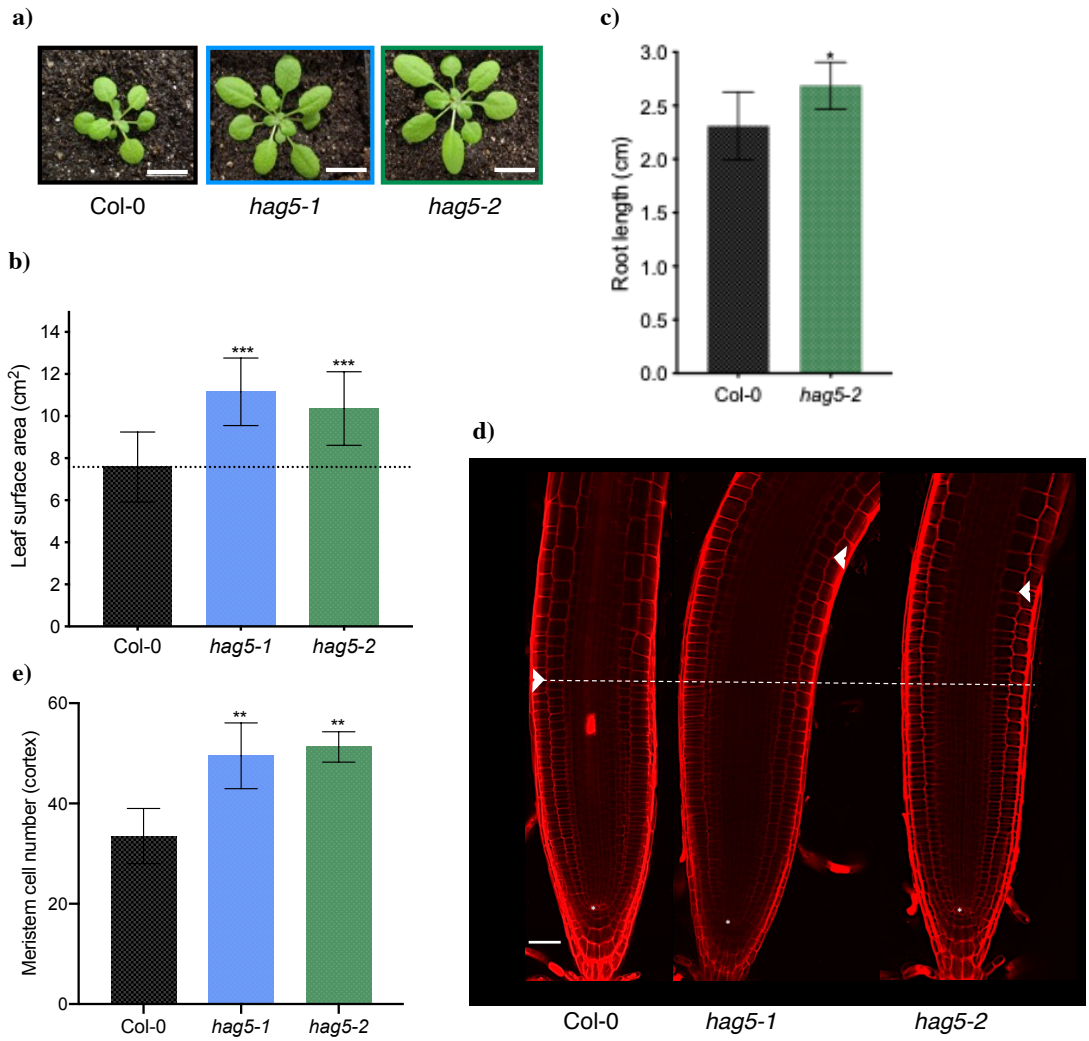

Figure 3.5. hag5 mutants have increased leaf surface area, longer primary roots and increased root meristem. a) Representative pictures of the rosettes of 5-week-old Col-0, *hag5-1* and *hag5-2* mutants grown under short-day photoperiod. Scale bars represent 1.5 cm. b) Leaf surface area of Col-0 and *hag5* mutants. Pictures of fully expanded rosettes in 5-weeks-old plants were taken for analysis using ImageJ (https://imagej.net). Error bars indicate SD (n = 24). Statistical differences between *hag5* mutants and Col-0 were obtained using one-way ANOVA, *** $P \leq 0.0001$. c) Root length of 14 day old Col-0 and hag5-2 seedlings measured using ImageJ. Error bars represent SD (n = 40). Statistical differences were calculated using two-tailed t-test (*$P \leq 0.05$, n = 50). d) Confocal images of the meristem of Col-0, *hag5-1* and *hag5-2* roots. Roots of 4 day old seedlings were treated with Propidium Iodide (10µg/µL) and imaged using a confocal microscope Leica TSC SP5. White arrows indicate the transition zone from the dividing cortical cells to the elongating meristem, and the white line indicates meristem size of Col-0 roots. e) Meristem cell number of Col-0, *hag5-1* and *hag5-2* roots. Meristem cell number was calculated as the number of cortical cells from the quiescent centre to the first expanding cortical cell. Error bars indicate SD (n=10). Statistical testing: one-way ANOVA, **$P \leq 0.0002$.

3.3. HAG5 is a negative regulator of innate immunity

After studying the developmental phenotypes of *hag5* mutants, we decided to further characterise their response to biotic stress through different pathogenesis assays. To this end, bacterial growth assays were repeated to confirm the results of the *P. syringae* DC3000 screening described above (Figure 3.2b). As previously observed, *hag5-1* and *hag5-2* mutants displayed increased tolerance to *P. syringae* DC3000 (Figure 3.7a) after 3 dpi.

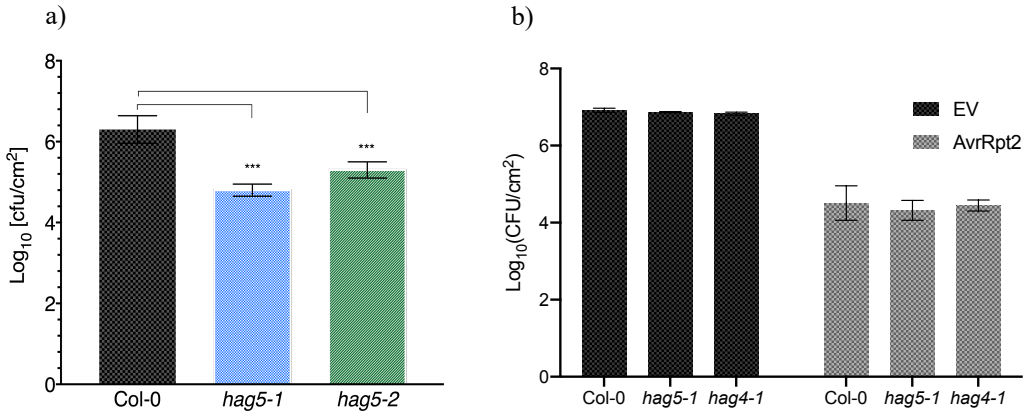

Figure 3.6. *hag5* mutants are more resistant to infection with Pseudomonas through spraying. **a)** 5-week-old plants were sprayed with OD_{600} = 0.01 solution of *Pseudomonas syringae* DC3000. Differences from Col-0 were calculated using One-way ANOVA, *** P < 0.05. **b)** Col-0, *hag5-1* and *hag4-1* mutants infiltrated with *P. syringae* DC3000 EV or *P. syringae* DC3000 *AvrRpt2* (OD_{600} = 0.001). Samples were collected 3 days post-inoculation. Error bars represent SD (n = 6).

The plant defence response has been extensively described in section 1.3 of Chapter 1, and the data presented this far suggest that HAG5 has a role in MTI. As described previously in section 1.3, there is a second line of defence that arised from recognition of effector proteins (Dangl and Jones, 2006). When these effectors are detected by the resistant proteins (R), there is an activation of the effector-triggered immunity (ETI). ETI is associated with a rapid and localized programmed cell death, known as the hypersensitive response (HR), expression of defence genes and the production of metabolites to limits pathogen growth and spread (Greenberg, 2003). To investigate whether HAG5 has a role in ETI, we syringe-inoculated leaves from Col-0 and both *hag5* mutants with *P. syringae* DC3000 expressing an empty vector (EV) or expressing the type III effector *AvrRpt2*. This effector is recognised by NB-

LRR receptors, triggering ETI (Axtell and Staskawicz, 2003). As a consequence, infiltrating *P. syringae* DC3000 expressing the effector *AvrRpt2*, results in decreased bacterial growth when compared to bacteria expressing an empty vector (EV) (Figure 3.7b). By using syringe inoculation as a method for infection, the bacteria gets directly delivered into the apoplast through the stomata. This approach ensures that equal amounts of *P. syringae* are infiltrated into the infected leaf, and as a consequence, the strength of the immune response is inversely correlated to the pathogen growth levels (Liu et al. 2015). As seen in Figure 3.7b. there were no differences between genotypes on bacterial growth with the control strain (EV). Furthermore, *hag5* mutants responded similarly to Col-0 after infiltration with the *AvrRpt2* expressing bacteria. These results suggest that the defence mechanism in which HAG5 participates is MTI, the plant first line on defence (Felix et al., 1999), but does not function in ETI at least in the case of *AvrRpt2*-induced immune responses.

3.3.1. Transcriptional response to flg22 elicitation in *hag5-2* mutant

Plant recognition of potential pathogens results in the activation of signal transduction pathways leading to transcriptional reprogramming, changes in the metabolism and production of antimicrobial compounds to overcome the potential threat. This early detection of potential pathogens takes place through recognition of conserved microbe associated molecular patterns (MAMPs), such as bacterial flagellin, by transmembrane pattern recognition receptors (Dangl and Jones, 2006). Activation of receptors by MAMPs triggers an array of immune responses that restrict pathogen growth and limit damage to the host (Denoux et al., 2008, Zipfel et al., 2004).

As described in the previous section, *hag5* mutants have increased tolerance to the bacterial pathogen *P. syringae* DC3000. To investigate whether this phenomenon is due to differences in gene expression changes following pathogen recognition, we performed a transcriptional profiling analysis with Col-0 and the loss-of-function mutant of *HAG5*, *hag5-2*, treated with the bacterial flagellum-derived peptide flg22. flg22 is a 22-amino acid sequence of the conserved N-terminal motif of flagellin, the protein that forms the bacterial flagellum. This motif is recognised by the FLS2 receptor in the plasma membrane, triggering an array of plant immune responses (Chinchilla et al., 2007b) By using flg22 as an elicitor, we are exclusively

characterising the transcriptional response directly associated with the recognition of this peptide by the plant receptor, since using *P. syringae* DC3000 would also result in effector dampening of MTI.

For this experiment, 16 day old Col-0 and *hag5-2* seedlings grown *in vitro* and transferred for 1 hour into ½ MS plates supplemented or not with 1μM flg22. 16 seedlings of each genotype were kept untreated as control samples, and four biological replicates per condition were performed independently. Since *hag5-1* and *hag5-2* have very similar phenotypes, we decided to exclude *hag5-1* in this experiment.

Experimental procedures regarding RNA extraction, sample preparation and hybridisation were carried out by Sophie Piquerez (post-doctoral research assistant), and further details regarding methodology and data processing can be found in section 2.10 of Chapter 2. Samples were hybridised onto Agilent Arabidopsis (V4) microarrays containing 43,803 probes. The average probe intensity was taken for each probe across replicates following array normalisation. To check reproducibility across replicates, correlation plots were generated for each sample between different biological replicates (Figure 3.8).

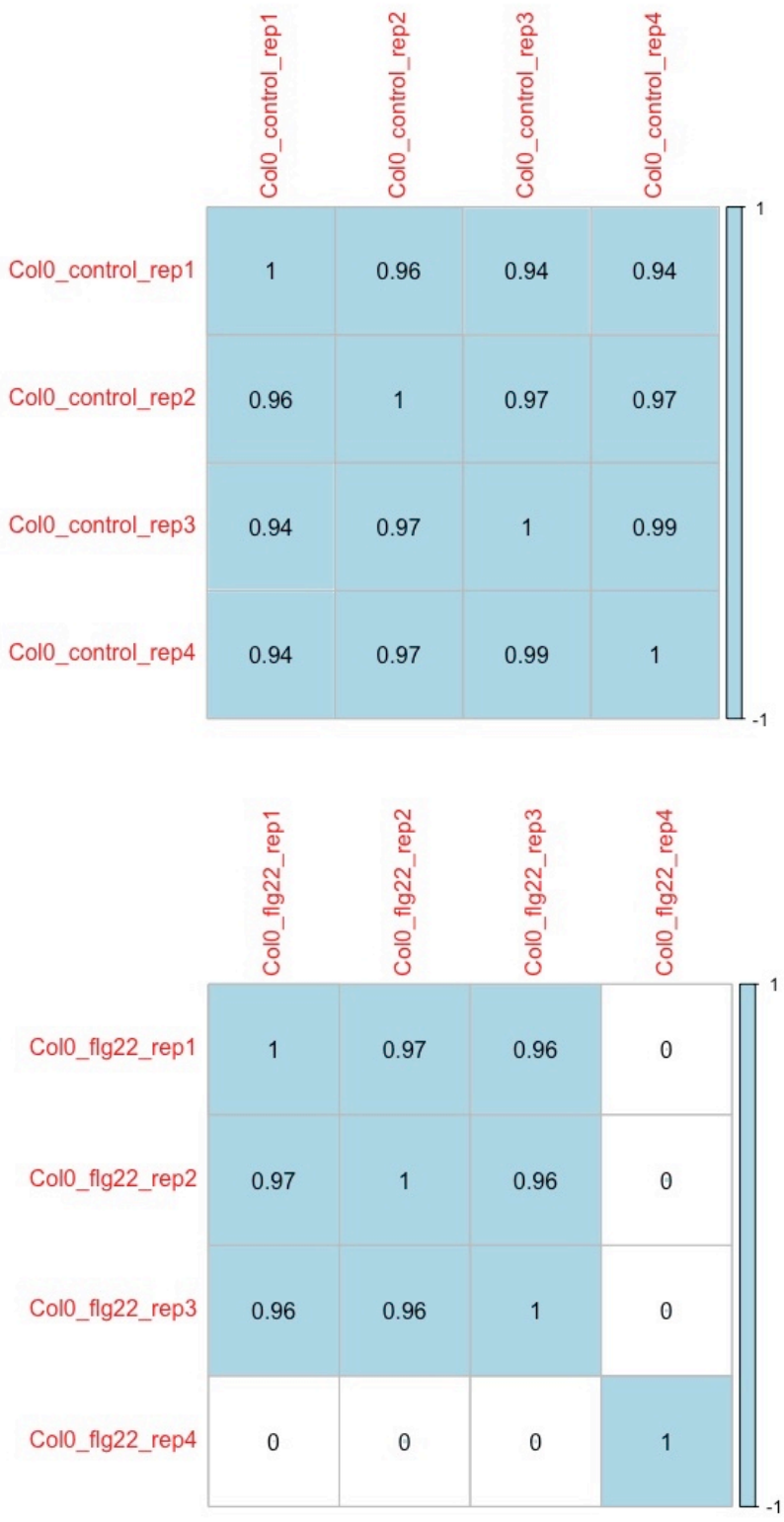

Figure 3.8. Visualization of the Pearson's correlation coefficient between Col-0 replicates. Every biological replicate of Col-0 control (above) and Col-0 flg22 treated samples (below) respectively is represented. The graphs were generated using the R package "corrplot" (Taiyun Wei, 2017).

This graph visualises the degree of similarity between biological replicates through the Pearson's correlation coefficient. This coefficient calculates the value of Cauchy–Schwarz inequality, where 1 represents total positive linear correlation, 0 is no linear correlation, and −1 is total negative linear correlation (Cauchy, A.L., 1821). This step of quality control was crucial to discard, prior analysis, the samples that did not correlate across replicates. Correlation plots for *hag5-2* samples were also generated in order to discard potential defective replicates (data not shown). As a consequence, Col-0 flg22 (replicate 4), *hag5-2* control (replicate 1) and *hag5-2* flg22 (replicate 4) samples were discarded to avoid introducing noise in the analysis and reducing the significance of the results. These samples did not correlate to their equivalents from other biological replicates, probably due to errors during the experimental procedure.

An additional step for quality control is the quantile array normalisation, which was performed with the Bioconductor LIMMA (Linear Models for Microarray Data) software package in R (Ritchie et al., 2015).

a)

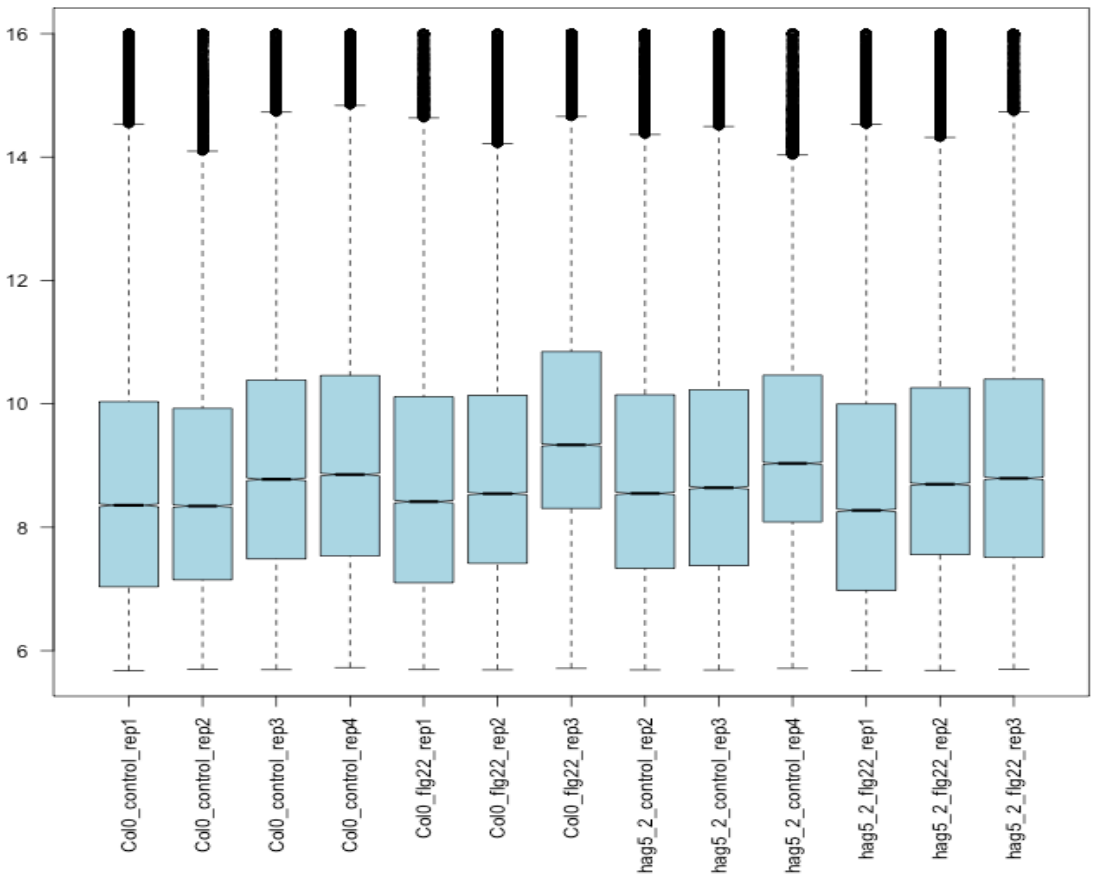

b)

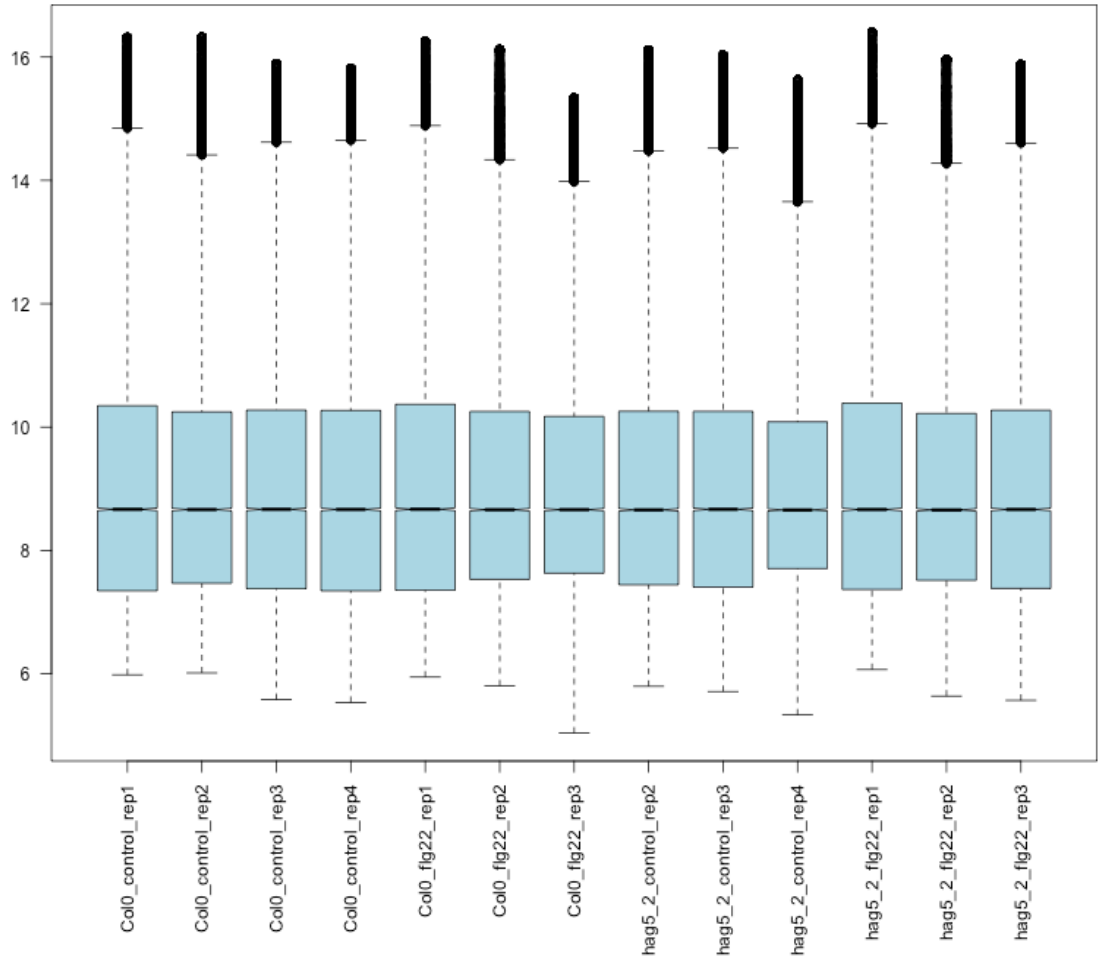

Figure 3.7. Overall microarray intensities before and after quantile normalisation. **a)** Array intensities before normalisation. **b)** Array intensities after normalisation. The centre of the box indicates the median, the box length indicates the interquartile range (IQR, 3rd quartile 1st quartile), the upper whisker indicates the 3rd quartile + 1.5 * IQR, whereas the lower whisker indicates the 1st quartile 1.5 * IQR of the data.

Box-plots were produced to indicate the overall intensity of arrays before and after normalisation. Figure 3.9 illustrates that the normalisation produced was successful, since the median intensity is aligned across samples.

Initial analysis of differentially expressed genes (DEGs) indicated that results from this microarray experiment are in agreement with those published from similar experiments (Denoux et al., 2008), in which approximately 10% of the genome gets up or down-regulated after flg22 elicitation. We used the thresholds of FDR-adjusted p-value ≤ 0.05 and log2 fold-change ≥ 1.5 to establish the level of significance. As a consequence, the genes that undergo an increase or decrease of 1.5-fold change

between comparisons will appear as DEGs. After identifying the lists of DEGs for each comparison, we performed a GO term enrichment analysis using TopGO (Alexa, 2014) and the *Arabidopsis* genome from the Ensemble database (version 79) (Kersey et al., 2018) to identify biological mechanisms and signalling pathways associated to the transcriptional response between genotypes and conditions.

DEGs between Col-0 and *hag5-2* in basal conditions

To investigate the effect of silencing *HAG5* in the transcriptome of seedlings without flg22 elicitation, we compared Col-0 and *hag5-2* seedlings in their basal state. We found only 3 DEGs with p-value ≤ 0.05 and log2 fold-change of 1.5. As expected, *HAG5* was down-regulated in *hag5-2* mutants. The other two genes were up-regulated when compared to Col-0.

- *HAG5* (AT5G09740)
- *WHY2* (AT1G71260), involved in DNA repair, defence response and regulation of transcription.
- *AT5G26270*, a transmembrane protein.

These small differences indicate that HAG5 does not alter the transcriptional landscape at that particular developmental stage (16 day old seedlings) in the absence of stimuli. This means that the developmental phenotypes of *hag5* mutants are a result of mutant plants undergoing development in the absence or down-regulation of *HAG5*, instead of there being a direct effect between HAG5 and the up or down-regulation of developmental genes. However, since the RNA extraction for this experiment was performed in whole seedlings, transcriptional differences inherent to the root might have been diluted. Consequently, investigating the root transcriptomes of Col-0 and *hag5-2* could provide more specific answers to whether the bigger root meristem of *hag5-2* mutants is due to transcriptional differences related to HAG5 or merely a developmental pleiotropic effect.

Common DEGs after flg22 treatment

When comparing each genotype before and after flg22 elicitation, 1869 differentially expressed genes were found in Col-0, and 1964 DEGs in *hag5-2*, both up and down-regulated (Figure 3.10).

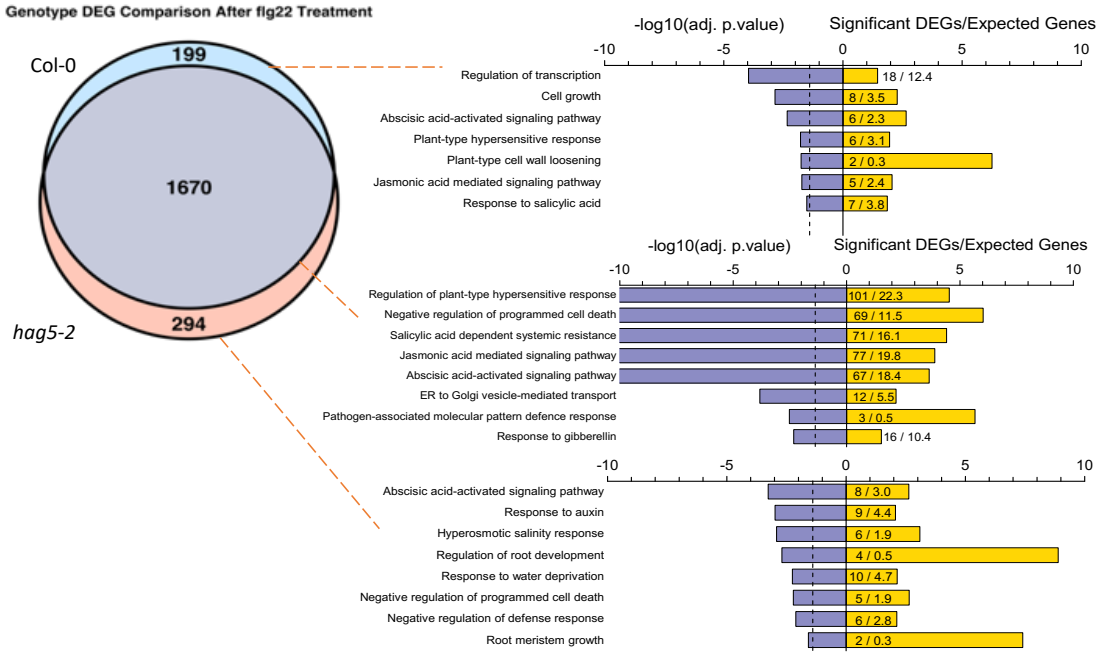

Figure 3.8. Venn diagram of DEGs between Col-0 and *hag5-2* after *flg22* elicitation. In Col-0, 1869 genes were up or down-regulated, and in *hag5-2*, 1964 genes between control and treated samples (1µM flg22). The Venn diagram represents three subsets of genes: Exclusive to Col-0 (blue), common DEGs between both genotypes (grey) and exclusive to *hag5-2* (orange). The GO term enrichment for each subset of genes was calculated using the R package "TopGO" (Adrian Alexa and Jorg Rahnenfuhrer, 2016). The Arabidopsis Col-0 genome available in Bioconductor (Carlson M, 2019) was used as reference genome. Next to each GO term, the -log (10) of the adjusted p-value and the ratio of significant over expected DEGs is represented.

As illustrated in the Venn diagram above, from all the DEGs after flg22 treatment, 1670 genes are common to both genotypes. The graph situated on the right-hand side of the Venn diagram shows the result of the GO term enrichment for each section of the diagram. GO terms are used to characterise subsets of genes based on associated biological processes, molecular functions or cellular components. Next to each GO term there are two different graphical representations of their significance:

in yellow, the number of significant DEGs belonging to each particular GO term over the number of hits that would have occurred randomly; in purple, the -log10 of the adjusted p-value (Figure 3.10).

Within these GO terms, some refer to well characterised mechanisms associated to plant defence, such as "HR response", "programmed cell death" or "MAMP defence response". These mechanisms have been described in section 3.1.1 as part of the pathogen-triggered immune response. In addition, several hormonal pathways are present as key players in that common response. Indeed, "salicylic acid (SA) dependent systemic resistance", "jasmonic acid (JA) mediated signalling pathway" and "abscisic acid (ABA)-activated signalling pathway" appear has highly enriched GO terms, with very similar significant/expected DEGs rate. These results indicate that most of the transcriptional response following MTI gets activated in *hag5-2* mutants, implying that *hag5-2* mutants display a fairly robust immune response. Something to take into account is that this microarray assay was performed after 1h of flg22 treatment, which constitutes early MTI responses. Analysing the transcriptomes of Col-0 and *hag5-2* seedlings at later time points after the treatment would give a more complete overview of the core immune responses of *hag5-2* mutants.

Even though there are 1670 common DEGs between Col-0 and *hag5-2* mutants upon flg22, the level of up or down regulation of these genes could be different between genotypes, causing a different response to the elicitor and a differential immune response. In order to visualise whether these DEGs displayed similar levels of expression in Col-0 and *hag5-2*, we generated a heatmap using the pheatmap package in R (Raivo Kolde (2019)) (Figure 3.11). As seen in this heatmap, the level of expression of these genes is conserved between genotypes. This confirms that *hag5-2* mutants display a robust response to flg22, since there is a core shared response in the magnitude of the changes in gene expression.

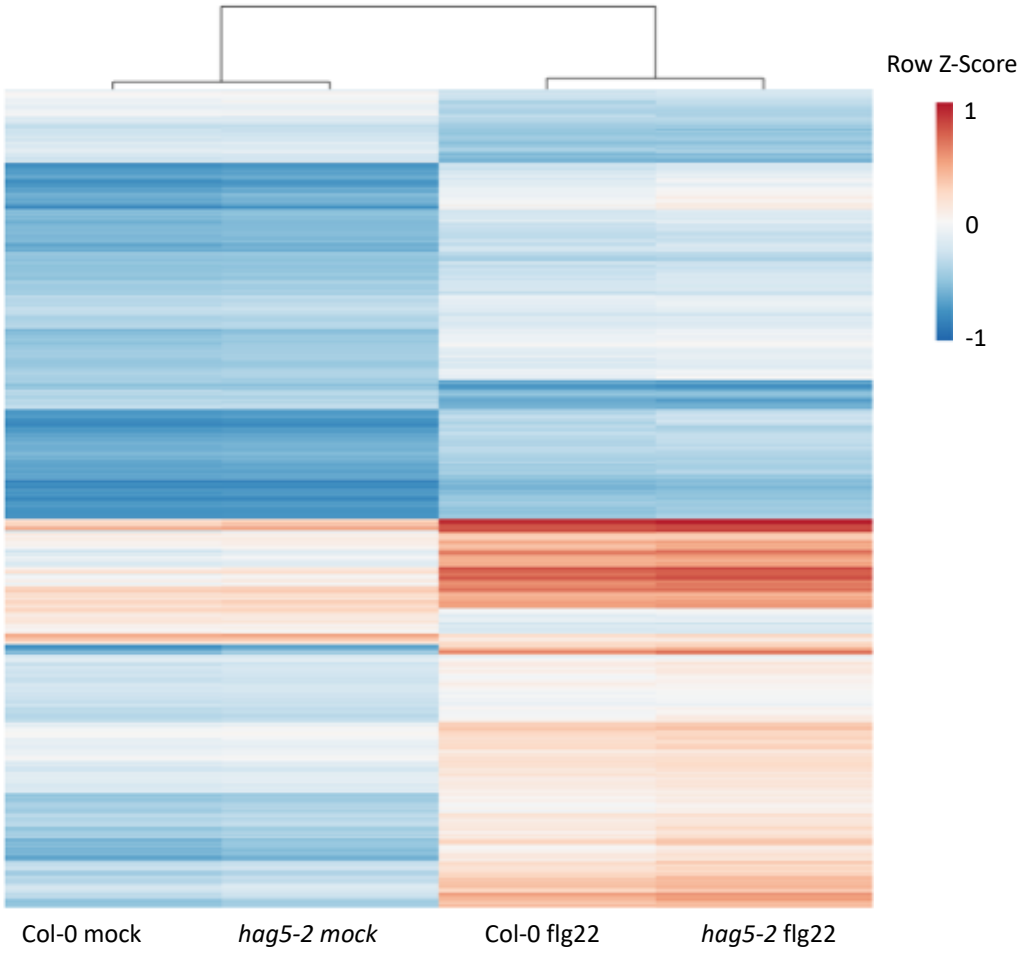

Figure 3.9. Heatmap of the expression of 1670 common DEGs between Col-0 and *hag5-2* under mock and flg22 treatments. Up-regulated genes are represented in red and downregulated, in blue, according to their Z-score values.

Col-0 exclusive DEGs after flg22 treatment

There are 199 flg22-depedent DEGs in Col-0 that do not get differentially expressed in *hag5-2* after elicitation (Figure 3.10). Within these genes, there are several transcription factors, such as *ERF14*, involved in ethylene responses, and several leucine zipper TFs such as *BZIP53* and *HB22*. These genes are up-regulated exclusively in Col-0 after flg22 treatment, indicating that HAG5 acts as a positive transcriptional regulator for these TFs. In addition, multiple genes involved in cell growth and the HR response, which are key processes of the immune response, are not differentially expressed on the *hag5-2* mutant after flg22 elicitation. Furthermore, HAG5 is involved in flg22-depedent transcriptional regulation of JA and ABA signalling pathways.

An interesting finding is that the ABA signalling pathway is represented across all three groups of DEGs (Figure 3.10), which indicates that HAG5 plays a role in the signalling cascade and transcriptional response to the phytohormone. This preliminary observation provides a hint about the role of HAG5 and the molecular mechanisms behind the *hag5* mutant phenotypes

hag5-2 exclusive DEGs after flg22 treatment

On the previous section, the genes that require HAG5 to be differentially expressed after flg22 elicitation were described. This section is dedicated to the description of flg22-depedent genes that are only differentially expressed in the *hag5-2* mutant. As seen in the Venn diagram of Figure 3.10, there are 294 genes that are not part of the common flg22 response of Col-0 plants. Looking at the pathways that these genes belong to might give some insight into which biological processes are affected by HAG5, and perhaps shed some light into the mechanisms that confer the disease resistance of *hag5* to *P. syringae* DC3000 discussed in section 3.2. The GO terms associated to these genes can be grouped into 3 categories: those related to root growth (response to auxin and root meristem growth), defence response (negative regulation of programmed cell death and defence response) and drought responses (ABA-activated signalling pathway, salinity response and response to water deprivation). As seen in Table 3.3 below, several genes involved in the ABA signalling pathway and hyperosmotic salinity response are overexpressed in *hag5-2* mutants after flg22 elicitation. These results suggest that HAG5 acts as a regulatory hub for biotic and abiotic stress responses. In this context, HAG5 would be a negative regulator of drought responses upon pathogen perception. The role of HAG5 in the ABA signalling pathway and tolerance to drought will be further investigated in Chapter 4, but these microarray results already highlight the involvement of this enzyme in regulating such responses.

The developmental phenotypes of *hag5* mutants have been previously characterised within this chapter. Indeed, *hag5-2* mutants have longer roots with increased root meristem. Having DEGs associated to root growth after flg22 exclusively on the *hag5-2* mutant means that, in the absence of HAG5, the transcription of root growth-related genes remains active. Whereas this finding does

not directly explain why *hag5-2* seedlings have longer roots, it highlights that HAG5 is involved in the regulation of root development. Indeed, the observed phenotype could be the product of a miss-regulation of cell growth and division at the root meristem throughout plant development.

Overall, this microarray experiment evidences that HAG5, even though is not crucial to initiate a defence response upon pathogen perception, acts in the regulation of hormonal responses, particularly those related to ABA. Furthermore, its role in development and drought tolerance can be perceived within the miss-regulated genes exclusive to *hag5-2* after flg22 elicitation.

Up to date, the reported activity of HAG5 *in vitro* is the acetylation of H4 at lysine 5 (H5K4ac) (Earley et al., 2007). As a consequence, our hypothesis relies on the non-overlapping DEGs between Col-0 and *hag5-2* being associated to H4K5 and regulated by this acetylation. Hence, the lack of H4K5ac in *hag5-2* mutant plants on loci related to hormone signalling, plant defence and growth, results in an altered transcriptional response to biotic stress and, phenotypically, in better performing plants with increased tolerance to *P. syringae* DC3000.

3.4. HAG5 is not involved in defence responses to *Verticillium dahliae*

After characterising the phenotype of *hag5* mutants with *P. syringae* DC3000 and knowing their transcriptional profile after flg22, the next arising question was whether these mutants displayed increased tolerance to other pathogens. To this end, the known fungal pathogen *Verticillium dahliae*, with known pathogenicity against *A. thaliana* plants, was selected for pathogenesis assays (Tjamos et al., 2005).

V. dahliae Kleb. is a soil-borne pathogenic fungus that affects more than 160 plant species, causing vascular wilt and resulting in billions of dollars in crop losses annually (Barbara W Pennypacker, 2004). This fungi colonises the root systems of host plans, invading the xylem and spreading towards the aerial parts of the plant through spores known as conidia (Barbara and Clewes, 2003). The diseased plants display several symptoms, such as leaf flaccidity, chlorosis and necrosis, stunting and vascular discoloration in stems (Pegg, 1981).

Our collaborator Danai Gkizi from Sotiris Tjamos laboratory in the Agricultural University of Athens, performed a pathogenesis assay with the fungi as described in

section 2.5.2 of Chapter 2. In brief, Col-0, *hag5* and *hag4* plants were inoculated with the pathogen and disease severity was recorded every day. Disease severity at each observation was calculated as a percentage of the number of leaves that showed wilting in the inoculated plants. The level of disease is expressed as a percentage of the maximum possible area of wilting for the whole duration of the experiment (25 days), which is referred to as the relative AUDPC (area under disease progress curve). The experiment was repeated two times with 30 plants per treatment and plant genotype. *hag4* mutants were included in the assay as control, since *hag4-1* mutants showed no bacterial growth phenotype in the *P. syringae* DC3000 screening (Figure 3.2).

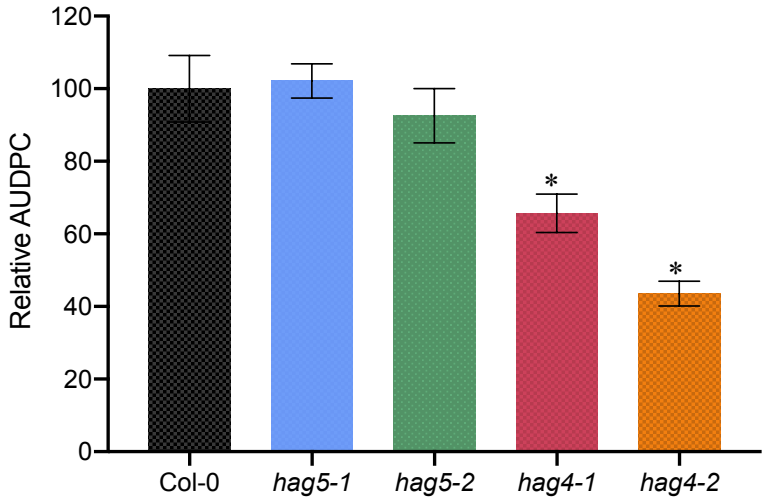

Figure 3.10. *hag4* mutants are more resistant to infection by the root pathogen *V. dahliae*. Three-week-old plants were challenge-inoculated with *V. dahliae* by root drenching with 10ml of a suspension of 1×10^7 conidia per millilitre of sterile distilled water (Tjamos et al. 2005). Control plants were mock-inoculated with 10ml of sterile distilled water. Disease severity at each observation was calculated from the number of leaves that showed wilting as a percentage of the total number of leaves of each plant, and was periodically recorded for 25 days after inoculation. Disease was expressed as a percentage of the maximum possible area for the whole period of the experiment, which is referred to as the relative AUDPC. Disease ratings were plotted over time to generate disease progression curves. AUDPC was calculated by the trapezoidal integration method (Campbell and Madden 1990). The experiment was repeated two times with 30 plants per treatment and plant genotype (a total of 60 plants). Statistical significance between genotypes was calculated with Tukey's test, *P < 0.05. This experiment was performed by Dr. Danai Gkizi.

As seen in Figure 3.12, *hag5* mutants have no significant decrease in AUDPC, which means that the wilted area produced by the fungus in the infected leaves was

very similar to those in Col-0 plants. These results suggest that HAG5 might be exclusively involved in defence responses to bacterial pathogens or pathogens that colonise via the aerial parts of the plant. Interestingly, the two T-DNA insertion mutants of *hag4* included in the assay had AUDPC values of 65.6% and 43.5%, respectively. The fact that *hag4* and *hag5* mutants show distinct phenotypes in terms of immune responses to different pathogens opens the question of whether the two paralogues have specialised in some distinct and exclusive functions over time. This subject will be further discussed in the following section and throughout the progression of this thesis.

3.5. HAG4 and HAG5 have distinct and redundant functions

As shown at the beginning of this chapter, the results of the screening of HATs mutants revealed that only *hag5* mutants but not *hag4* displayed increased resistance to infection with *P. syringae* DC3000 (Figure 3.2b). That suggested that even though HAG4 and HAG5 have been previously reported to have redundant functions, they might also be involved in different processes. A previous study of the two MYST histone acetyltransferases in yeast showed that the double mutant *esa1 esa2*, the orthologs of *HAG4* and *HAG5* respectively, were inviable, hence confirming their functional redundancy in terms of cell cycle regulation. In this study, the *esa1* KO mutant displayed susceptibility to thermal, genotoxic and oxidative stresses but tolerance to osmotic, cold and cell wall stresses. In contrast, *esa2* KO mutants was more resistant to high temperatures and cold (Wang et al., 2013b). The authors concluded that both proteins play opposite roles in cell growth and morphogenesis although they share common targets for acetylation.

Taking these findings into account, differential phenotypes between *hag4* and *hag5* mutants were investigated. As seen in Figure 3.13a, *hag4-2* mutants do not display the increased surface area observed in both *hag5* mutants.

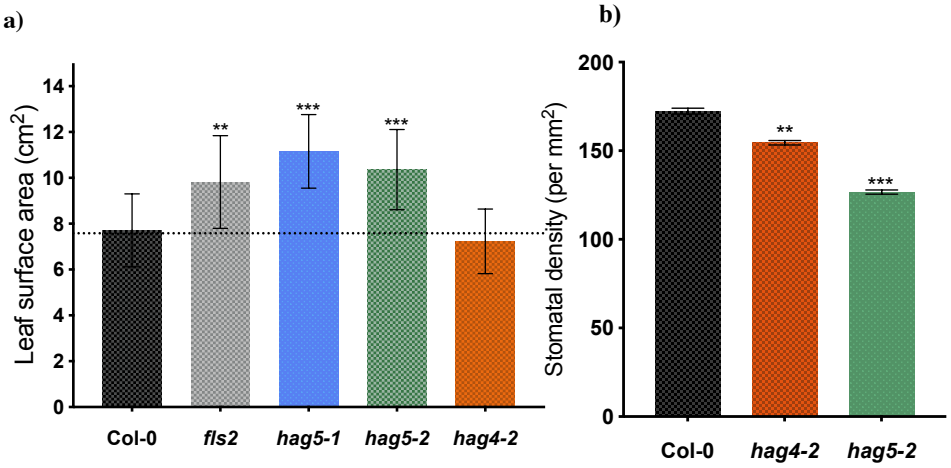

Figure 3.11. *hag4* and *hag5* mutants have common and distinct phenotypes. **a)** Leaf surface area of Col-0, *fls2*, *hag4* and *hag5* mutants. *fls2* mutant was included as a control since it has increased leaf area (Gomez-gomez et al., 2000). Pictures of fully expanded rosettes of 5-weeks-old plants were taken for analysis using ImageJ (https://imagej.net). Error bars indicate SD (n=24). Statistical differences between mutants and Col-0 were obtained using one-way ANOVA, ** P ≤0.001, *** P ≤0.0001. **b)** Stomatal density of *hag4-2* and *hag5-2* mutants. Leaves 6 and 7 from 5-weeks-old plants were collected and imaged using a magnification of 320x240 µm. Stomatal density was calculated from 2 sections of each leaf. Error bars represent SD (n = 12). Statistical differences between mutants and Col-0 were obtained using one-way ANOVA **P ≤0.001, ***P<0.0005.

Bacterial colonisation happens through the stomata, hence suggesting that the increased resistance to Pseudomonas in *hag5* mutants could be due to a decreased stomatal density. Stomatal density measurements of both *hag4-1* and *hag5-2* leaves showed that mutants had reduced stomata per mm^2 of leaf, although the difference was more significant in *hag5-2* mutants (Figure 3.13b). The stomatal determination happens during development, and HAG4 and HAG5 seem to play a redundant role in terms of cell determination but not in growth. This information also suggests that even though the reduced number of stomata might provide *hag5* mutants increased resistance to bacterial colonisation, there might be other defence mechanisms affected downstream of pathogen recognition.

In this chapter, the first evidence of both Arabidopsis MYST HATs having distinct functions has been presented. The evolutionary divergence between *HAG4* and *HAG5* will be further investigated and discussed throughout the next chapters, exploring the possibility of diversification through specialisation caused by the initial redundancy of both proteins.

3.6. Complementing and overexpressing *HAG5* in the mutant background

Insertional mutagenesis is a tool widely used in reverse genetics approach, consisting of the disruption of gene function through the insertion of foreign DNA into the gene of interest. In Arabidopsis, this involves the use of either transposable elements or T-DNA. This T-DNA not only disrupts the expression of the gene into which is inserted, but also acts as a marker for the subsequent identification of the mutation through genotyping. Because Arabidopsis introns are small, and because there is very little intergenic material, the insertion of a piece of T-DNA on the order of 5 to 25 kb in length generally produces a dramatic disruption of gene function (Krysan et al., 1999).

In order to characterise the function of HAG5, two different T-DNA insertion lines from the NASC institute (Alonso et al., 2003) were selected: *hag5-1* and *hag5-2*. The phenotypes of both allelic mutants have been thoroughly described in this chapter. However, confirmation that a phenotype of interest resulted from a given mutation or T-DNA insertion is crucial to validate the gene function attributed to such phenotypes. That requires the re-insertion of the wild type allele into the mutant background to rescue the wild type phenotype.

Over expressing the gene of interest in the mutant background and investigating the phenotypes of such plants can confirm the processes affected by the protein of interest. Furthermore, over expression can bring new information about the roles of HAG5 that were not evidenced through the lack-of-function approach. Complementation testing as described by (Weigel and Glazebrook, 2008) was performed to rescue the wild type phenotypes and investigate the phenotypes of the overexpressor lines. *Agrobacterium tumefaciens* GV3101 expressing the WT *HAG5* genomic DNA and promoter in a pEG302 vector was used to generate the complemented lines. For the overexpressor lines (OE), the same transformation procedure was followed introducing *HAG5* cDNA under a CaMV 35S promoter available in the pEG202 vector. Both vectors confer resistance to BASTA (glufosinate ammonium), which was used for the selection of positive transformants. T0 female gametes of *hag5-2* plants were transformed through floral dipping by Dr. Sophie Piquerez, as described in Chapter 2, section 2.3.

Figure 3.14a shows a diagram of *HAG5* genomic DNA and cDNA used for transformation, with the locations of the FLAG tag and the primers used for confirming the presence of the insert in both complemented and OE lines. Genotyping through PCR was performed to check for the presence of the insert within the transformed plants, amplifying the fragment of HAG5 directly associated with the FLAG tag, a sequence that is not naturally present in the Arabidopsis genome. As seen in Figure 3.14b, the respective insertion was present in complemented lines number 1, 3, 9, 10, 11 and 13 and in overexpressor lines 1, 2, 8, 9 and 10. Seeds obtained from these lines were sown into selective media to check for homozygosity (data not shown). Due to mendelian inheritance, the seeds from heterozygous plants have around 75% survival rate, whilst those from homozygous ones display a 100% survival rate. As seen in Figure 3.14c, Col-0 seeds cannot germinate in the selective media, and seeds from the complemented line #1 were homozygous, since all of them germinated in the presence of BASTA (10μg/mL). However, only heterozygous OE lines were identified, which required a step of selection or genotyping prior assay testing of these lines.

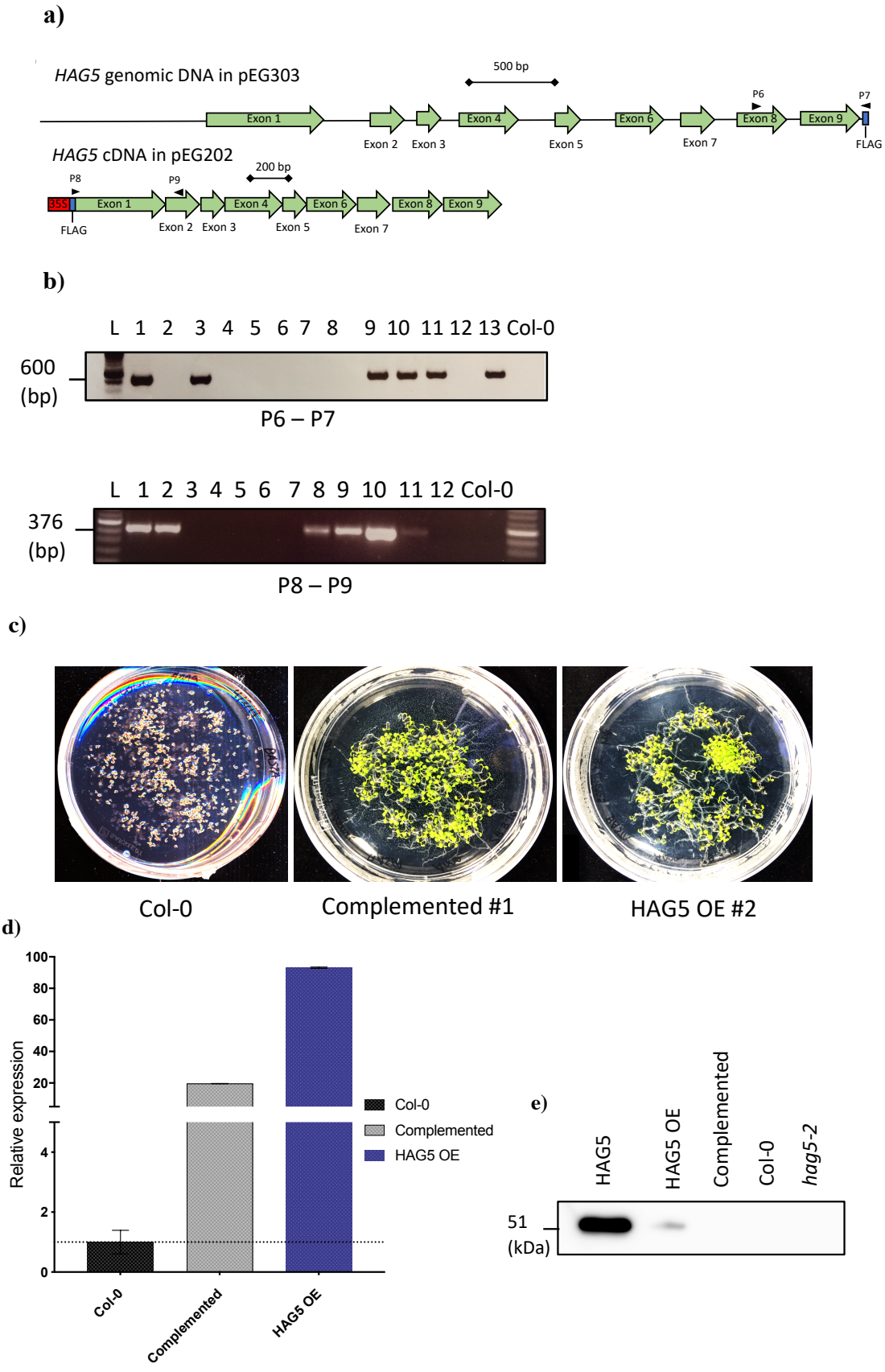

Figure 3.12. Strategy for complementing and over expressing *HAG5* in *hag5-2* background. **a)** Diagram of *HAG5* genomic DNA and cDNA with the tags, promoters and primers used for selecting positive transformants. **b)** Gel

electrophoresis of PCR products from DNA extracted from 4 weeks-old Arabidopsis complemented or overexpressor (OE) T1 plants post-BASTA selection. The amplicons correspond to the presence of *HAG5* genomic DNA expressed in pEG303 vector (up) or 35S:*HAG5* cDNA in pEG202 expression vector (down), using the primers from section a. **c)** Germination of seeds from Col-0 and T1 positive transformants (T2) of complemented and overexpressor lines in selective media (1/2 MS 1% Sucrose + 10µg/mL BASTA). Pictures were taken 7 days after vernalisation. **d)** Expression of *HAG5* in Col-0, complemented and OE lines in basal state. RNA was extracted from 10 day old seedlings grown in plates. Relative expression of *HAG5* was determined by qPCR using gene-specific primers (section 2.9.5). Error bars represent SD between technical replicates (n = 3). **e)** Immunoblot blot analysis of nuclear extracts from 35s:*HAG5*-FLAG (OE) and complemented transgenic lines immunoprecipitated using M2 FLAG beads (Sigma). The first line corresponds to purified HAG5-FLAG from E. coli Rosetta™ competent cells (Novagen). Col-0 and *hag5-2* mutants were included as negative controls. The hyphen indicates the location of the tagged HAG5 protein (51.2 kDa of HAG5 + 1012 Da of FLAG-tag).

To check the expression levels of *HAG5* in the complemented and OE lines, we used Real Time PCR in 10 day old seedlings grown in MS plates. Col-0 plants were used as a control to normalise the levels of *HAG5* expression. As seen in Figure 3.14d, the expression of *HAG5* in the complemented lines is 20 times higher than in Col-0 seedlings in basal state. Even though *HAG5* is being expressed under its native promoter, *HAG5* expression in the complemented lines is higher than in Col-0 plants at basal sate. This is a common event during complementation. On the other hand, the OE lines had an expression of *HAG5* of 100-fold when compared to the wild type. Since *HAG5* cDNA is under the expression of the CaMV 35S promoter this is an expected level of up regulation of the gene. Nonetheless, quantifying the abundance of *HAG5* transcripts does not necessarily reflect the actual levels of cellular HAG5, since protein degradation and turnover are downstream processes that are not being accounted for in this assay. In order to visualise HAG5 at the protein level, nuclear extraction, immunoprecipitation and western blot assays were carried out as described in section 2.12.1 of Chapter 2. In brief, nuclear proteins from seedlings were isolated and incubated with M2 FLAG beads (Sigma). FLAG elution was used to concentrate the tagged HAG5. The resulting eluate was mixed with an affinity matrix (StrataClean Resin, Agilent) and after several washes, the beads were resuspended in 60 µL of SDS-PAGE loading buffer and incubated at 100ºC for 10 min for protein denaturation. Approximately 100 seedlings per genotype were used for the nuclear extraction

following FLAG elution (Chapter 2, section 2.12.1). 45µL of eluate + 1X SDS-PAGE loading buffer per sample were loaded into the acrylamide gel. For the first line of the immunoblot,15µL of purified HAG5-FLAG in 1X SDS buffer + DTT were loaded as control. Proteins were transferred into a PVDF membrane which was then probed with the corresponding antibodies targeting the FLAG tag. The bands were visualised using a chemiluminescence approach.

The immunoblot diagram in Figure 3.14e confirms the detection of HAG5-FLAG in the OE lines. Yet, HAG5 in the complemented lines was not identified, probably due to the relatively low level of expression of the protein. As expected, due to the lack of FLAG-tagged HAG5 in the Col-0 and *hag5-2* lines, no protein was detected in these samples. This assay confirms that, at least in the OE lines, HAG5 is being overexpressed in the mutant background, allowing for further experimentation with these lines to investigate the resulting phenotypes.

3.6.1. Phenotypes of HAG5 complemented and OE lines

With the complemented and OE lines available, the developmental phenotypes of these plants were characterised in pursuance of confirming the role of HAG5 as a negative regulator of growth. As previously done with *hag5* mutant lines, leaf area of 5 weeks old plants was measured, as well as the root length of 10 day old seedlings (Figure 3.15).

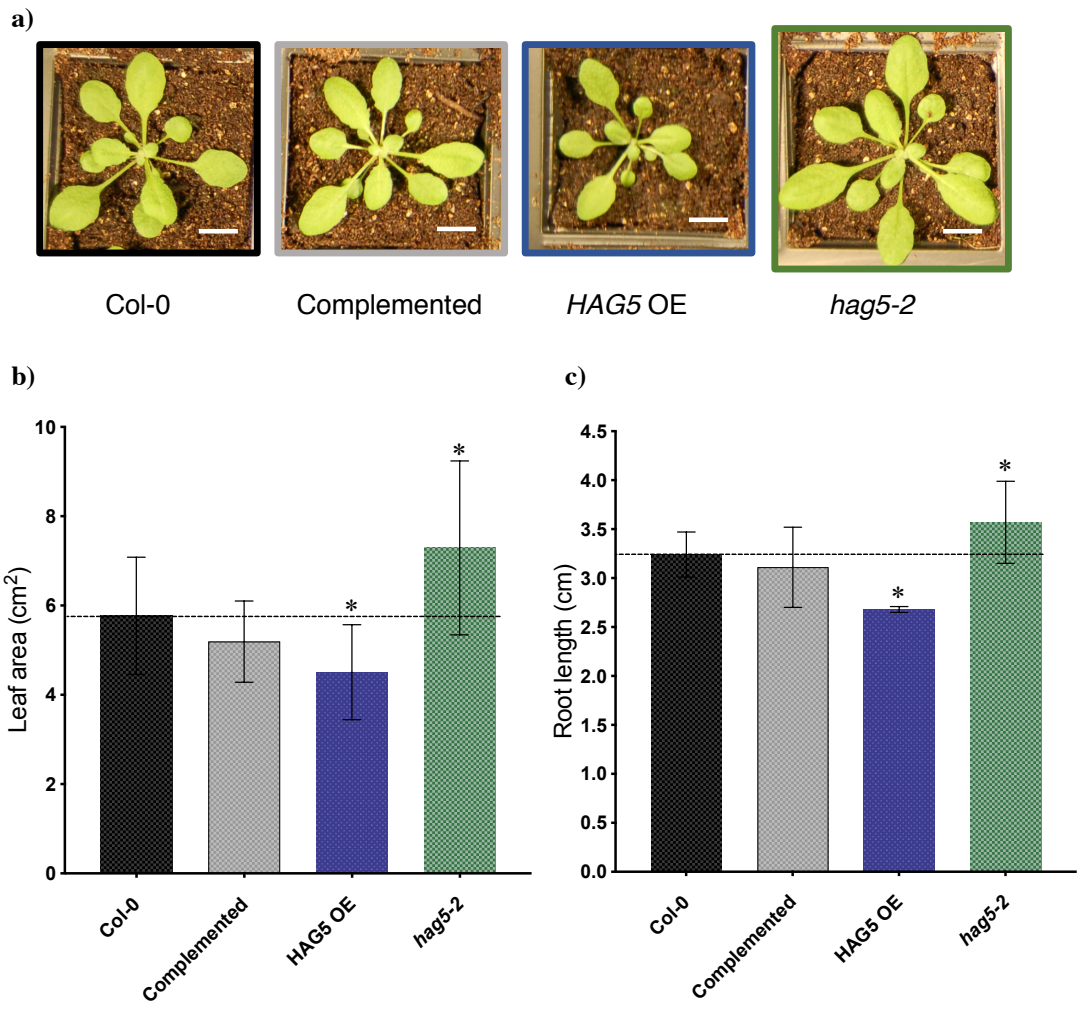

Figure 3.13. Phenotypes of complemented and *HAG5* OE lines. **a)** Representative pictures of the rosettes of 5-weeks-old Col-0, *hag5-2* complemented, *HAG5* OE and *hag5-2* mutants grown under short-day photoperiod. Scale bars represent 1.5 cm. **b)** Leaf surface area of Col-0, complemented, *HAG5* OE and *hag5-2* mutants. Pictures of fully expanded rosettes in 5-weeks-old plants were taken for analysis using ImageJ (https://imagej.net). Error bars indicate SD (n = 24). Statistical differences between transgenic lines and Col-0 were obtained using one-way ANOVA, * $P \leq 0.05$. **c)** Root length of Col-0, *hag5-2* complemented, HAG5 OE and *hag5-2* mutants roots measured using ImageJ. Error bars represent SD (n = 40). Statistical differences were calculated using one-way ANOVA (*$P \leq 0.05$).

Because the OE lines are heterozygous, Col-0 and *hag5*-2 were germinated in MS plates, and the complemented and OE lines in ½ MS plates with BASTA, letting them grow for 5 days horizontally. Seedlings were then transferred to vertical plates (½ MS 1% Sucrose), selecting those OE seedlings that germinated, and grown for 5 more days before measuring root length. As observed in Figure 3.15c, the

complemented lines show no difference in root length when compared to Col-0, evidencing a successful rescue of the wild type phenotype. Interestingly, the OE lines had significantly shorter roots than the wild type. *hag5-2* mutants were included as a control, since it was previously found that these plants have longer roots. It would be interesting to further investigate the meristem size of root tips from both transgenic lines to see if its size is restored or decreased in the complemented and *HAG5* OE lines respectively. Similarly, the leaf area phenotype was rescued in the complemented line. *hag5-2* mutants are bigger plants and the OE ones are smaller than the wild type. These results confirm that HAG5 is indeed a negative regulator of root and leaf growth.

Due to the opposite phenotypes between *hag5-2* and the OE lines, investigating the bacterial growth phenotypes resulting from re-introducing or over expressing *HAG5* in the loss-of-function background arose as the next logical step. The bacterial growth assay described previously on section 3.3 of this chapter was repeated using *P. syringae* DC3000 in 5 weeks old plants and collecting samples 3 days post-inoculation. Since the OE lines are heterozygous, plants were genotyped to confirm the presence of the insert before the bacterial assay, using the primers and approach shown in Figure 3.3b (data not shown).

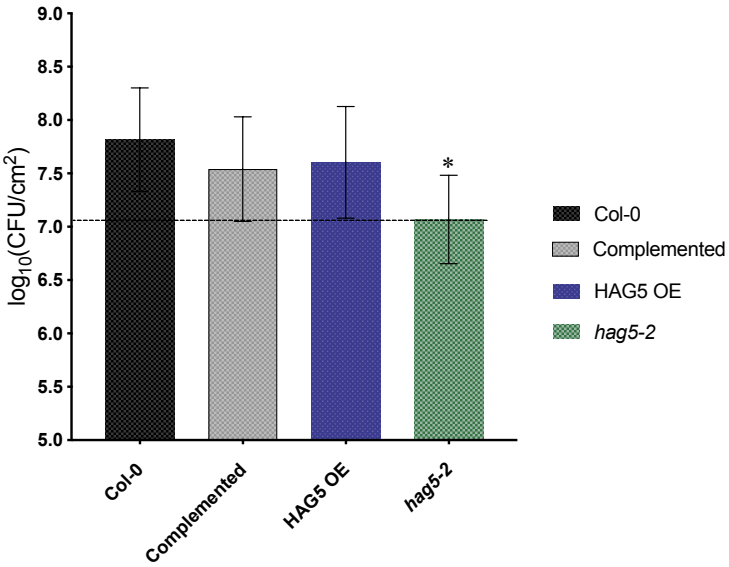

Figure 3.14. Re-introducing *HAG5* in the *hag5-2* mutant background restores the Col-0 bacterial growth phenotype, whilst over expressing the protein has no effect. 5-week-old plants were sprayed inoculated (OD_{600} = 0.01) with *P. syringae* DC3000. Bacterial growth was assessed 3 days post-inoculation. Error bars represent SD (n = 6). Differences from Col-0 were calculated using One-way ANOVA, * $P \leq 0.05$.

Figure 3.16 shows that indeed *hag5-2* mutants are more tolerant to Pseudomonas infection, with a decrease of half a $\log_{10}(CFU/cm^2)$ when compared to Col-0. There were not significant differences in the bacterial growth in the complemented line when compared to the growth of the pathogen in Col-0. Interestingly, the OE lines did not display a different phenotype either, with no difference in susceptibility to *P. syringae* DC3000. Given that the bacterial growth phenotype might be caused by the lower stomatal density of *hag5-2* mutants, it would be interesting to measure the density of stomata in the leaves of the complemented and overexpressor lines, and see if the obtained values are similar to those from Col-0 in both lines. Furthermore, the high concentration of bacteria used (OD_{600} = 0.01) might be masking a resistance phenotype. As a consequence, repeating the experiment with different concentrations of *P. syringae* would be useful to further characterise the resistance or susceptibility of each line.

From this experiment it can be concluded that HAG5 is indeed a negative regulator of immunity in the context of *P. syringae* DC3000. The mutant *hag5* plants are more tolerant to the pathogen, and re-introducing or over-expressing the gene results in normal susceptibility. These results are not surprising, since it is possible that, if HAG5 is involved in defence responses as hypothesized previously, not only its expression but also its degradation and turnover at the protein level might be regulated during the immune response. As a consequence, the over expressed transcripts or even the protein could be degraded during the 3 days of infection as part of the plant's mechanism to regulate immunity, resulting in normal susceptibility to *P. syringae* DC3000. Checking the protein levels of HAG5 through western blot over the course of the infection in complemented and OE lines would determine whether there are differences in the levels of HAG5. On the other hand, the growth phenotype of the OE lines can indeed be a consequence of the plant developing with more HAG5 expressing throughout the whole period in which the plant is growing. Furthermore, if the molecular processes in which HAG5 is involved are dependent on HAG5 interacting with other proteins, those proteins and their level of expression can turn into a limiting factor. Consequently, increasing cellular amounts of HAG5 would not be enough to see any phenotype related to such pathways or processes.

Overall, the complemented lines are a useful tool to confirm the function of HAG5 as modulator of growth an immunity, and the overexpressor line provided some

evidence that HAG5 negatively regulates growth throughout different developmental stages and tissues.

3.7. Findings

- *hag5* mutants display increased tolerance to infection with *P. syringae* DC3000 and have a robust transcriptional response to flg22 treatment.
- HAG5 is involved in the transcriptional regulation of abscisic acid responses and drought-related mechanisms upon flg22 treatment.
- *hag5* mutants have several developmental phenotypes: increased leaf area, longer roots and bigger root meristem.
- *hag5* and *hag4* mutants display some different phenotypes, stating that both homologues have distinct and redundant roles.
- *hag5* mutant phenotypes are complemented after expressing HAG5 under the genomic promoter in the *hag5* KO background.
- Overexpressing HAG5 results in smaller plants, without an immunity phenotype.

3.8. Discussion

HATs have been previously reported to act as positive and negative regulators of growth, since they have a role in cell cycle transition (Rosa et al., 2015). In this chapter it has been demonstrated that HAG5 is a negative regulator of growth in the terms of root length, meristem size and leaf area by investigating the phenotypes of *hag5* mutant plants. Since there are no transcriptional differences between Col-0 and *hag5-2* seedlings in basal state, there is not a direct link between HAG5 being a regulator of any specific growth, cell cycle or development genes that would explain the growth phenotypes. The ongoing hypothesis is that these developmental phenotypes are a result of *hag5* mutant plants undergoing development with low levels of HAG5 or completely lacking the enzyme. These phenotypes have been confirmed with two different T-DNA insertion lines (*hag5-1* and *hag5-2*), and through complementation of the *knock-out* mutants, reassuring that the described phenotypes are not due to off-target effects produced by the T-DNA insertion. The fact that the

knock-down and knock-out *hag5* mutants have similar phenotypes suggests that specific levels of HAG5 are required to perform its function. Hence, HAG5 acts in a threshold-dependent manner. An approach to test this hypothesis would be to quantify the endogenous protein levels of HAG5 in Col-0 plants with a specific antibody, and compare them with the levels in the knock-down mutants, both in basal state and before and after treatment with Pseudomonas.

Activation of immunity implies a severe developmental trade-off to prioritize defence over growth-related cellular functions (Huot et al., 2014a). As a consequence, the better performing *hag5* mutants would have been expected to display increased susceptibility to pathogen infection. However, *hag5* mutants are more tolerant to infection with *P. syringae* DC3000 and a loss of function of HAG5 still provides a robust transcriptional immune response following flg22 elicitation, as discussed in section 3.3.1 of this chapter. Since the microarray assay was performed only looking at early MTI (1h after flg22 elicitation), a root-growth arrest assay in Col-0 and *hag5* seedlings using exogenous flg22 treatment (Gómez-Gómez and Boller, 2000) would help determine whether *hag5* mutants have a differential MTI response in roots over time.

MYST HATs in mammals have been implicated in transcriptional repression (Thomas and Voss, 2007). In concordance with these results, HAG5 negatively regulates many of the ABA responsive genes upon activation of immunity. However, these genes still get up-regulated after treatment, which shows that HAG5 only modulates their level of expression rather than being a direct negative regulator. The displayed increased tolerance to pathogen infection in mutants does not prevail with other pathogens such as *V. dahliae* (section 3.4), which suggests that HAG5 is involved in immune responses to bacteria or pathogens that colonise through the aerial parts of the plant. In addition, *hag5-1* mutants do not have an increase tolerance to *P. syringae* DC3000 *AvrRpt2*, implying that the mechanism in which HAG5 participates is MTI, the plant first line on defence (Felix et al., 1999). Furthermore, *hag5-2* mutants have decreased stomatal density, which would partially explain why bacterial colonisation through spray inoculation is less successful in these mutants. However, *hag4* KO mutants have a similar phenotype and are not more resistant to *P. syringae* DC3000, supporting the evidence of HAG5 being a modulator of immune responses.

As seen in Figure 3.17, *HAG5* (also known as *HAM2*) is conserved throughout different plant species.

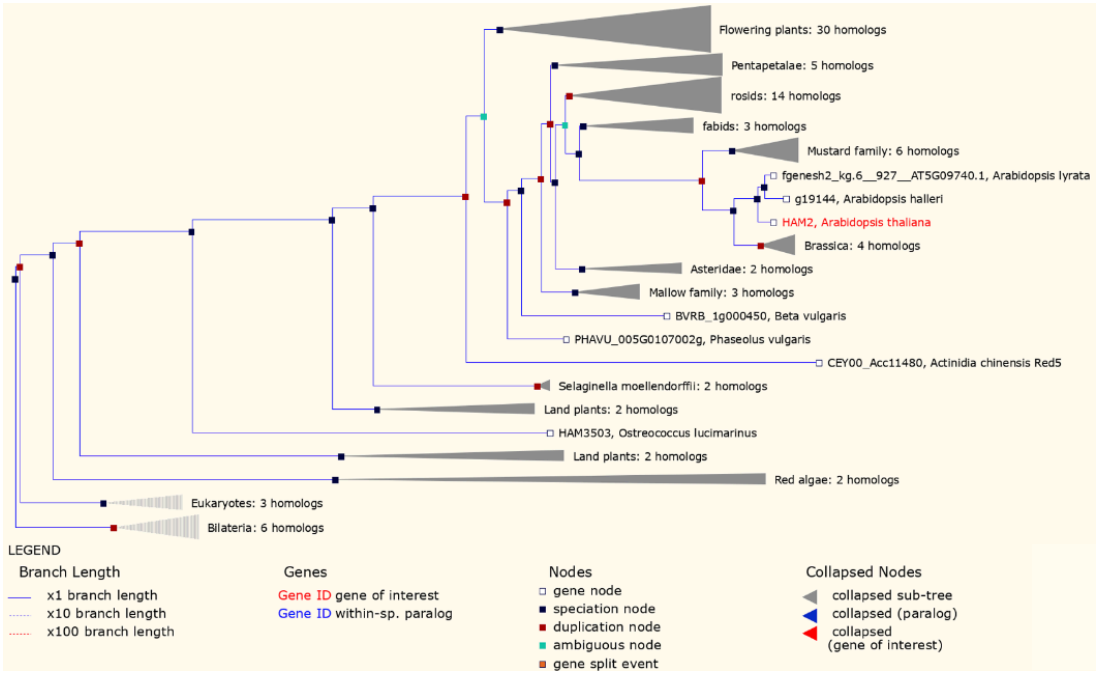

Figure 3.15. *HAG5* is conserved across plant lineages. Phylogenetic tree of *HAG5* (displayed as *HAM2*) obtained through the pan-taxonomic comparison using Ensembl (http://plants.ensembl.org).

The characterised benefits of supressing *HAG5* in order to increase plant fitness and response to pathogens questions the conservation of *HAG5* across plant lineages. The current hypothesis regarding this high conservation is that even though a lack of HAG5 confers beneficial phenotypes, its role in modulating plant fitness and response to stress in changing environmental conditions is important for better adaptation. Indeed, *hag5* mutant phenotypes have been investigated under controlled growth conditions (temperature, light and humidity), without nutrient or water deficits. Under these circumstances HAG5 seems to have a negative effect in plant performance. As a consequence, supressing the expression of *HAG5* in Arabidopsis, and potentially other Brassicaceae crops, would result in better performing plants. However previous publications have described negative effects of disrupting the expression of *HAG5*. Indeed, *hag5* mutants display increased levels of DNA damage following UV-B treatment (Campi et al., 2012). Consequently, total disruption of *HAG5* expression might have some detrimental effects. Thus, the motivation within this thesis, and the

main focus of Chapter 5, will therefore be to develop a novel agrochemical to inhibit HAG5 targeting its catalytic activity, aiming at modulating plant transcriptional responses to stress under specific conditions.

During the next chapter, the molecular mechanisms by which HAG5 regulates biotic and abiotic stress responses will be further investigated. This thesis comprises an effort to better understand the role of HAG5, its evolutionary divergence from its close paralogue *HAG4* and the ways in which its expression and activity can be altered to create better performing plants without a developmental trade-off.

Chapter 4 HAG5 is involved in abscisic acid signalling and drought responses

4.1. Context of this chapter

In the previous chapter, HAG5 was identified as a negative regulator of growth and immunity. The *hag5* mutants are bigger plants with longer roots, increased meristem size and increased tolerance to bacteria. However, in the previous chapter, the molecular mechanism underlying these developmental and immunity phenotypes was not identified. Since the only role of HAG5 known to date is to acetylate H4K5 *in vitro* (Earley et al., 2007), the current hypothesis is that the growth and immunity phenotypes displayed by *hag5* mutants are a result of an altered acetylation state of the chromatin. Regarding the immunity phenotypes, we investigated the transcriptional response of *hag5* loss-of-function mutant to the elicitor flg22 to further understand the increased tolerance of *hag5* mutants to *P. syringae* DC3000 (section 3.3 of Chapter 3). The microarray results indicate that the regulation of hormone-related and defence associated genes is indeed impaired in *hag5-2* seedlings. Consistent with the initial hypothesis, the assumption was that the lack of HAG5 translates into different acetylation status for some of those miss-regulated loci, resulting in the observed differential response and bacterial growth phenotype.

In mammals, histone acetyltransferases are known to acetylate histones, transcription factors, nuclear receptors and enzymes affecting their activity or their binding capacity through protein-protein interactions via bromodomain (Strahl and Allis, 2000). HATs can impact the transcriptional activity of the transcription factor they interact with (Pelletier et al., 2002), regulating their activity or specificity through direct acetylation (Wang et al., 2018) (Figure 4.1).

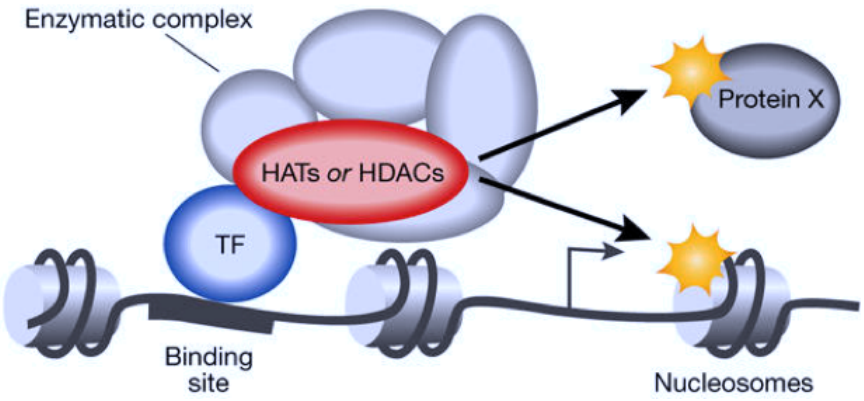

Figure 4.1. Model of local action of histone acetyltransferases and histone deacetylases. Histone acetyltransferases (HATs) and histone deacetylases (HDACs) can be recruited to their target promoters through a physical interaction with a sequence-specific transcription factor (TF). They usually function within a multimolecular complex in which the other subunits are necessary for them to modify nucleosomes around the binding site. These enzymes can also modify factors other than histones (protein X) to regulate transcription (Legube and Trouche, 2003).

In plants, it has been previously reported that histone acetyltransferases interact with other proteins such as transcription factors or HADCs and form chromatin remodelling complexes (Bieluszewski et al., 2015, Tsuzuki and Wierzbicki, 2018). Indeed, through their physical interaction with sequence-specific transcription factors, HATs target specific promoters, where they locally modify histones or transcription factors and thus regulate gene transcription (Figure 4.1) (Legube and Trouche, 2003). To date, HAG5 has not been shown to interact with any transcription factor. As a consequence, we proceeded to screen for transcription factors that interact with HAG5 and either recruit HAG5 to their target promoters for H4K5 acetylation or are direct substrates of HAG5.

4.1.1. Yeast 2-Hybrid screening of HAG5 interactors

In order to identify potential TFs interacting with HAG5, we performed a Yeast 2-Hybrid screening using a library of Arabidopsis transcription factors generated by (Dreze et al., 2010, Pruneda-Paz et al., 2014) . This library was built by proteins that were identified through a high-throughput DNA binding assay (Pruneda-Paz et al., 2014), and consists of 1,956 sequence-confirmed pENTR/D-TF clones representing

78.5% of all predicted Arabidopsis TFs. Almost all TF genes included in the collection (99%) encode polypeptides predicted by the current Arabidopsis genomic annotation (TAIR10). A fraction of these clones (4.6%) contain silent point mutations likely generated during gene amplification. 93 out of 97 (96%) predicted Arabidopsis TF families are represented in this library, with a clone coverage higher than 50% for 89% of these TF families. Due to cloning limitations, only four TF family singletons (hATP, LFY, NOT, and TBP) are not present in the collection, whereas other families, suchas ARF, PHD, and SNF2, are significantly underrepresented (Pruneda-Paz et al., 2014).

This high-throughput experiment is a yeast-based screen for the identification of protein-protein interactions based on auxotrophy. In brief, this system consists of the reconstitution of a transcription factor through the expression of two hybrid proteins, one fusing the DNA-binding (DB) domain to a protein X (DB-X) and the other fusing an activation domain (AD) to a protein Y (AD-Y). In this library, the TFs are fused to the activation domain (AD), whilst *HAG5* cDNA was fused to the DNA-binding domain (DB). If the two fused proteins interact, the DB and AD of the GAL1-HIS3 transcription factor activate the expression of the *GAL1-HIS3* reporter gene (Figure 4.2). This results in Histidine (HIS3) production by the yeast, allowing it to survive in media without the supplemented amino acid. To avoid false positives through autoactivation, we used increasing concentrations of 3AT (3-amino-1,2,4-triazole), a competitive inhibitor of the HIS3 gene product.

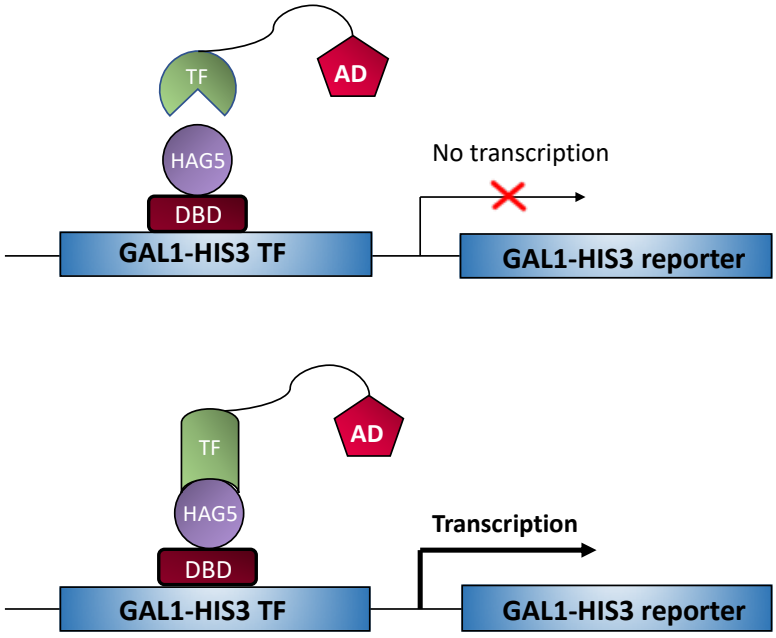

Figure 4.2. Detecting protein-protein interactions with the yeast two-hybrid system. Protein-protein interactions are detected by the mating of two haploid complementary yeast strains, each expressing a distinct expression plasmid. The first strain expresses a protein prey fused to a transcription activation domain (AD). The second strain expresses a protein bait fused to a DNA-binding domain (DBD) that binds to its recognised binding site, usually a transcription factor (GAL1-HIS TF) that activates the expression of a reporter (*GAL1-HIS3* reporter). If there is interaction between bait and prey, the AD is brought into proximity of the DBD to cause transcriptional activation of the TF and the subsequent activation of the reporter, leading to selection. Adapted from (Ratushny and Golemis, 2008).

Yeast transformed with *HAG5-DB* synthesise Leucine, and the yeast with the different TF candidates synthesise Tryptophan, which allows successfully transformed cells to grow in selective media without the respective amino acids provided. This system is required for the selection of mated yeast expressing both *HAG5-DB* and *TF-AD* vectors (mated), which can then survive in -Leu-Trp media. Positive interactions are then identified when the mated yeast can synthesise HIS3 due to the physical binding of the DB and AD domains fused to HAG5 and the interacting partner respectively. This allows yeast to grow in rich media (SC) without Leucine, Tryptophan and Histidine.

4.1.2. HAG5 interacts with bHLH91, a TF involved in anther and pollen development

The Yeast 2-Hybrid screening revealed two potential interacting partners of HAG5. The first candidate is the transcription factor *bHLH91* (AT2G31210). Negative (C1) and positive controls (C2-C5) included in the library were used to verify the mattings and media used for yeast selection (Figure 4.3) (Dreze et al., 2010). In order to confirm the specificity of the interaction, two paralogues of *bHLH91* available in the library were added as controls, *bHLH10* (AT2G31220) and *bHLH89* (AT1G06170) (Figure 4.3a). These three genes occurred from duplication events in the most recent common ancestor of the *Brassicaceae* (crucifers) (Zhu et al., 2015). We performed a multiple sequence alignment between the three paralogues, which compares all protein sequences identifying the homologous residues between them. It

it is assumed that all aligned residues in a multiple sequence alignment derive from a common ancestral residue, which provides information about the evolution of proteins (reviewed by (Gabaldón, 2007)). Figure 4.3b represents the evolutionary distance between the three genes, which is an estimate of the evolutionary divergence calculated through their protein sequence alignments (Brocchieri, 2013), showing the great degree of conservation between all three paralogues. These bHLH genes have been previously shown to interact with DYT1, another bHLH transcription factor required for tapetum development. DYT1 is the central regulator of the Arabidopsis anther transcriptome, and it is required for normal male reproductive development. It regulates the expression of more than 1000 genes involved in peptide and lipid transport, pollen exine formation, pollen development and phenylpropanoid biosynthesis (Zhang et al., 2006, Feng et al., 2012).

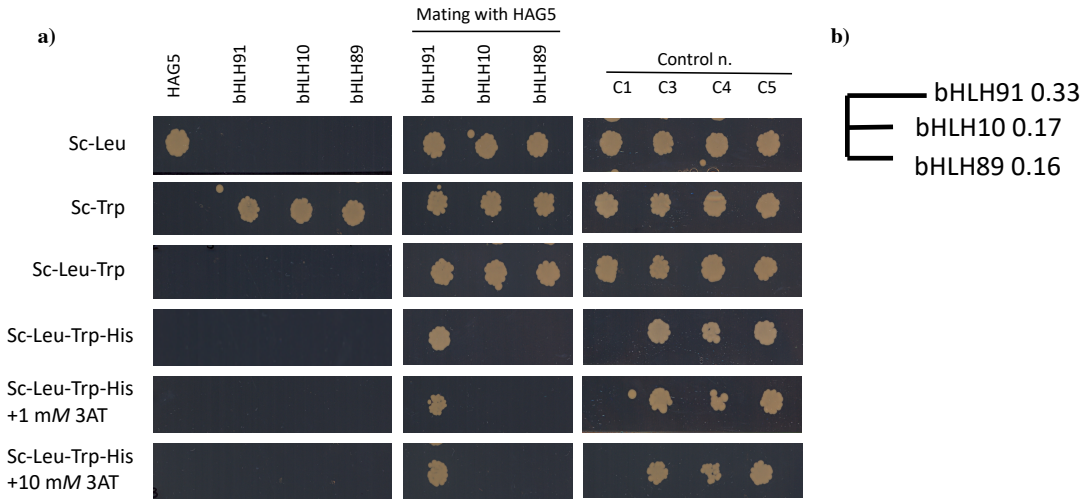

Figure 4.3. a) Phenotypes of Y2H interactions between HAG5 and three bHLH transcription factors. The controls consist of four strains C1–5, each containing a different pair of DB-X and AD-Y hybrid proteins. C1: negative control; C3, C4, C5: positive controls as described in (Dreze et al., 2010). **b)** Phylogenetic distances were calculated through ClustalW2, using the Newick/PHYLIP format tree and the Neighbour-joining algorithm (Naruya Saitou, 1987). The multiple sequence alignment was produced by CLUSTAL O (1.2.4).

These three bHLH TFs are required for the expression of the majority of DYT1-dependent genes. The functional redundancy of the three genes was investigated with

single, double and triple mutants, where only *bhlh91* showed defective anthers with abnormal pollen (Zhu et al., 2015).

The fact that HAG5 interacts with only one of the three bHLH paralogues suggests that, just like it might have occurred between HAG4 and HAG5, redundancy over time led to specialisation of these proteins. As a consequence, *bHLH91*, which is indeed further apart in evolutionary distance from the other two paralogues, might have acquired extra functions through its interaction with HAG5.

HAG4 and *HAG5* have been previously shown to be involved in gametophyte development. In fact, Delaure et al., revealed through genetic analysis that *hag4hag5* partial silencing through RNAi induces severe defects in male and female gametophyte formation due to an arrest of mitotic cell cycle at early stages of gametogenesis (Delarue et al., 2008). The fact that HAG4 and HAG5 are redundant in regulating gametophyte development suggests that both proteins are required to acetylate H4K5 at the respective loci and/or that both HATs interact with bHLH91. Since the other two bHLH transcription factors function redundantly with bHLH91, it is not very probable that HAG4/HAG5 interacting with bHLH91 is the determinant factor for the proper regulation of the anther and pollen development genes. Nonetheless, Alexia Tornesaki, another member of the Ntoukakis group, performed the Y2H screening looking for interactors of HAG4 (Figure 4.5). Her results confirm that HAG4 does not interact with any of the bHLH TFs, corroborating that the HAG5-bHLH91 interaction is a product of evolutionary diversification and acquirement of new functions of both paralogues. These findings bring us closer to the hypothesis of HAG5 being responsible for the acetylation status of some of the genes regulated by bHLH91 (and the other two paralogues) required for gametophyte development. This hypothesis is based on the assumption that if these loci do not get acetylated through HAG5, none of the three bHLH transcription factors could access the chromatin, resulting in the observed lethal phenotypes of the *hag4hag5* mutant. That would not explain the redundancy of *HAG4* and *HAG5* in anther and pollen development, since only in the absence of HAG5 the acetylation status of the developmental genes would be compromised. It is possible that HAG4 interacts with other transcription factors, that together with bHLH91, bHLH10 and bHLH89 regulate anther and pollen development. An interesting approach to test this hypothesis would be to investigate if bHLH-dependent genes are associated to HAG4 and/or HAG5-dependent H4K5

acetylation. Since HAG4 and HAG5 might act redundantly acetylating H4K5, using *hag4-2* or *hag5-2* mutants for a ChIP-seq experiment looking at chromatin associated to H4K5ac could result in no differences in enrichment when compared to Col-0. An alternative approach will be to see whether HAG4 and/or HAG5 are associated with bHLH-dependent genes by performing a ChIP-seq using HAG4 or HAG5 complemented mutants. This would reveal the physical interactions between both HAG4 and HAG5 with different chromatin regions, bringing information about the genes that are regulated by their HAT activities.

In the previous chapter, we described that HAG4 and HAG5 mostly differ structurally in their TUDOR domains. As a consequence, we hypothesize that this specificity grants the unique interactions of both HATs. In order to test this hypothesis, we propose an experiment swapping the TUDOR domains between HAG4 and HAG5 and performing a Y2H with the positive interactors. This experiment would reveal whether such interactions are indeed dependent on the TUDOR domain and would bring more information about the mechanism behind the differential roles of both paralogues.

Our current understanding of the HAG5-bHLH91 interaction is that it is not crucial for of anther and pollen development, but it probably facilitates bHLH91 TF activity. However, yeast is a heterologous system in which post-translational modifications do not necessarily take place. This might result in false positives for protein-protein interaction, and a confirmation *in planta* is required to establish such relationship between HAG5 and bHLH91.

4.1.3. HAG5 interacts with ARIA, a TF involved in ABA responses

The Y2H screening revealed a second potential HAG5 interactor (Figure 4.4). This transcription factor, *ARIA* (AT5G19330), is an ARM repeat TF previously shown to act as a positive regulator of ABA responses (Kim et al., 2004a). As previously done with the bHLH TF interactor, we included the closest TFs to ARIA available in the library as controls for the specificity of the interaction between ARIA and HAG5. As a consequence, we used *BOP2* (AT2G41370) and an ankyrin repeat family protein (AT2G04740).

As seen in Figure 4.4b, the evolutionary distances between these three transcription factors is approximately 0.4. HAG5 did not interact with any of those two TFs, which reflects the specificity of the interaction with ARIA. In order to verify this interaction *in planta*, we transiently co-expressed *HAG5-FLAG* and *ARIA-YFP* in *N. benthamiana* using Agrobacterium transformation as described in section 2.8.4 and 2.8.5 of Chapter 2.

We proceeded to perform a co-immunoprecipitation (Co-IP) experiment pulling down ARIA fused with YFP using GFP trap® beads and testing for HAG5-FLAG presence amongst the pulled-down protein. The immunoblot in Figure 4.4c shows that both fusion proteins were successfully expressed in *N. benthamiana*. The input samples constitute the proteins from the nuclear extract before the immunoprecipitation (IP). The input corroborates the successful expression of HAG5-FLAG (51.7 kDa) and ARIA-YFP (78.2 kDa + 27.0 kDa YFP). The empty vectors (EV) were co-expressed with each single protein as a control to test that if there is any interaction, is due to the expressed protein and not because of its fused tag. As seen in the IP section of the immunoblot, HAG5 is found bound to ARIA when co-expressed in *N. benthamiana* (Figure 4.4c), confirming the interaction between both proteins *in planta*.

ARIA was initially discovered through its interaction with AREB1/ABF2 (Kim et al., 2004a) a known bZIP transcription factor involved in abscisic acid signalling and osmotic stress responses (Kim et al., 2004b). Through the study of the mutant and overexpressor lines of *ARIA*, Kim et al., concluded that ARIA is partially responsible for a subset of ABF2-dependent ABA responses.

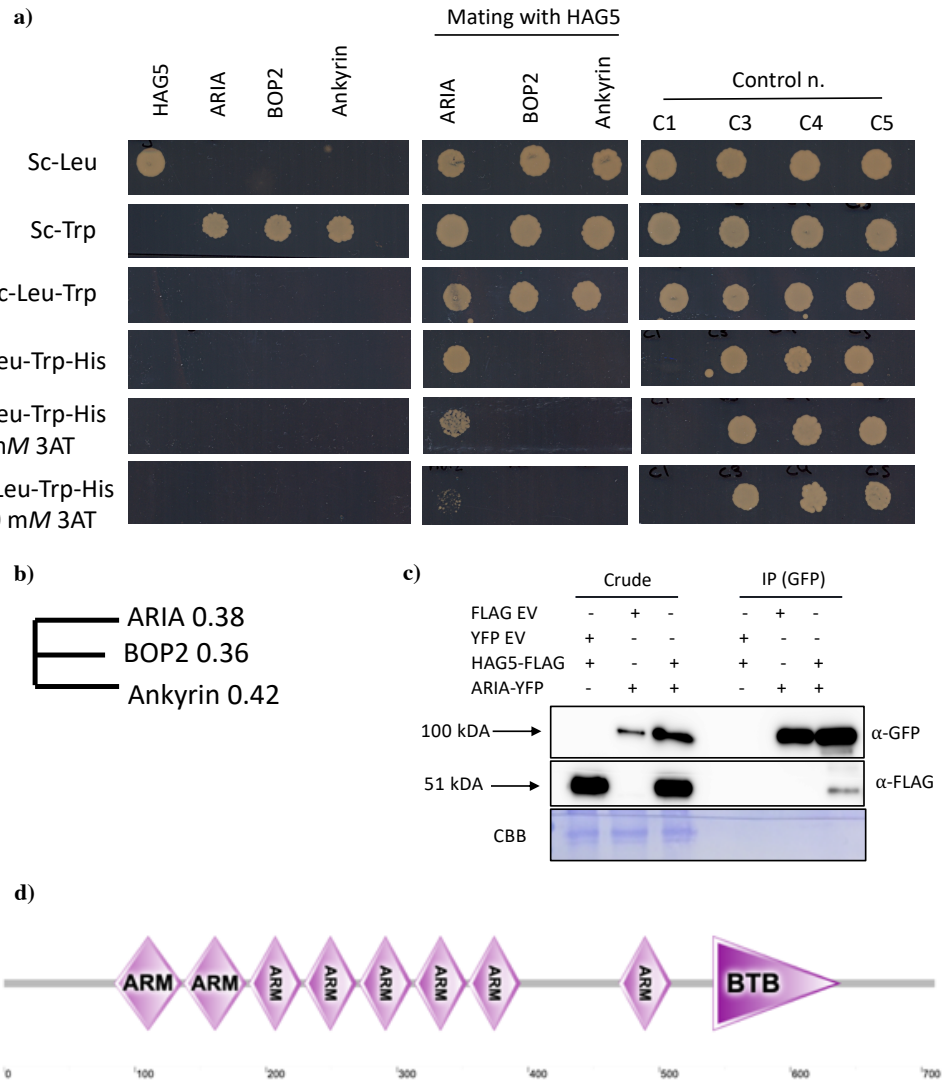

Figure 4.4. a) Phenotypes of Y2H interactions between HAG5 and three BTB/POZ transcription factors. The controls consist of four strains C1–5, each containing a different pair of DB-X and AD-Y hybrid proteins. C1: negative control; C3, C4, C5: positive controls as described in (Dreze et al., 2010). **b)** Phylogenetic distances were calculated through ClustalW2, using the Newick/PHYLIP format tree and the Neighbour-joining algorithm (Naruya Saitou, 1987). The multiple sequence alignment was produced by CLUSTAL O (1.2.4). **c)** HAG5 and ARIA physically interact *in planta*. The protein-protein interaction was confirmed by co-immunoprecipitation. *HAG5* and *ARIA* were transiently expressed in *N. benthamiana* plants using *Agrobacterium tumefaciens* transformation. Plants were co-transformed with either HAG5 in pEG202 (FLAG) vector + PEG104 EV or ARIA in pEG104 (YFP) + PEG202 EV. Lysates were immunoprecipitated using GFP-trap beads (Chromotek), separated by PAGE and electroblotted to PVDF. The immunoblot analysis probing with α-GFP or α-FLAG antibodies showed that HAG5 co-immunoprecipitated with ARIA, confirming the interactions between the two proteins. Protein extracts were indicated by staining with Coomassie-brilliant blue (CBB). **d)** Diagram of ARIA showing the different arm repeats and BTB/BOZ domain. The numbers

below indicate the position within the amino acid sequence (total length 710 aa). The figure was generated using the EMBL domain protein annotation tool SMART (http://smart.embl.de) (Letunic and Bork, 2018).

From its structural domains, ARIA has been characterised as an arm repeat protein. Armadillo (arm) repeat is a 42-amino acid protein-protein interaction motif (Andrade et al., 2001), which in Eukaryotes is involved in cell signalling or cellular architecture. In addition, ARIA has another conserved sequence motif, BTB/POZ (broad complex, tramtrak, and bric-a-brac/poxvirus and zinc finger) domain, in the C-terminal region (Figure 4.4d) (Kim et al., 2004b). This domain is found in many transcription factors and in some actin-binding proteins in animals (Aravind and Koonin, 1998, Collins et al., 2001). In *Caenorhabditis elegans*, the BTB domain has been reported to act as a substrate-specific adapter for the CUL-3-based E3 ubiquitin ligases (van den Heuvel, 2004). Although arm repeat and BTB domain proteins play diverse roles, the basic functions of the two motifs are to mediate protein-protein interactions. As a consequence, it is predicted that ARIA has the potential to form complexes with other proteins or to function as a scaffold (Kim et al., 2004b). In fact, two other proteins have been identified as ARIA interactors through Y2H assays. One of those proteins is ADAP, which contains two AP2 domains and regulates seed germination, growth, responses to salt and drought and overall ABA responses (Lee et al., 2009). The second interactor, AtNEK6, is a protein kinase involved in epidermal cell morphogenesis, plant growth regulation, responses to ABA and high osmolarity during the seed germination stage (Lee et al., 2010a).

The Y2H screen performed by Alexia Tornesaki identified a novel interactor of HAG4 and showed that HAG4 does not interact with bHLH91 or ARIA (Figure 4.5). MD2B and At4g03250 were included in the plate assay because they were positive hits in the liquid culture screening. However, these false positive interactions were not confirmed in further assays.

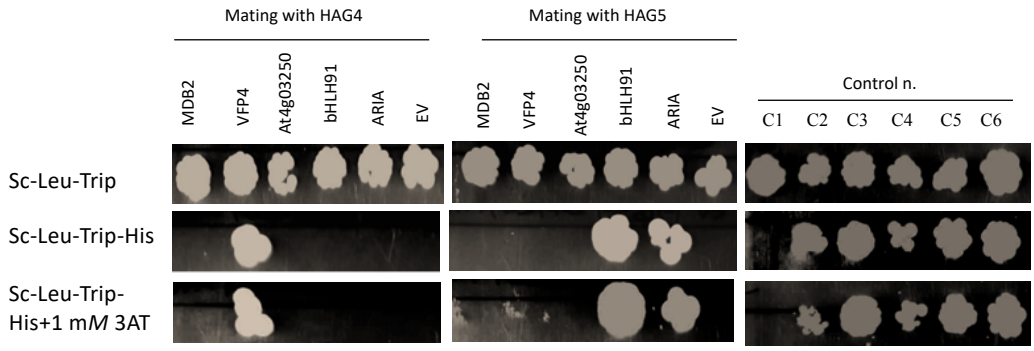

Figure 4.5. Phenotypes of Y2H interactions between HAG5, HAG4 and four different transcription factors. Matings with yeast transformed with the same EV bearing the TF library were included as negative controls to test for autoactivation. The controls consist of four strains C1–5, each containing a different pair of DB-X and AD-Y hybrid proteins. C1: negative control; C3, C4, C5: positive controls as described in (Dreze et al., 2010). This assay was performed by Alexia Tornesaki.

As seen in Figure 4.5, HAG4 interacts with VPF4, a member of the GeBP/GPL family of leucine zipper transcriptions factors. VFP4 acts as an activator of defence responses and gets targeted by the F-box proteins from *A. tumefaciens* VirF and VBF (Garcia-Cano et al., 2018). These exclusive interactions with TFs involved in pant development, defence and stress responses give further support to the hypothesis regarding the evolutionary diversification between *HAG4* and *HAG5*.

In this chapter we will further investigate the nature of ARIA-HAG5 interaction, trying to elucidate the role of this HAT in modulating ARIA or even ABF2 activity through either histone acetylation or scaffolding with transcription factors.

4.1.4. Roles of abscisic acid in plant development and stress responses

Phytohormones regulate numerous important biological processes in plant development and biotic and abiotic stress responses. In section 1.4.4 of Chapter 1, the role of ABA in regulating plant drought responses has been extensively reviewed. Besides being crucial for abiotic stress responses, ABA is a phytohormone involved in many aspects of plant development. In fact, this plant hormone affects seed

maturation, germination, seedling growth, stomatal regulation, pathogen responses, flowering, and senescence (Finkelstein, 2013) (Figure 4.6).

Figure 4.6. Diagram of developmental processes and stress responses regulated by the phytohormone abscisic acid (ABA). ABA is a negative regulator of seed dormancy, and it is produced during germination. ABA negatively regulates root and shoot growth. This hormone also triggers senescence in ethylene dependent and independent manners and is known to be involved in stress responses. ABA synthesis is promoted during abiotic stress such as drought, high salinity and cold. ABA also plays a role in regulating biotic stress responses through the control of stomata opening upon pathogen perception and hormonal cross-talks with SA and JA. Reviewed by (Vishwakarma et al., 2017).

During the early phase of seed development, ABA is synthesised to promote embryo growth, but high ABA levels in later developmental phases inhibit embryo growth by suppressing gibberellin signaling (Finkelstein et al., 2002).

In terms of the roles of ABA in plant growth, this hormone affects the development of the root system, which is of great importance for both plant stress response and nutrient absorption. The key phytohormone that regulates root growth is auxin, especially in the maintenance of the root stem cell niche (Aida et al., 2004). However, ABA and gibberellic acid (GA) are also involved in the control of root development. A previous study revealed that low concentrations of ABA enhanced quiescence of the quiescent centre and suppressed stem cell differentiation in the primary root meristem in Arabidopsis (Zhang et al., 2010). An earlier study showed

that ABA promoted the transcription of *ICK1/KRP1*, which encodes a negative regulator of the cell cycle, suggesting that ABA delays cell expansion and proliferation (Wang et al., 1998). Exposing seedlings to high concentrations of exogenous ABA, as well as the accumulation of ABA resulting from abiotic stress, inhibits Arabidopsis primary root growth. However, the molecular mechanisms involved in this process are not fully understood. Recently, the Gong lab showed that the ethylene biosynthesis inhibitor L-alpha-(2-aminoethoxyvinyl)-glycine reduced ABA-mediated root growth inhibition. These results imply that ABA inhibits root growth by promoting ethylene biosynthesis (Luo et al., 2014).

The regulation of flowering time during the plant life cycle is crucial for growth and survival, especially under adverse environmental conditions. The role of ABA in the regulation of flowering time at the molecular level was first clarified by a study showing that the SnRK2 kinases that transduce the ABA response, phosphorylate flowering time regulators. Supporting this idea, the authors observed that the *snrk2.2/2.3/2.6* triple mutant, which lacks key kinases responsible for acetylating downstream TFs in the ABA signalling pathway, has an early flowering phenotype (Wang et al., 2013a). An increase in ABA can also induce overexpression of the ABA-insensitive *ABI5*, which also delays floral transition, suggesting that ABA inhibits flowering (Wang et al., 2013c). A more recent study reported that *ABSCISIC ACID-INSENSITIVE 4* (*ABI4*), a key component in the ABA signalling pathway, directly promotes *FLOWERING LOCUS C* (*FLC*) transcription, negatively regulating floral transition (Shu et al., 2016). The drought-escape response is a mechanism by which drought stressed plants shorten their life cycle to produce seeds before the severe stress is fatal (Riboni et al., 2013). Even though the molecular basis of this response is still unknown, the flower promoter gene *GIGANTEA* and the florigen genes *FLOWERING LOCUS T* and *TWIN SISTER OF FT* have been identified as flowering promoter factors under these stress conditions. In fact, ABA is required to positively regulate flowering under long day conditions by promoting the expression of these genes in an ABA and photoperiod dependent manner (Riboni et al., 2013). As a consequence, the contribution of ABA to the control of flowering time is still controversial, and more evidence is required to establish whether ABA acts as a positive or negative regulator in the transition between the vegetative to the reproductive stage.

One of the most well-studied processes regulated by ABA is stomata closure. Water loss in plats occurs primarily through the stomata, which are required for gas exchange. Under drought conditions, ABA synthesis is stimulated and the phytohormone accumulates in the guard cells. ABA signalling then activates the efflux of anion and potassium ions via membrane proteins. As a consequence, guard cell turgor pressure and volume decrease, leading to stomatal closure and preventing water loss and CO_2 influx and assimilation (Mori et al., 2006). Foliar bacterial plant pathogens colonise host tissue trough natural surface openings, such as stomata (Melotto et al., 2006). Thus, stomatal closure also serves as a mechanism of plant defence, since it prevents bacteria from colonising the plant. In fact, the bacterial pathogen *P. syringae* DC3000 uses the virulence factor coronatine to actively open stomata (Melotto et al., 2008). Coronatine is a phytotoxin secreted by virulent strains of *Pseudomonas syringae p.v. tomato* which mimics JA activating JA signalling and reopening stomata, counteracting plant defence mechanisms to prevent bacterial colonisation through such openings (Melotto et al., 2006). However, this mechanism remains controversial, since exogenous MeJA does not antagonise ABA-dependent stomatal closure (Montillet et al., 2013). In fact, it has been proposed that 12-OPDA (12-oxo-phytodienoic acid), a precursor of JA, is the responsible of promoting stomatal closure in response to drought (Savchenko et al., 2014).

The role of ABA in biotic stress responses has been further characterised throughout the years. However, the role of this hormone in Arabidopsis defence against *P. syringae* differs depending on the stage of infection. At the early post-invasive stage of the disease, ABA supresses callous deposition and SA-mediated plant resistance, enhancing plant susceptibility (De Torres-Zabala et al., 2007). In contrast, prior to bacterial colonisation, ABA promotes resistance to bacterial infection by favouring stomatal closure (Cao et al., 2011).

In vegetative tissues under osmotic stress conditions, ABA-dependent and ABA-independent signaling pathways function cooperatively to induce a large number of genes involved in signal transduction and stress tolerance (Yoshida et al., 2019), diverting resources away from growth to enhance stress tolerance. The biological functions of ABA have mostly been studied in the context of osmotic stress and seed dormancy. However, ABA also modulates growth under non-stress conditions. Endogenous ABA is associated with the maintenance of shoot growth in

Arabidopsis and tomato (*Solanum lycopersicum*) (LeNoble et al., 2004). In the following section, we will describe the usage of exogenously applied ABA to investigate its effects on seed germination and root growth in *hag5* mutants.

4.2. *hag5* mutants are less sensitive to ABA

Given the role of ARIA as a positive regulator of ABA responses, we investigated whether *hag5* and *aria* mutant plants display similar phenotypes in response to the phytohormone. Lack-of-function *aria* mutants are bigger plants and less sensitive to ABA and glucose treatments (Kim et al., 2004a). In section 3.2 of the previous chapter we discussed the developmental phenotypes of *hag5*, which are indeed bigger plants. ABA is a negative regulator of plant growth, and it also plays a central role in regulating seed dormancy and inhibiting the transition from embryonic to germination growth (Rodríguez-Gacio et al., 2009). As seen in Figure 4.7a, when treated with exogenous ABA wild type seeds suffered from germination arrest, but a significant percentage of *hag5-1* and *hag5-2* mutant seeds were able to proceed to radicle formation even under increasing concentrations of ABA (Figure 4.7b). These results demonstrate that *hag5* mutants, like *aria* mutants, are less sensitive to ABA.

Generally, ABA is functioning as an negative regulator of shoot and root growth of plants under well-watered conditions (Sharp and Lenoble, 2002). However, under water scarcity, root-specific activation of ABA signalling promotes root growth towards soil exploration, which suggests that ABA can modulate root architecture to adapt to the environmental stress conditions (Li et al., 2017b). In fact, although auxin is considered the primary hormone regulating root meristem function, ABA modulates cell division and elongation in the root meristem (Petricka and Benfey, 2008). In the previous chapter (section 3.2), the root growth dependency on the cell division/growth in the meristematic and elongation zones respectively was described. ABA has been reported to promote quiescence of the quiescent centre and to supress cell differentiation in the Arabidopsis root meristem, in order to maintain the stem cell population (Zhang et al., 2010). ABA regulates root growth by directly regulating the population of dividing cells in the root tip. Li et al., studied the biphasic root growth response to ABA in Arabidopsis, which depends on the concentration of ABA and the environmental conditions, and involves cross-talk with ethylene and auxin signalling

pathways (Li et al., 2017b). In that study, the authors determined that low concentration of ABA such as 0.1µM promote root growth, whilst 1µM and 10µM of ABA result in root growth inhibition. Based on these findings, the concentration used in this report for assessing root growth inhibition is 5µM of ABA.

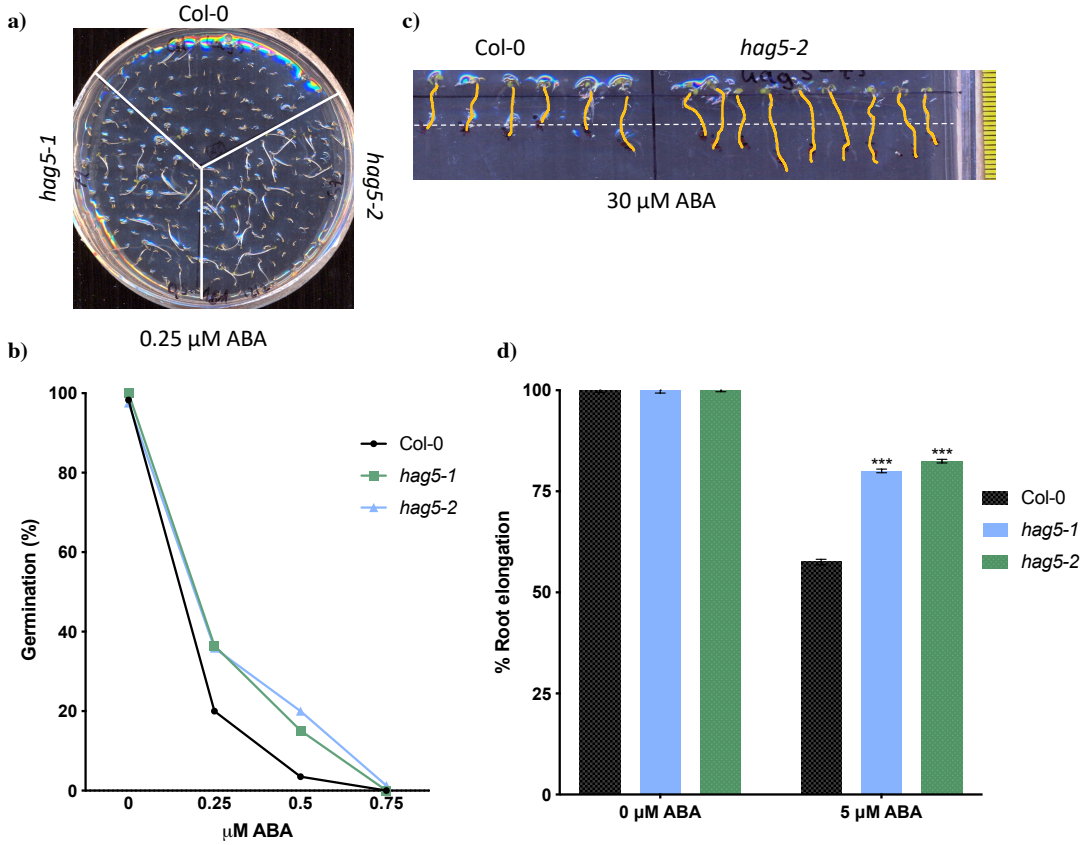

Figure 4.7. *hag5* mutants are less sensitive to exogenously applied ABA. **a)** Germination of Col-0, *hag5-1* and *hag-2* mutants in ½ MS media supplemented with 0.25µM of ABA. Seedlings were grown in short photoperiod for 4 days and transferred to dark conditions for 3 days before pictures were taken. **b)** Germination percentage of Col-0, *hag5-1* and *hag5-2* seeds germinated in MS plates supplemented with 0, 0.25, 0.5 and 0.75µM of ABA. Measurements were taken at day 4 (n = 40). **c)** Root length of Col-0 and *hag5-2* seedlings in high concentrations of ABA. 4-days-old seedlings were transferred to ½ MS plates supplemented with 30µM of ABA. Pictures were taken 7 days after the transfer. Roots were highlighted using the free-hand tool from ImageJ. **d)** 7 day old seedlings were transferred to media supplemented with 0 or 5µM of ABA and grown vertically for 12 days after germination. Root elongation was measured for each genotype, condition and time point using ImageJ (https://imagej.net). The growth rate in the treatment plates was calculated as a percentage of the root growth that took place in the control plates (no ABA). Error bars represent. SD (n = 20). Statistical testing: one-way ANOVA, *** $P \leq 0.001$.

In order to characterise the effects of ABA in root growth, 4-days-old seedlings were germinated horizontally in ½ MS plates and transferred to ½ MS media or ½ MS media supplemented with 5µM of ABA (Figure 4.7d). The seedlings were then grown vertically for 10 days and the root length was measured daily to estimate growth rate. As seen in Figure 4.7d, the root growth rate in Col-0 seedlings decreases to 60% in the presence of ABA, whilst in both *hag5* mutants is around 80% when compared to mock conditions. Even when increasing ABA concentration to 30µM, roots of *hag5-2* seedlings were visible longer than those in Col-0 (Figure 4.7c). Since ABA is a negative regulator of germination and growth, these results show that *hag5*, like *aria* mutants, are less sensitive to ABA, implying that they are positive regulators of ABA responses.

4.3. HAG5 participates in the activation of downstream genes in the ABA signalling pathway

ABA induces the expression of many genes whose products are important for stress responses and tolerance, such as enzymes for osmoprotectant synthesis (Fujita et al., 2011). Transcriptome studies have shown that over 50% of the genes regulated by ABA are also differentially expressed by drought or salinity. In a microarray study by Seki et al, 245 ABA-inducible genes were identified in Arabidopsis. Amongst the ABA-inducible genes, 63% (155 genes) were induced by drought, and 54% (133 genes) by high salinity (Seki et al., 2002). These results indicate a significant overlap between ABA response and abiotic stress signalling pathways, especially drought and high salinity.

Since H4K5 acetylation is the only known function of HAG5 to date, we hypothesized that the differential phenotypes under ABA treatment were due to a transcriptional miss-regulation of ABA responsive genes. To test this hypothesis, we selected genes known to be regulated by ARIA and/or ABF2 in an ABA-dependent manner (Kim et al., 2004b, Kim et al., 2004a), as well as genes that belong to different stages of the ABA signalling cascade (Table 4-1).

Table 4-1. List of ABA responsive genes used for qPCR analysis of mock and ABA treated samples. The primer sequences used for each gene can be found in section 2.9.5 of Chapter 2.

Name	GENE ID	Gene description	Position in the ABA response pathway
RAB18	AT5G66400	ABA, cold and drought induced dehydrin. Plays a protective role during cellular dehydration.	ABA downstream signalling pathway induced by ABF2
RD29A	AT5G52310	Induced by ABA, cold and drought stresses The cis-acting region of the rd29A promoter contains three dehydration-responsive elements (DRE) and one abscisic acid responsive element (ABRE).	ABA downstream signalling pathway induced by ABF2
RD29B	AT5G52300	Induced in response to ABA triggered by water deprivation, cold, high-salt and drought. The promoter region contains two ABA-responsive elements (ABREs).	ABA downstream signalling pathway induced by ABF2
CYP707A2	AT2G29090	Encodes a protein with ABA 8'-hydroxylase activity. Involved in ABA catabolism, it plays a major role in the rapid decrease of ABA levels during early seed imbibition.	ABA hydrolase

We treated 14-days-old seedlings with 50μM of ABA for 7h and quantified the expression of the selected genes by qPCR as described by (Kim et al., 2004b) and in section 2.9.5 of Chapter 2. Following treatment, genes downstream the ABA signalling pathway (*RAB18, RD29A, RD29B*) and an ABA hydrolase (*CYP707A2*) are only partially upregulated in the *hag5-2* mutant in comparison with Col-0 plants (Figure 4.8a). Since HAG5 is partially responsible of the upregulation of at least some ABA responsive genes, we next tested the expression of *HAG5* after ABA induction in Col-0 plants (Figure 4.8b). *HAG5* is upregulated upon ABA induction (Figure 4.8b), which further suggests that HAG5 has a role in modulating ABA responses.

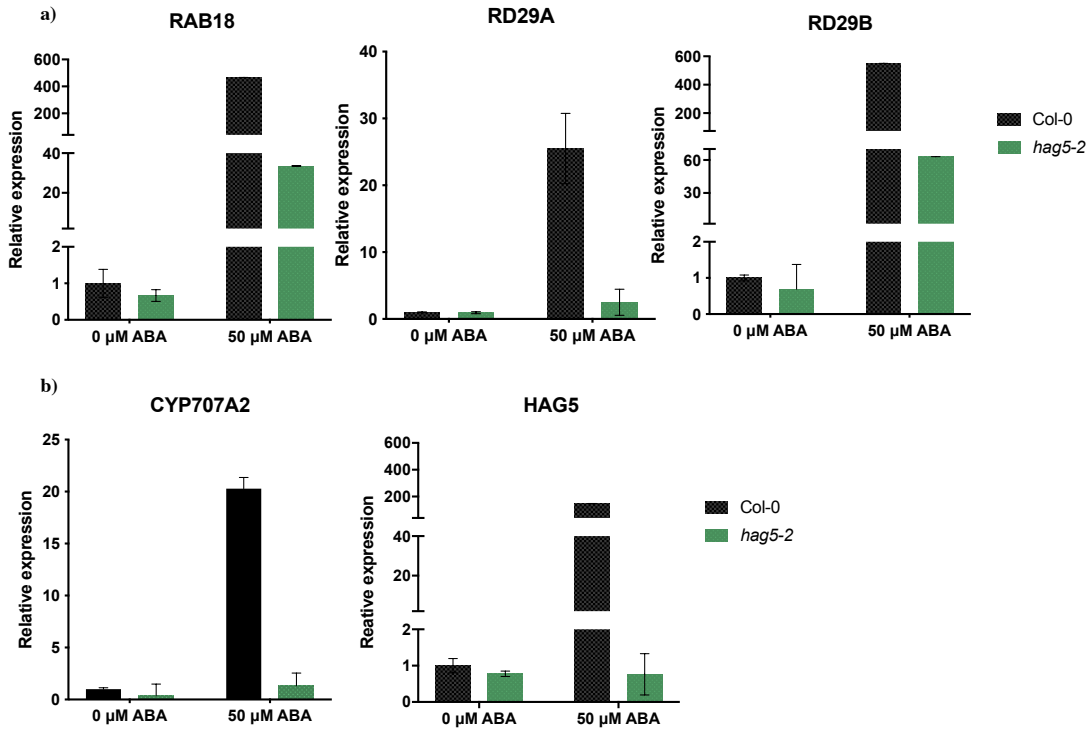

Figure 4.8. *hag5-2* mutants have a weaker transcriptional response to ABA treatments. **a)** Expression of ABA marker genes (*RAB18*, *RD29A* and *RD29B*) after ABA treatment. **b)** Expression of the ABA hydrolase *CYP707A2* and *HAG5* after ABA induction. In all cases, 15 day old seedlings were treated with 0 or 50µM of ABA for 7h. The relative expression was normalised against the house keeping gene *α-tubulin*. The primer sequences used for each gene can be found in section 2.9.5 of Chapter 2. Error bars represent SD between technical replicates (n = 3). The experiment was repeated three times, and the trends in gene expression were conserved between biological replicates.

The partial up-regulation of those ABA marker genes upon treatment in *hag5-2* mutants led us to question whether there was an insensitivity or a delay in the transcriptional response of these mutant plants. To address this question, we analysed the expression of *RAB18*, a gene regulated by ABF2, at 0, 1, 3 and 7h after treatment with mock or 50µM of ABA.

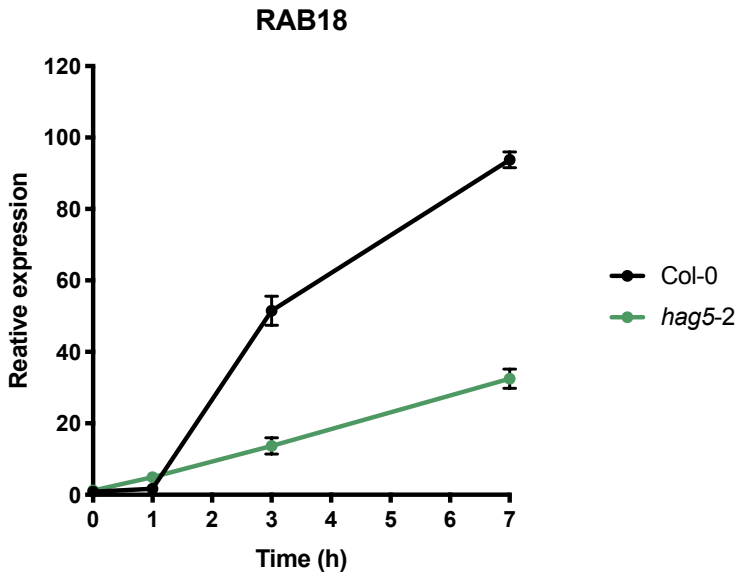

Figure 4.9. *hag5-2* mutants have delayed transcriptional response to ABA. Expression of *RAB18* in Col-0 and *hag5-2* plants at 0, 1, 3 and 7h after treatment with 50μM of ABA. The relative expression was normalised against the house keeping gene *α-tubulin*. Error bars represent SD between technical replicates (n = 3).

The time-course qPCR results in Figure 4.9 show that there is a delay in the up-regulation of *RAB18* in *hag5-2* mutants. Whilst *RAB18* expression rapidly increases in Col-0 after 3h of ABA treatment, the increment of expression in *hag5-2* mutants is slower. However, later data points would provide further information about the timing of peaking and decreasing of this transcriptional response in Col-0 plants and reveal whether *RAB18* expression in *hag5-2* follows a similar trend or is shifted. Overall, this data conveys into the idea of HAG5 being a positive regulator of the ABA downstream signalling pathway, with a role on fine-tuning the timing of the transcriptional response through its interaction with ARIA and/or ARIA-ABF2 complex.

In order to fully characterise the transcriptional response of *hag5-2* mutants to ABA, we performed an RNA-seq experiment that will be further discussed in Chapter 5 of this thesis.

4.3.1. Measuring ABA content in *hag5* mutants

Differences in ABA content due to miss-regulation of ABA biosynthesis or hydrolysis can result in different transcriptional responses to the hormone. In order to

justify that the different transcriptional response to ABA observed in *hag5-2* mutants is due to signalling events downstream of the ABA response pathway, ABA content of *hag5-2* and Col-0 seedlings was determined as described in Chapter 2, section 2.7.4. Mutants of known ABA regulators such as *snrk2.2/2.3* (positive regulator) and *brm-3* (negative regulator) were included in the assay as controls. Indeed, the SWItch/Sucrose Non-Fermentable (SWI2/SNF2) chromatin remodelling ATPase BRAHMA (*BRM*) is known to act as a transcriptional repressor of *ABI5* during post-germination development. ABI5 is a TF that mediates ABA-dependent growth repression, seed germination and seedling growth (Skubacz et al., 2016). BRM decreases accessibility of the genomic DNA by promoting high occupancy of a well-positioned nucleosome at the *ABI5* locus (Han et al., 2012). As a consequence, BRM is a negative regulator of ABA signalling, and the observed mutant phenotypes (ABA hypersensitivity, growth repression and drought tolerance) are not related to differential ABA content.

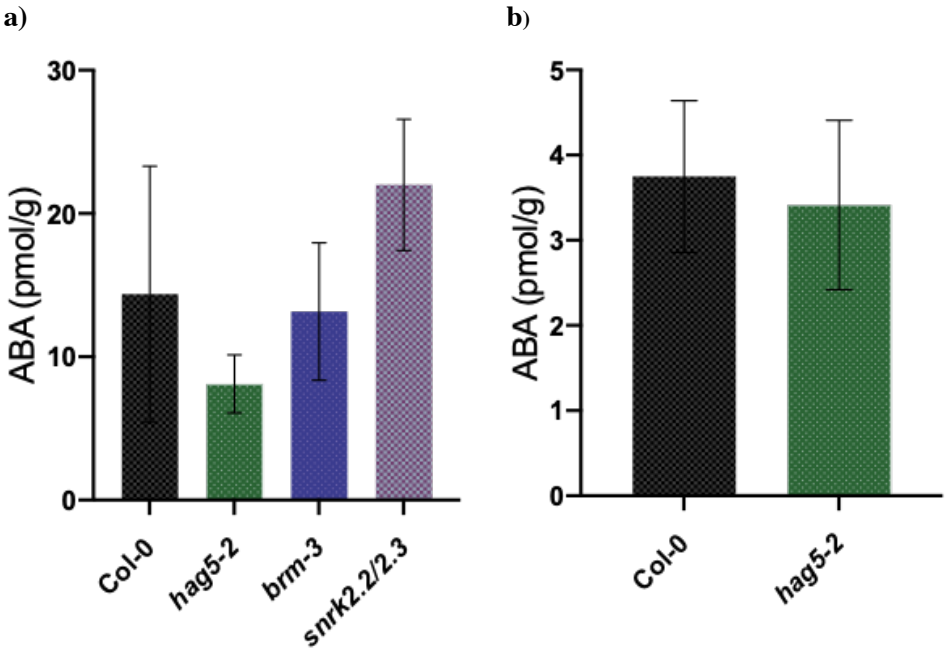

Figure 4.10. ABA content of Col-0 and *hag5-2* seedlings. **a)** First biological replicate, featuring Col-0, *hag5-2* and *brm-3* (SALK_088462, (Farrona et al., 2007)) and *snrk2.2/2.3* mutants (Fujii et al., 2007) as controls. **b)** Second biological replicate of ABA content measurements in Col-0 and *hag5-2* mutant. Error bars indicate SD (n = 3). One-way ANOVA and Student T-test were performed, with no significant differences identified between samples. ABA content was determined by HPLC-ESI-MS/MS as described by (Bacaicoa et al., 2011). Plants were grown by Dr. Selena Gimenez-Ibanez and experimental

procedures, carried out by Jose Maria García Mina and Dr. Ángel María Zamarreño.

SnRK2.2 and SnRK2.3 are activated by ABA and can phosphorylate the ABA-responsive b-ZIP transcription factors, which are important for the activation of ABA-responsive genes (Fujii and Zhu, 2009). In a study by Fuji et al., the *snrk2.2/2.3* double mutant was characterised as ABA insensitive, and the authors concluded that SnRK2.2 and SnRK2.3 are positive regulators of ABA signalling. In basal conditions *snrk2.2/2.3* double mutant is published to contain similar ABA levels than Col-0 (Fujita et al., 2009), indicating that SnRKs are likely involved in signalling instead of ABA biosynthesis or hydrolysis.

As seen in Figure 4.10a, there are no significant differences in ABA content between genotypes. The second biological replicate performed only between Col-0 and *hag5-2* mirrored these results, with no differences at basal state. These results indicate that HAG5 is not involved in ABA accumulation, and that the ABA insensitivity and transcriptional delay in *hag5* mutants are due to the role of HAG5 in ABA signalling and response.

4.4. *hag5* mutants are more tolerant to drought

ABA regulates biotic and abiotic stress responses as well as other aspects of plant development under non-stress conditions. Either by itself or through cross-talk with other hormones, ABA participates in seed maturation and germination, vegetative growth, stomatal regulation, pathogen responses, flowering, and senescence (Finkelstein, 2013). But most importantly, ABA is a messenger that acts as the signalling mediator for regulating the adaptive response of plants to different stresses (Sah et al., 2016). Thus, ABA is a crucial factor that controls stress responses through many layers of regulation. These include the transcriptional response through the activity of core transcription factors regulated by ABA, the regulation of ABA metabolism, transport and post-transcriptional and post-translational regulation of metabolic regulators.

When facing a stress, the levels of ABA in the plant increase via ABA biosynthesis. Water shortage, high salinity and extreme temperatures are some of the

stresses that trigger ABA biosynthesis (Zhu, 2002). Then, the increased ABA binds to its receptor to initiate signal transduction, which results in cellular responses to stress (Ng et al., 2014). Salt and drought stress signal transduction consists of ionic and osmotic homeostasis signalling pathways, detoxification response pathways, and pathways for growth regulation (Zhu, 2002).

Since we identified ARIA as a transcription factor interacting with HAG5, we decided to test *hag5* mutants for ABA-related phenotypes such as drought tolerance. There are many ways to assess drought tolerance in plants. One common experiment is to subject 5-weeks-old Arabidopsis plants to drought by withdrawing watering for 2-3 weeks, and re-watering afterwards in order to allow the surviving plants to recover (Figure 4.11a). When *hag5* mutant plants were subjected to drought and re-watered, a higher percentage of plants recovered when compared to Col-0 (Figure 4.11b). ABA regulates stomatal aperture, which is required to limit water loss from leaves under drought conditions through regulation of water transpiration (Kim et al., 2010). To assess transpiration rates in the different genotypes, we measured water loss rates and standardised water contents of whole rosettes after detachment (Figure 4.10c) following published protocols (Fujita et al., 2011).

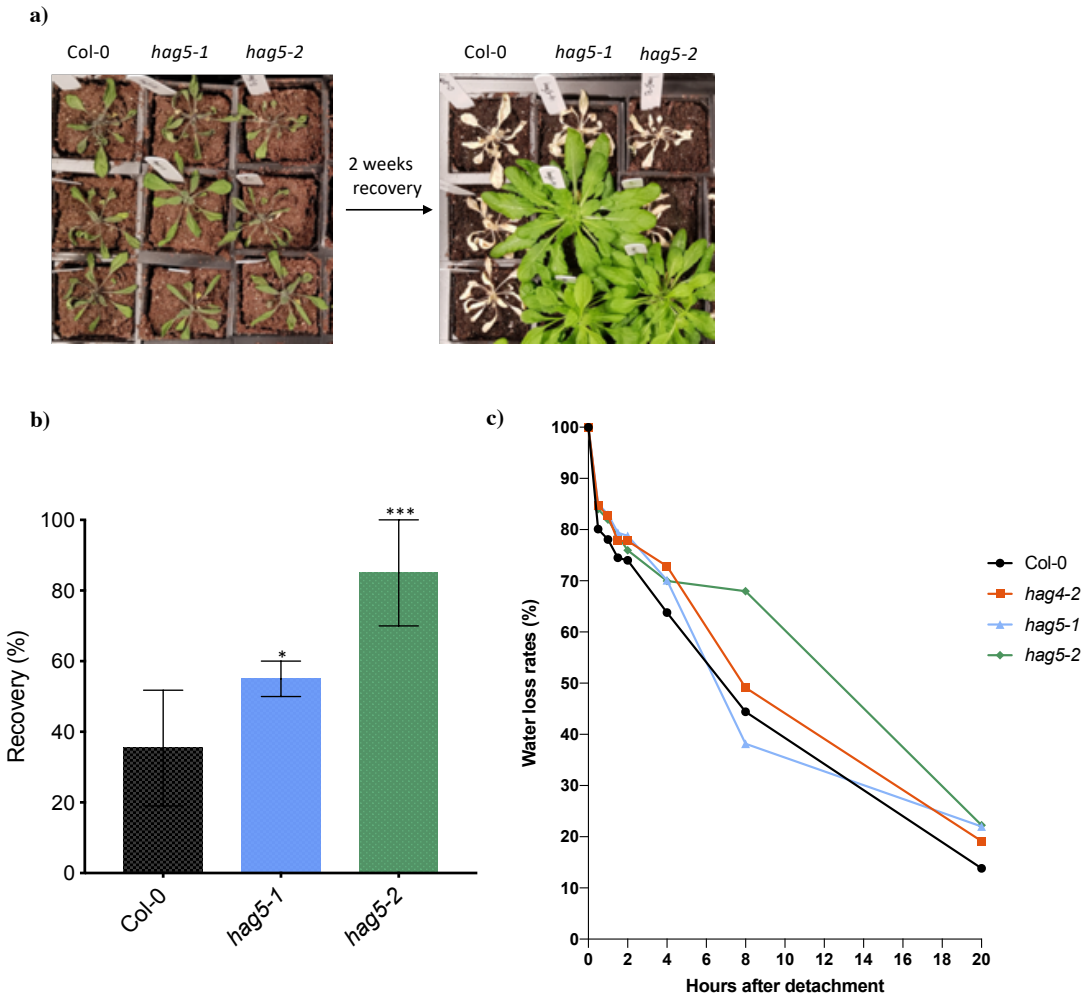

Figure 4.11. *hag5* mutants are more tolerant to prolonged drought stress. **a)** Pictures of 5-weeks-old Col-0, *hag5-1* and *hag5-2* plants withheld from watering for 14 days (left) and after 2 weeks of recovery through watering (right). **b)** Percentage of recovery calculated from 3 independent drought experiments. Error bars represent SD (n = 12). Statistical testing: one-way ANOVA, * $P \leq 0.05$, *** $P \leq 0.001$. **c)** Analysis of plant-water relations in Col-0 and *hag4* and *hag5* mutants. Water loss and final water content were measured as described (Yoshida et al., 2002; Fujita et al., 2005), with minor modifications. Aerial parts from 5-week-old soil-grown plants were excised and weighed to determine fresh weight over time. Detached aerial parts were then dried to determine dry weight. Water content was standardized as a percentage relative to the initial water content of aerial parts of the plant. Water content was calculated as [(FWi – DW)/(FW0 – DW)] * 100, where FWi and FW0 are fresh weight for any given interval and original fresh weight, respectively, and DW is dry weight. Final water content was determined at 20h post-detachment.

As seen in the figure above, there are no differences in the water-loss rate between genotypes in the first hours after detachment. However, *hag5-2* mutants' water-loss rate remains stable 8 hours post-detachment. Even though measurements

in further time points would give more insight into the water-loss dynamics of *hag5-2* mutants, these results show that these mutants' rosettes suffer a lower degree of dehydration over time, which might explain the increased survival rate of the mutants. However, there are other factors such as stomatal density and root length, as well as the regulation of the transcriptional response to drought that play a role in drought tolerance. As a consequence, a detailed analysis of stomatal closure in *hag5* mutants upon stress is required to determine if this mechanism is responsible for, or contributes to the drought tolerance of *hag5* plants, amongst other factors. Furthermore, assessing the ABA content of Col-0 and *hag5* plants after drought would provide additional information on whether HAG5 influences ABA accumulation upon stress resulting in the increased tolerance, or if other mechanisms are responsible for this phenotype.

Assessing drought tolerance in soil is challenging, since there are many different factors that might change the severity of the drought stress amongst replicates sown in different pots. Achieving uniform watering, soil compaction and even relating the water use efficiency to the transpiration rate and size of each genotype can be challenging. Those factors can in fact determine the degree of drought stress that is inflicted upon each individual pot. Consequently, an observed drought tolerant phenotype can be an artefact of milder drought conditions inflicted. Hence, we decided to perform additional drought-response tests by using 1/2 MS plates, where the number of variables that can influence the severity of drought are reduced. To this end, 15 seedlings per row were sown in plates containing exactly 50 ml of solid ½ MS media (Figure 4.12a). The distance between seeds was kept even, and seedlings were let to grow vertically until the water from the media had been consumed and plants started desiccating. Figure 4.12a shows that *hag5-2* mutants kept their turgor and green leaves when experiencing the same degree of drought as Col-0 plants, which complements the previous data regarding the drought tolerance of these mutants.

An even more accurate method for assessing drought is by decreasing the water potential of the media (Ψw) by using polyethylene glycol (PEG)-infused plates (Kumar et al., 2015). Indeed, drought is defined as a decrease in soil water availability, which can be quantified as a decrease in water potential. Mathematically, Ψw is the chemical potential of water divided by the partial molar volume (Kramer, 1995). Decreased Ψw translates into higher difficulty of water uptake by the plant, which then starts an array of responses to either avoid water loss and facilitate water uptake

or to tolerate reduced water content in the tissues (Kumar et al., 2015). In addition, loss of water availability causes a number of rapid stress responses including high levels of ABA accumulation and induction of stress and ABA-regulated genes (Kumar et al., 2015).

Alexia Tornesaki, a PhD student in the lab, prepared the PEG-infused plates pouring a PEG-containing overlay solution on top of the solidified ½ MS plates. As seen in Figure 4.12b, increasing concentrations of PEG result in greater decrease in water potential.

a)

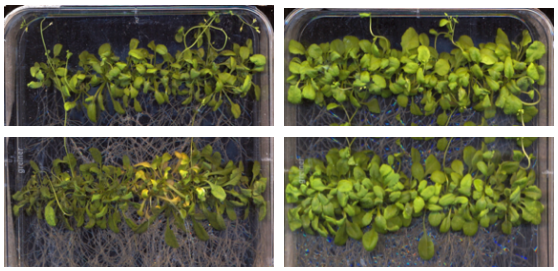

b)

Final water potential of the PEG-infused plate (MPa)[1]	PEG added per liter of media to make the overlay solution (g)[2,3]
-0.25	0
-0.5	250
-0.7	400
-1.2	550
-1.7	700

c)

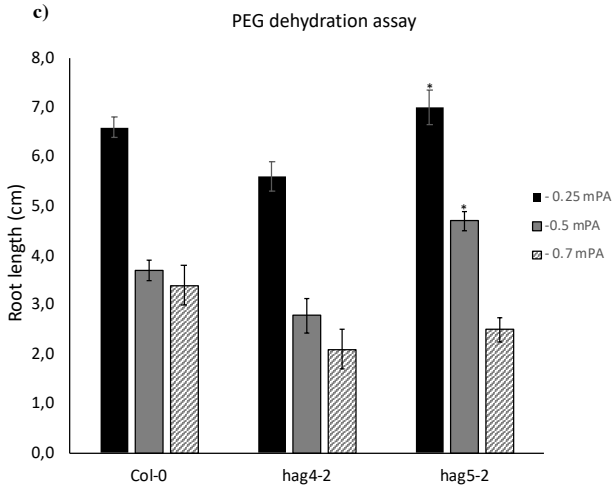

Figure 4.12. Drought phenotypes of *hag5-2* seedlings in plates. **a)** Dehydration in plates. 30 seedlings genotype (15 in each row) were sown in plates containing exactly 50 ml of solid ½ MS 1% sucrose media. The distance between seeds was kept even, and seedlings were let to grow vertically until the water from the media had been consumed and plants started desiccating. **b)** Table indicating the final water potential (Ψw) in MPa achieved in 1/2 MS media infused with different concentrations of PEG. **c)** Col-0, *hag4-2* and *hag5-2* root elongation in ½ MS media with standard (Ψw = -0.25 MPa) or reduced water potential (Ψw = 0.7 MPa). * $P \leq 0.05$ calculated with one-way Anova, for samples that are greater than Col-0. Error bars represent SD (n = 10) Experimental procedures were carried by Alexia Tornesaki as described by (Kumar et al., 2015).

Seedlings of Col-0, *hag4-2* and *hag5-2* were germinated in ½ MS plates without sucrose for 4 days, and then transferred into the PEG-infused plates for a week to quantify root growth. Ψw (-0.25 MPa) corresponds to unstressed conditions, Ψw (-0.5 MPa) mimics mild stress and Ψw (-0.75 MPa) or below correspond to severe drought stress that leads to rapid dehydration of the seedlings. Figure 4.12c shows that under non-stress conditions Ψw (-0.25 MPa), seedling growth in all three genotypes is successful. Under mild drought conditions Ψw (-0.5 MPa), *hag5-2* seedlings root growth arrest was less severe than in Col-0 or *hag4-2*. Finally, all three genotypes display similar levels of root growth arrest under severe drought Ψw (-0.75 MPa).

These results altogether manifest that *hag5-2* mutants have increased survival rate after drought and recovery, longer lasting drought tolerance in plates and less root growth arrest in media with reduced water availability. In addition, once again *hag4* and *hag5* mutants display different phenotypes in response to stress.

The mechanisms at the morphological, physiological, biochemical, cellular and molecular levels that plants have developed in order to overcome water deficit have been extensively studied and reviewed in the section 1.4.1 of Chapter 1. In brief, drought resistance in plants is divided in different strategies: drought avoidance, drought tolerance, drought escape, and drought recovery. Various drought-related traits, including root traits, leaf traits, osmotic adjustment capabilities, water potential, ABA content, and stability of the cell membrane, have been used as indicators to evaluate the drought resistance of plants (Fang and Xiong, 2015). Therefore, HAG5 has role in regulating such mechanisms in a way that negatively affects drought recovery. The mechanisms by which HAG5 regulates drought stress remain partially unknown, but we hypothesize that the slower ABA transcriptional response of *hag5* mutants translates into a delayed commitment to senescence after severe stress. This concept will be developed in the following sections of this chapter, as the nature of the ABF2-ARIA-HAG5 interaction is further tested.

4.5. Using the phenoscope to investigate drought tolerance in *hag5* mutants

Another measure of drought tolerance is to monitor the decrease in growth rate over a prolonged period of time when plants are subjected to mild or severe drought conditions (Tisne et al., 2013). We established a collaboration with Dr. Olivier Loudet from INRA in Versailles (France), using a phenoscope to determine these changes in plant growth under different degrees of drought stress. The phenoscope is a high-throughput phenotyping platform that continuously rotates the individual pots, automatically adjusts watering and images rosette size and expansion rate during vegetative growth (Tisne et al., 2013). This allows for high uniformity of drought conditions applied, avoiding position effects and differential soil watering encountered in other soil-based drought assays. In this high-throughput screening, 200 plants per genotype (Col-0 from phenoscope, Col-0 from Ntoukakis lab and *hag5-2*) were randomised and periodically monitored for rosette growth rate in control and water deprived conditions. Growth conditions (control, mild and severe drought stress) were as described in detail by (Tisne et al., 2013). Briefly, seeds were stratified for 2 days and germinated for 8 days before transferring them to single pots in the phenoscope. Individual plants were then grown on the phenoscope for 15 days under short day photoperiod. During germination, soil was saturated with water. In the first 7 days of growth after transferring onto the phenoscope (Day 9 to 15 after sowing), soil water content was gradually decreased through controlled watering until it reached either 60% (control), 30% (mild stress), 25% (severe stress) or 20% (extreme stress). The respective levels of drought stress were then strictly maintained until day 23 after sowing. Zenithal rosette images of each individual plant were taken daily and segmented as described previously (Tisne et al., 2013) to extract projected rosette area (PRA; a measure of rosette biomass at these development stages), rosette radius (the radius of the circle encompassing the rosette) and compactness (the ratio between PRA and the rosette circle area).

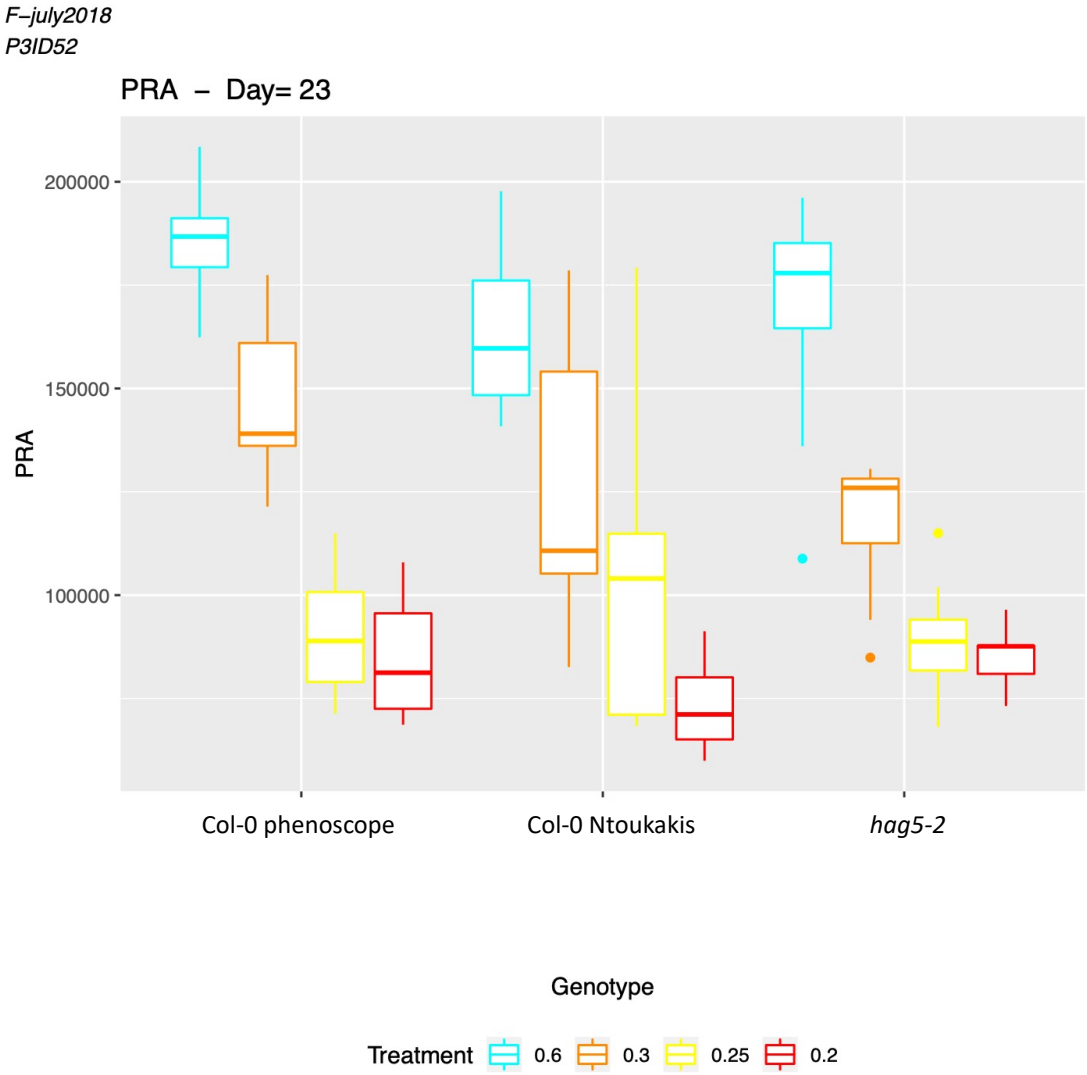

Figure 4.13. Effect of degrees of drought stress in rosette area over time in Col-0 and *hag5-2* mutants. Box plot of the projected rosette area (PRA) of different genotypes on day 23 of the experiment. Colours represent degrees of drought stress: blue = 60% (control), orange = 30% (mild stress), yellow = 25% (severe stress) and red = 20% (extreme stress). n = 23 plants per genotype and watering condition. Error bars represent SD between replicates, and statistical differences were assessed using Tukey test with $P < 0.05$. Measurements of rosette leaf area and data analysis were performed as described in (Tisne et al., 2013).

As seen in Figure 4.13, the PRA at day 23 of plants subjected to the 4 different watering conditions progressively decreases as the severity of drought increases. However, there seems to be no significant differences in rosette area between genotypes. If anything, *hag5-2* mutants seem to be more susceptible under mild

drought (0.3). Interestingly, the mortality rate of plants is lower in the mutants under normal (0.6) and mild conditions (0.3) and higher under more extreme drought (0.2).

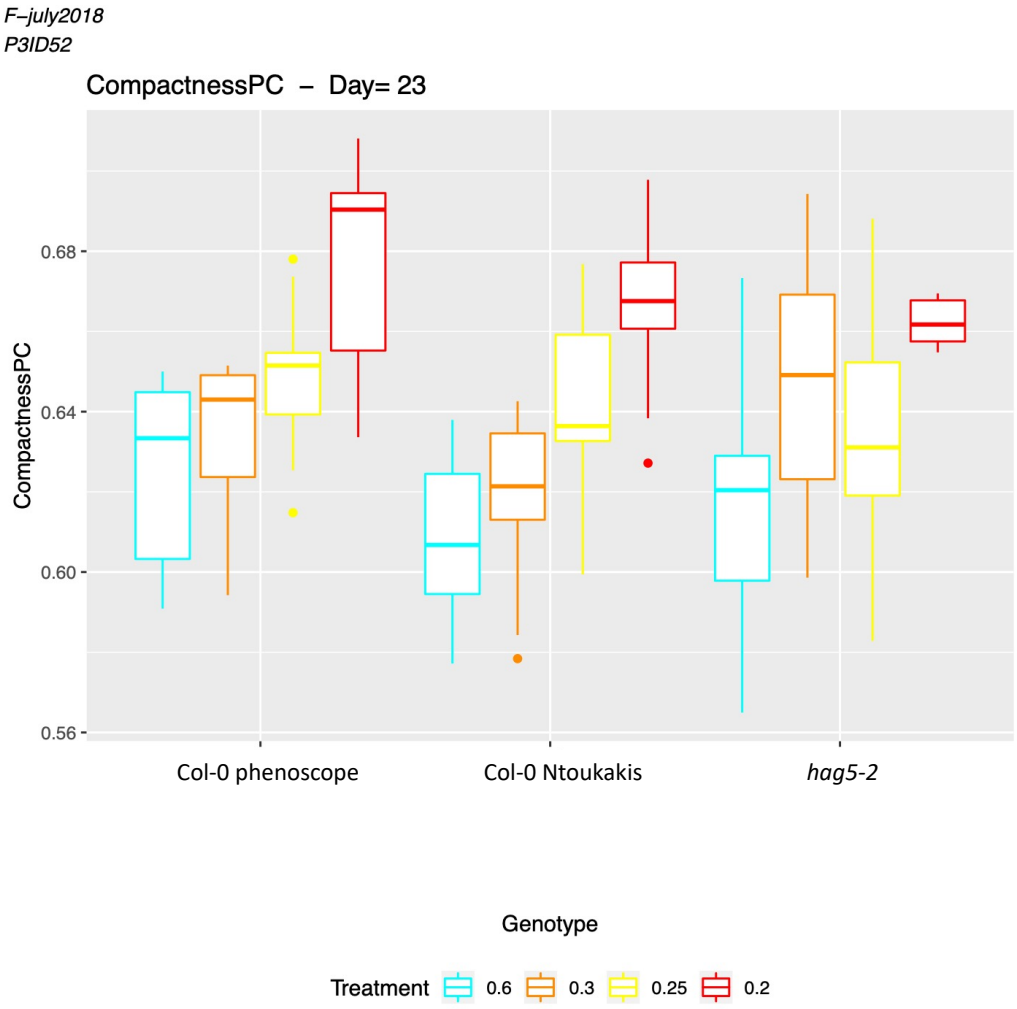

Figure 4.14. Effect of different degrees of drought stress in compactness of Col-0 and *hag5-2* mutants. Box plot of the Compactness (ratio between PRA and rosette circle area) of different genotypes on day 23 of the experiment. Colours represent degrees of drought stress: blue = 60% (control), orange = 30% (mild stress), yellow = 25% (severe stress) and red = 20% (extreme stress). n = 23 plants per genotype and watering condition. Error bars represent SD between replicates, and statistical differences were assessed using Tukey test with $P < 0.05$. Measurements of rosette leaf area and data analysis were performed as described in (Tisne et al., 2013).

The compactness signifies the ratio between PRA and the rosette circle area. Figure 4.14 illustrates no differences between the two control groups (Col-0 phenoscope and Col-0 Ntoukakis). If anything, the linear trend between the increasing

drought conditions gets slightly distorted in *hag5-2* mutants, but overall there are no significant differences between genotypes.

Figure 4.15 shows the relative growth rate (RER) in stress conditions over control in the different phenotypes Figure 4.15a shows the growth rate of plants subjected to mild stress (30%) normalised to the mock conditions (60%). At day 7 there is a decrease in growth rate that restores from day 10 onwards. As seen in 4.15b-c, there is a significant decrease in growth rate on day 7 after the more severe drought conditions are applied (25% and 20%), and there is a recovery period of 5 days until plants reach a steady rosette growth, which still remains below the growth in mock conditions. However, there seems to be no significant differences between genotypes at any point.

a)

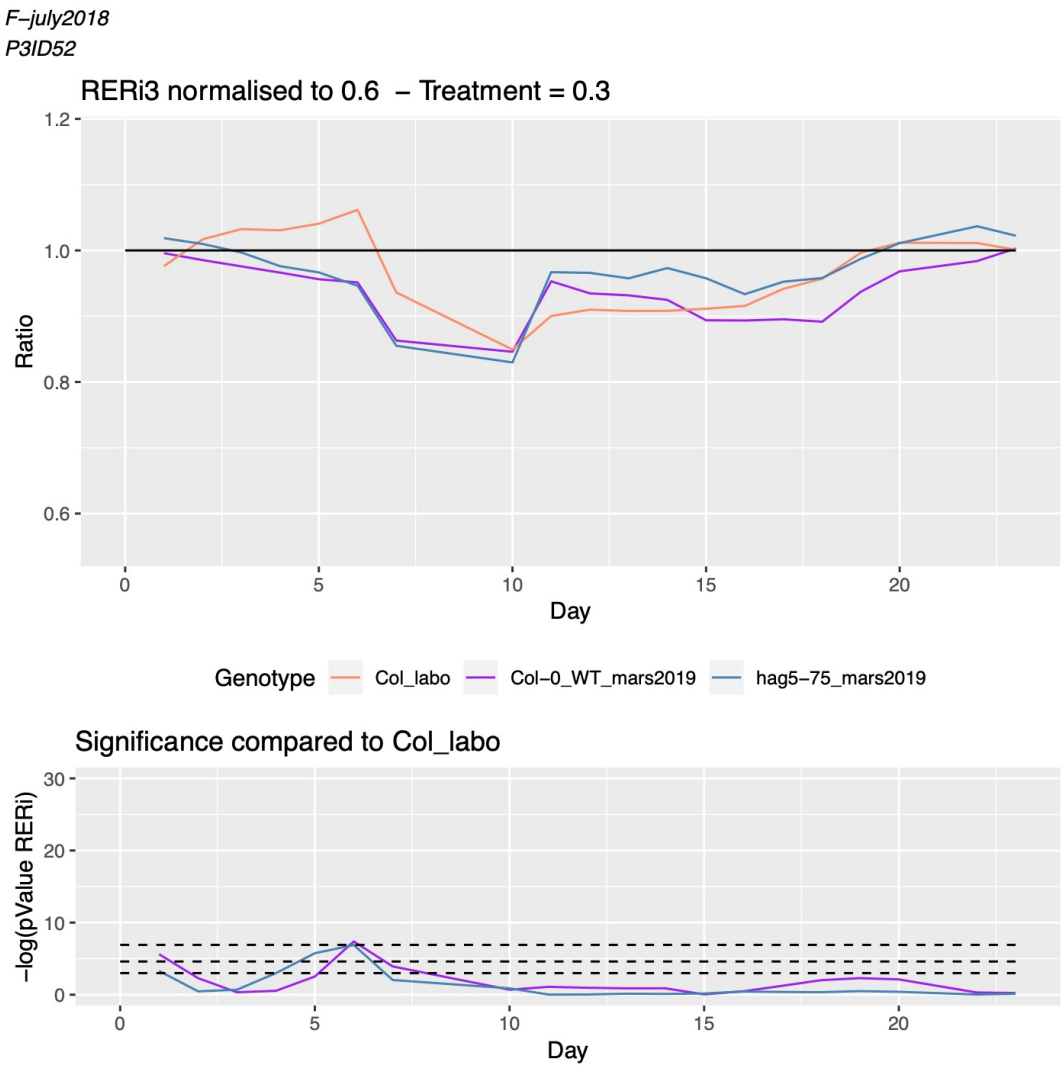

b)

F–july2018
P3ID52

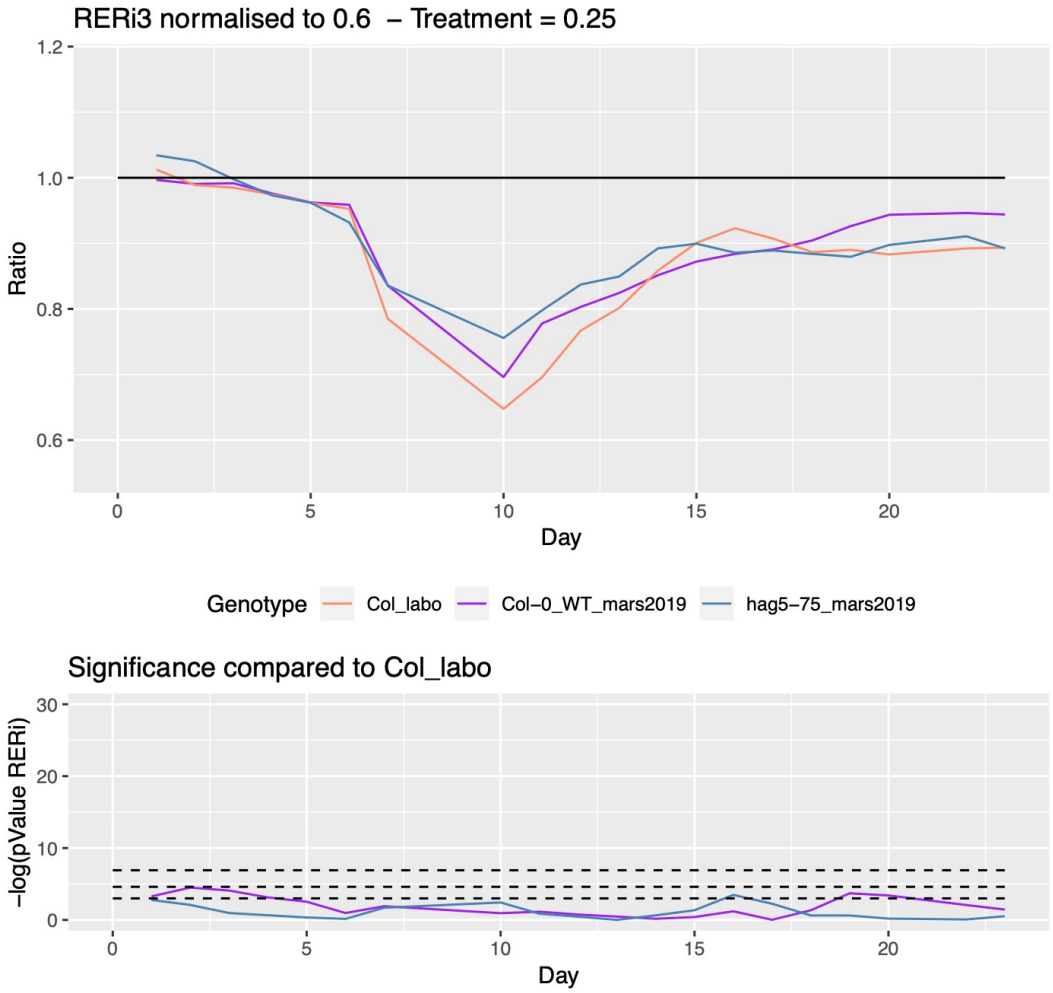

c)

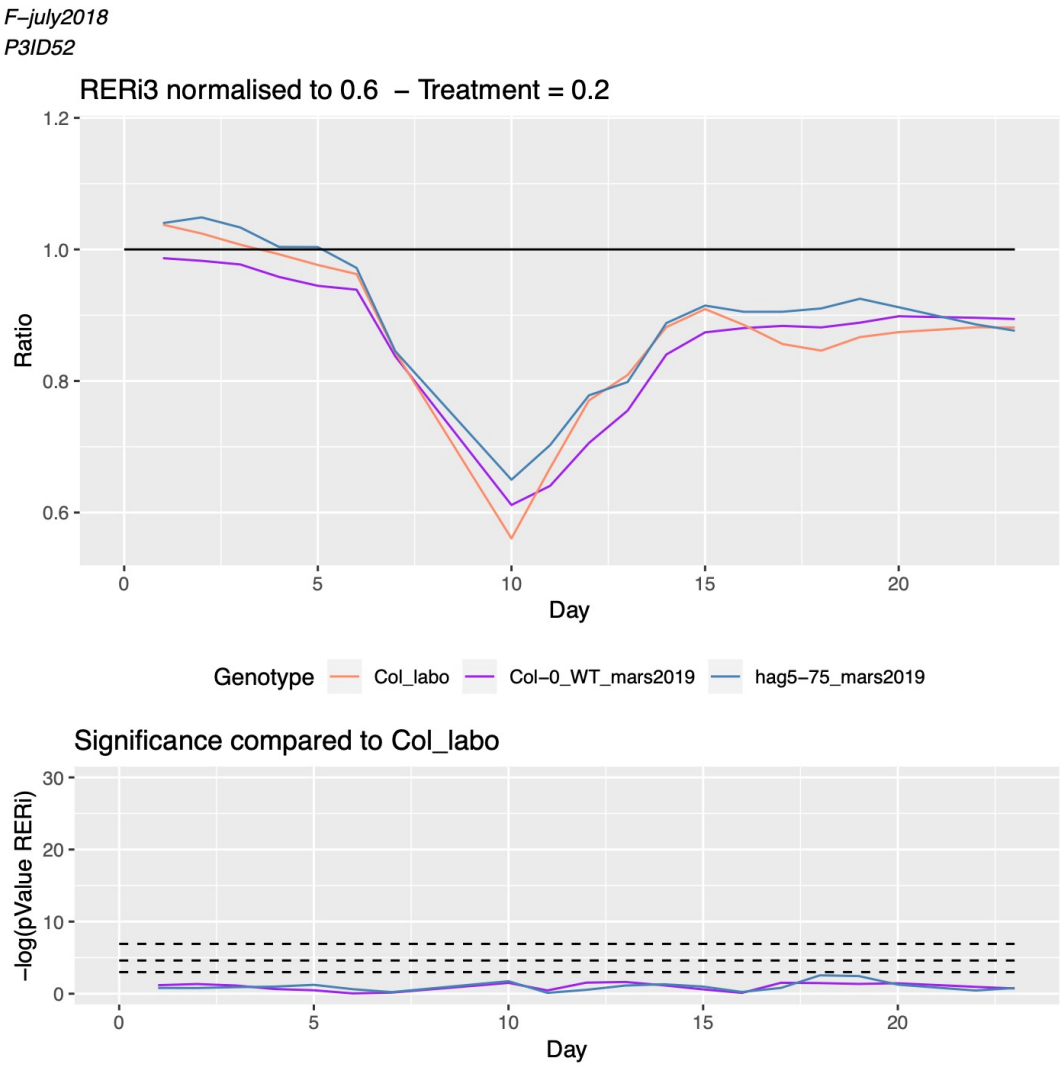

Figure 4.15. Relative growth rate (RER) in different degrees of drought conditions over control conditions of Col-0 and *hag5-2* mutants. **a)** RER in plants watered under mild drought stress (30% watering). **b)** RER of plants under severe drought (25% watering). **c)** RER in plants under extreme drought conditions (20% watering). n = 23 plants per genotype and watering condition. The RER was calculated over a time window corresponding to day 5–23 as the slope of the linear regression between the log-transformed PRA and time.

These results indicate, that *hag5-2* mutants do not differ in rosette growth rate arrest under different degrees of drought stress. In the previous chapter we described *hag5* mutants as bigger plants with increased leaf area. However, this observation was only significantly when plants were at least 5 weeks old, which might explain the lack of differences in the non-stressed plants in this experiment of only 23 days of length. An interesting approach would be to perform the phenoscope assay of plants subjected

to a drought stress and recovery, like the assay in Figure 4.11a, were *hag5-2* mutants display an increased recovery rate after water withdrawal and subsequent re-watering. Our hypothesis underlaying this observed drought recovery phenotype in *hag5-2* mutants in light of these results will be further developed in section 4.10.3 of this chapter.

4.6. Model of HAG5, ARIA and ABF2 regulation of ABA responses

After characterising the ABA-related phenotypes of *hag5* mutants, we confirmed that they convey with the *aria* mutant phenotypes, further supporting the idea that both proteins are involved in the same signalling pathway and regulate common ABA-mediated responses. *aria* mutants are bigger plants, with ABA sensitivity during germination and early development but without differential stomatal closure or drought tolerance (Kim et al., 2004a). During the initial characterisation of the *aria* mutant and its comparison with the *abf2* mutant by Kim et al., the authors concluded that ARIA affects only a subset of the ABA-dependent processes regulated by ABF2 (Kim et al., 2004a). Since *hag5* mutants display drought recovery and drought tolerance phenotypes, we hypothesised that the role of HAG5 as a positive regulator of ABA signalling also involves ABF2.

As detailed in section 4.1.3, ARIA has 8 arm repeats and BTB/POZ domain. In animals, the arm protein, β-catenin has been demonstrated to be a transcriptional coactivator, since it can be translocated into the nucleus in response to a hormone signal and forms complexes with transcription factors to activate target gene expression (Polakis, 2000). The BTB/POZ domain has also been described to have different functions. One of them is being involved in protein degradation through ubiquitination (van den Heuvel, 2004). Thus, ARIA might regulate the stability of ABF2 or other proteins that possibly associate with it, such as HAG5, or the transcription factor DREB2C (Lee et al., 2010b). A study published by Collins et al., showed that the BTB/POZ domain can recruit a histone deacetylase to mediate transcriptional repression (Collins et al., 2001). As a consequence, since ARIA possesses two protein-protein interaction domains, a more promising hypothesis is that it could function as an adaptor for ABF2 to form a protein complex with HAG5, resulting in the transcriptional activation of ARIA and/or ABF2-dependent genes. This

would mean that the expression of ABF2, ARIA and HAG5-dependent genes should be parallel. In addition, it has been previously described that ARIA interacts with two proteins with DNA binding domain, ADAP and NEK6. These proteins could interact with ARIA independently of ABF2 and HAG5 or form a complex.

Here we propose a first model of interaction between all three proteins (Figure 4.16). Upon ABA recognition, the ABA receptors (PYR/PYL/RCAR) get activated, releasing PP2C from its repressive activity over SnRK2. This kinase phosphorylates and activates bZIP transcription factors such as ABF2 (Fujita et al., 2011), that initiate the transcription of ABA-responsive genes through the recognition of their regulatory elements. Indeed, ABA-regulated genes are controlled by the cis-regulatory elements sharing the (C/T)ACGTGGC consensus. This conserved sequence motif is generally known as "ABA- responsive element (ABRE)". Amongst the ABREs, those sharing the ACGTGGC core sequence are found to be ubiquitous, and their role in ABA-responsive gene expression has been characterized in detail (Hattori, 2002).

We hypothesize that, upon ABA perception, HAG5 associates with ARIA and ABF2 and acetylates H4K5 associated to the promoters of the ABRE-regulated ABA responsive genes. This acetylation mediated by HAG5 would then result in an opening of the chromatin that would allow ARIA and/or ARIA-ABF2 to initiate the transcription of target genes (Figure 4.16). In the absence of HAG5, there is either lack of H4K5 acetylation on the ABA-responsive loci, or the impossibility to form the protein complex that would directly drive ARIA and/or ARIA-ABF2 to the promoters of the ABA responsive genes. As a consequence, there is a delay the transcriptional activation of such genes, as shown by the time course qPCRs in the *hag5-2* mutant (Figure 4.9).

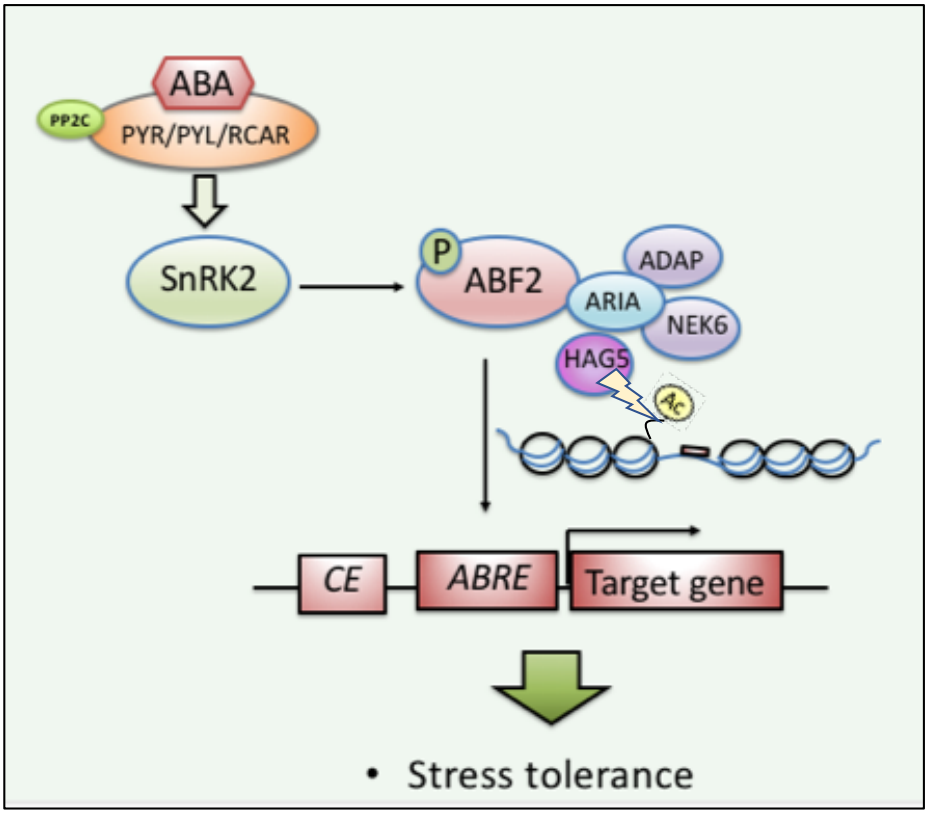

Figure 4.16. Model of the molecular mechanism by which HAG5 regulates ABA signalling. PYR/PYL/RCAR ABA receptor-PP2C complexes control SnRK2-AREB/ABF pathways to regulate major ABA-mediated ABRE-dependent gene expression. bZIP TFs such as ABF2 regulate ABA-mediated gene expression by interacting with cis-elements in the promoter regions upstream of the target genes in response to ABA. HAG5 might be the responsible of acetylating H4K5 in association with those cis elements, guiding ARIA and/or ABF2 to their targeted genomic regions and facilitating gene expression.

This mechanism is based on the concept that HAG5 acquired specialised functions to fine-tune stress responses. Thus, HAG5 is not necessary for the transcriptional activation of genes downstream the ABA signalling pathway, but it contributes to the timing of that response by quickening the action of the ARIA-ABF2 complex.

4.6.1. Chip-seq of H4K5ac after ABA treatment

In order to test our hypothesized model, we established a collaboration with Dr. Moussa Benhammed from the University of Paris-Saclay to perform RNA-seq and

H4K5 acetylation ChIP-seq experiments on Col-0 and *hag5-2* mutants treated or untreated with ABA. At first, we aimed to characterize the whole transcriptional response of *hag5-2* mutants to ABA at the time point in which the mutants show delayed induction (7h). That would facilitate the identification of genes that are dependent on HAG5 for timed upregulation. The results of the RNA-seq will be extensively revised in Chapter 5. Secondly, we wanted to know if these HAG5-dependent genes were associated to H4K5ac. This would confirm that the way HAG5 modulates ABA responses is through histone acetylation, and that it does so independently from its paralogue *HAG4*. Finally, we wanted to see how the ABA treatment in Col-0 and the lack of HAG5 in the mutant would affect H4K5ac enrichments throughout the genome.

In this section, the ChIP-seq experiment results are presented. In brief, this experiment consists of immunoprecipitating chromatin isolated from differently treated samples using antibodies specific to the histone mark of interest (H4K5ac). The DNA physically associated to such mark is then purified, used for library preparation and sequenced. For this experiment, we used 12-days-old Col-0 or *hag5-2* seedlings grown vertically in ½ MS plates under short photoperiod. Approximately 100 seedlings/genotype were transferred to either ½ MS plates or plates supplemented with 50μM of ABA for 7h. The detailed protocols for cross-linking, nuclear enrichment, immunoprecipitation, DNA purification and library preparation can be found in section 2.11 of Chapter 2. The sequencing results were then analysed by Dr. Lorenzo Concia, a bioinformatician in the Benhammed research group. The first striking observation whilst looking at the data is that there were no significantly different levels of enrichment between genotypes and treatments.

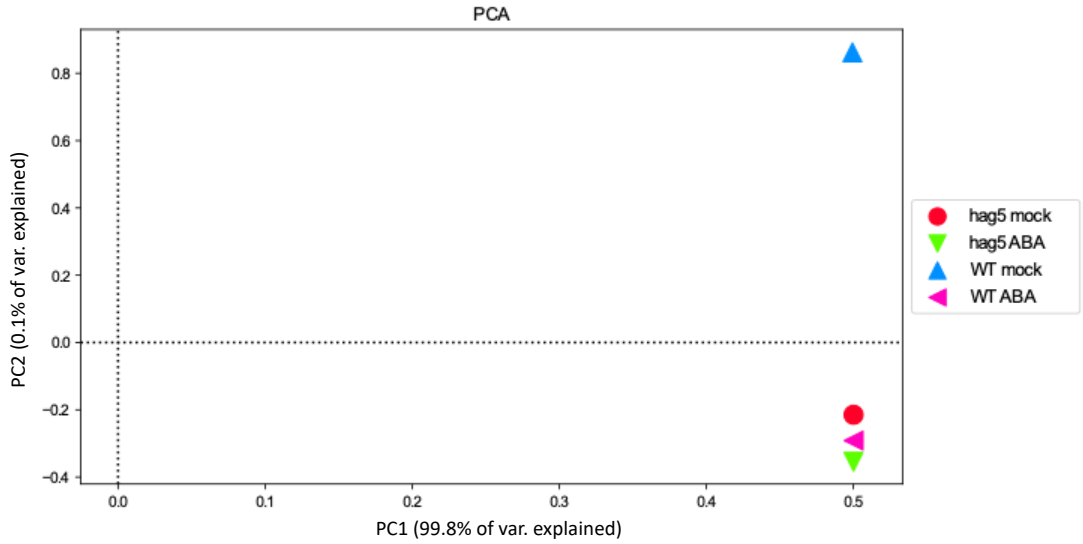

Figure 4.17. ChIP-seq of H4K5ac in Col-0 and *hag5-2* mutants mock and ABA treated. Principal Component Analysis (PCA) of all samples. The PC1 accounts for 99.8% of the variation, whilst PC2 accounts for 0.1% of the variation between samples. Data analysis was performed by Dr. Lorenzo Concia as specified in Chapter 2.

When using PCA to cluster the samples, all four different samples (WT mock, WT ABA, *hag5* mock and *hag5* ABA) grouped/aligned within the first principal component (PC1), which accounted for 99.8% of the variation (Figure 4.17). Even though the WT mock sample seems to separate within the PC2, that only accounts for 0.1% of the variation (Figure 4.17). In order to see the level of correlation between samples, we generated a scatter plot and calculated the spearman correlation coefficient (Figure 4.18).

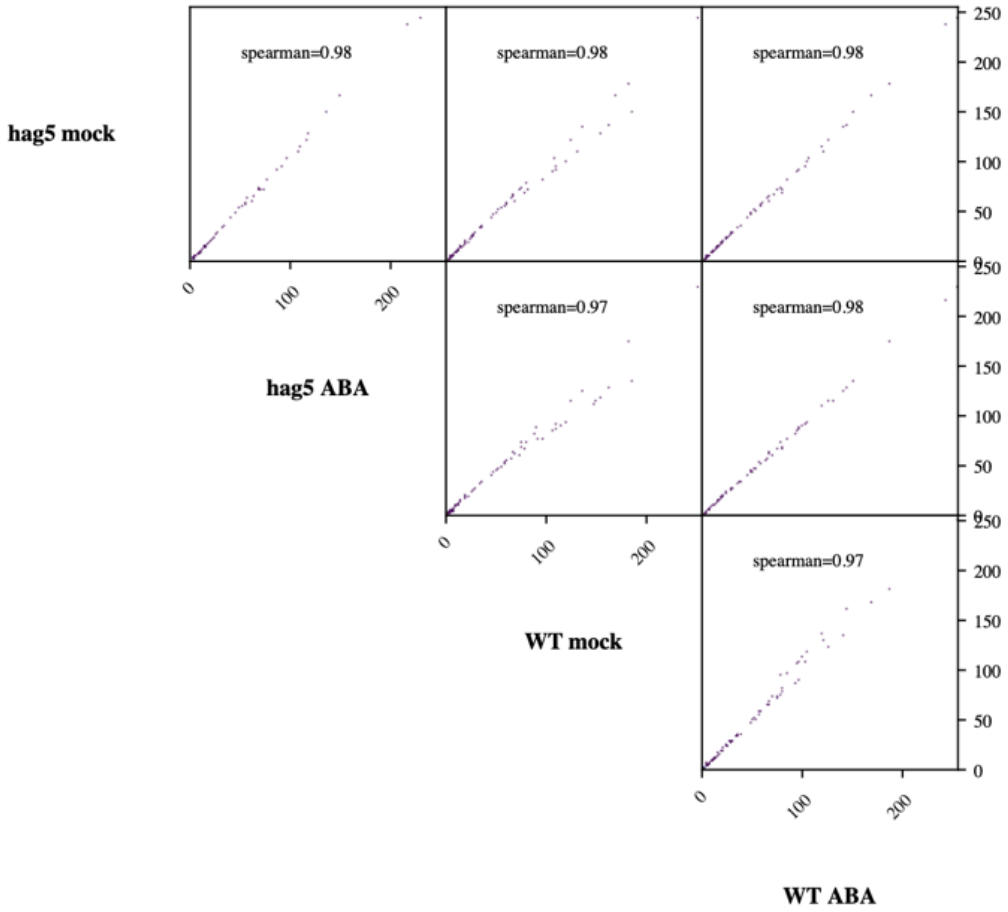

Figure 4.18. ChIP-seq of H4K5ac in Col-0 and *hag5-2* mutants mock and ABA treated. Scatter plots and spearman coefficient calculated from plotting all samples against each other as measure of correlation. The spearman coefficient being ~1 in all comparisons evidences the lack of differences in H4K5ac enrichment between genotypes and treatments. Data analysis was performed by Dr. Lorenzo Concia as specified in Chapter 2.

As seen in Figure 4.18, due to the straight line generated by plotting samples against each other, and the correlation coefficient being nearly 1 for all comparison, we can conclude that there are no differences in H4K5ac enrichment between genotypes and between treatments. Whilst the antibody worked, the same regions of the genome and with the same degree of enrichment were identified for all samples. In order to take a closer look at the data, we decided to select the list of genes that belong to the ABA signalling pathway and look for differential enrichment amongst those.

We obtained the list of genes using the gene ontology database AmiGO2 (http://amigo.geneontology.org).

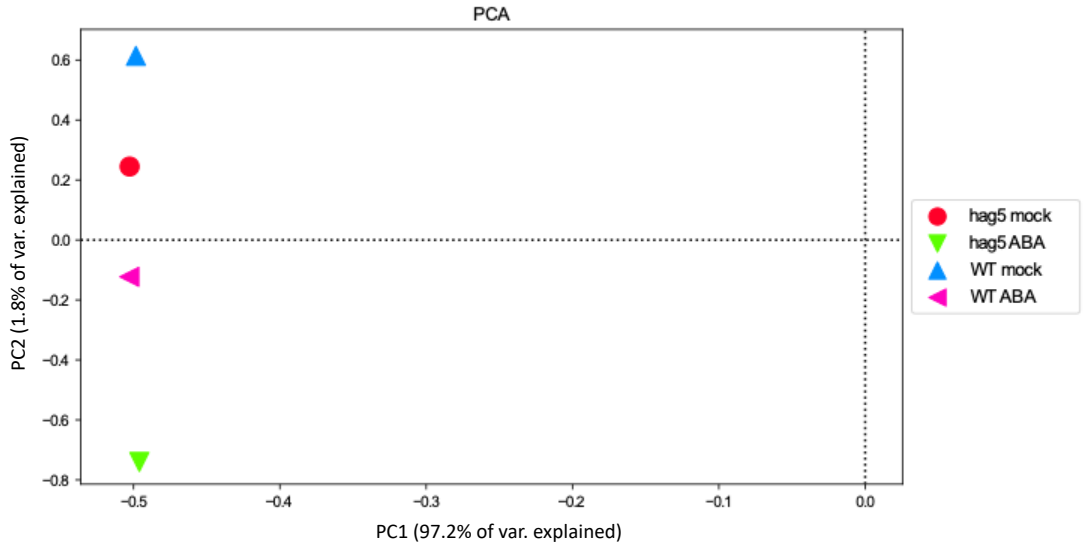

Figure 4.19. ChIP-seq of H4K5ac in Col-0 and *hag5-2* mutants mock and ABA treated for genes that belong to the ABA signalling pathway. Principal Component Analysis (PCA) of all samples. The PC1 accounts for 97.2% of the variation, whilst PC2 accounts for 1.8% of the variation between samples. Data analysis was performed by Dr. Lorenzo Concia.

We ran a principal component analysis on the samples based on those genes (Figure 4.19) and found out that all four samples aligned within the first PC, accounting for 97.2% of the variation. Whilst using scatter plot and Spearman's coefficient, we also found a strong degree of correlation between samples, suggesting that this subset of genes is not differentially enriched due to ABA treatment or the lack of HAG5 in *hag5-2* mutants. The most obvious conclusion for the lack of differences between Col-0 and *hag5-2* both treated and untreated samples was that the ABA treatment did not work. Since the microarray in Chapter 3 section 3.3.1 showed that there are no transcriptional differences between Col-0 and *hag5-2* mutants in basal state, a defective ABA treatment could result in such high correlation between samples. In order to test the effectivity of the treatment, we performed RNA extraction, cDNA synthesis and qPCR analysis from samples kept frozen before crosslinking and nuclear extraction. We tested the expression of ABA marker genes (*RAB18* and *RD29B*) and verified the induction in the Col-0 ABA treated samples, and a lesser increment of expression in *hag5-2* treated seedlings (Figure 4.20). As a consequence, the lack of differences is not due to the ABA treatment but probably due to HAG5 acting through a different mechanism than H4K5 acetylation in response to ABA.

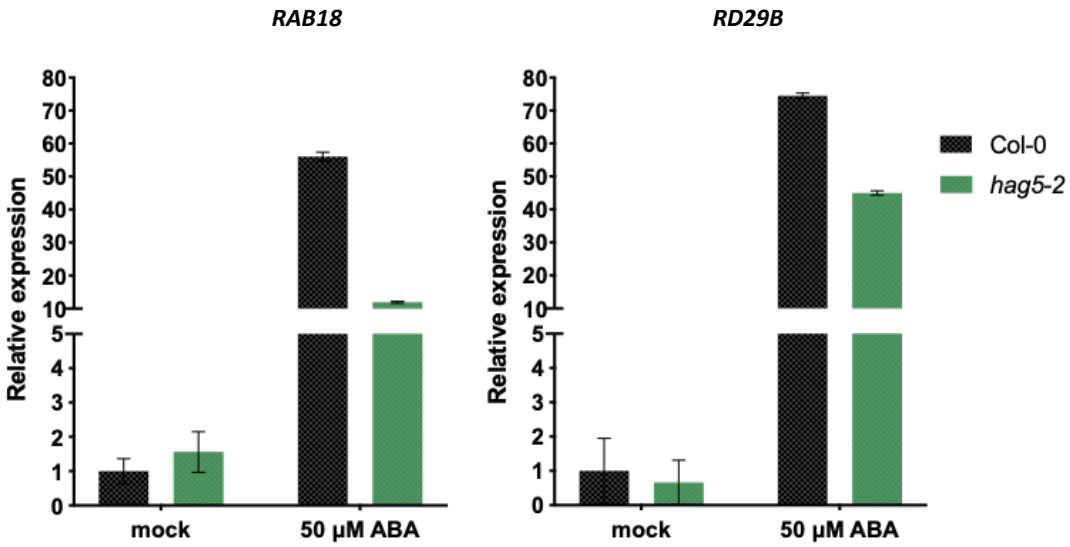

Figure 4.20. qPCR for testing the ABA induction in ChIP-seq samples. 14-days-old seedlings were treated with 0 or 50µM of ABA for 7h. The relative expression was normalised against the house keeping gene *α-tubulin*. The primer sequences used for each gene can be found in section 2.9.5 of Chapter 2. Error bars represent SD between technical replicates (n = 2).

There are several conclusions that can be extrapolated from this experiment. First, since *hag5-2* seedlings display the same level of H4K5 acetylation as the wild type, either HAG4 is redundantly acetylating H4K5 in the absence of HAG5, or HAG5 does not acetylate H4K5 *in vivo*, and/or that it might target a different histone lysine. Secondly, ABA treatment does not modify the levels of acetylation of H4K5 in Col-0 plants. Hence, this epigenetic mark does not appear to be involved in ABA responses. Previous ChIP-qPCR analysis of the ABA marker gene *RAB18* showed enrichment of the promoter region (150 bp form the TSS) in the H4K5ac mark in Col-0, whilst such enrichment was lost in *hag5-2* mutants (data not shown). This preliminary data established the foundation for this ChIP-seq experiment. The lack of differential enrichment amongst genotypes in the ChIP-seq, could indeed imply that HAG5 is not involved in H4K5ac, at least under the tested conditions. However, it is possible that these results are not determinant, since only one biological replicate was sequenced. As a consequence, sequencing at least a second biological replicate would help discerning between the contradictory results from the ChIP-qPCR and ChIP-seq experiments.

In light of these results, we propose an alternative mechanism by which HAG5 regulates the transcriptional response to ABA without acting as a histone

acetyltransferase. This model is based on *TIP60*, *HAG5* orthologue in mammals. It is known that TIP60 can modulate the activity of its interacting transcription factor, p53, through acetylation (Wang et al., 2018). We hypothesize that this mechanism might be conserved in plants, and we propose an alternative model in which HAG5 acetylates ARIA by targeting lysine residues (Figure 4.21). ARIA acetylation by HAG5 could happen in an ABA-dependent or independent manner. Furthermore, this acetylation could either regulate the transcriptional activity of ARIA or interfere with ABF2 activity. Finally, this modification could potentially regulate the formation of the transcriptional complex between HAG5, ARIA and ABF2. This model and the nature of HAG5, ARIA and ABF2 interactions will be further discussed throughout this chapter.

Nonetheless, it is possible that the observed phenotypes of *hag5* mutants are not due to the enzymatic activity of HAG5. A way to test if HAG5 acetyltransferase activity is responsible for such phenotypes, we propose complementing the knock-out *hag-2* plants with a dead version of HAG5, unable to acetylate any substrates because of mutations in the active centre. If these complemented lines display the same phenotypes as the mutant lines, it would imply that the acetyltransferase activity of HAG5 is necessary to regulate Arabidopsis growth, development and stress responses. However, if Col-0 phenotypes are rescued, it would imply that HAG5 might have different cellular activities, or be part of a complex without directly modifying specific substrates.

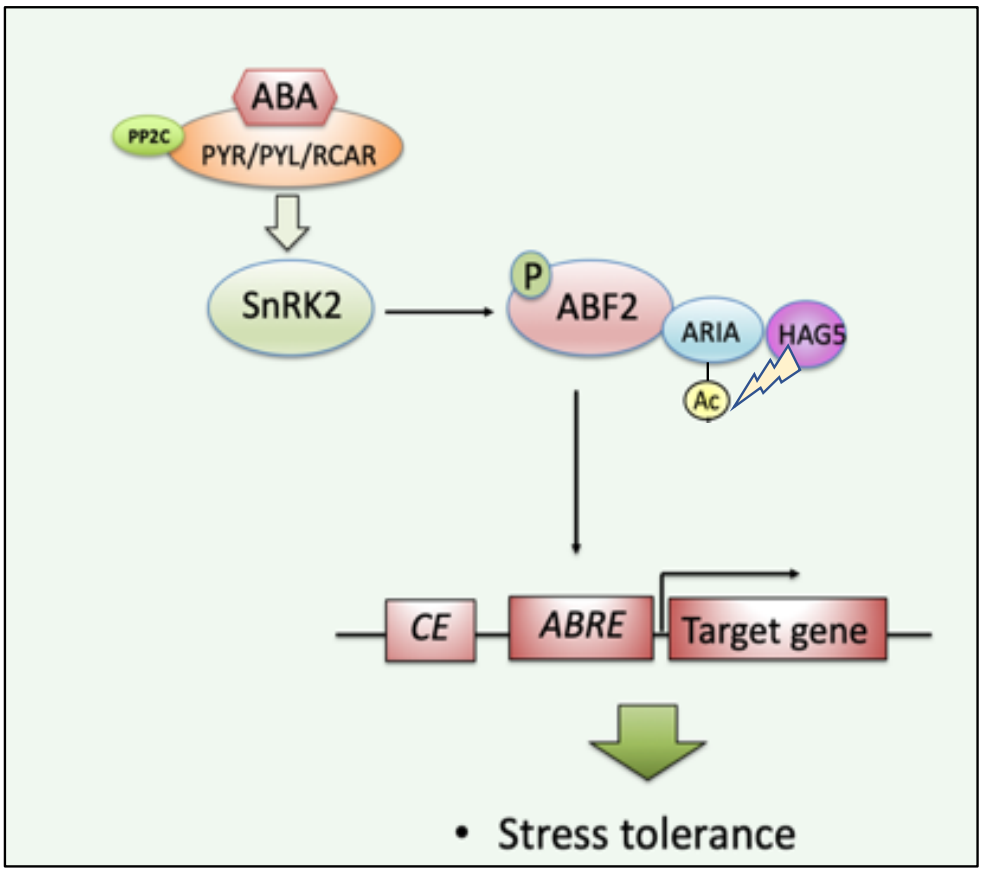

Figure 4.21. Second model for HAG5 regulation of ABA signalling pathway. PYR/PYL/RCAR ABA receptor-PP2C complexes control SnRK2-AREB/ABF pathways to regulate major ABA-mediated ABRE-dependent gene expression. bZIP TFs such as ABF2 regulate ABA-mediated gene expression by interacting with cis-elements in the promoter regions upstream of the target genes in response to ABA. HAG5 might affect the transcriptional activity of ARIA and/or ABF2 by directly acetylating a lysine residue in ARIA. ARIA acetylation might result in a more active TF, or it might play a role in the assembly of the transcriptional complex formed by ABF2, ARIA and HAG5.

4.7. Investigating HAG5 possible acetylation of ARIA

In order to test this second hypothesis, we designed several approaches to identify acetylation of lysine residues in ARIA by HAG5. Our fist approach was to purify recombinant HAG4, HAG5 and ARIA proteins from IPTG-induced *Escherichia coli* Rosetta™ cells for an *in vitro* acetylation assay (Active Motif Cat N. 56100). This fluorescence-based HAT activity assay is based on the transfer of acetyl groups from acetyl-coA to substrates, generating CoA-SH. Briefly, this assay consists

of incubating a recombinant HAT (provided p300 active centre, HAG4 or HAG5) in a provided assay solution, adding acetyl-coA and a substrate (ARIA, H3 or H4). A stop solution is added to stop the acetylation after a given incubation period, and a developer solution is provided that reacts with the free sulfhydryl groups on the CoA-SH to give a fluorescent reading of HAT activity in AFU (Arbitrary Fluorescence Units). The kit provided H3 and H4 as substrates, so we included them to test whether HAG4 and HAG5 acetyltransferase activity *in vitro* was, as published, acetylating H4K5 (Earley et al., 2007). The assay provides recombinant p300 catalytic domain as a HAT control. The protein purification was performed by Dr. Veselina Uzunova, a post-doctoral researcher in the Ntoukakis group.

As a method of control, we tested the AFU of the substrates (H3, H4 and ARIA) in the presence of assay buffer and acetyl-coA, but in the absence of HATs (Figure 4.22a). This would give the background fluorescence of the substrates in absence of acetyltransferase activity. As seen in Figure 4.22a, ARIA on its own gave high background signal, (~40000 AFU) whilst H3 and H4 background was considerably lower (~2000 AFU).

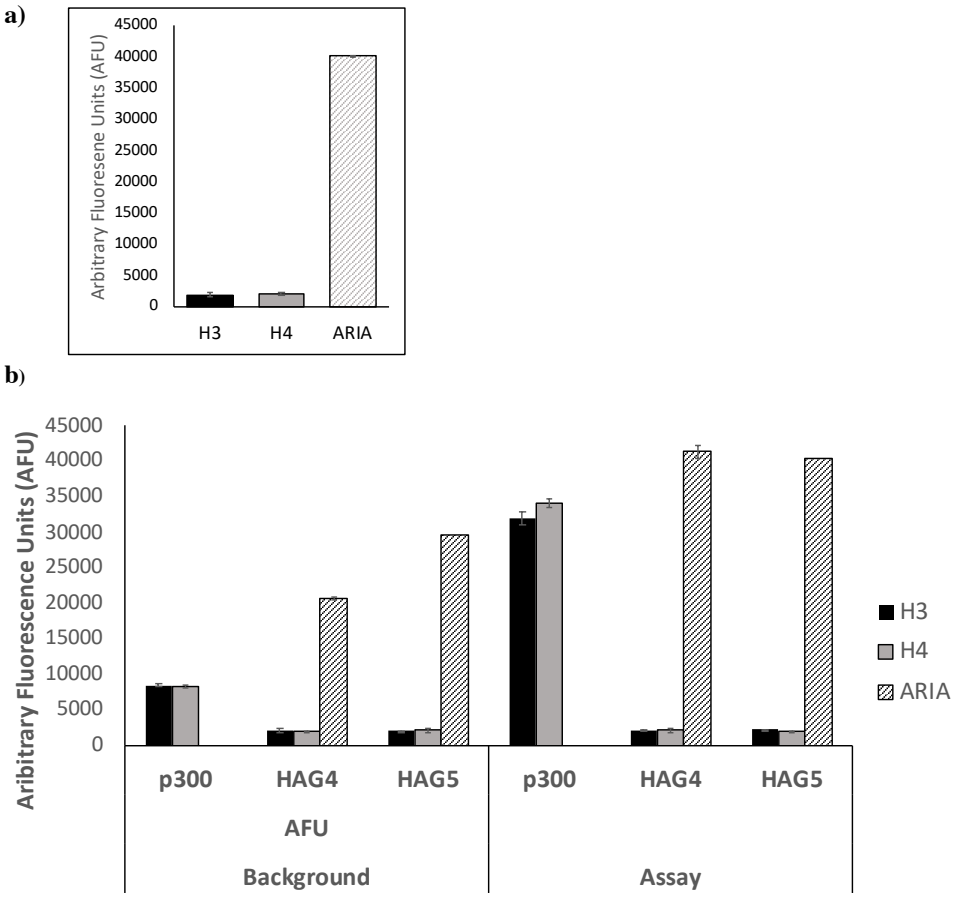

Figure 4.22. Histone acetyltransferase activity (HAT) assay using HAT activity kit (Active motif). **a)** Arbitrary fluorescence units in control wells incubating the different substrates (H3, H4 or ARIA) in assay solution. **b)** HAT activity assay using recombinant p300 catalytic domain, HAG4 and HAG5 as enzymes and H3, H4 and ARIA as substrates. The AFU of background wells represents the signal due to the mixture of all the components of the enzymatic reaction (enzyme, substrate, acetyl-coA and assay buffer) before acetylation. The assay wells correspond to the AFU after transfer of acetyl groups from the enzyme to the substrate. Fluorescence of reaction wells was measured after incubating reaction mixtures for 20 min in the dark, using a fluorescence plate reader (Magellan™). Error bars correspond to SD of technical replicates (n = 3).

There are four amino acids, such as the two aromatic amino acids phenylalanine and tyrosine, the heterocyclic tryptophan, and the disulphide cystine, that exhibit characteristic ultraviolet absorption. These aromatic and heterocyclic amino acids re-emit the absorbed ultraviolet light in the form of fluorescence (Lakowicz, 1988). Given the high fluorescent background of ARIA, we checked its amino acid composition in order to see the percentage of these fluorescent residues using the ProtParam tool in ExPASy (web.expasy.org) (Wilkins et al., 1999). According to this analysis, the percentage of these amino acids according to the composition of ARIA is: phenylalanine (3%), tyrosine (2.3%), tryptophan (0.4%) and cysteine (1.4%). Since these low percentages do not justify the high fluorescent background of the recombinant ARIA, we hypothesize that it could be due to low purity of the protein caused by methodological issues during the purification.

For the HAT activity assay, we included background wells in which each enzyme (p300, HAG4 or HAG5) was incubated with assay buffer, acetyl-coA, and stop solution before adding the substrate (Figure 4.22b). Adding the stop solution before the substrate ensured that there was no HAT activity when all the reagents were combined in a single well, and the resulting AFU measurement corresponded exclusively to background signal from all the components. Whilst HAG4 and HAG5 gave very low levels of background when incubated in the presence of H3 or H4, adding ARIA as a substrate dramatically increased the signal background. For the assay wells, each enzyme was incubated in assay buffer with acetyl-coA and the substrate. The stop solution was added 20min post-incubation, after acetylation had taken place. Figure 4.22b shows that the acetyltransferase activity of 50ng of p300 *in vitro* was detected, reaching a significant increase in Arbitrary units of fluorescence

in the presence of both H3 and H4 (~40000 AFU). Both histones are known substrates of p300, and the reached levels of AFU were consistent with the recommended ones by the supplier, indicating that the assay successfully worked. When incubating HAG4 or HAG5 with H3 or H4, the detected levels of fluorescence were similar to the ones from the background wells. Since both HAG4 and HAG5 have been proven to acetylate H4K5 *in vitro* (Earley et al., 2007), the lack of signal in the H4 wells indicates that the purified proteins are not active and cannot acetylate *in vitro*, probably due to denaturation during the purification steps. Thus, when ARIA was included as a substrate in the assay wells, the increased signal could only be due to the background produced by ARIA itself, rather than any HAT activity by either HAG4 or HAG5. Overall, the HAT activity kit can be a useful tool to detect acetylation *in vitro*. However, further optimization is required in the protein purification steps in order to maintain the HAT activity of the enzymes. In addition, some substrates might give high background, resulting in difficulties detecting acetylation levels. In these cases, even though the HAT activity could not be measured through fluorescence, the substrate could be purified from the assay reaction either through IP or by using StrataClean Resin (Agilent) to wash the reagents away. The concentrated protein could then be prepared for mass-spectrometry in order to identify differences in acetylation between assay and background samples.

Given the lack of success with the *in vitro* acetylation assay, we designed a second strategy to identify HAG5-dependent ARIA acetylation based on mass-spectrometry. We proceeded to either express ARIA fused with a YFP tag on its own or co-expressed with HAG5 fused with a FLAG tag in *N. benthamiana*. The plants expressing both proteins were either sprayed with water or a solution containing 50μM of ABA. Leaf tissue was collected 7h after treatment, and at least 5g of tissue per sample were used for protein extraction. The methodological procedures are described in section 2.12. of Chapter 2. TSA was used in the protein extraction buffer as a deacetylase inhibitor to avoid loss of acetylation during the extraction procedure. The identification of ARIA-YFP was successful in all samples (expressed on its own, co-expressed with HAG5 and mock treated and co-expressed with HAG5 and ABA treated). However, the identified peptides for each sample covered 18%, 15% and 8% of the total protein sequence respectively (data not shown). Most of the lysine residues were not identified, so the lack of differential acetylation between the samples is

probably due to low coverage. We propose repeating the experiment using three biological replicates and incrementing the amount of starting material to at least 20g of tissue per sample.

If HAG5 was found responsible for acetylating lysine residues of ARIA, the following step would be to complement *aria* mutants with a point mutated variant of ARIA. Investigating the phenotypes of this line and comparing them with *hag5-2* and *aria* mutant phenotypes would give an insight into which mechanisms are specifically dependent on HAG5 acetylation of ARIA.

4.8. *hag4* and *hag5* display different structural domains, interacting partners and ABA-related phenotypes

A recurrent theme in this thesis is the characterisation of *hag4* and *hag5* mutants showing distinct phenotypes, which evidences the evolutionary divergence between both paralogues. After the initial Y2H screen for the identification of HAG5-interacting transcription factors (sections 4.1.2 and 4.1.3), a second screen was performed using HAG4 against the same library of transcription factors. As seen in Figure 4.5 HAG4 interacted the transcription factor VFP4 and did not interact with either ARIA or bHLH91. In addition, HAG5 did not interact with VFP4, which means that both paralogues have different interactors. In light of these results, Dr. Veselina Uzunova has performed *in silico* modelling of both proteins trying to characterise structural differences in the interaction domains that would explain the specificity of the interactions (Figure 4.24). The first produced model was for HAG4, in which two templates were used: the 1wgs Tudor Hypothetical Protein Homologous from mouse to Histone Acetyltransferase from the PDB database and the 2pq8 Probable histone acetyltransferase MYST1 from *KAT8* in *Homo sapiens*.(Figure 4.23a). The rest was modelled using Molecular Dynamics (MD)-based protocols (Mai et al., 2018) to create the initial model in Figure 4.23b. A similar strategy was used to build the model of HAG5. However, since this model was done later, further crystal structures were available, covering almost the whole sequence. The following crystal templates: 2rnz, 3lmm and 3to7 from PDB were used for the *in silico* modelling of HAG5.

a)

1wgs for Tudor domain

2pq8 for MYST HAT

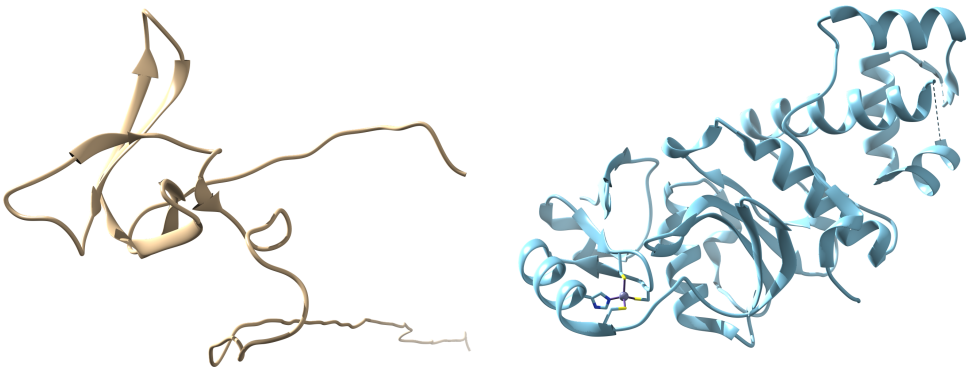

b)

Initial model

Figure 4.23. Templates for building the initial 3D *in silico* model of HAG4. **a)** Template used to model the chromodomain or Tudor domain (1ws form mouse) and template used for the HAT domain (2pq8 from humans). B) Initial model produced through homology modelling subjected to molecular dynamics. The pink and the cyan regions folded over. The green remained disordered. Both templates were obtained from the PBD database. The initial model was produced by Dr. Charo del Genio and Dr. Veselina Uzunova.

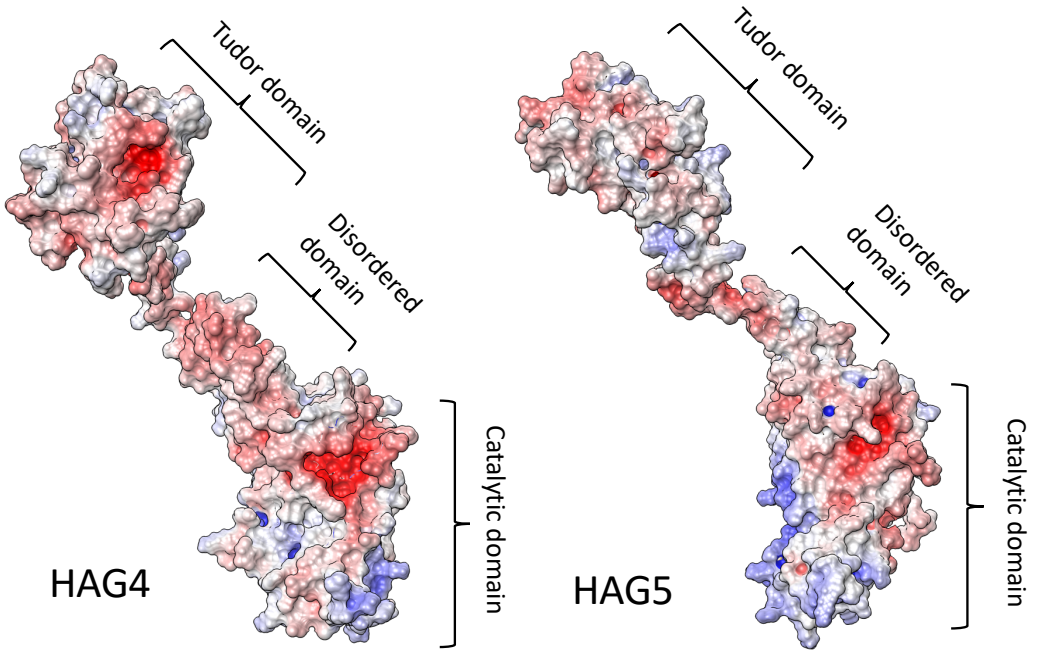

Figure 4.24. HAG4 and HAG5 have different TUDOR domain organisation. 3D *in silico* modelling of HAG4 and HAG5 folded proteins through MD refinement. Electrostatic potential is coloured in the models. Blue is positive electrostatic potential and red, negative. The three distinct domains (catalytic, disordered and Tudor) are identified between the brackets. The homology modelling was done by Dr. Veselina Uzunova, a post-doctoral researcher at the Ntoukakis group.

As seen in the 3D homology model, the active centre is conserved between both enzymes. Since the catalytic activity takes place due to the active centre, this conserved domain shows that both enzymes display the characteristic structure of an acetyltransferase. Interestingly, the disordered and Chromodomain/TUDOR domains display structural differences between HAG4 and HAG5, supporting the specialisation of both enzymes through interaction with different partners.

The Tudor domain was originally identified in 1985 as a region of 50 amino acids found in the Tudor protein encoded in Drosophila (Boswell and Mahowald, 1985). The Tudor protein contains 11 repeats of the later named Tudor domain, which consists of 60 amino acids. Later studies identified this domain being present in many other proteins involved in RNA metabolism (Ponting, 1997), and processes like RNA splicing and small RNAs pathways. Over the past two decades, Tudor domain proteins have been identified to participate in a number of other processes, such as histone modification and DNA damage response (reviewed by(Chen et al., 2011)).

Furthermore, Tudor domain proteins function as molecular adaptors, and they promote the assembly of macromolecular complexes by binding methylated arginine or lysine residues on their substrates (Pek et al., 2012). The research of this domain in Drosophila has linked it to various processes that take place during development, including cell division, differentiation and genome stability (Pek et al., 2012). A study from 2015 identified the Agenet/Tudor domain family in the plant kingdom by using bioinformatics and phylogenetic analyses. The authors identified 30 members of this family in Arabidopsis, classified in four subgroups (Brasil et al., 2015). Proteins belonging to the Agenet/Tudor domain family are currently known as histone modification "readers" and classified as chromatin remodelling proteins, with important roles in regulating different aspects of plant development (Brasil et al., 2015). The structural differences found on the Tudor domain of HAG4 and HAG5 proteins could explain their diverse functions, possibly due to specific interactor partners, resulting in the different phenotypes of the mutants.

Following the confirmation that the interaction with ARIA is exclusive to HAG5, we investigated the ABA sensitivity of *hag4* mutants. Since *hag5* mutants are hyposensitive to the effect of ABA in seed germination, we decided to test *hag4-1* knock-down and *hag4-2* loss-of-function mutants (described in Chapter 3) for their response to ABA. Exogenous ABA has a negative effect on germination and cotyledon greening (Sharp and Lenoble, 2002), hence, we germinated Col-0, *hag4-2* ad *hag5-2* seeds in 0, 0.25, 0.5 and 0.75µM of ABA under short day photoperiod (Figure 4.25). Seedlings were grown for 7 days before pictures were taken.

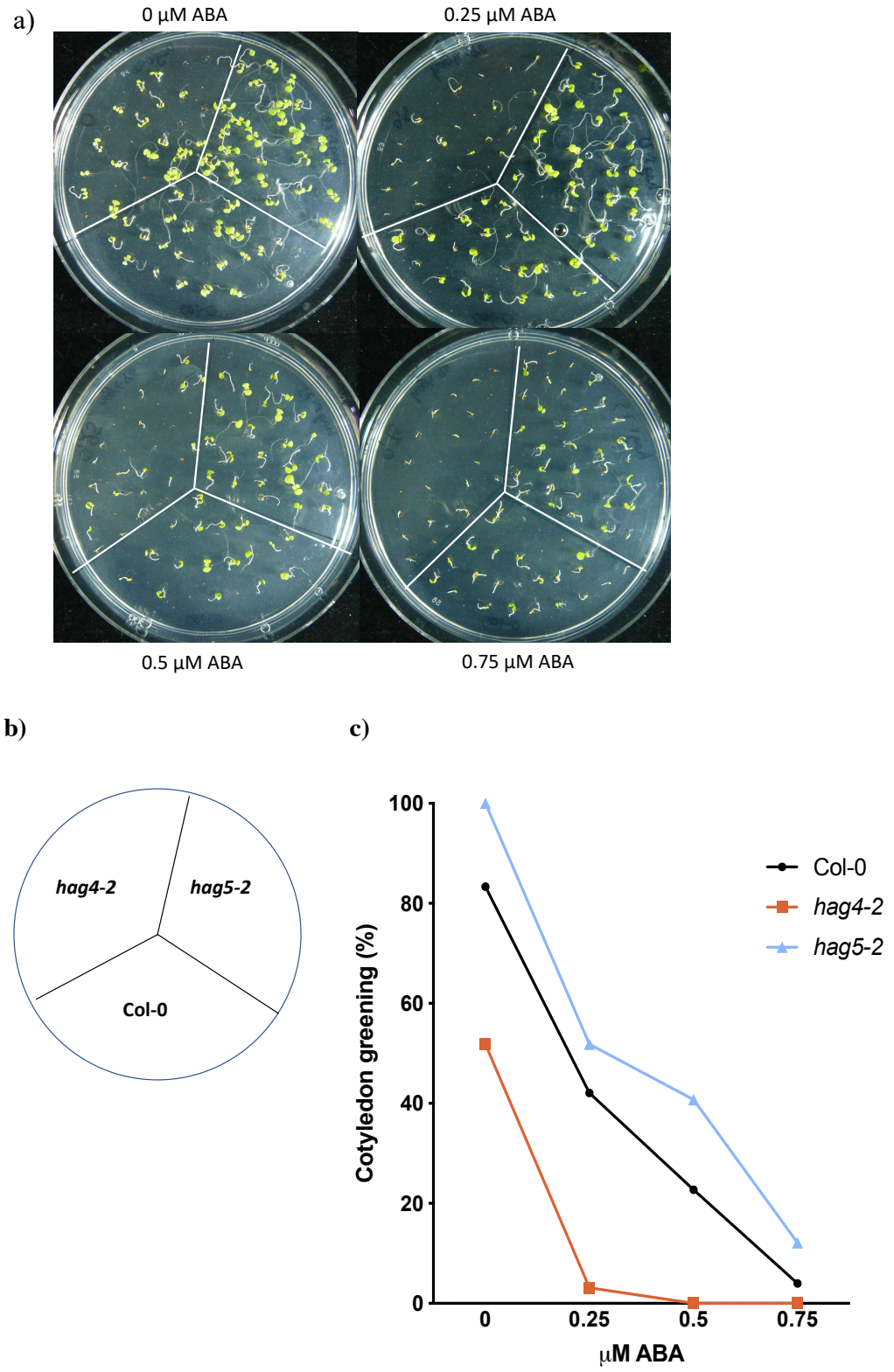

Figure 4.25. *hag4* and *hag5* mutants have different ABA response phenotypes. **a)** Cotyledon greening of Col-0, *hag4-2* and *hag5-2* 7 day old seedlings sown in ½ MS media with increasing concentrations of ABA (0, 0.25, 0.5 and 0.75µM of ABA). **b)** Diagram showing the distribution of the different phenotypes in plates from section a. **c)** Percentage of cotyledon greening scored as number of seedlings that presented the first set of green cotyledons over the

total number of seeds (n = 20). This figure represents a unique biological replicate representative of three independent experiments.

Figure 4.25a-c shows that *hag4-2* mutants display lower rates of germination and cotyledon formation in the control media, whilst *hag5-2* seedlings displayed enhanced development. In addition, increasing concentrations of ABA dramatically decrease the germination and cotyledon greening of *hag4-2* mutants when compared to Col-0. *hag5-2* seedlings display a higher percentage of green cotyledons and are less sensitive to intermediate concentrations of ABA (Figure 4.25c). These results suggest that HAG4 and HAG5 have opposite roles in regulating ABA responses. Our hypothesis is that HAG4 might be involved in the ABA biosynthesis or turnover. That could result in *hag4* plants displaying higher levels of ABA in basal conditions or in processes that require ABA production, such germination. That would explain the higher sensitivity and the decreased germination rate. In order to further understand the role of HAG4 in ABA signalling and response, we suggest a hormone content measurement to determine the levels of ABA in *hag4* mutants at different developmental stages and after ABA induction through processes that are ABA-dependent, such as drought or cold stresses.

Further characterisation of these mutants is needed, both in terms of their response to drought, cold and salt tolerance, as well as looking into the transcriptional regulation of response to ABA. We propose qPCRs looking at the induction of ABA biosynthesis, degradation and response genes, or even RNA-seq to identify all the miss-regulated genes resulting from the lack of HAG4.

4.9. Findings

- HAG5 interacts with bHLH91, a TF involved in anther and pollen development.
- HAG5 interacts with ARIA, a TF involved in abscisic acid responses through its interaction with ABF2.
- *hag5* mutants are less sensitive to treatment with exogenous ABA, implying that HAG5 is a positive regulator of ABA responses.
- *hag5* mutants have regular endogenous levels of ABA, suggesting that the altered ABA responses in these mutants are due to the role of HAG5 in ABA signalling.

- *hag5* mutants are more tolerant to low water availability and display higher recovery rates after prolonged periods of drought stress.
- The up-regulation of ABA marker genes after induction is delayed in *hag5*, implying that HAG5 participates in the timing of the transcriptional responses to ABA.
- H4K5ac is not an epigenetic mark involved in the regulation of the transcriptional response to ABA.
- *hag5-2* seedlings have no altered levels of H4K5 acetylation.
- HAG4 and HAG5 have different Tudor domains, suggesting evolutionary diversification between both paralogues.
- HAG4 interacts with a different set of transcription factors than HAG5.
- *hag4* mutants are hypersensitive to exogenous ABA treatment, displaying opposite phenotypes from *hag5* mutants.

4.10. Discussion

4.10.1. Interaction between HAG5 and ARIA

The most exciting novel finding of this chapter was the interaction between HAG5 and ARIA, a transcription factor involved in abscisic acid responses (Kim et al., 2004a). ARIA is known to interact with the well-studied bZIP transcription factor ABF2, which is responsible for the expression of many ABA-responsive genes upon ABA perception (Kim et al., 2004b). Furthermore, *aria* and *hag5* mutants display similar phenotypes, such as increased rosette size, longer roots and ABA hyposensitivity (Kim et al., 2004b). This suggests that both proteins might be taking part on the same cellular processes and metabolic pathways.

The interaction between ARIA and HAG5 was initially identified using a heterologous system, through a screening with a library of proteins with *in silico* identified DNA-binding domain. This system has several limitations, one of them being that not all the potential Arabidopsis transcription factors are cloned in the library, with some TF families being underrepresented or not present at all (Pruneda-Paz et al., 2014). But the greatest limitation of this system is the fact that the library is

restricted to proteins with DNA-binding domains, excluding all the possible interactions with proteins with different functions. Currently, there are cDNA libraries of more than 12000 Arabidopsis proteins, like the one available at SPOmics-InterATOME (the IPS2 protein-protein interaction platform), as well as more sophisticated methods of screening protein-protein interactions using such libraries (Erffelinck et al., 2018). Using these resources to screen for HAG4 or HAG5 interactors might reveal novel interactor partners, helping define the molecular functions of these proteins.

The HAG5-ARIA interaction and has been confirmed *in planta* using *N. benthamiana* transient expression of proteins. Nonetheless, a third method for testing protein-protein interactions in *Arabidopsis thaliana* would give supporting evidence for the interaction between HAG5 and ARIA. We propose using a split-YFP strategy in Arabidopsis protoplasts overexpressing both *HAG5* and *ARIA* with the N and C-terminal domains of YFP. If this interaction happens in Arabidopsis, when HAG5 and ARIA are physically bound to each other, the two domains of YFP will reconstitute the entire protein, whose fluorescence can then be identified using confocal microscopy. Furthermore, exogenous ABA can be applied to the protoplasts to monitor changes in the intensity of the YFP signal, which is an indirect measure of the interaction between HAG5 and ARIA. This would answer the question of whether ARIA and HAG5 interaction depends on or strengthens upon ABA perception.

4.10.2. The role of HAG5 in regulating ABA responses

Based on the detection of ARIA as an interacting partner of HAG5, we have investigated the ABA-related phenotypes of *hag5* mutants. We concluded that *hag5* mutants are less sensitive to exogenous ABA in terms of germination rate and root elongation. In addition, the expression of ABF2-dependent genes was delayed in *hag5* mutants and *HAG5* expression got induced upon ABA treatment. Hence, HAG5 plays a role in the regulation of ABA-responsive genes, facilitating a quick response to the phytohormone. Because ARIA only regulates a subset of ABF2-dependent genes, we proposed a model in which HAG5, through its interaction with ARIA, facilitates ABF2 transcriptional activity either through H4K5ac in the vicinity of ABA responsive loci or by enhancing the activity of the transcription factor. In order to test if the role of

HAG5 in ABA signalling is related to its histone acetyltransferase activity, we performed a ChIP-seq experiment looking for H4K5ac enrichment in the genome after ABA and in the absence of HAG5. The lack of differences between treated and untreated samples suggested that, even though we found several ABA-responsive genes associated to H4K5ac, the ABA treatment did not increase or decrease the acetylation status of these loci. These results show that H4K5ac is not promoted nor decreased after ABA treatment, and that this epigenetic mechanism is not playing a regulatory role in abscisic acid signalling, at least under the tested conditions. Furthermore, the lack of differences in the levels of H4K5ac between *hag5-2* mutants and the wild type seedlings suggested that either HAG5 does not acetylate H4K5 *in vivo*, or that HAG4 redundantly performs HAG5 acetylation duties. Nonetheless, the transcriptional differences observed in the mutants can only be attributed to a process independent of H4K5ac, either through the assembly of a transcriptional protein complex with ARIA, ABF2 and potentially other components, or through the acetylation of the interacting transcription factors to modulate their activity. However, complementing *hag5-2* mutants with an enzymatically dead version of HAG5 would provide further insight into whether the acetyltransferase activity of HAG5 is responsible for the observed phenotypes.

Further research focusing on the nature of the ARIA-HAG5 interaction is required in order to answer the questions regarding the molecular mechanism by which HAG5 regulates ABA responses. We suggest using the 35S:*HAG5*-FLAG overexpressor Arabidopsis lines generated to pull down HAG5 and, through mass-spectrometry, identify possible interactors and members of the hypothesized complex between HAG5, ARIA and ABF2. In addition, performing this pull-down in ABA treated and untreated plants would give us information about whether the HAG5-ARIA interaction or even the formation of a transcriptional complex is ABA-dependent. In order to test if HAG5 facilitates ABF2 binding to the chromatin, we propose Fluorescence Recovery After Photobleaching (FRAP) assays in Col-0 and *hag5-2* mutant protoplasts transformed with 35S:ABF2 with a GFP tag. With this technique, we can measure the time it takes for ABF2 to bind to the chromatin by imaging the nuclei in the transformed protoplasts, looking at the recovery of the GFP signal after bleaching the nuclei. The use of protoplasts will allow looking into the dynamics of ABA signalling in different mutants. Other members of the Ntoukakis

group have designed a protoplast-based system using hormone related markers as reporters of transcriptional activity. Using the luciferase (LUC) as a reporter under the control of *RAB18* promoter, a gene regulated by ABF2, we can quantify the timing and amplitude of *RAB18* transcriptional activation in *aria*, *abf2* and *hag5* mutant protoplast by measuring the LUC activity over time. If the activity of the promoter over time is similar between all mutants, it will imply that all three proteins are involved in the same ABA response mechanism.

4.10.3. HAG5 regulation of drought recovery

hag5-2 mutants display increased tolerance to drought stress in terms of seedling growth under reduced water availability and recovery of adult plants after a prolonged period of drought. The most prominent drought phenotype took place under prolonged stress, and the phenoscope data revealed that the mechanism underlying this increased resistance was not related to growth arrest. The recovery phenotype suggests that the senescence and programmed cell death activated through drought (Sade et al., 2018), as opposed to leaf growth arrest, are delayed processes in *hag5* mutants. A previous study in tobacco plants showed that it was possible to enhance drought tolerance of plants by delaying the drought-induced senescence of leaves during the drought treatment (Rivero et al., 2007). Their hypothesis was that if senescence is to be considered a type of programmed cell death, suppressing this mechanism would prolong the drought tolerance over time. To test this hypothesis, the authors suppressed drought-induced senescence by promoting cytokinin biosynthesis through the expression of a rate-limiting factor under a stress inducible promoter. To test the drought tolerance, the authors grew transgenic and wild type plants for 40 days under standard conditions, and after this period, the plants were subjected to severe drought for 15 days. During the drought period, the wild type plants showed progressive wilting and senescence, whilst the transgenic plants partially wilted but did not display drought-induced senescence. After 1 week of re-watering, the wild type plants did not recover and died, whilst the transgenic plants' leaves recovered their turgor and finally resumed their growth (Rivero et al., 2007). Both the experimental settings and the observed recovery phenotype coincides with our drought recovery assays and *hag5-2*

increased drought tolerance. Hence, we hypothesize that HAG5 regulates drought responses through the control of ABA-induced senescence during drought stress.

Programmed cell death resulting in leaf senescence is a mechanism that regulates growth and development in plants. It is considered an evolutionarily acquired strategy tightly associated with reproduction and survival, since it results in the re-direction of nutrients towards developing and storage tissues (Guo and Gan, 2014). One of the most intriguing incognitos for plant biologist has been which are the mechanism by which plants decide when and how to initiate senescence. It is known that senescence develops in an age-dependent manner, but it can also be triggered by environmental stresses such as drought, low or high temperatures and darkness, as well as phytohormones such as ABA, ethylene, salicylic acid and jasmonic acid, whilst being delayed by cytokinin (Guo and Gan, 2014). Upon initiation of leaf senescence, genetic reprogramming resets the regulatory network of senescence-associated genes (SAGs) (Li et al., 2017d). ABA was thought to regulate senescence by promoting ethylene production (Riov et al., 1990). However, a recent study identified that an ABA receptor (PYL9) promoted ABA-induced senescence by inhibiting PP2Cs, with the subsequent activation SnRK2s to mediate phosphorylation of RAV1 (Related to ABI3/VP1), an ABA-dependent TF, and ABF2. These transcription factors up-regulate the expression of *ORE1* and other *NAC* transcription factors to activate the expression of senescence-activated genes (SAGs) (Zhao et al., 2016). These findings are crucial, since the participation of ABF2 in up-regulating senescence-related genes might explain the delay in senescence of *hag5* mutants, resulting in the drought recovery phenotype. This would be based on the hypothesis that HAG5 forms a protein complex with ARIA and potentially, ABF2, to facilitate transcription of target genes. However, further evidence is needed to link the drought recovery phenotype of *hag5* plants to delayed senescence. We propose quantifying the expression of the previously mentioned senescence marker genes (SAGs) in *hag5* mutants after drought stress, as well as studying the transcriptional landscape of Col-0 and *hag5*-2 plants when differences in senescence are observed between both genotypes during the drought treatment. If the activation of the senesce-related genes is delayed in *hag5-2* mutants, it could be either because HAG5 facilitates ABF2 binding to its target SAGs, or because HAG5 acetylates H4K5 in the vicinity of these loci.

Chromatin remodelling through histone modifications has been identified as a mechanism involved in the regulation of leaf senescence. A study combining ChIP-seq and RNA-seq data identified a strong correlation between temporal changes in levels of H3K4me3 and transcription of SAGs during leaf senescence. (Brusslan et al., 2015). Further evidence for a link between regulation of leaf senescence and histone modifications was provided by a study characterising *hda9* mutants, which displayed delayed senescence phenotypes (Chen et al., 2016). A genome-wide occupancy profiling revealed that HDA9 directly binds to the promoters of key negative regulators of senescence. Thus, there is strong evidence for the importance of histone deacetylases in modulating global gene expression during leaf senescence. In order to identify if H4K5 acetylation is responsible for regulating the expression of senescence associated genes, we propose a ChIP-seq experiment looking at chromatin associated to H4K5 in Col-0 plants under well-watered and drought-induced senescence conditions.

Even though further characterisation is needed to understand the molecular mechanisms in which HAG5 participates, the drought recovery phenotypes, together with the increased fitness (leaf area and root length) and tolerance to *P. syringae* DC3000 of *hag5* mutants, manifest that there are beneficial effects of inhibiting HAG5. In the following chapter, we will investigate the transcriptional response of *hag5-2* mutants to ABA through RNA-seq experiments. In addition, we will propose different strategies to translate our findings to generate better-performing crop plants without a developmental trade-off. We will discuss how to mimic the *hag5* mutant phenotypes in wild type plants without using transgenesis, as well as investigating the conservation of *HAG5* across plant lineages and the generation and partial characterisation of CRISPR/Cas9 *Brassica oleracea* plants lacking this enzyme.

Chapter 5 Developing HAG5 inhibitors to improve crop performance

5.1 Context of this chapter

The findings presented in Chapter 3 and Chapter 4 indicate that reducing or repressing the expression of *HAG5* results in beneficial phenotypes, both in the context of response to pathogens and tolerance to drought. Indeed, HAG5 acts as a negative regulator of defence and drought tolerance by modulating the transcriptional activation of ABA responsive genes. This confers increased tolerance to infection with *P. syringae* DC3000, as well as higher rates of drought recovery, with minimal impact in plant growth. In fact, *hag5* mutants are bigger plants, with increased leaf area, longer roots and bigger root meristem. As a consequence, and due to the high conservation of *HAG5* across plant lineages, targeting HAG5 in an agricultural context has the potential to translate these advantageous phenotypes to crop plants. Two different approaches for improving plant performance are implemented on this chapter. The first approach consists of screening chemical inhibitors identified using *in silico* modelling of HAG5 by performing different phenotypic assays to evaluate if inhibitors are able to replicate *hag5* mutant phenotypes when applied to Col-0 plants. The most promising inhibitor candidate will then be tested following a transcriptomic approach in order to evaluate the effects that the compound has in regulating gene expression in Col-0 plants at basal state and in response to ABA, as an indirect measure of its specificity. The transcriptional response of inhibitor-treated plants to ABA will then be compared to that of *hag5-2* mutants in order to find common elements, revealing whether the compound is able to inhibit the catalytic activity of HAG5 *in vivo* and mimic the transcriptional effects caused by the loss-of function mutation of *HAG5* in response to ABA.

The second approach consists of targeting *HAG5* homolog in *Brassica oleracea* using gene editing through CRISPR/Cas9 to investigate whether the advantageous phenotypes observed in *hag5-2* Arabidopsis mutants can be translated to other members of the *Brassica* family through loss-of function of the conserved homolog. To this end, a collaboration was established with members of the Biotechnology Resources for Arable Crop Transformation (BRACT) facility at John Innes Centre to

design RNA guides targeting *HAG5* orthologue in *B. oleracea* DH1012, and create non-transgenic *HAG5* loss-of function Brassica lines.

5.1.1 Identifying inhibitors of HAG5 *in silico*

Since *hag5-1* (knock-down) and *hag5-2* (loss-of function) display similar phenotypes, and due to the current controversy about the use of GM crops in Europe, an approach for developing inhibitors of HAG5 catalytic activity in order to replicate the observed mutant phenotypes was adopted. Previous research has described the role of HAG5 in DNA-damage repair, and addressed the negative effects of silencing *HAG5*, which results in increased DNA damage after UV-B treatment (Campi et al., 2012). In light of these findings, using chemical inhibition of HAG5 implies that the treatment can be applied under specific conditions, avoiding any potential detrimental effects of permanently knocking out *HAG5*. To this end, Dr. Stephanie Kancy performed *in silico* docking to identify chemical inhibitors of HAG5. To begin, she created a homology model of HAG5. Once the model had been quality-evaluated, the ChemBridge library of structural data of over a million compounds was used to screen for compounds with agrochemical properties (foliar absorbed, able to translocate into the plant trans vascular system, able to translocate into the nucleus and with low reactivity towards non-plant HATs). Subsequently, an *in silico* docking was performed with the filtered 979,672 compounds to identify candidate inhibitors (Figure 5.1). The details of the homology model generated, and the computational docking performed against the AtHAG5h homology model can be found within her PhD thesis.

Given the phenotypic differences resulting from silencing *HAG4* or *HAG5*, the inhibitor screening had to be refined so that the inhibitors were specific for HAG5. Indeed, *hag4* mutants do not present the increased leaf area or root length, and they display ABA hypersensitivity. In addition, compounds were also filtered out for their affinity to bind to a homology model of the HAG5 human monologue *HsKAT8* (*TIP60*), in order to select for compounds with low toxicity.

The list of identified candidates is displayed in Figure 5.2. These inhibitors target HAG5 active centre to compete against Acetyl-CoA, the natural ligand of HAG5. Their high affinity to the conserved residues and low affinity to the non-

conserved ones ensures that the inhibitor will have low toxicity due to their plant specificity. In order to investigate whether the inhibitors were specific for HAG5 and do not bind to HAG4, Dr. Veselina Uzunova ran several docking simulations with the selected list of inhibitors against a homology model created for HAG4 following the same approach for modelling HAG5.

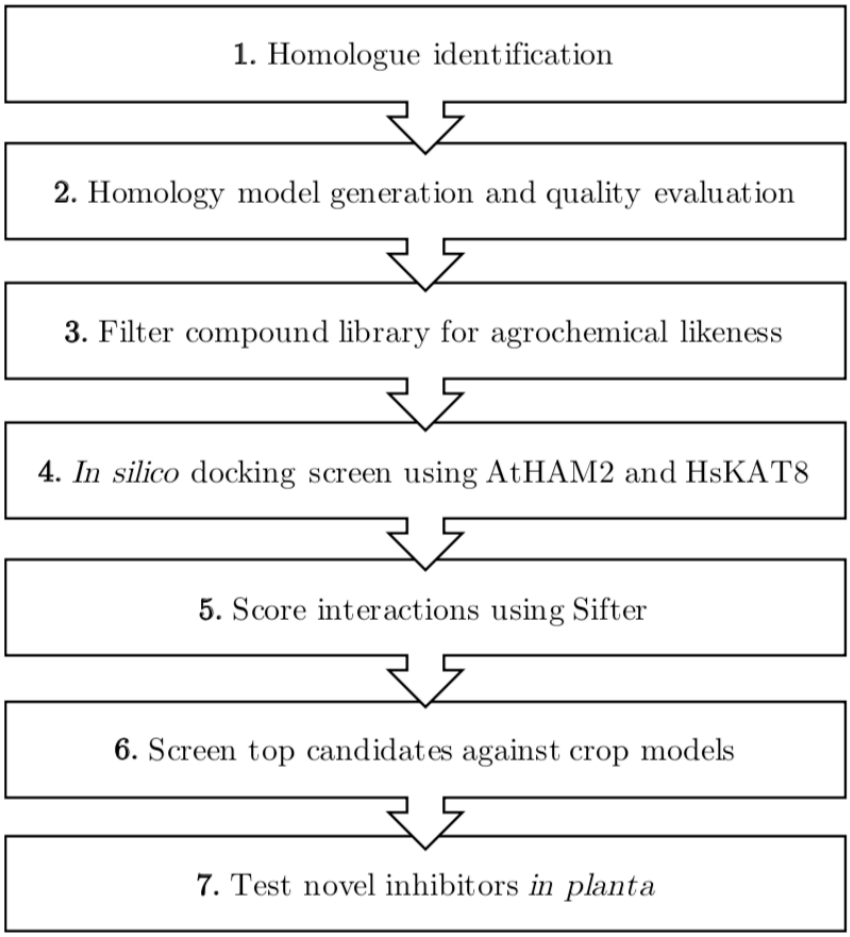

Figure 5.1. Diagram of the work-flow followed by Dr. Stephanie Kancy and Dr. Veselina Uzunova from homologue identification to novel inhibitor discovery.

The aims of the following section are to identify the best candidate amongst the selected inhibitors following three approaches:

- Testing inhibitors *in planta* to mimic mutant phenotypes.
- Investigating the transcriptional response of Col-0 and *hag5-2* mutants to ABA.

- Comparing the transcriptional response to ABA in Col-0 seedlings treated with candidate inhibitor to define specificity and similarity to *hag5-2* transcriptional response.

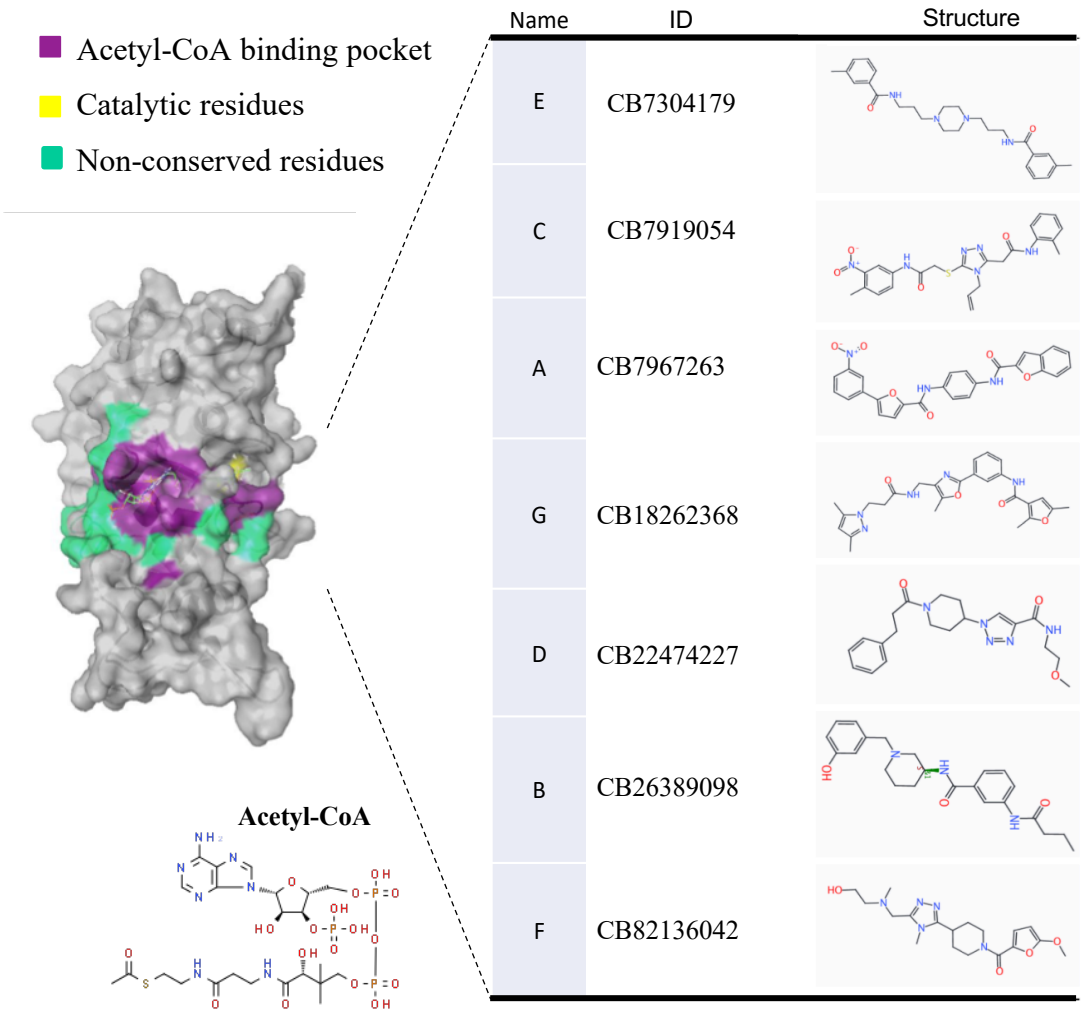

Figure 5.2. Graphical representation of Acetyl-CoA binding site in HAG5 and list of candidate inhibitors. Left: Homology model AtHAG5 catalytic domain. Acetyl-CoA binding pocket (purple), catalytic residues (yellow) and non-conserved residues (green) are represented. Below, the chemical ring structure of acetyl-CoAis displayed. Right: List of candidate inhibitors with their compound ID and chemical ring structure. Hydrophilic and hydrophobic residues are represented in blue and red respectively.

5.2 Screening of HAG5 inhibitors *in vivo*

5.2.1 Effect of inhibitors in root meristem size

Due to the evidence between HAT dysfunction and human pathologies, there have been many studies looking for inhibitors targeting the human MYST subfamily of HATs to develop novel therapeutics. Coffey et al. carried out a high-throughput *in vitro* screen to identify inhibitors of the human MYST Tip60 amongst 80,000 compounds. The inhibitor 1,2-bis(isothiazol-5-yl) disulfane (NU9056) was identified as a relatively potent inhibitor (IC50 2μM), and the authors confirmed its cellular potency by analysis of acetylation of histone and non-histone proteins in a prostate cancer cell line model (Coffey et al., 2012).

A way to test for successful HAG5 inhibitor candidates is to treat Col-0 seedlings with the *in silico* identified candidate inhibitors and investigate whether the treatment reproduces *hag5* mutant phenotypes in the wild type plants. In Chapter 3, the developmental phenotypes of *hag5* mutants were described, concluding that *hag5* seedlings have longer roots with increased meristem size. To measure the meristem size, seedlings are grown on ½ MS plates before imaging. Due to this highly controlled experimental set up, this assay was chosen in order to test for the efficacy of the inhibitors, since a precise concentration of inhibitor can be supplemented to the MS media, and the use of seedlings minimises time constraints and variables introduced by the use of adult plants.

Thus, measurements were taken from the meristem of Col-0 and *hag5-2* roots in 4 day old seedlings that were transferred overnight to ½ MS plates supplemented with DMSO (solvent of the inhibitors, used as control) or the candidate inhibitors A and B. Tip60 NU9056 was used as a control inhibitor, supplemented at the IC50 concentration calculated by (Coffey et al., 2012) (Figure 5.3). As seen in Figure 5.3, Tip 60 inhibitor and inhibitors A and B increased the meristem size of Col-0 plants, resembling the phenotype of *hag5-2* mutants. This pilot assay confirmed that meristem size differences can be measured using IC50 concentration of inhibitors calculated by (Coffey et al., 2012).

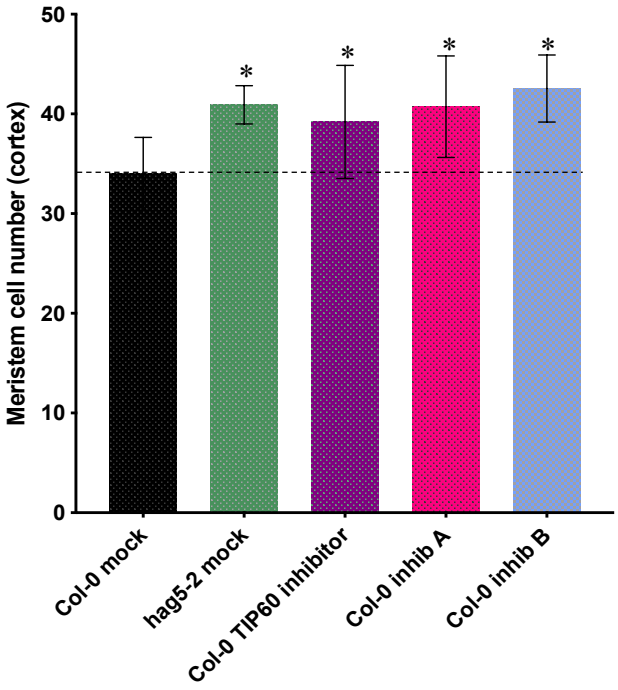

Figure 5.3. Meristem cell number in response to HAT inhibitors. Col-0 and *hag5-2* seedlings were germinated *in vitro* and grown vertically for 4 days. 10 seedlings/genotype were transferred overnight into ½ MS plates supplemented with DMSO (mock) or 2µM of Tip 60 inhibitor (NU9056) (Coffey et al., 2012) or inhibitors A and B. Roots were imaged using propidium iodide in a confocal microscope Leica SP5. The graph represents the number of cortical cells form the quiescent centre. One-way ANOVA was used to determine significant differences between groups, * $P \leq 0.05$. Error bars represent SD (n = 10). The experiment was repeated three times with similar results.

Alexia Tornesaki, a PhD student within the Ntoukakis group, performed the screening of all the HAG5 inhibitor candidates (A-G) using the described experimental setup (Figure 5.4). In this experiment, Col-0 seedlings were transferred overnight to plates supplemented with 2µM of each inhibitor (A-G) or DMSO as control. Confocal images of roots stained with propidium iodide were taken and root meristems size was then calculated for seedlings in each treatment. As seen in Figure 5.4 all inhibitors except E and F increased the meristem size of Col-0 seedlings, mimicking the root phenotype of *hag5* mutants. This screening was repeated by a visiting student in the lab (Ellie Fletcher) with similar results. As a consequence, inhibitors E and F were discarded from further assays.

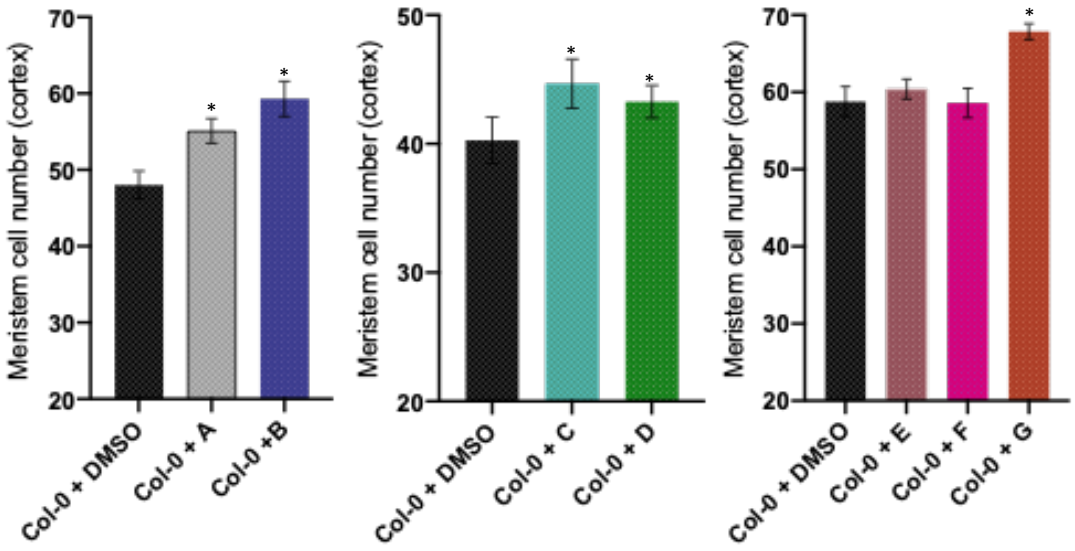

Figure 5.4. Screening of HAG5 inhibitors using meristem size. 10 day old Col-0 seedlings were transferred to ½ MS plates supplemented with DMSO or 2µM of each candidate inhibitors (A-G) and left to grow overnight. Meristem size was determined as the number of meristematic cells form the QC to the first expanding cell. Col-0 plants were transferred to normal ½ MS plates (50ml of media per plate) with the chemical compounds A-G for 24 hours. Error bars indicate SD (n = 10). Asterisks indicate statistically significant differences to the control samples (Col-0 DMSO), calculated using One-way Anova ($P < 0.05$).

5.2.2 Effect of inhibitors in tolerance to dehydration

In order to narrow down the lists of inhibitors, dehydration assays in plates were performed to assess whether supplementing Col-0 plants with the inhibitors would confer increased tolerance to desiccation, as previously observed in *hag5-2* mutants (Chapter 4). In this assay, 14 day old Col-0 seedlings were germinated and grown vertically in ½ MS plates, then transferred to plates supplemented with DMSO (control) or 2µM of each inhibitor. Each plate contains exactly 50mL of solid media to ensure equal conditions amongst samples. 10 seedlings per genotype were transferred per plate and left to grow under short photoperiod until the media was consumed, exposing the plants to drought.

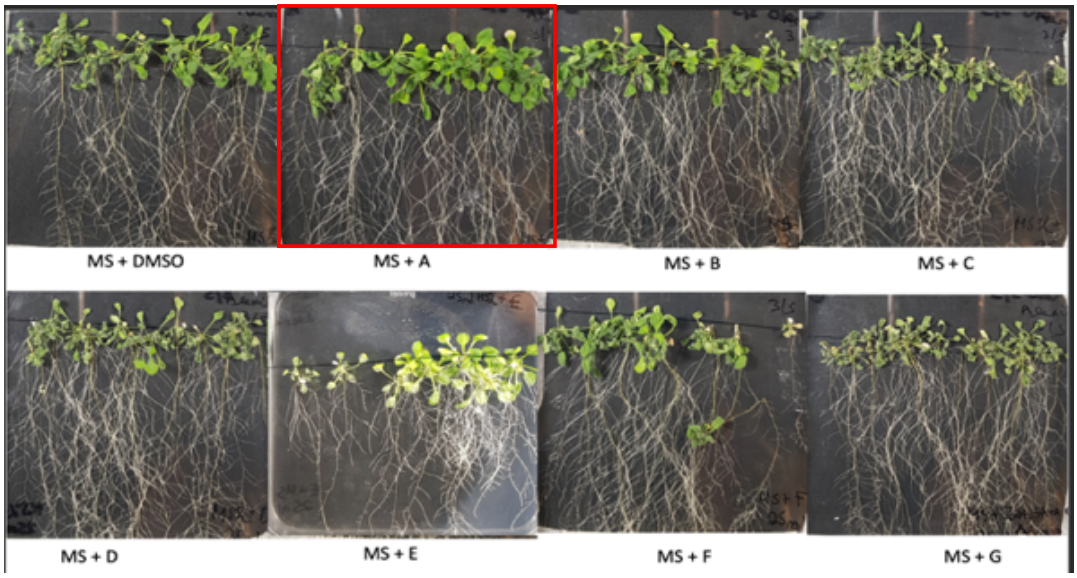

Figure 5.5. Dehydration assays in plates supplemented with the inhibitors. 14 day old Col-0 plants germinated and grown in ½ MS plates were transferred to plates containing 50mL of media and DMSO (control) or 2µM of each inhibitor. 10 seedlings were transferred per condition. Seedlings were grown under short photoperiod until dehydration was observed (loss of turgor and drying of the cotyledons). Pictures of the plates were taken using a scanner HP (methods). Seedlings with best performance under drought are highlighted in red (inhibitor A). The assay was performed by Alexia Tornesaki.

Figure 5.5 shows that between the inhibitors that confer increased root meristem (A, B, C, D and G), inhibitor A provides increased tolerance to desiccation in Col-0 plants, since the plants displayed increased green colour and turgor when compared to the control (Col-0 in DMSO). However, this assay is based on a qualitative measurement. Hence, quantifying this tolerance by measuring fresh weight of dehydrated seedlings would be a more reliable, quantitative measurement of this phenotype. Combining the root meristem phenotype and the desiccation tolerance conferred by inhibitor A, we proceeded to test the effects of this inhibitor in *hag5* mutants as an indirect measure of specificity.

5.2.3 Effect of inhibitor A in *hag5* mutants

To characterise the effects of inhibitor A in both Col-0, *hag5-1* and *hag5-2* mutant plants, meristem size assays were repeated using the three genotypes in order to test the effects of the inhibitor A in the knock-down and knock-out mutants. The

aim of this experiment was to look for phenotypic differences in *hag5* mutant roots caused by non-specific binding to other acetyltransferases or other off-target activities (Figure 5.6a).

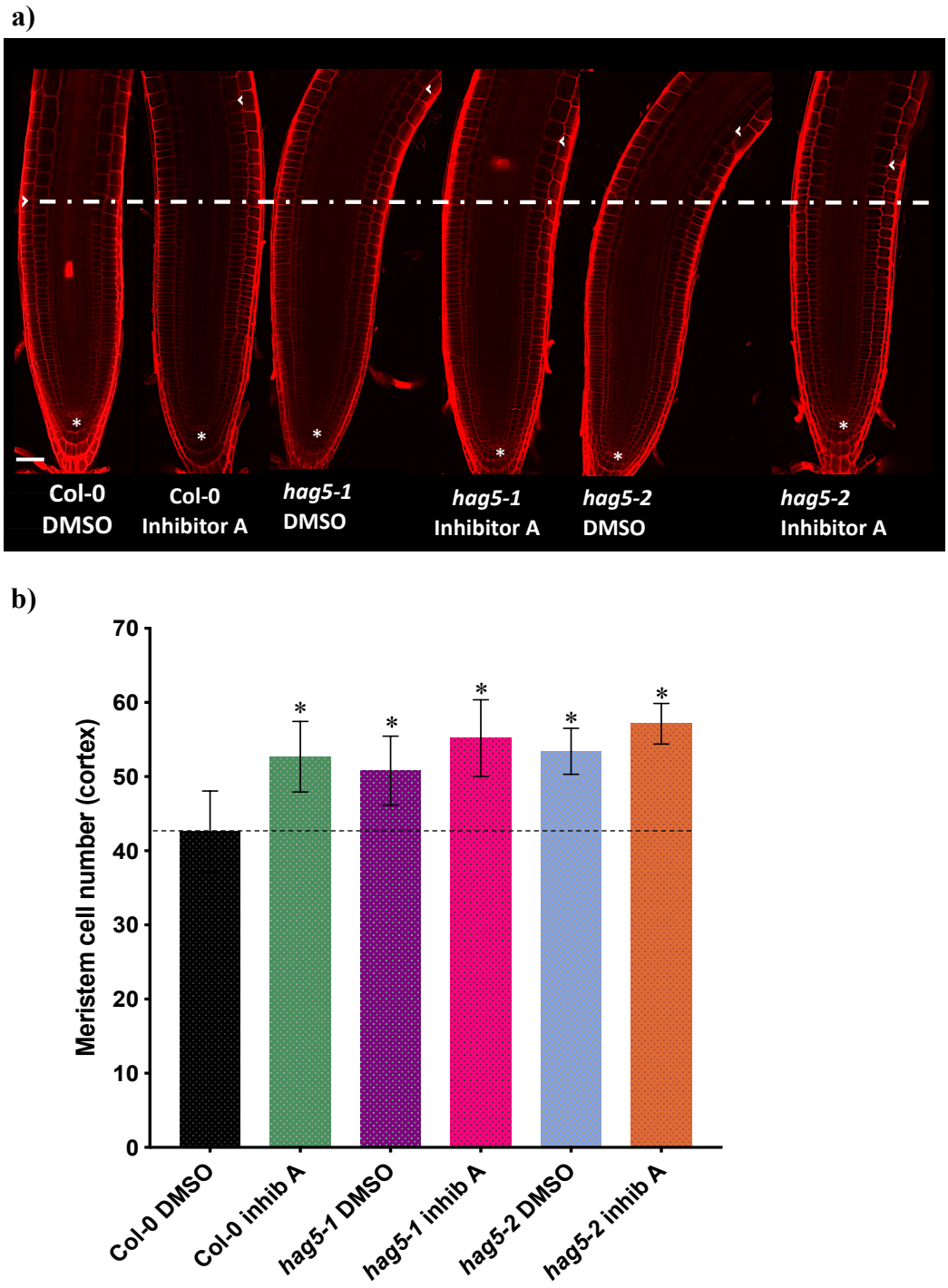

Figure 5.6. Effects of inhibitor A in meristem size of Col-0, *hag5-1* and *hag5-2* roots. **a)** Propidium iodide staining of 4 day old Col-0, *hag5-1* and *hag5-2* roots form seedlings transferred to ½ MS with DMSO or 2µM of inhibitor A overnight. Pictures were taken using a confocal microscope Leica SP5. The quiescent centre (QC) is marked with an asterisk, and the transition between the meristem and the elongation zone, with an arrow. **b)** Meristem cell number in

response to inhibitor A. Number of cells was determined from the quiescent centre (QC) to the first expanding cortical cell. Asterisks indicate statistically significant differences to the control samples (Col-0 DMSO), calculated using One-way Anova ($P < 0.05$). Error bars represent SD ($n = 10$).

As seen in Figure5.6a-b, inhibitor A increased the meristem size of Col-0 roots, resembling *hag5-1* and *hag5-2* roots, without significant additional phenotypic effects observed in any of the *hag5* mutants. Collectively, our results indicate that chemical A is a promising candidate to inhibit HAG5 *in vivo*. However, other phenotypic tests must be run in order to elucidate if inhibitor A confers beneficial effects comparable to those of down-regulating or silencing *HAG5*. Phenotypic assessment of treated plants is just an indirect measure to test for the inhibitory activity of the candidate compounds. Thus, additional methods assessing the specificity of the inhibitor and the effect that it has on plant homeostasis at the molecular level are needed to verify that the effects observed after treatment are indeed due to a successful inhibition of HAG5. In the following sections, the effects of compound A in plant homeostasis under non-stress conditions, as well as its effect on ABA responses will be assessed and compared to those of *hag5-2* mutants. The aim of this characterisation is to evaluate whether inhibitor A could be used as an exogenous treatment in wild type plants to reproduce some of the advantageous phenotypes of *hag5* mutants.

5.3 Investigating the transcriptional response of *hag5* to ABA treatment

In the previous chapter, interactors of HAG5 were identified through a yeast-2 hybrid screening using a library of Arabidopsis transcription factors. One of the two interacting TFs was ARIA, an arm repeat protein previously shown to interact with AREB1/ABF2 (Kim et al., 2004a). In light of these results, phenotypical and transcriptional response of *hag5* mutants to ABA treatment was investigated. *hag5* mutants are hyposensitive to treatment with exogenous ABA and display a delay in the transcriptional response to the phytohormone, as assessed by a time course qPCR looking at the expression of an ABA marker genes (*RAB18*) in seedlings treated with 50µM ABA. These results altogether suggest that HAG5 is a positive regulator of ABA signalling, possibly due to its interaction with ARIA or ARIA-ABF2 protein complex.

To better understand the role of HAG5 in regulating ABA signalling, RNA-sequencing (RNA-seq) parallel to the ChIP-seq experiment was performed to have an overview of the whole transcriptional response of *hag5* loss-of function mutants. Looking at the transcriptomic differences between Col-0 and *hag5-2* mutants will provide an insight into all the pathways in which HAG5 directly or indirectly participates upon ABA signalling, bringing some light into the currently unknown molecular mechanism underlying HAG5 activity towards ABA-dependent regulation of stress responses.

In the previous sections of this chapter, inhibitor A was identified as a potential candidate to mimic *hag-5* mutant phenotypes in wild type (Col-0) Arabidopsis plants. However, the effect of the inhibitor (increased meristem size) observed in the phenotypic assays used for the screening could be due to an indirect effect rather than due to HAG5 inhibition.

An indirect way to test if compound A is inhibiting the catalytic activity of HAG5 is to look at the transcriptional landscape of Col-0 inhibitor-treated plants and compare it with that of the *hag5-2* mutants. However, the results from the microarray analysis in Chapter 3 showed that there are very few differences in gene expression between both genotypes at basal state. The major transcriptional and phenotypical differences between Col-0 and *hag5-2* mutants occur after stress.

Addressing these uncertainties, Col-0 and *hag5-2* samples treated with the inhibitor and in the presence or absence of ABA were included in the RNA-seq experiment in order to see if inhibitor A could reproduce the ABA response of *hag5-2* mutants upon ABA treatment. To this end, 10 day old seedlings germinated *in vitro* were transferred to ½ MS media supplemented with DMSO, DMSO + 2µM inhibitor A, 50µM ABA or 50µM ABA + 2µM inhibitor A for 7h. 3 seedlings were used per genotype and condition, and three biological replicates were performed independently. RNA was extracted as described in section 2.9.2 of Chapter 2. Multiplex RNA library construction and Illumina sequencing were carried out at the Beijing Genome Institute (BGI).

In order to estimate differential gene expression and fold change between one-to-one comparisons, average sequencing data from the three biological replicates sequenced per sample were compared using DESeq2 (Love et al., 2014), with a fold change ≥ 2.0 and adjusted p-value ≤ 0.05. The diagram for each sample comparison,

with its description and the identified number of DEGs is illustrated in Figure 5.7a-c. Comparisons 1 and 2 look into the differences between Col-0 and *hag5-2*, and Col-0 with or without inhibitor A at basal state, respectively. As seen in Figure 5.7c, the numbers of DEGs between Col-0 and *hag5-2* at basal stage are very low (only 31 genes differentially expressed), in agreement with the microarray data from Chapter 3. Comparisons 3-5 are within genotypes in response to ABA treatment (Col-0, *hag5-2* and Col-0 + inhibitor A, respectively). The transcriptional response to ABA for each comparison results in ~2000 DEGs due to the hormone treatment (Figure 5.7c).

a)

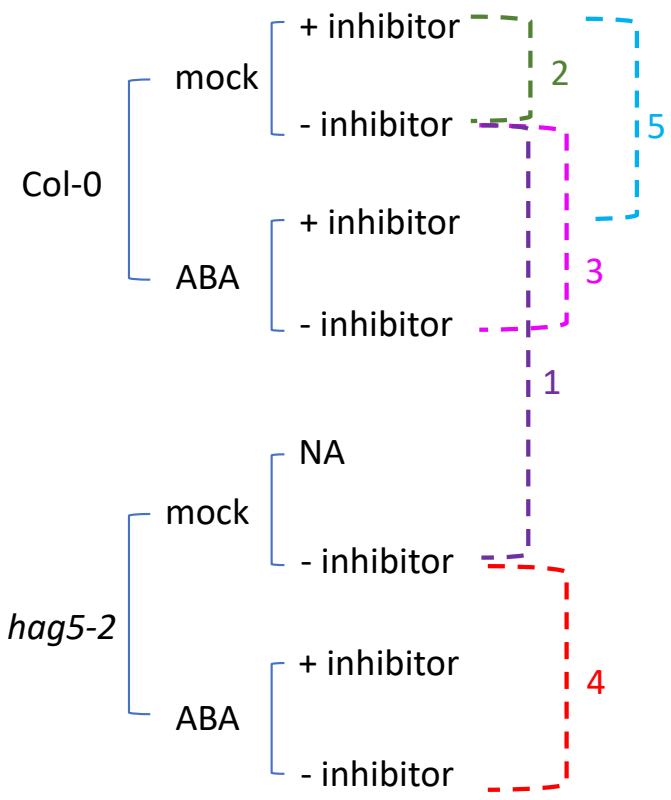

b)

		Comparison	Description	Significance
Basal conditions	1	Col-0 vs *hag5-2*	DEGs between genotypes in basal state	Transcriptional response to *HAG5* mutation
	2	Col-0 (+/- inhibitor)	DEGS after inhibitor A	Transcriptional changes induced by inhibitor A
After ABA treatment	3	Col-0 (+/- ABA)	DEGs in response to ABA	Transcriptional response of Col-0 to ABA
	4	*hag5-2* (+/- ABA)	DEGs in response to ABA	Transcriptional response of *hag5-2* mutants to ABA
	5	Col-0 + ihibitor (+/- ABA)	DEGs in response to ABA and inhibitor	Transcriptional response to ABA in the presence of the inhibitor

c)

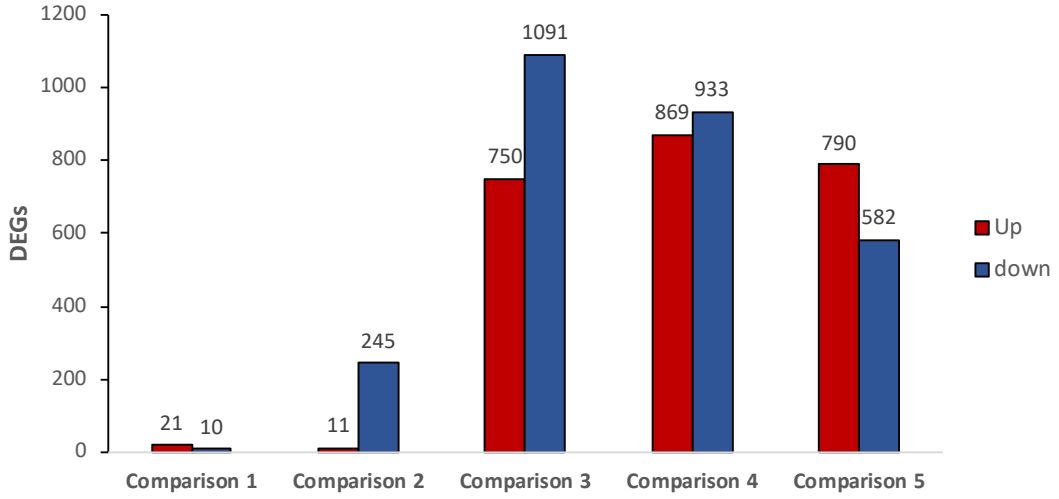

Figure 5.7. Sample comparisons for the RNA-seq experiment. **a)** Diagram of the different samples sequenced. The dashed lines indicate the one-to-one comparisons between samples to calculate differential expression (DEGs). **b)** Table displaying the various comparisons between samples and their biological significance. **c)** Bar plot displaying the total number of up and down-regulated genes identified between each comparison. Number of DEGs was calculated using DESeq2 (Love et al., 2014), with a fold change ≥ 2.0 and adjusted p-value ≤ 0.05.

5.3.1 Transcriptomic differences in basal state

In order to assess the specificity of the inhibitor, the common and distinct DEGs between comparison 1 and comparison 2 (Col-0 after inhibitor A and Col-0 vs *hag5-*

2) were obtained. This comparison revealed that there is no overlap between the transcriptional response resulting from treating Col-0 with inhibitor A or resulting from silencing *HAG5*. As seen in the Venn diagram from Figure 5.8, the inhibitor treatment itself results in a strong repressive transcriptional response, since the majority of the DEGs are down regulated after treatment with the compound. Regarding the DEGs between Col-0 and *hag5-2,* results were very similar to those discussed in Chapter 3, with no major transcriptional differences between genotypes in basal state, besides the strong repression of *HAG5*.

Gene ontology (GO) term enrichment of the DEGs from comparison 2 revealed that treatment with inhibitor A results in the transcriptional repression of genes related to biotic and abiotic stress responses, such as ABA, SA, drought, oxidative stress or immunity (Figure 5.8b). Looking into the molecular function of the same group of genes, most of them are associated with DNA binding and transcriptional regulation (Figure 5.8c). As a consequence, inhibitor A represses the signalling response to biotic and abiotic stress-related genes in the absence of stimuli. The lack of overlap between the inhibitor treatment and *hag5-2* can be due to several reasons. The *hag5-2* mutant seedlings have germinated and undergone development in the total absence of HAG5, achieving a level of homeostasis that is reflected through the small number of DEGs between genotypes. On the other hand, Col-0 plants were only treated with the inhibitor for 7h. Hence, it is not surprising that the transcriptional landscape is completely different between both comparisons. In addition, it is possible that inhibitor A binds to other HATs besides HAG5, which would explain the transcriptional repression observed resulting from a reduction in the acetylation status of stress-related genes that have basal low levels of expression. However, the inhibitor-induced transcriptional changes do not necessarily imply lack of affinity. A study assessing the transcriptional differences in salt-stressed Arabidopsis seedlings treated with *in vitro* confirmed HDACs inhibitors showed that the inhibitor treatment under mock conditions (DMSO) resulted in between ~400 and ~200 DEGs, depending on the inhibitor (Nguyen et al., 2018). Nonetheless, the inhibitors conferred increased tolerance under salt stress and induced gene expression of salt tolerance genes typically repressed by HDACs. These results suggest that treatment with HADC or HAT inhibitors might produce transcriptional changes in basal state due to the

alteration of the acetylation state of genes that keep defined levels of expression, and not necessarily due to non-specific binding.

Yet, more phenotypic characterisation of plants treated with inhibitor A is required in order to understand the physiological effects that the compound has under non-stress conditions.

The following sections will focus on the transcriptional response between h*ag5-2* mutants and Col-0 plants after ABA treatment, and how that response differs from both comparisons in the presence of the inhibitor.

a)

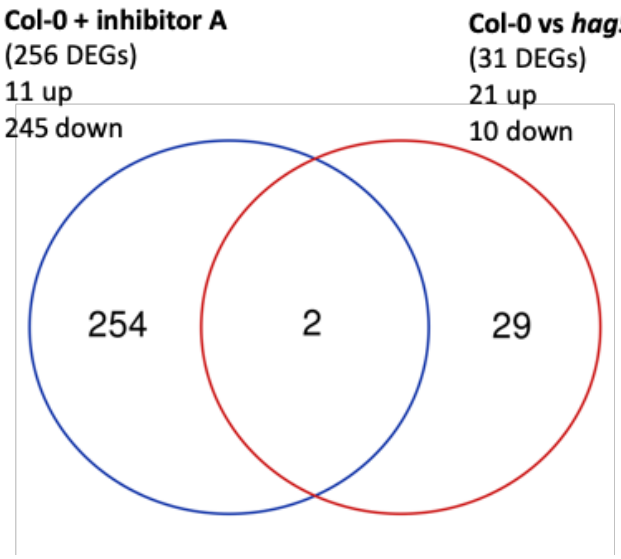

GO-term enrichment of DEGs after inhibitor A in Col-0

b)

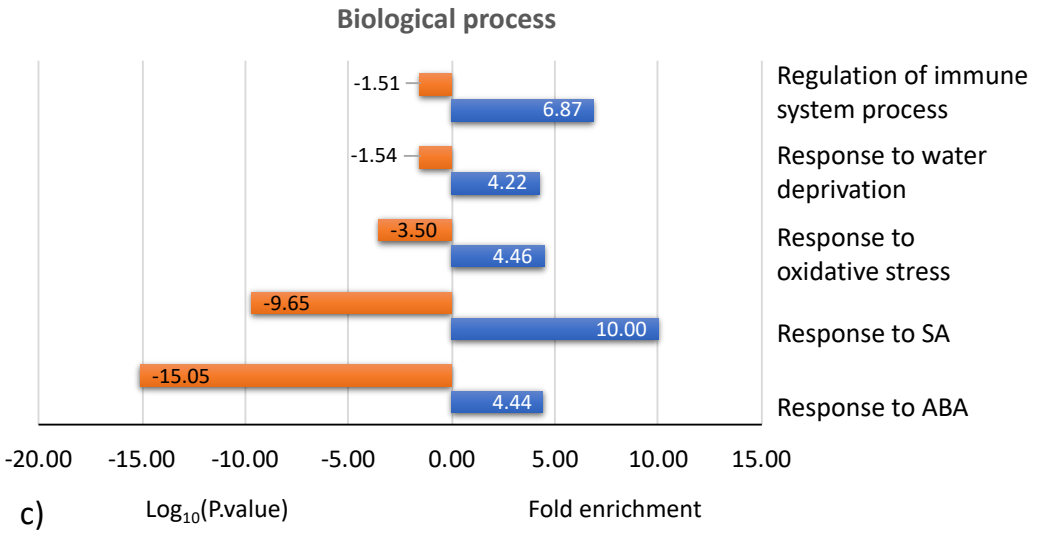

c)

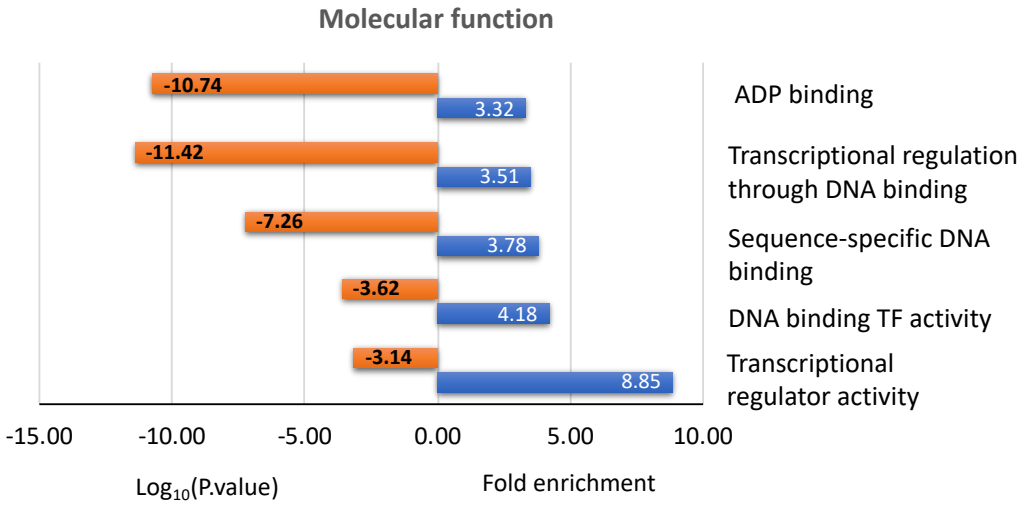

Figure 5.8. Common and unique DEGs in response to inhibitor A or *HAG5* silencing. **a)** Venn diagram of overlapping DEGs between Col-0 after 7h of treatment with 2µM of inhibitor A and Col-0 in comparison to *hag5-2* mutants. **b)** Biological process GO term enrichment of non-overlapping DEGs in response to inhibitor A. **c)** Molecular function GO term enrichment of non-overlapping DEGs in response to inhibitor A. Fold enrichment was calculated by dividing the number of obtained DEGs for a particular GO term over the total number of random hits predicted for that GO term. The GO term enrichment was performed using PantherDB, applying the Bonferroni correction for multiple testing (Mi et al., 2009).

5.3.2 Transcriptomic response to abscisic acid

This section is dedicated to the characterisation of the transcriptional response of Col-0 and *hag5-2* seedlings to the phytohormone abscisic acid. In Chapter 4, it was described that *hag5-2* mutants have a delayed upregulation of ABA response genes upon treatment, with an overall lower expression levels in comparison to Col-0 at 7h after induction. This RNA-seq experiment aims to understand the common and different transcriptional landscape after treatment between both genotypes (comparisons 3 and 4 in Figure 5.7a) in order to further comprehend the role of HAG5 in regulating ABA signalling and response.

As seen in Figure 5.9, Col-0 differentially regulates 1841 genes after ABA, and *hag5-2*, 1802. A study using a similar transcriptomic approach investigated the effects of treating Arabidopsis seedlings for 3h with 50µM of ABA. The ABA treatment resulted in 2,825 upregulated genes and 1,616 downregulated genes (Weng et al., 2016). However, the authors used a lower p-value (adjusted p-value at 0.1) and different treatment conditions, which might explain the vast differences in DEGs in response to ABA.

The overlap between DEGs before and after ABA treatment for each genotype is illustrated in the Venn diagram below. The common response between genotypes comprises a total of 1320 DEGs.

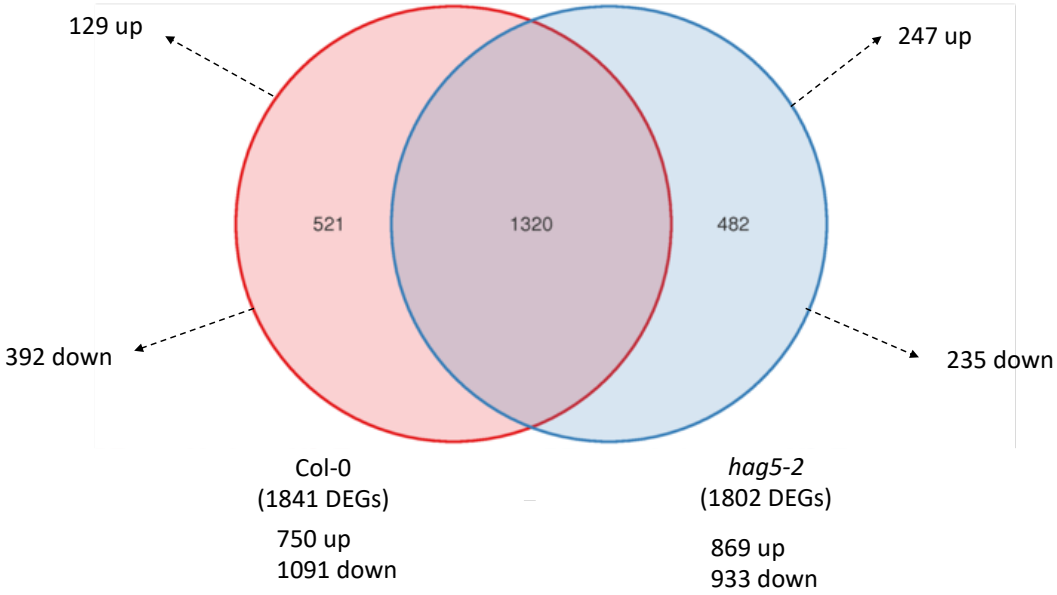

Figure 5.9. Venn diagram of DEGs between Col-0 and *hag5-2* in response to ABA. 10 day old Col-0 and *hag5-2* seedlings germinated *in vitro* were transferred to ½ MS media or media supplemented with 50µM ABA for 7h. 3 seedlings were used per genotype and condition, and three biological replicates were performed independently. The number of up and down-regulated genes from the non-overlapping DEGs is indicated with arrows.

GO term enrichment analysis of these common DEGs was performed using AgriGo (Du et al., 2010), in order to characterize the shared biological processes that both genotypes alter in response to abscisic acid. The list of GO terms was plotted in Cytoscape (Figure 5.10) (Shannon et al., 2003) to represent the network of biological processes this group of genes are part of. Figure 5.10 displays the GO terms represented as circles, where the size of the circle is proportional to the fold enrichment, and the intensity of red color, to the p-value.

Some of the overrepresented GO terms in response to ABA are "response to hormone", "water deprivation", "response to stress" or "response to chemical", among others. These common GO terms coincide with the ones identified in a similar RNA-seq study, where Col-0 seedlings were subjected to 10µM of ABA treatment for 4 and 8h (Song et al., 2016). Indeed, the authors found that ABA-related GO terms such as "seed development" and "response to salt/osmotic stress/water deprivation" were enriched in up-regulated genes, whereas a growth-related terms such as "response to auxin stimulus" and "cell wall organization" were over represented in down-regulated genes after ABA (Song et al., 2016).

Hence, the overlapping transcriptional response to ABA implies that *hag5-2* mutants have a core ABA response since 71% (1320 genes out of 1841) of the ABA DEG are shared between the wild type plants and the mutant. Not surprisingly, the most overrepresented GO terms characteristic to ABA are the ones being part of this shared response.

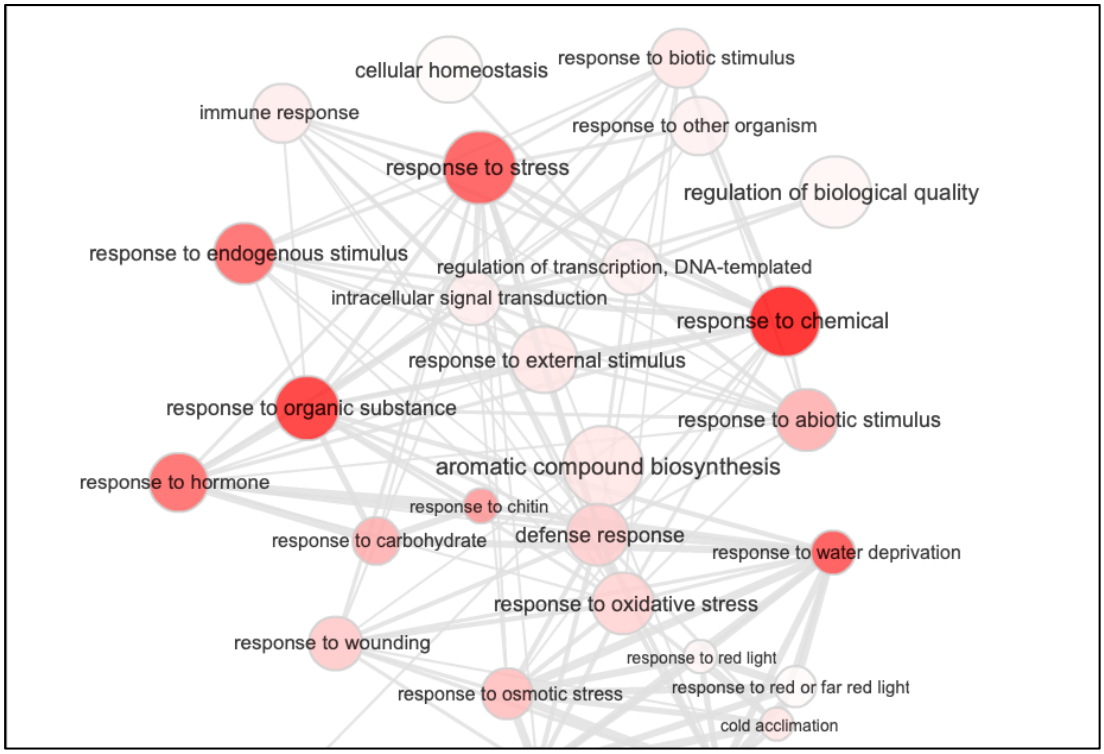

Figure 5.10. GO term enrichment of common DEGs between Col-0 and *hag5-2* seedlings in response to ABA. GO term enrichment analysis was performed using AgriGo (Du et al., 2010). The list of GO terms was plotted in Cytoscape (Shannon et al., 2003). GO terms are represented as circles, where the size of the circle is proportional to the fold enrichment, and the intensity of red colour, to the p-value.

In order to investigate if the common DEGs follow the same trend in both genotypes after ABA, we produced a heatmap representing the expression values of these 1320 common DEGs in the 4 samples (Figure 5.11).

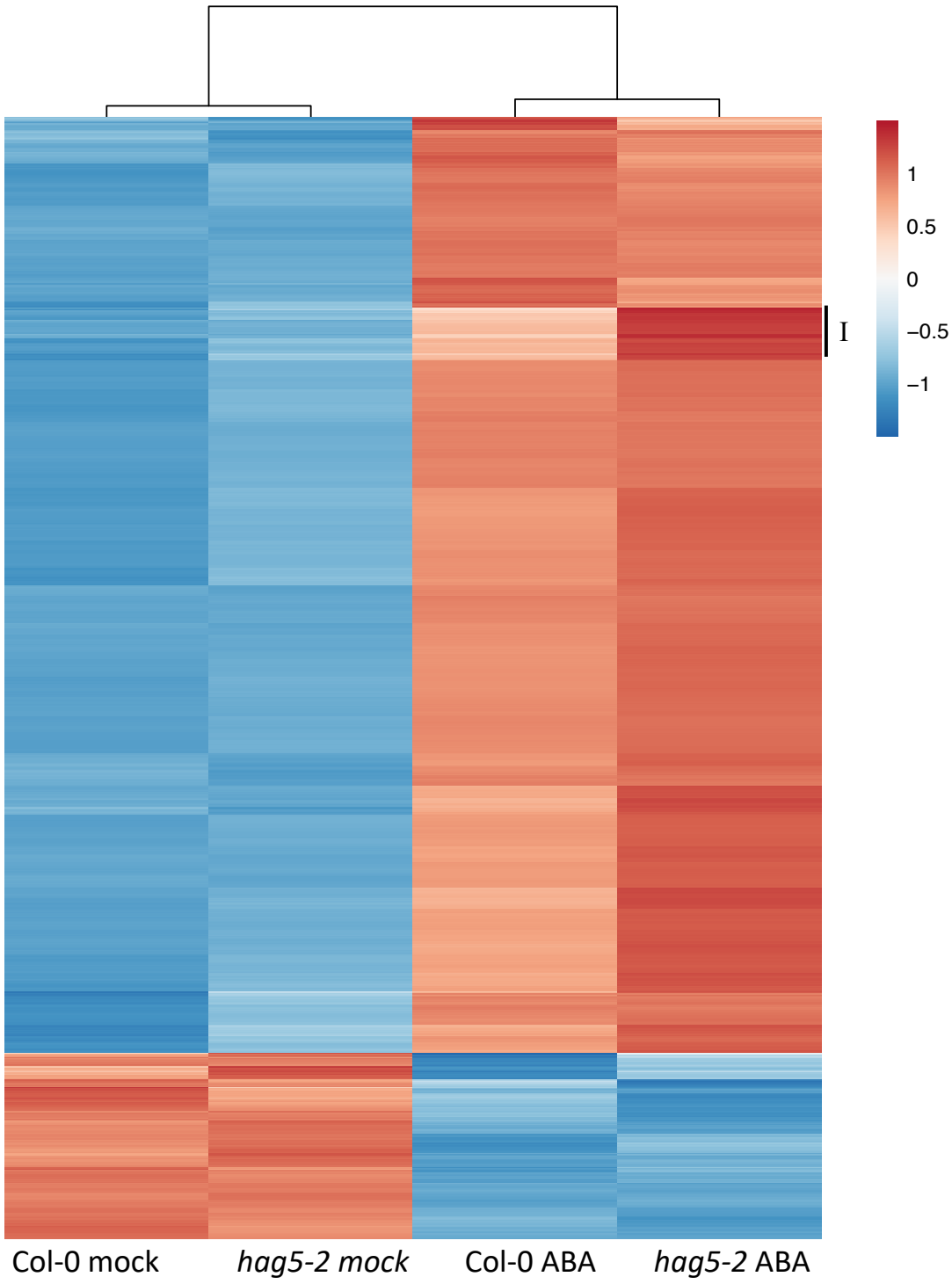

Figure 5.11. Heatmap of the expression of 1320 common DEGs between Col-0 and *hag5-2* under mock and ABA treatments. Up-regulated genes are represented in red and downregulated, in blue, according to their Z-score values.

As seen in this heatmap, the levels of expression of the 1320 common DEGs between Col-0 and *hag5-2* before and after ABA is similar between genotypes, with

a small subset of genes (Group I in Figure 5.11) that has a stronger up-regulation in *hag5-2* mutants upon ABA. As a consequence, the basal shared ABA response is similar not only in the genes that are differentially expressed, but also in the magnitude of expression of such genes.

Examining the genes that are differentially expressed exclusively in Col-0 provides an insight into the molecular processes that are HAG5-dependent. From the 1841 ABA-dependent DEG 521 (28%) are not differentially expressed in the *hag5* mutant, clearly demonstrating that HAG5 regulates a significant subset of the ABA-responsive genes. Discerning between up and down-regulated non-overlapping DEGs from Col-0 provides information about the processes that require HAG5 to get activated (up-regulated genes) and the ones that are negatively affected by HAG5 (down-regulated genes). The GO term enrichment of the 129 up-regulated genes in Col-0 alone reveal that these genes are part of abiotic stress, flavonoid biosynthesis and phenylpropanoid biosynthesis processes (Figure 5.12).

Flavonoids are known to play a role in UV-B protection. However, there is increasing evidence of their antioxidant properties, their involvement in ROS scavenging and even in hormone signal transduction (Brunetti et al., 2018). In Arabidopsis, stress induced-ROS triggers ANP1-mediated MAPK cascade, which leads to stressed plants diverting energy from auxin-promoted activities to stress protection (Kovtun et al., 2000). Furthermore, flavonoids have been hypothesized to regulate ABA-signalling pathway and fine tune stomata movement (Brunetti et al., 2018). On the other hand, phenylpropanoids are secondary metabolites produced by plants, which, by differential expression, are involved in responses to biotic and abiotic stresses, maintaining plant homeostasis. There is evidence that one of the pathways regulating phenylpropanoids induction depends on abscisic acid (ABA) and it is generated by a signalling cascade involving calcium (Ca^{2+}) and Ca^{2+}-dependent protein kinases (CDPKs) (Vighi et al., 2019). Both flavonoid metabolism and phenylpropanoid biosynthesis were processes overrepresented in the DEGs after ABA treatment analysed by (Song et al., 2016). *hag5-2* mutants do not upregulate these genes upon ABA, confirming that the transcriptional response is either inhibited or delayed. In addition, this transcriptional response is correlated with ROS detoxification and stomatal movement, two processes that might affect both the response to drought and bacterial colonization through the stomata.

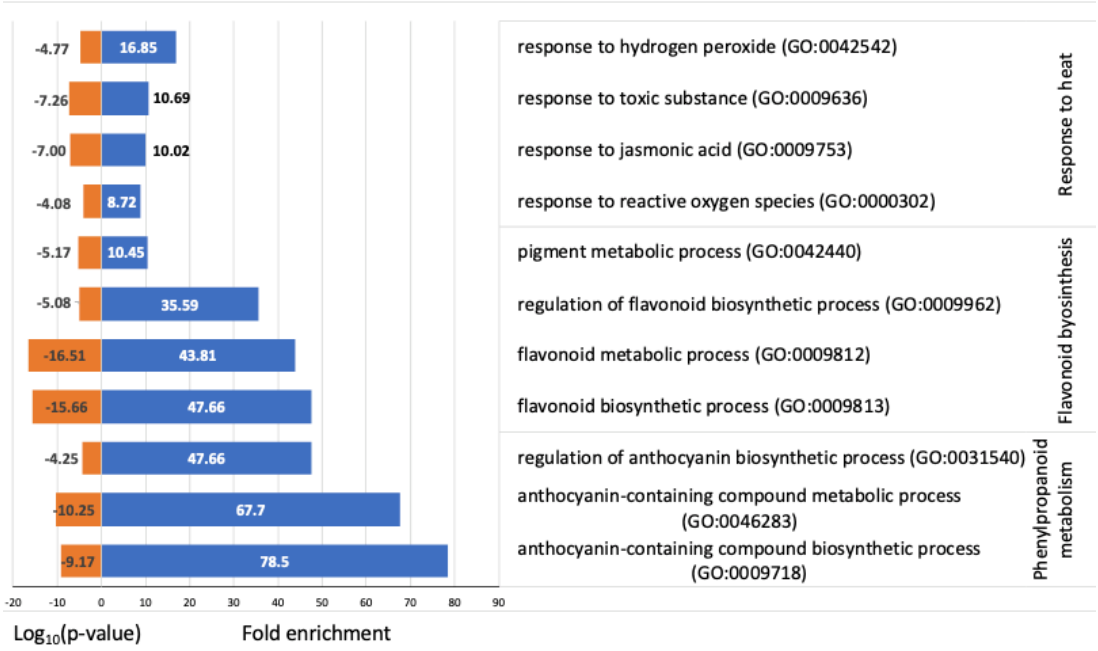

Figure 5.12. Molecular function GO term enrichment of non-overlapping DEGs up-regulated in Col-0 after ABA. Fold enrichment was calculated by dividing the number of obtained DEGs for a particular GO term over the total number of random hits predicted for that GO term. The GO term enrichment was performed using PantherDB, applying the Bonferroni correction for multiple testing (Mi et al., 2009).

In order to characterise the transcription factors that regulate the expression of Col-0 unique DEGs, TF-binding motif enrichment analysis was performed in the 500 bp upstream of the transcription start site (TSS) region of such DEGs. This region often comprises the promoters of protein-coding genes under low-nucleosome occupancy, which relates to higher transcriptional activity.

This analysis identified overrepresented known TF-binding sites using the AME (Analysis of Motif Enrichment) algorithm developed by (McLeay and Bailey, 2010). This enrichment analysis is based in two different databases: *Arabidopsis* PBM database, consisting of 113 TF-binding motifs found by protein binding microarrays (PBM) (Franco-Zorrilla et al., 2014); and the Arabidopsis DAP-seq database of 872 TF-binding motifs identified using DNA affinity purification sequencing (O'Malley et al., 2016). The five most enriched motifs found in the PBM database were the bHLH, MYC2, MYC3 and MYC4 (Table 5-1). These TFs are known to be involved in JA regulated plant defence responses, crosstalk between ABA, SA, GA and auxin, and

biosynthesis of secondary metabolites in response to stress (Chung et al., 2008, Fernández-Calvo et al., 2011). PIF binding motifs are also enriched within this subset of genes (Table 5-1). PIF4 and PIF5 are transcription factors that act in the signalling pathways of ethylene and ABA, and modulate the expression of *EIN3*, *ABI5* and *EEL*, which directly activate NAC TF ORESARA1, the major TF regulating and promoting leaf senescence in Arabidopsis (Sakuraba et al., 2014). As a consequence, *hag5-2* mutants are defective in up-regulating abiotic stress response genes and the biosynthesis of secondary metabolites involved in plant homeostasis in response to ABA.

Table 5-1. Over-represented known transcription factor binding motifs in unique up-regulated genes in Col-0 after ABA treatment. One-tailed Wilcoxon rank-sum was used, threshold p-value ≤ 0.05.

Database	Logo	ID	p-value	TP (%)
PDB		REM19	3.65E-15	29.30%
		bHLH31	5.67E-13	22%
		ABF2	3.00E-47	18.80%
DAP-SEQ		MYC4	6.59E-10	22.80%
		MYC2	8.22E-11	30.10%
		MYC3	8.49E-11	18.70%
		PIF5	7.12E-07	20.30%
		PIF4	8.86E-04	20.30%
		PIF3	1.81E-02	10%
	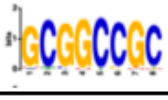	DREB2C	2.32E-02	2.40%

DREB2C stands for Dehydration-responsive element-binding protein 2C. This transcription factor binds to the C-repeat/dehydration response element and is known

to interact with ABF2, cooperating to activate the transcription of ABA-responsive genes (Lee et al., 2010b). Interestingly, the ABF2 binding motif is enriched within this gene list, according to the PDB database. This motif is also known as ABRE (ABA Response Element), which consists of "ACGTGGC" as core sequence, and its role in ABA-responsive gene expression has been characterized in detail (Hattori, 2002) and described in Chapter 1. Overall, *hag5-2* mutants lack some of the transcriptional response to ABA regulated by key TFs and motifs. These results agree with the results of the qPCRs of the ABA marker genes from Chapter 4, in which *hag5-2* mutants display partial up-regulation of ABA marker genes due to a delayed response. Overall, these results indicate that HAG5 is required for the up-regulation of ROS-activated and oxidative stress response genes under the control of ABRE and DRE promoters. Nonetheless, having transcriptional data at earlier and later time points would provide further information about whether these up regulated genes in Col-0 are repressed in *hag5-2* mutants or will be differentially expressed at later time points.

On the other hand, genes that are down-regulated in Col-0 but not in *hag5-2* upon ABA are those that are negatively regulated by HAG5. The most overrepresented GO terms for this group of DEGs are related to biotic stress, with significant enrichment of "immune system process", "response to biotic stimuli" or "defence response" (Figure 5.13).

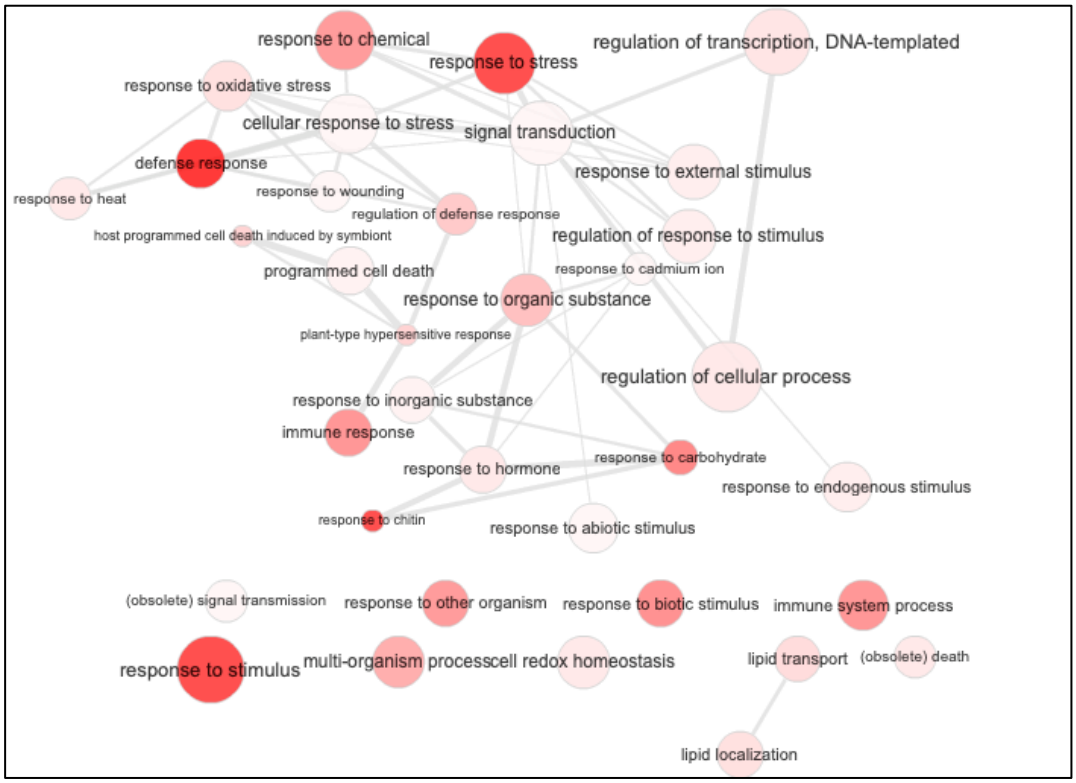

Figure 5.13 GO term enrichment of down-regulated unique genes in Col-0 after ABA treatment. GO term enrichment analysis was performed using AgriGo (Du et al., 2010). The list of GO terms was plotted in Cytoscape (Shannon et al., 2003). GO terms are represented as circles, where the size of the circle is proportional to the fold enrichment, and the intensity of red color, to the p-value.

In Chapter 3, HAG5 was identified as a negative regulator of immunity, with an increased tolerance to *P. syringae*. In agreement with these results, the immunity-related genes that get suppressed upon ABA, do not get down-regulated in *hag5-2*. The enriched TF binding motifs identified in the DAP-seq database (O'Malley et al., 2016) pointed out three known WRKY TFs (Table 5-2). *WRKY* genes respond to pathogens, elicitors, and defence-related phytohormones such as salicylic acid (SA) or jasmonic acid (JA), playing a major role in plant immune responses, although they are also involved in abiotic stress responses (reviewed by (Bai et al., 2018)).

WRKY38 has been characterized as a negative regulator of plant defense in response to *P. syringae* since it suppresses the expression of *NPR1* through its interaction with HDA19 (Kim et al., 2008b). WRKY12 is involved in response to abiotic stress and cold (Bai et al., 2018) and WRKY45 functions as a critical component of the GA-mediated signalling pathway to positively regulate age-triggered leaf senescence (Chen et al., 2017). These three enriched motifs in the group

of genes down-regulated in Col-0 after ABA but not in *hag5-2* bring further evidence of the role of HAG5 in immunity, abiotic stress responses and senescence. Indeed, these results suggest that HAG5 is directly or indirectly involved in the downregulation of the WRKY-dependent defence response upon ABA treatment. A valid hypothesis is that HAG5 acts as a modulator of plant homeostasis by regulating the expression of defence-related or drought-response genes according to the type of stress, repressing defence-response genes upon abiotic stress, and facilitates the expression of ROS scavenging and antioxidant compounds like flavonoids or phenylpropanoid at the early stages of abiotic stress. However, transcriptomic experiments under drought stress and infection with *P. syringae* under the conditions in which *hag5-2* displays increased tolerance phenotypes would be crucial for understanding how HAG5 fine-tunes the transcriptional responses to drought and immunity.

Table 5-2. Over-represented known transcription factor binding motifs in unique down-regulated genes in Col-0 after ABA treatment. One-tailed Wilcoxon rank-sum was used, threshold p-value ≤ 0.05.

Database	Logo	ID	p-value	TP (%)
PBD		WRKY38	1.26E-13	31%
		WRKY12	2.28E-12	22.60%
		WRKY45	2.99E-11	26.20%

Finally, the GO term enrichment of the 482 genes that are differentially expressed exclusively in *hag5-2* mutants in response to ABA mostly belong to the ontologies related to ROS scavenging (“oxygen binding”), “hydrolase activity”, as well as antioxidant and peroxidase activities (Figure 5.14).

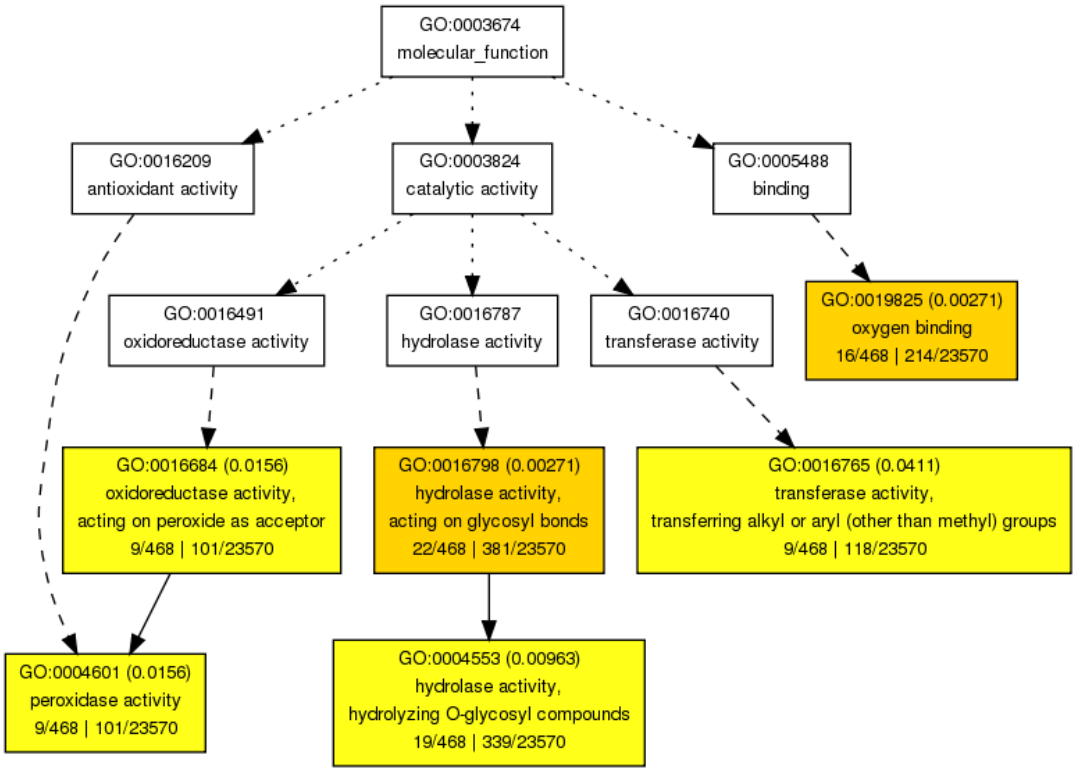

Figure 5.10. Map of GO term enrichment found in *hag5-2* unique DEGs after ABA. GO term enrichment analysis was performed and plotted using AgriGo (Du et al., 2010) and DAG (Directed Acyclic Graph). Each node shows the name of the GO term and the p-value. The darker (yellow) the color is, the lower p-value which indicates the more significant enrichment

As a consequence, genes involved in cellular detoxification are miss-regulated in *hag5-2,* supporting the idea that HAG5 is involved in the regulation of ROS activation upon ABA. Nevertheless, the p-values of these enriched GO terms indicate that there is not a strong overrepresentation of GO terms from these DEGs in *hag5-2* mutants. This suggests that the observed ABA-related phenotypes in *hag5-2* mutants are due to a miss-regulation of ABA response genes that require HAG5 to get overexpressed (or expressed in time), rather than due to the exclusive independent events that take place because of the absence of HAG5.

5.3.3 ABA responses are altered by inhibitor A

In the previous section, the common and distinct differentially expressed genes between Col-0 and *hag5-2* seedlings as a result of ABA treatment were extensively

described. In order to demonstrate the specificity at the transcriptional level of inhibitor A, analysis of DEGs after ABA treatment in the presence of the inhibitor was conducted. The aim was to investigate if the transcriptional response to ABA in the presence of the inhibitor resembles that of *hag5-2* mutants, or if there are off-target processes affected by the compound. To this end, the DEGs from comparisons 3, 4 and 5 (Figure 5.15) were combined to find the common and distinct genes in response to ABA for each condition (Col-0 plants, mutant *HAG5* or Col-0 inhibitor-treated plants). As seen in the Figure 5.15, there are 1372 DEGs in Col-0 plants treated with the inhibitor in the presence or absence of ABA. 895, or 65 % of these genes belong to the common transcriptional response to ABA shared between Col-0 and *hag5-2* mutants as described above. Inhibitor-treated Col-0 samples share 137 DEGs with Col-0 and 130 DEGs with *hag5-2* after ABA, somewhat displaying an intermediate response between the two genotypes. The fact that the response of inhibitor treated samples is not more similar to that of *hag5-2* is not surprising. The inhibitor treatment was performed for 7h, meaning that HAG5 catalytic activity was fully functioning in Col-0 seedlings up until that point, as opposed to *hag5*-2 mutants. Furthermore, the inhibitor was supplied at the IC50 concentration calculated for Tip60 NU9056, which is based on achieving half of the maximal inhibitory concentration of the compound, thus only inhibiting a maximum of half of the present HAG5 molecules in Col-0.

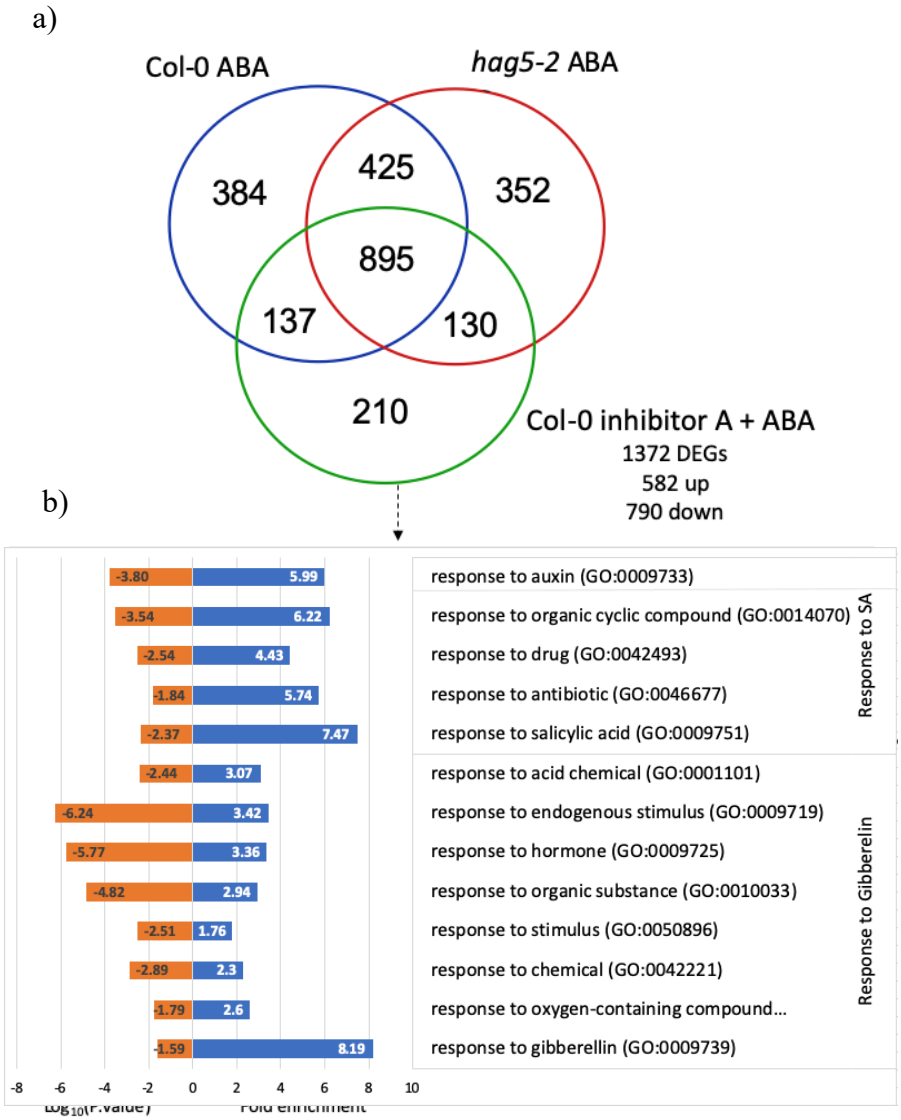

Figure 5.15. Overlapping and unique DEGs between Col-0, hag5-2 and inhibitor-treated Col-0 in response to ABA. **a)** Venn diagram Comparison 3, 4 and 5. **b)** Molecular function GO term enrichment of non-overlapping DEGs up-regulated in Col-0 after ABA. Fold enrichment was calculated by dividing the number of obtained DEGs for a particular GO term over the total number of random hits predicted for that GO term. The GO term enrichment was performed using PantherDB, applying the Bonferroni correction for multiple testing (Mi et al., 2009).

In total, 1162 (137 + 895 + 130) DEGs are common to the ABA response of Col-0, *hag5-2* or both. This comprises 84.7% of the total transcriptional response, suggesting that inhibitor A does not inhibit major responses. In addition. 74.7 % of the DEGs in inhibitor treated plants are common to *hag5-2* mutants, which highlights certain specificity of the inhibitor. However, there are 210 DEGs (15.3% of the total

transcriptional response to ABA) that are unique to the inhibitor-treated samples, hence being a by-product of either unspecific binding of compound A to other acetyltransferases or a result of the treatment itself having different effects at the cellular level. To characterise and understand the off-target response to the inhibitor, GO term enrichment of those 210 DEGs was performed (Figure 5.15b). As seen by the gene ontology enrichment, these genes cluster in groups that respond to either auxin, salicylic acid or gibberellins, suggesting that the inhibitor affects the hormonal crosstalk in response to ABA. The most overrepresented molecular functions associated with these DEGs are "catalytic activity", "transcription regulatory activity" and "binding". From the 210 unique DEGs, 83 are down-regulated and 127 up-regulated. The 83 downregulated genes are related to the phytohormone auxin, such as "auxin-activated signalling pathway", "cellular response to auxin stimulus" or "regulation of growth" (Figure 5.16). Since those are down-regulated genes, it appears that inhibitor A negatively regulates auxin responses and stimulates growth suppression upon ABA treatment. Significant overrepresented GO terms were not found for the 127 up-regulated genes.

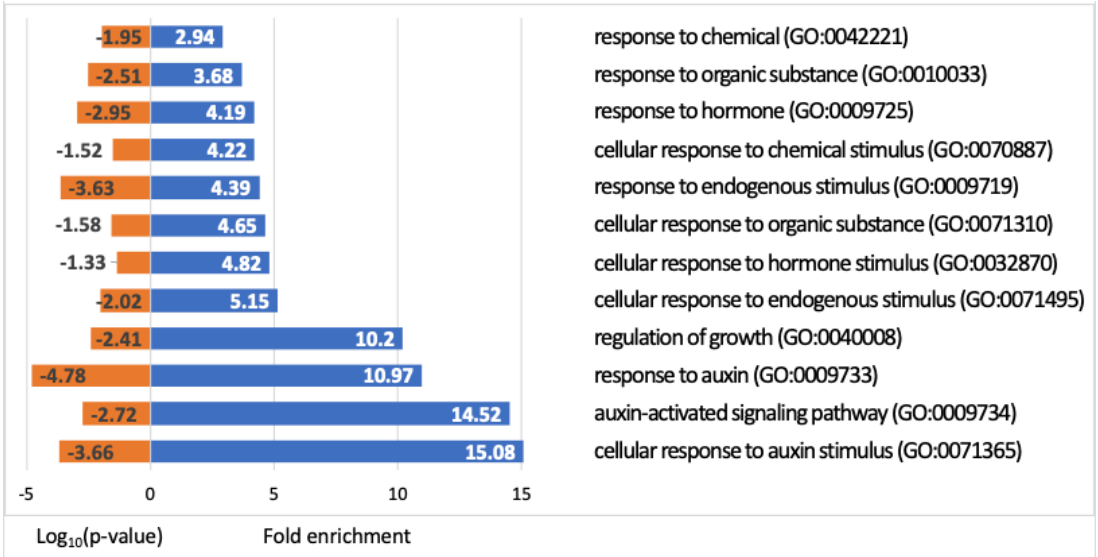

Figure 5.11. Biological process GO term enrichment of non-overlapping DEGs down-regulated in inhibitor-treated Col-0 after ABA. Fold enrichment was calculated by dividing the number of obtained DEGs for a particular GO term over the total number of random hits predicted for that GO term. The GO term enrichment was performed using PantherDB, applying the Bonferroni correction for multiple testing (Mi et al., 2009).

According to these results, treating Col-0 samples with inhibitor A for the duration of the ABA treatment results in a substantially different transcriptional response to the phytohormone. From the 521 ABA-regulated genes whose expression did not change in *hag5-2* following ABA treatment , 384 were also supressed by the inhibitor (Figure 5.15a). As a consequence, inhibitor A is interfering both at the phenotypic and transcriptional level with ABA responses. This interference seems to be predominantly due to the catalytic inhibition of HAG5, since 74.7% of the miss-regulated genes upon treatment are common to those exclusive to *hag5-2* mutants. However, an inhibitor treatment cannot completely mirror the transcriptional response of a loss-of-function mutant, since the long-term developmental consequences of mutating HAG5 are not comparable to partially inhibiting the enzyme for few hours. Furthermore, the concentration of inhibitor used was based on the IC50 of the Tip60 inhibitor and may not be sufficient for a complete inhibition of HAG5.

Overall, in order to refine the inhibition activity of compound A in Col-0 plants, dose-effect response phenotypic assays with the inhibitor and enzymatic binding experiments *in vitro* between HAG5 and inhibitor A are required in order define the best working concentration and conditions for *in vivo* and *in vitro* inhibition. To this end, Dr. Veselina Uzunova, a researcher within the Ntoukakis group, is studying the binding of inhibitor A to the purified HAG5 *in vitro* using Surface Plasmon Resonance (SPR). This assay measures of the association and dissociation curves between the immobilised purified HAG5 and the inhibitor, and once optimised will provide direct information about whether inhibitor A is able to bind to HAG5, as well as the affinity of the binding and the competition against acetyl-CoA, the natural ligand of HAG5.

5.4 Gene editing of *HAG5* homologue in *Brassica oleracea*

One of the milestones of this thesis is to translate our current research to other crop plants based on our knowledge about Arabidopsis HAG5 and its role in modulating plant development, homeostasis and responses to stress. As previously mentioned in Chapter 3, *HAG5* is conserved across plant lineages, with homologues in different Brassica crop varieties (Figure 5.17a). Figure 5.17b shows the high degree of conservation between both proteins. In fact, the sequence differences are mainly in

the TUDOR domain, whilst the linker domain and the active centre remain highly conserved. As a consequence, the phylogenetic proximity and sequence homology between HAG5 in Arabidopsis and Brassica can be exploited to extrapolate our findings from the model system to crop plants (Figure 5.18). Thus, we wanted to investigate the effects of using CRISPR/Cas9-based gene editing to generate *HAG5*-orthologue (*Bo9g173870*) knock-out mutant lines in *Brassica oleracea* DH1012 in plant performance. To this end, we participated in the BRACT initiative in collaboration with Penny Hundleby and Tom Lawrenson. This initiative was initially established as part of a Defra funded project (AR1005) in 2003 to develop and provide simple transformation protocols and resources to the UK research community for wheat (Rothamsted Research), barley and Brassica (John Innes Centre).

a)

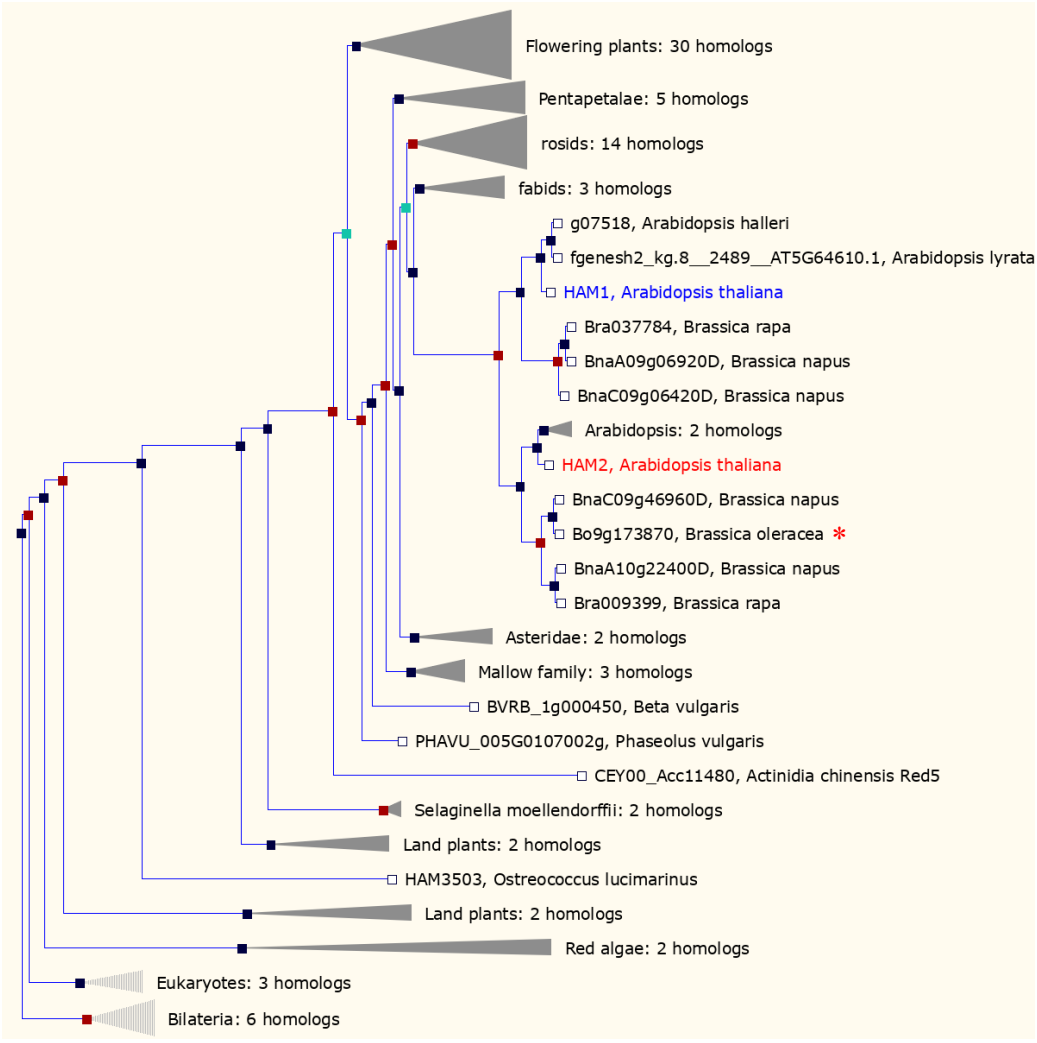

Figure 5.12. *HAG5* and its orthologue in *B. oleracea*. **a)** Gene tree of *HAG5* homologs across plant species. The phylogenetic tree was created using the Ensemble database (http://plants.ensembl.org). Arabidopsis *HAG5* is highlighted in red and referred to as H*AM2*. A red asterisk is placed next to *HAG5* homologue in *B. oleracea*. **b)** Protein sequence alignment of Arabidopsis HAG5 and its orthologue in *B. oleracea* (*Bo9g173870*) using Clustal Omega (version 1.2.4). The same colouring for aligned residues indicates conservation of amino acid chemical properties. (ClustalX colouring: blue: hydrophobic, red: positively charged, magenta: negative charged, green: polar, cyan: aromatic, pink: cysteine, yellow: proline, orange: glycine).The black box represents the Chromodomain/TUDOR domain, the red box the linker domain and the blue box, the acetyltransferase catalytic domain.

Brassica oleracea has been cultivated for at least 2,000 years, and a wide variety of forms have been developed. Cabbage, kale, kohlrabi, cauliflower, broccoli and Brussels sprouts are all cultivars of *Brassica oleracea* (Figure 5.18a-b) highlighting the economic importance of the Brassica (Brassicaceae) family . We chose the diploid species *B. oleracea* using the doubled-haploid genotype AG DH1012 (a broccoli-like Brassica) from the *Brassica oleracea var. alboglabra* (A12DHd) × *B. oleracea var. italica* (Green Duke GDDH33) mapping population (Lawrenson et al., 2015) to investigate the effects of mutating *HAG5* in Brassica crop, due to the already available

toolbox of biochemistry methods and transformation protocols (Lawrenson et al., 2015).

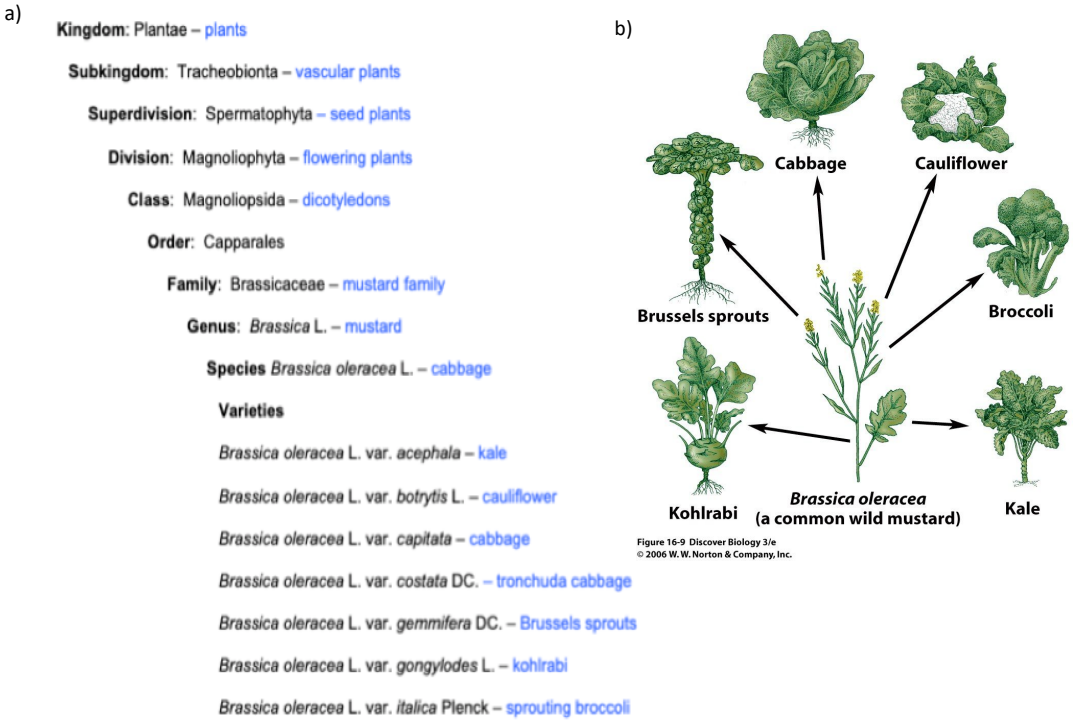

Figure 5.13. Multiple edible crops are varieties of *Brassica oleracea*. **a)** Taxonomy of *Brassica oleracea*. Adapted from (http://plants.usda.gov) **b)** The vegetables broccoli, cabbage, cauliflower, brussels sprouts and kale are closely related varieties of the species *Brassica oleracea*. Picture from (Shin, 2006).

Targeted genome editing technologies have been developed to avoid the detrimental effects of random mutagenesis approaches, and to speed the process of acquiring stable lines with targeted inheritable mutations. In recent years, methods involving sequence-specific nucleases to create targeted DNA double-stranded break (DSB) genetic tools, such as zinc-finger nucleases and transcription activator-like effector nucleases (TALENs), have been used for genome editing (Voytas and Gao, 2014). However, the technical difficulties of these approaches have resulted in a lack of use by the scientific community. Recently, the type II clustered regularly interspaced short palindromic repeats (CRISPR)-associated protein (Cas) system (CRISPR/Cas9) has emerged as a highly efficient, cost-effective, simple and versatile gene editing tool. So far, this technique has been demonstrated to be efficient for gene disruption in many plant species, including Arabidopsis, *Nicotiana benthamiana*, *N.*

tabacum, rice, wheat, maize, sorghum, tomato, potato, sweet orange, poplar, and liverwort (reviewed by (Ma et al., 2019)). CRISPR/Cas9 provides the opportunity to make precise changes at specific genomic locations to induce gene insertions, gene replacements, or insertions or deletions that disrupt the function of a specific gene (Hsu et al., 2014). CRISPR/Cas9 genome editing is based on a site-directed nuclease that introduces one or more breaks in the DNA at the targeted locus, which will be repaired by the cell's endogenous DNA repair mechanisms. Imperfect repair can produce mutations or deletions in the genes of interest, causing inheritable mutations. To generate site-specific breaks, the RNA-guided Cas9 system uses a small non-coding RNA, known as the single guide RNA (sgRNA), which directs the Cas9 nuclease to the DNA target of interest based on sequence-specificity. The first applications of RNA-guided Cas9 in plants were described in 2013 using transient systems (Nekrasov et al., 2013, Li et al., 2013, Shan et al., 2013). Feng et al., demonstrated inherited induced mutations in Arabidopsis (Feng et al., 2014), and recently, a protocol for inheritable CRISPR/Cas9 genome editing in *B. oleracea* has been developed by (Lawrenson et al., 2019). This protocol uses Agrobacterium-mediated transformation to deliver Cas9 and dual sgRNAs into 4-day-old cotyledonary petioles of *Brassica oleracea.* Details of experimental procedures followed can be found in (Lawrenson et al., 2019).

Using this approach, 2 independent lines (CRISPR line 1 and CRISPR line 2) were identified with indels in the desired area through direct sequencing (Figure 5.19). Figure 5.19a displays a diagram of the *HAG5* orthologue gene (Bo9g173870) with the sequences used as RNA guides to direct the Cas9 to the first exon of the gene, mimicking the disruption in *hag5-2* mutants, which have a T-DNA insertion within the first exon. Figure 5.18b displays the tracking of both indels in each positive T0 lines as analysed through TIDE.

a)

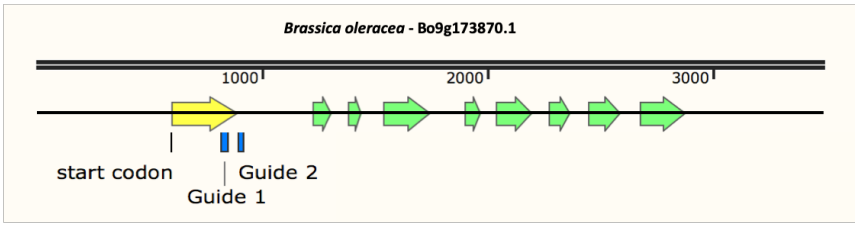

Guide 1: GTACTCGTGTCCTGTGCCGG
Guide 2: GAGCGGCGGAGGATTCATAA

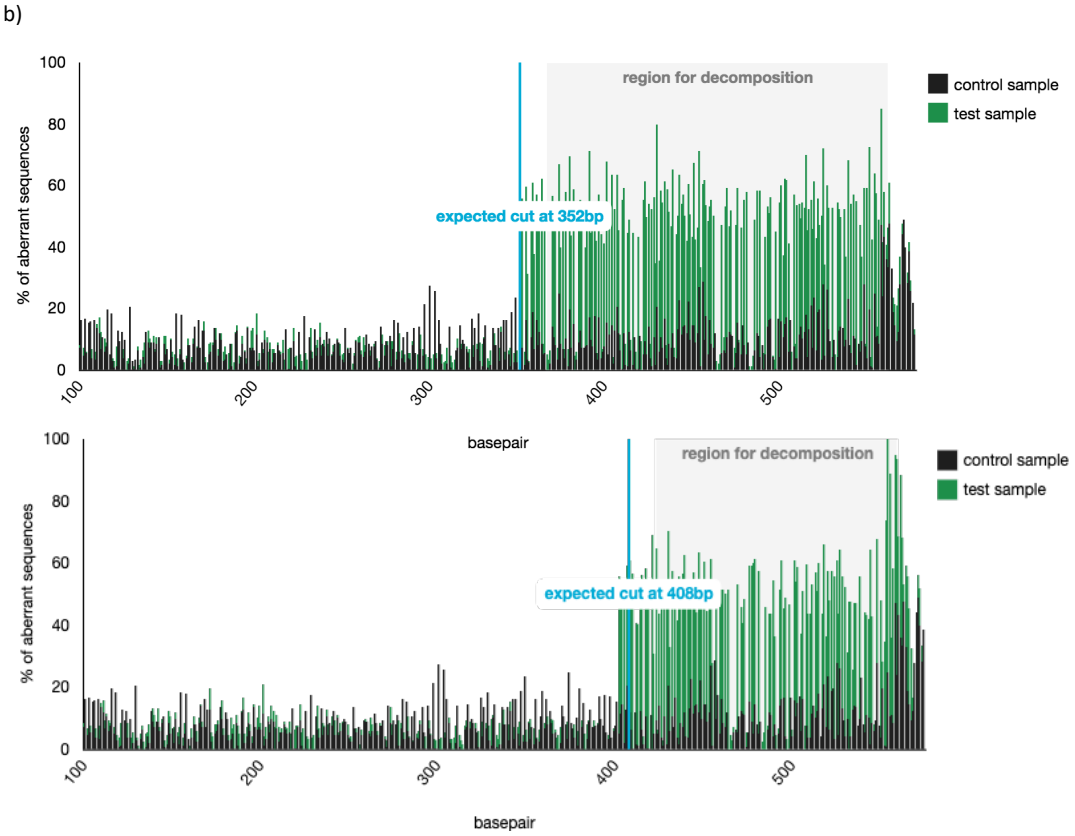

Figure 5.14. Targeting *HAG5* orthologue in *B. oleracea*. **a)** Diagram of Bo9g173870. Exons are represented as arrows. The targeted location of the RNA guides as well as the sequences are displayed below the gene cartoon. **b)** Quality control vs aberrant sequence signal of the two positive CRISPR lines using TIDE (Brinkman et al., 2014). Control sequence (form wild type plants) is represented in black, whilst test sample (from edited lines) is represented in green. Decompositions settings used: Alignment window (bp) = 100 – 342, decomposition window (bp) = 367 – 563, indel size = 10, p-threshold = 0.001.

Due to imperfect DNA repair after cutting by the Cas9, the DNA in the analysed cell pool consists of a mixture of indels, which results in a combined sequence trace after the break site. As consequence, the online tool TIDE was used to align the sgRNA sequence to the control sequence (sequence of *Bo9g173870* in wild type plants, represented in black) to determine the position of the expected Cas9 break site and the abundance of detected indels. The control sequence region upstream of the break site is aligned to the experimental sample sequence (sequence of base pairs in CRISPR lines, represented in green) in order to determine any offset between both sequence reads. The software uses the peak heights for each base from the capillary sequencing data to determine the relative abundance of aberrant nucleotides over the

length of the whole sequence trace (Brinkman et al., 2014). As seen in Figure 5.19b, the positively selected edited lines have a predicted cut in the following positions from the TSS: 352 bp and 408 bp of the input wild type sequence from the TSS, respectively. Since the input sequence contained 158 bp of the upstream promoter region before the TSS, one indel is in the position 194 after the TSS (Indel 1), and the second one, at the 250 (Indel 2) (Figure 5.20). The first intron is 298 bp long, which means that both indels fall within the first intron.

Figure 5.15. First exon of *HAG5* homologue (Bo9g173870) in *B. oleracea* featuring sgRNA sequences and detected indels. Start codon is represented in red. RNA guides are highlighted above DNA sequence and Indel 1 and 2 are represented in green. The figure was generated using SnapGene® software (GSL Biotech).

In order to estimate the abundance of a particular indel within the targeted regions, the indel spectrum was analysed using TIDE (Brinkman et al., 2014). Figure 5.20 displays the percentage of insertions, deletions or no changes in the targeted region within the pool of sequences sequenced. Regarding the first edit (indel 1) 27.7% were identified as deletions, 35.6% as native base pair and 8.8% as insertions (Figure 5.21a) in the CRISPR line 1. Regarding indel 2.45% corresponded to a deletion, whilst 41.5%, to the native base pair. (Figure 5.21b).

In CRISPR line 2, 29.2% of identified indel 1 corresponded to a deletion and 45.3 % to the native base pair (Figure 5.21c). For indel 2, 44.5 % was a deletion and 42.7%, the native base pair (Figure 5.21d).

a)

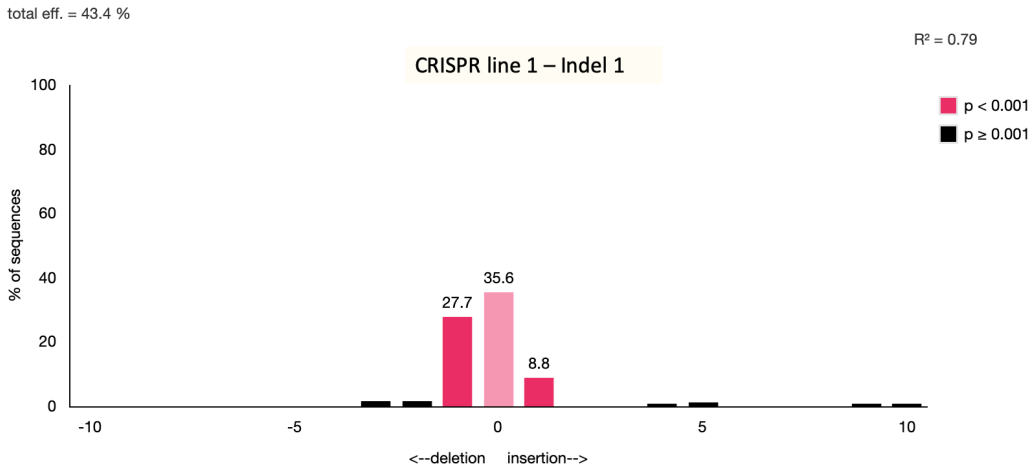
total eff. = 43.4 %
R² = 0.79
CRISPR line 1 – Indel 1
p < 0.001
p ≥ 0.001
% of sequences
100
80
60
40
20
0
27.7
35.6
8.8
-10
-5
0
5
10
<--deletion
insertion-->

b)

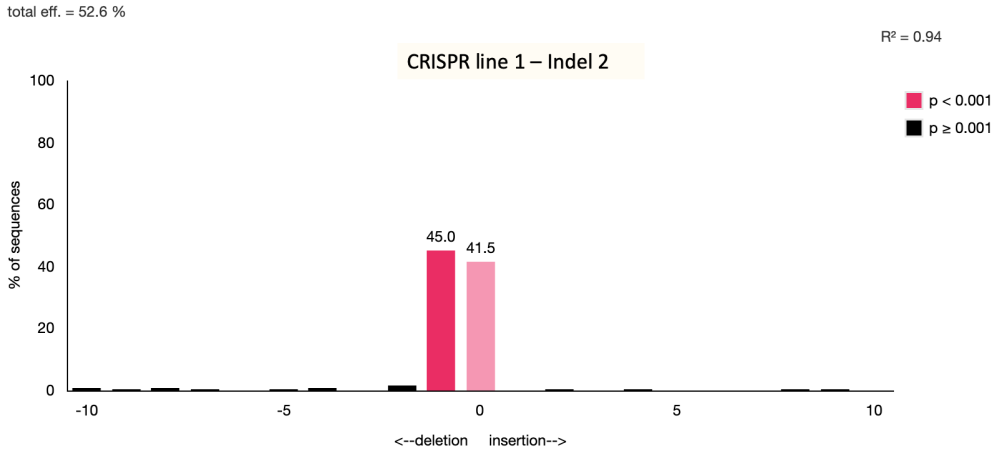
total eff. = 52.6 %
R² = 0.94
CRISPR line 1 – Indel 2
p < 0.001
p ≥ 0.001
% of sequences
100
80
60
40
20
0
45.0
41.5
-10
-5
0
5
10
<--deletion
insertion-->

c)

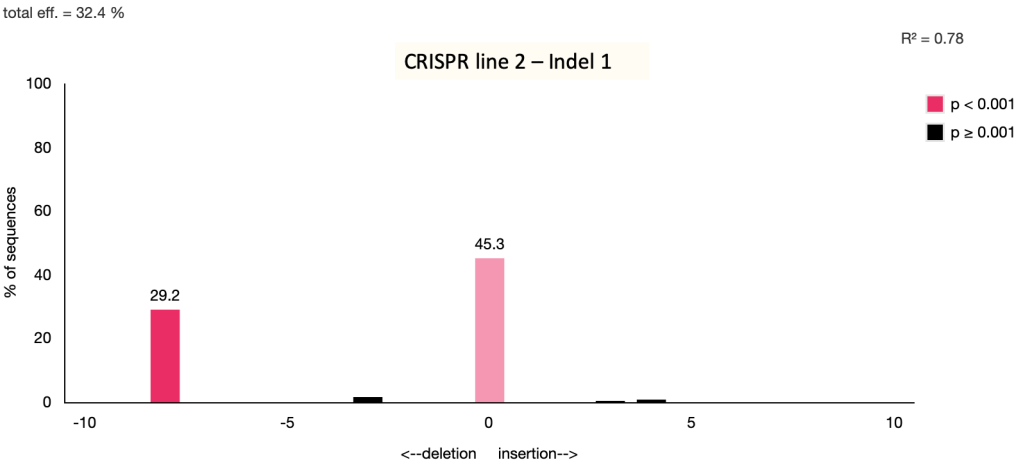
total eff. = 32.4 %
R² = 0.78
CRISPR line 2 – Indel 1
p < 0.001
p ≥ 0.001
% of sequences
100
80
60
40
20
0
29.2
45.3
-10
-5
0
5
10
<--deletion
insertion-->

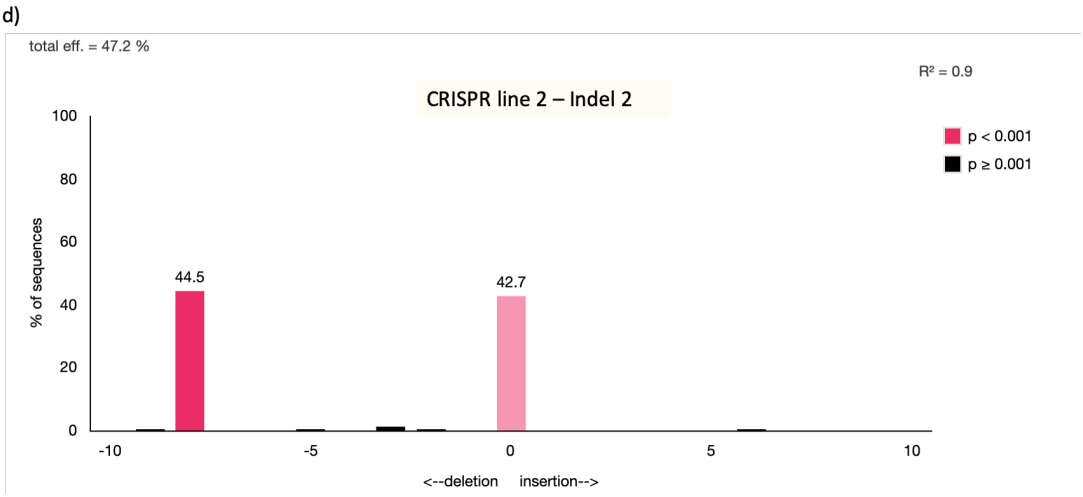

Figure 5.21. Percentage of indel sequences identified per line. **a)** Percentage of inserts, deletions or native sequences identified in CRISPR line 1 for indel 1. **b)** Percentage of inserts, deletions or native sequences identified in CRISPR line 1 for indel 2. **c)** Percentage of inserts, deletions or native sequences identified in CRISPR line 2 for indel 1. **d)** Percentage of inserts, deletions or native sequences identified in CRISPR line 2 for indel 2. Graphs were generated using the inline tool TIDE (Brinkman et al., 2014).

According to these results, both lines have both edits/indels, with higher probability of deletions over insertions identified. In CRISPR line 1, one single copy of the insert encoding the Cas9 was identified, whilst 19 copies were found in CRISPR line 2 (data not shown). Since ultimately the Cas9 has to be segregated in subsequent generations in order to avoid future indels, we focused our work in CRISPR line 1.

In order to explore the phenotypical differences caused by these indels, CRISPR line 1 and a control line displaying a copy of the same Cas9 insert without detected indels were grown under long day photoperiod for approximately 30 days, when pictures were taken (Figure 5.22). As seen in the figure below, at this developmental stage there are no obvious phenotypical differences between genotypes. However, it is important to note that these lines are T0 mosaic lines. In order to get stable edited lines, T1 plants have to be sequenced to detect the presence and abundance of indels.

Figure 5.16. 30 day old *B. oleracea* plants with one copy of the Cas9 and presence or absence of described indels.

The abundance of the indels in the tested mosaic lines (CRISPR lines 1 and 2) suggests that the transformation event took place at the early stages of tissue culture, which increases the probability of the indels being in gametic cells in order to create future stable edited lines.

Once the stable edited lines have been generated and the Cas 9 segregated, the presence of the *HAG5* homologue (Bo9g173870) will be tested through qPCR to detect the levels of transcripts. If the indels results in a loss-of-function mutation, plants will be characterised for their developmental phenotypes (leaf area and fresh weight) under basal conditions. Plants will also be tested for ABA sensitivity by germinating seeds in media with different concentrations of the phytohormone, and their tolerance to drought will be assessed through dehydration assays.

5.5 Findings

- Inhibitor A increases root meristem of Col-0 plants and confers tolerance to dehydration.
- Inhibitor A represses transcriptional biotic and abiotic stress responses in basal conditions.
- Inhibitor A is a negative regulator of transcription and supresses the expression of stress-related genes in basal conditions.
- *hag5-2* mutants display core ABA transcriptional responses.
- HAG5 is required to up-regulate ROS and oxidative stress responses under the control of ABRE and DRE promoters upon ABA.
- HAG5 is required to repress the WRKY-dependent transcription of immune response genes upon ABA.
- Response to ROS is miss-regulated in *hag5-2* mutants.
- Inhibitor A is able to partially reproduce *hag5-2* response to ABA in Col-0 treated plants, accounting for 73.7% of the DEGs found in *hag5-2* mutants after treatment.
- Inhibitor A negatively regulates auxin signalling and growth upon ABA.

5.6 Discussion

The aim of this chapter was to explore different ways of translating our research, bringing the knowledge gathered about *hag5* mutant phenotypes and the molecular mechanisms regulated by HAG5 to improve plant performance in crop plants.

Within the last two chapters, the roles of HAG5 in regulating plant development and responses to biotic and abiotic stresses have been extensively explored and developed. In brief, HAG5 is a negative regulator of growth and immunity, and is required for the timing of the transcriptional response to ABA, which affects drought responses. *hag5* mutants are bigger plants, with longer roots, increased tolerance to the bacterial pathogen *P. syringae* and higher recovery rates after prolonged periods of drought. These findings have highlighted HAG5 as a target for improving agricultural crops, since inhibiting this enzyme results in better performing plants under stress, without a developmental trade-off.

5.6.1 Identifying HAG5 inhibitors *in silico* and *in planta*

The first approach consisted on the identification of chemical inhibitors of HAG5 to mirror the phenotypes of *hag5* mutants. To this end, a homology model of HAG5 was generated by Dr. Steph Kancy in order to perform an *in silico* screening of potential inhibitors with desired agrochemical properties and specificity towards HAG5. This model was used for screening a library of over a million synthetic compounds looking for potential compounds with increased affinity for HAG5, with a final output of 7 potential candidates for *in planta* assays.

One effective way to test for the efficacy of inhibitors was based on the increased root meristem size of *hag5* seedlings, described in Chapter 3 of this thesis. We tested a previously published inhibitor of Tip60, NU9056 (Coffey et al., 2012), and its effect on root meristem size along with two of the candidate inhibitors (A and B) identified through *the in silico* screening to test the efficacy of the *in planta* assay. Through his assay we concluded that all three inhibitors were able to mimic the *hag5* mutant phenotypes when applied to Col-0 seedlings, increasing the root meristem size after overnight treatment. As a consequence, this assay was selected for the *in planta* screening of all HAG5 inhibitor candidates (A-G). The outcome of this inhibitor resulted in 5 positive candidates able to increase meristem size when exogenously applied to Col-0 seedlings.

In chapter 4, the increased desiccation tolerance of *hag5* mutants was successfully tested through assays in plates. In order to narrow down the list of inhibitors, dehydration assays in plates were performed testing whether supplementing the inhibitors in ½ MS media would increase the desiccation tolerance of wild type plants. Combining the outcomes of both screening assays, inhibitor A arose as the most promising inhibitor, since it conferred increased meristem size and desiccation tolerance in Col-0 seedlings, without observable phenotypes when applied to *hag5-1* or *hag-2* seedlings.

5.6.2 Transcriptomic analysis: effect of inhibitor A in basal state

Once a candidate inhibitor had been identified through phenotypic assays, we decided to test for the specificity of inhibitor A to HAG5. Comparing the transcriptional response that results from knocking out *HAG5* versus treating wild type plants with the inhibitor provided information about the effect that inhibitor A has at basal state conditions. Overall, 256 genes were differentially expressed due to inhibitor A treatment, and 95.7% of those genes were down-regulated, highlighting the repressor activity of compound A. These genes were part of biotic, abiotic stress responses and hormone signalling pathways, and were mostly associated with the regulation of transcriptional activity. As a consequence, inhibitor A supresses the expression of genes that display low expression levels in the absence of stimuli. Assuming that inhibitor A targets HAG5, these results suggest that HAG5 is required to maintain basal expression levels of stress-related genes in normal conditions. This would confirm our hypothesis of HAG5 being required to regulate plant homeostasis. There was no significant overlap between the DEGs resulting from treatment with compound A with the DEGs due to the *hag5-2* mutation. However, since *hag5-2* seedlings have undergone development in the absence of HAG5, we hypothesize that a level of homeostasis to maintain low levels of stress-related genes in basal conditions has been achieved in these mutants.

Whilst most of the research regarding stress tolerance in plants is based on characterising the cellular responses to stress at the transcriptional, molecular and cellular levels, maintenance of low levels of stress responses in basal conditions is equally important for plant performance. Indeed, as reviewed in section 1.3.1 of Chapter 1, stress responses normally compromise other cellular functions and aspects of plant growth and development. Hence, the role of HAG5 in maintaining basal expression of stress-related genes would justify the high conservation of this enzyme across plant lineages.

5.6.3 Transcriptional response to ABA in *hag5-2* mutants

Since the discovery of the HAG5-ARIA interaction, gathering information about the responses to ABA in *hag5-2* mutants has been one of the milestones of this thesis.

To this end, RNA-seq of *hag5-2* ABA treated and untreated samples was performed alongside Col-0. In this assay, approximately 2000 genes were differentially expressed after ABA treatment on each genotype. Looking at the overlapping responses between Col-0 and *hag5-2*, 71% of those DEGs are common between genotypes, and the GO term enrichment analysis concluded that these genes comprise the core of the transcriptional response to ABA, as published in previous studies (Song et al., 2016). Hence, *hag5-2* mutants display most of the transcriptional response to ABA. However, 28% of the transcriptional response to ABA depends on HAG5. These results prove the regulatory role of HAG5 in ABA signalling. From these genes, the ones that require HAG5 to get up-regulated are related to abiotic stress, flavonoid biosynthesis and phenylpropanoid biosynthesis processes, which are processes related to cellular detox through ROS scavenging. Motif enrichment analysis identified that ABF2 binding motifs such as ABRE were enriched within this list of genes. These results show that HAG5 is required for a subset of the up-regulation of ABA responsive genes of antioxidant compounds under the regulatory elements recognized by ABF2, suggesting that HAG5 might assist ABF2 in ABA signal transduction. On the other hand, the DEGs negatively regulated by HAG5 are part of immune response and biotic stress processes under the regulatory elements recognized by WRKY TFs. Consequently, HAG5 is required to suppress the expression of biotic stress responses upon ABA. When exclusive DEGs in *hag5-2* mutants in response to ABA, these genes are mostly involved in the regulation of ROS responses, bringing further evidence of the role of HAG5 in this particular mechanism to ABA.

Chapter 4 investigated the drought tolerance phenotypes of *hag5-2* mutants, which displayed a higher recovery rate after prolonged drought. Since ABA is the main phytohormone that regulates plant responses to drought, the role of HAG5 in regulating ROS activation upon ABA can explain the recovery phenotype through modulation of senescence. This concept will be further investigated within the general discussion in Chapter 6.

5.6.4 Effect of inhibitor A in transcriptional responses to ABA

When investigating the effect that inhibitor A had in regulating ABA responses, an overlap of 73.7% of the DEGs were common to those observed in *hag5-2* mutants,

which highlight this compound as a potential inhibitor of HAG5 *in planta*. The exclusive genes differentially expressed due to the inhibitor were mostly down-regulated and related to growth and development through auxin signalling which can be attributed to the homeostatic effect that treatment with the compound might have when applied. Whilst we have shown that inhibitor A increases drought tolerance in seedlings, further research is required in order to identify if inhibitor A confers drought tolerance and recovery to adult plants as well as increased tolerance to bacterial pathogens, due to its effect in ROS signalling and senescence, Nonetheless, the RNA-seq results are a stepping stone towards investigating the effects of transiently inhibiting HAG5 in wild type plants.

Within the next chapter, the molecular mechanisms that confer the beneficial phenotypes in *hag5-2* mutants will be discussed as well as how inhibitor A partially mimics these responses at the molecular level.

5.6.5 Using *B. oleracea* to translate *hag5* phenotypes to plant crops

The second approach taken to translate the ongoing research about HAG5 regulation of plant homeostasis and responses to stress was to generate CRISPR/Cas9 lines targeting the first exon of the HAG5 homologue in *B. oleracea*. So far, two independent lines have been identified with two deletions within the first exon, in an effort to mimic the disruption of the gene that occurs within *hag5-2* mutant. These lines require further segregation to select plants with the indels and without the insert containing the Cas9. Once stable lines are acquired, phenotypic characterization will allow to test whether HAG5 roles revealed throughout this thesis are maintained in other crops. Furthermore, exogenous application of inhibitor A in wild type *B. oleracea* can provide further information about the suitability of the compound to be used for foliar applications in other Brassica crops, in an effort to improve plant performance without genetic engineering of crops.

Chapter 6 Discussion

6.1. Characterising plant responses to stress to improve plant performance

Given the imminent effects of climate change in global food production, and the threat that the increasing population brings upon maintaining food security, identifying unique approaches with the potential to minimise crop losses by improving plant performance has been the main goal within this study. In Chapter 1 of this thesis we described with detail the negative effects of plat biotic and abiotic stresses in crop production. In light of the impact that plant diseases and severe periods of drought have in agriculture, improving plant performance under stress conditions emerges as a powerful strategy to reduce crop loses and maximise yield without increasing the demand for arable land and resources. Indeed, decreasing plant susceptibility to pathogens or water scarcity is the most inexpensive and sustainable method of disease control, when compared to the single-handed use of appropriate cultivation practices, the application of pesticides or the use of irrigation systems (Quirino and Bent, 2003).

Our strategy to improve plant performance was based on the plant model system *Arabidopsis thaliana* and the investigation of a particular group of enzymes known as histone acetyltransferases (HATs). These enzymes are able to modify chromatin organisation, which translates into global changes in transcription that affect plant homeostasis and response to environmental stresses (Boycheva et al., 2014). Understanding the molecular mechanisms that modulate plant fitness and govern responses to biotic or abiotic stress response is the steppingstone for developing strategies towards improving plant performance.

As described throughout Chapter 3 of this thesis, a screening using HAT mutant lines highlighted HAG5 as an interesting target to accomplish said goal. HAG5 is a member of the MYST family of histone acetyltransferases (Ritu Pandey, 2002), and it occurred from a duplication event that took place during polyploidisation on the Brassicaceae ancestor. In fact, HAG5 shares 87.9% protein sequence identity to its paralogue HAG4 (Delarue et al., 2008), and both enzymes are assumed to acetylate H4K5 *in vitro* (Earley et al., 2007). Up to date, HAG4 and HAG5 have been shown to act redundantly in several processes such as gametophyte formation (Delarue et al.,

2008), regulation of flowering time (Xiaoa et al., 2013) and DNA damage repair after Ultraviolet-B radiation stress (Casati et al., 2008, Campi et al., 2012). Furthermore, recent findings have identified HAG4 and HAG5 as part of a repressor protein complex involved in heterochromatin formation and gene repression through DNA methylation (Lian-Mei Tan et al., 2018), although the roles of HAG4 and HAG5 within this complex remain unknown.

To date, there were no reports of HAG4 or HAG5 having different functions, or of these enzymes being involved in the regulation of plant homeostasis and stress responses. In order to characterise the roles of HAG4 and HAG5 in plant stress responses, we selected two independent T-DNA insertion mutant lines for further studies. Our phenotypic characterisation of *hag5* mutants led to the discovery of several advantageous phenotypes product of down-regulating or knocking-out *HAG5*.

6.2. HAG5 is a negative regulator of growth and immunity

Indeed, throughout Chapter 3, we identified that HAG5 is a negative regulator of growth an immunity, since the mutant lines displayed increased leaf area, longer roots and bigger root meristem, as well as increased tolerance to the model pathogen *Pseudomonas syringae* DC3000. In order to understand the mechanisms by which HAG5 regulates plant immunity, we performed pathogenesis assays by spraying *hag5* and *hag4* mutants with *P. syringae* DC3000. The increased tolerance displayed by *hag5* mutants after spray-inoculation suggested that HAG5 participates in microbe-associated molecular pattern immunity (MTI), a mechanism that restricts the growth of the vast majority of potential pathogens encountered by plants (Boller and Felix, 2009). In addition, we tested the susceptibility of *hag4* and *hag5* mutants to *Verticillium dahlia*, a soil-borne fungal pathogen causing billions of dollars worth of crop losses annually (Barbara W Pennypacker, 2004). This assay revealed that only *hag4* mutants are more resistant to infection with *V. dahliae*. Interestingly, *hag4* mutants did not display increased tolerance to *P. syringae* or enhanced growth. Hence, we provided the first evidence of the diversification and lack of complete redundancy between HAG4 and HAG5. This is important through an evolutionary perspective, in the context of gene redundancy leading to specialisation and the acquirement of new functions resulting in advantageous traits.

In order to unveil the molecular mechanism by which HAG5 negatively regulates plant immunity, we followed a transcriptomic approach looking into the effects of knocking-out *HAG5* in basal conditions as well as in response to the bacterial elicitor flg22. This assay revealed that there are not major transcriptional differences between wild type (Col-0) or *hag5* seedlings in basal conditions, hence providing no direct link between the developmental genotypes of *hag5* mutants through HAG5-dependent regulation of growth-related genes. This assay also revealed that HAG5 is required for the activation of transcription factors and involved in jasmonic acid and abscisic acid signalling, two phytohormones involved in plant defence responses.

This experiment has some limitations, since it was performed under flg22 treatment instead of after direct spraying of *P. syringae* DC3000, conditions in which the disease tolerance phenotypes have been identified in *hag5* mutants. In addition, this assay was performed in seedlings, whilst the disease tolerance and some of the enhanced growth phenotypes have been characterised in adult plants. Therefore, we propose further transcriptomic analysis after infection of 5-weeks-old plants with *P. syringae* DC3000, as well as ChIP-seq approach based on H4K5ac enrichment to investigate whether the regulation of defence-related genes by HAG5 takes place through H4K5 acetylation of these loci.

To test that the observed phenotypes of *hag5* mutants were due to the loss-of function of HAG5 and not an artefact of the T-DNA insertion, we generated complemented and over expressor lines in *hag5* knock-out mutant background. Complementation of the growth phenotype was successfully achieved, and an opposite growth phenotype was observed in the over expressor lines. As a consequence, we confirmed that HAG5 is a negative regulator of growth. However, whilst the increased tolerance to *P. syringae* DC3000 was rescued in the complemented lines, there were not significant disease resistance phenotypes in the over expressor lines. This can be due to limiting factors downstream HAG5 regulation of immunity, as well as due to the turnover of HAG5 at the protein level. Including HAG5 over expressor lines in the transcriptomic and ChIP-seq approaches proposed above will bring information about whether there are increased levels of H4K5 acetylation in such lines, and which are the transcriptional effects of such enrichment. In addition, a ChIP-seq experiment with the complemented lines looking for genes directly associated to HAG5 positioning will provide information about the processes that are directly regulated by HAG5.

Combining this data with the transcriptomic response of *hag5* mutants and over expressor lines will allow discerning between genes that are directly regulated by HAG5 versus the ones that get altered due to downstream events. Overall, these approaches will improve our knowledge about HAG5 regulation of plant immune responses at the molecular level.

6.3. HAG5 regulates ABA downstream signalling pathway

Further information about protein function can be obtained through the identification of interacting partners. To this end, we performed a high-throughput yeast-based screen with a library of Arabidopsis transcription factors to find interactors of HAG4 and HAG5, described in Chapter 4. It is important to highlight the caveats of such screening, since the available library was limited to a subset of Arabidopsis proteins with *in silico* identified DNA-binding domains. Using more complete libraries would ensure that other potential interacting partners of HAG4 and HAG5 are not left out of the screening.

This screen revealed that both enzymes have different interacting partners involved in different developmental and stress responses. Subsequent homology modelling of both protein structures revealed that HAG4 and HAG5 have different disordered and Tudor domains, which could explain the exclusivity of these interactions. Further experiments swapping the TUDOR domains between HAG4 and HAG5 for subsequent Y2H assays could confirm if this structural difference is responsible for the specific interacting partners of both enzymes. Nonetheless, these results provide supporting evidence towards our hypothesis regarding the evolutionary diversification between both enzymes. We propose further transcriptomic approaches following bacterial infection or ABA treatment in order to understand the molecular basis of the different processes regulated by HAG4 and HAG5

The most interesting finding, and the main focus within Chapter 4, was the interaction between HAG5 and ARIA, a transcription factor known to interact with ABF2 (Kim et al., 2004a). ABF2 is a transcription factor that activates the transcription of ABA-responsive genes, hence acting as a positive regulator of the abscisic acid signalling pathway (Kim et al., 2004a). We confirmed this interaction in planta through co-immunoprecipitation assays expressing HAG5 and ARIA in *N.*

benthamiana. Even though a nuclear localisation signal was not added to the heterologous HAG5 or ARIA expressed, both proteins were found in the nuclear fraction of *N. benthamiana* leaves, which suggests that the complemented lines transformed with the same constructs properly express and localise HAG5.

These results, in combination with the previous transcriptomic data discussed above, provided supporting evidence about the link between HAG5 and ABA.

ABA is a phytohormone that negatively regulates seed germination and root growth when applied exogenously (Finkelstein et al., 2002). Taking that into account, we investigated the germination rate, cotyledon greening and root elongation of *hag5* mutants under different concentrations of ABA. These assays revealed that *hag5* plants are hyposensitive to ABA. Hence, we hypothesised that HAG5 is a positive regulator of ABA responses through its interaction with the ARIA-ABF2 complex. This proposed mechanism was confirmed by analysing the induction of ABA-marker genes over time. This analysis confirmed that HAG5 is responsible for the timing of the transcriptional response to ARIA/ABF2 regulated genes upon ABA.

Given these results, we proposed a model in which HAG5 positively regulates the timing of the transcriptional response to ABA (Figure 6.1). Since HAG5 is a histone acetyltransferase, we hypothesised that it acetylates H4K5, and that a subset of ARIA-ABF2 dependent genes are associated to this histone mark. As a consequence, upon ABA treatment, HAG5 acetylation of H4K5 results in an active chromatin status of the loci regulated by the ARIA-ABF2 complex. This would facilitate a quick transcriptional response and explain the delay observed in *hag5* mutants.

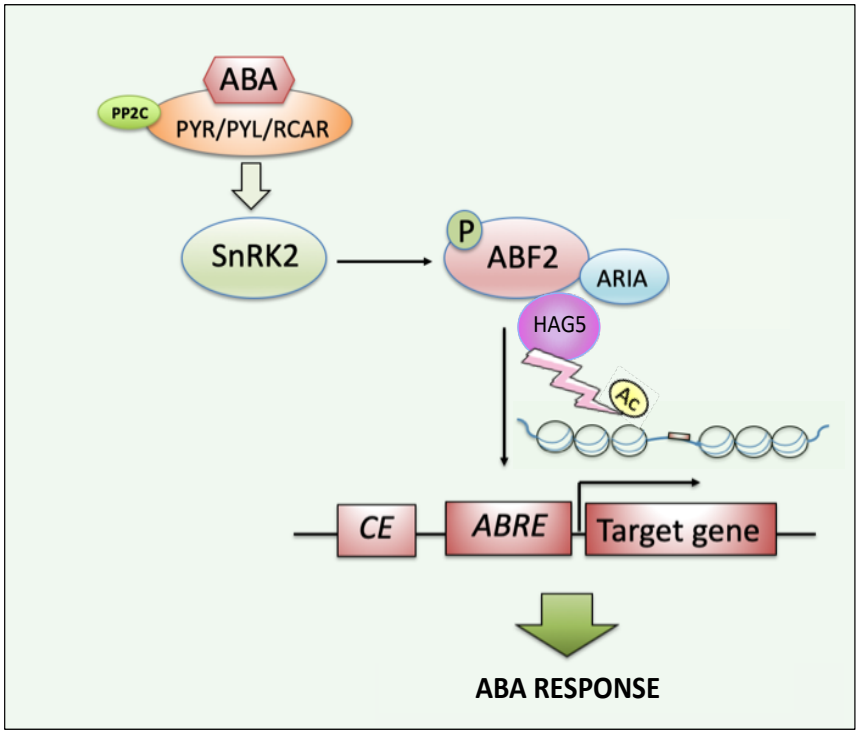

Figure 6.1. First model proposed for HAG5 regulation of ABA responses. In this model, HAG5 regulates the timing of transcriptional responses to ABA by increasing the accessibility of ABA response genes through H4K5 acetylation, facilitating the access to ARIA or ARIA-ABF2 complex.

To test our proposed model, we performed RNA-seq and ChIP-seq experiments in *hag5* mutants following ABA treatment. The aim of these experiments was to characterise the HAG5-dependent transcriptional response to abscisic acid and to explore the link between ABA signalling and H4K5ac.

6.4. HAG5 regulates ROS scavenging upon ABA

RNA-seq profiling resulted in the characterisation of a subset of genes regulated by HAG5. Indeed, 28% of the transcriptional response to ABA is positively or negatively regulated by HAG5. Genes that require HAG5 for their induction are involved in cellular detox processes through reactive oxygen species (ROS) scavenging, like flavonoid or phenylpropanoid biosynthesis. These results imply that HAG5 is required to maintain cellular homeostasis in a hormone-dependent manner. Furthermore, these genes are under the regulatory elements recognised by ABF2, such

as ABRE motifs. As a consequence, HAG5 assists ABF2 in ABA signal transduction to control cellular accumulation of ROS.

Accumulation of ROS levels within the cell results in oxidative stress, which can irreversibly damage proteins, DNA molecules, and membranes (Mittler, 2002). However, even though historically ROS have been considered damaging agents within cells, recent studies have demonstrated that these molecules also serve as second messengers in signalling pathways (Gilroy et al., 2016, Choudhury et al., 2017). In fact, ROS production is activated during early responses to abiotic stresses and senescence (Khanna-Chopra, 2012), and ABA-induced ROS production in guard cells results in stomata closure (Shi et al., 2015). In addition, ROS can reversely oxidise Cys residues in proteins, modulating enzyme structure or activity (Poole et al., 2004, Poole and Nelson, 2008, Choudhury et al., 2017). Therefore, ROS homeostasis is highly regulated in plant cells by enzymatic and small-molecule antioxidants, such as ascorbic acid, glutathione, and flavonoids (Watkins et al., 2017, Brunetti et al., 2018, Rice-Evans et al., 1997). These RNA-seq results show that HAG5 regulates ABF2-mediated transcription of antioxidant compounds, bringing novel information about additional molecular mechanisms that partially control cellular homeostasis through ROS levels. An important remark about this data is that it only reflects ROS regulation at the transcriptional level. Therefore, measuring ROS cellular levels upon ABA treatment in *hag5* mutants is required in order to validate this hypothesis.

In addition, quantifying the expression of ROS and senescence marker genes in Col-0 and *hag5-2* mutants upon *P. syringae* infection would help determine whether a miss-regulation of these pathways in the mutant partially explains the increased tolerance to the infection with this pathogen, besides the stomata density and/or opening.

6.5. Molecular mechanism of HAG5 regulation of ABA responses

In combination with the already discussed RNA-seq results, ChIP-seq analysis looking at H4K5ac enrichment upon ABA in Col-0 and *hag5* mutants unveiled two interesting findings. The first one was that H4K5ac seems to not participate in the regulation of ABA responses under the tested conditions, since there was no differential enrichment of this histone mark in ABA treated wild type samples. The

second finding was that there were not differential levels of H4K5ac in *hag5* mutants. This fact can be attributed to either HAG4 redundantly acetylating H4K5, or due to a different activity of HAG5 *in vivo* than the one previously reported *in vitro* by Earley et al., 2007. Indeed, it is possible that HAG5 is responsible for acetylating other histone marks or other interacting proteins.

In light of these results, our initial hypothesis about the molecular mechanism by which HAG5 regulates ABA responses was updated to the model described in Figure 6.2. In this model, HAG5 acetylates lysine residues in ARIA, modulating its transcription factor activity and/or indirectly affecting the transcriptional activity of ABF2. As a consequence, the lack of HAG5-mediated ARIA acetylation in *hag5* mutants results in a delay in the transcriptional response due to ARIA inactivation. This hypothesis was generated taking into account previous studies in *TIP60*, HAG5 orthologue in mammals. *TIP60* is known to modulate the activity of p53, an interacting TF, through direct acetylation (Wang et al., 2018). Hence, we contemplate the possibility of this mechanism being conserved in plants. If HAG5 was proven to acetylate ARIA, further steps would be required to characterise whether this acetylation is ABA dependent. In addition, the next approach would be to investigate the phenotypes resulting from complementing *aria* mutants with point-mutated versions of ARIA at the targeted lysine. Investigating the common and distinct phenotypes between this complemented *aria* lines and *hag5* plants would provide information about which HAG5-mediated processes depend on ARIA acetylation.

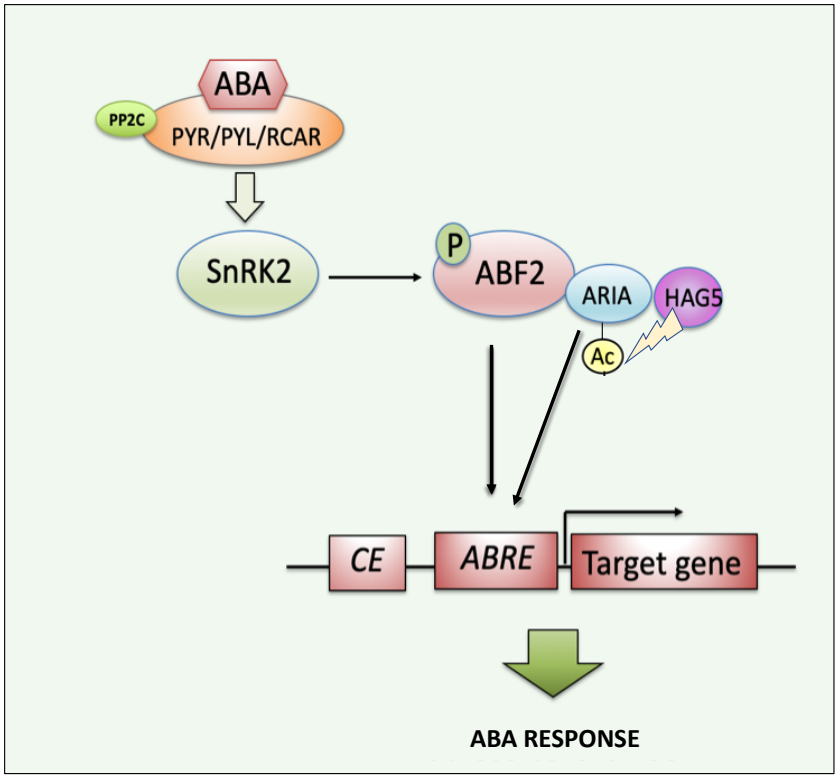

Figure 6.2. Second model proposed for HAG5 regulation of ABA responses. HAG5 positively regulates the transcriptional activity of ARIA through direct acetylation of lysine residues. This acetylation could also affect ABF2 transcriptional activity.

An alternative hypothesis is that HAG5 acetylation of ARIA might affect its ability to form protein complexes. Indeed, ARIA, due to its arm repeat structure, could function as scaffolding to assemble a transcriptional activator complex between HAG5, ABF2 and possibly, other proteins (Figure 6.3). In Chapter 4, several approaches were proposed to test each of the discussed possibilities. So far, acetylation of ARIA by HAG5 has been explored through *in vitro* assays measuring HAT activity, as well as through mass-spectrometry. The *in vitro* acetylation assay had the limitation of high background produced by the substrate (ARIA), as well as the technical difficulties of purifying HAG5 in an active catalytic state. Transient co-expression of ARIA and HAG5 in *N. benthamiana* has been performed successfully. However, in order to identify acetylation in specific lysine residues, high coverage of expressed ARIA is needed. As a consequence, we propose optimising this protocol by adding biological replicates and increasing the starting material for protein purification in order to obtain higher amounts of protein, maximising the chances of detecting most of the peptides that constitute ARIA.

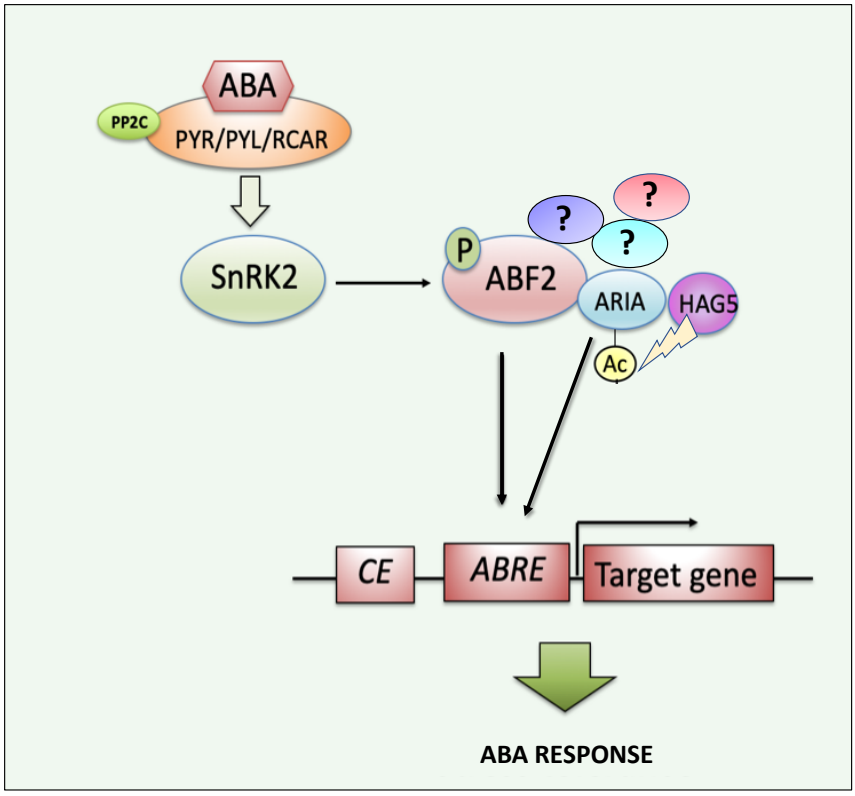

Figure 6.3. Third model proposed for HAG5 regulation of ABA responses. HAG5 acetylation of ARIA interferes protein scaffolding through ARIA, either recruiting or dissociating this transcriptional regulatory complex.

6.6. HAG5 regulates drought recovery strategies

ABA is a major phytohormone regulating plant responses to abiotic stresses such as cold, heat, increased salinity or drought (Fujita et al., 2006). The effect of climate change in global temperature and environmental conditions highlights drought as the abiotic stress with the greatest impact in agriculture.

When plants recognize water deficit conditions through their roots, they trigger changes in plant homeostasis, stress damage control and repair mechanisms. In addition, plants also initiate mechanisms of growth control through the production of abscisic acid (ABA) (Zhu, 2002). Due to the involvement of HAG5 in regulating ABA responses, we investigated the drought tolerance of *hag5* mutants in order to discover any potential role of HAG5 in biotic stress responses. By using different experimental settings, testing different aspects of drought stress, we demonstrated that *hag5* mutants are more tolerant to drought in terms of growth arrest, transpiration and recovery. Overall, *hag5* mutants display increased turgor upon desiccation, growth maintenance

upon mild drought stress, decreased water loss through the stomata and higher recovery rates after prolonged periods of drought.

From the three main strategies that plants use to overcome drought stress, these results confirmed that HAG5 is involved in the strategy known as “drought tolerance” or “drought recovery”. This mechanism confers plants the ability to function while at low water potential, maintaining a certain level of physiological activity even under severe drought stress conditions or whilst desiccated (Tardieu and Tuberosa, 2010, Fang and Xiong, 2015). Plants undertaking this approach can tolerate drought by promoting antioxidant defence mechanisms, production of dehydrins and late embryogenesis abundant (LEA) proteins, coordinating the abscisic acid (ABA) response and maximising water-use efficiency (Kumar et al., 2012). As a consequence, and in light of the RNA-seq results following ABA treatment, we propose that HAG5 participates in drought responses through regulating ROS production and scavenging at the transcriptional level to coordinate drought recovery strategies.

ROS enhancement under stress triggers defence responses and acclimation mechanisms by specific signal transduction pathways. In fact, ROS acts in ABA-mediated stress responses to sustain plant survival under adverse growth conditions (Lee et al., 2012). When plants are exposed to drought, ABA signals trigger ROS accumulation, which results in the induction of leaf senescence (Bhattacharjee, 2005). Drought-induced leaf senescence contributes to the maintenance of water balance in the whole plant body, reduces losses through transpiration and promotes the remobilization of nutrients from senescing leaves to youngest tissues (Munné-Bosch and Alegre, 2004). However, supressing ROS production and leaf senescence upon drought has been shown to result in increased drought tolerance similar to the one displayed by *hag5* mutants. In a study by Rivero et al., in 2007 transgenic plants with supressed ROS production were shown to maintain high water contents and retained photosynthetic activity during prolonged periods of drought stress. Moreover, these plants displayed minimal yield loss when watered with only 30% of the amount of water used under control condition. As a consequence, the authors concluded that suppression of ROS production delays leaf senescence and enhances drought resistance (Rivero et al., 2007). However, it is currently unclear how ROS metabolism is associated with ABA signalling in induction of leaf senescence upon drought. In

this study, we provide a link between HAG5, ABA signalling, ROS production and drought-induced senescence. Our hypothesis is based on the role of HAG5 in controlling the timing of ABA responses, based on the delayed transcriptional response of ABA marker genes in *hag5* mutants. Hence, upon ABA treatment, we hypothesize that HAG5 modulates ROS accumulation on a time-dependent manner. As a consequence, the regulation of the cellular levels of ROS upon ABA and drought is delayed in *hag5* mutants. This would result in a delayed initiation of drought-induced senescence and, overall, increased tolerance to drought. In order to test this hypothesis, we propose measuring the progression of senescence in drought-stressed *hag5* plants. To this end, we suggest a time course experiment measuring ROS content and photosynthetic activity of Col-0 and *hag5* as an indirect measure of senescence, over the course of prolonged drought stress.

6.7. Developing inhibitors of HAG5 to improve plant performance

Due to the beneficial phenotypes that plants display in the absence of HAG5, we developed two different strategies to implement our findings and improve crop plant performance. The first strategy is based on chemical inhibition of HAG5 catalytic activity to reproduce *hag5* mutant phenotypes. Through an *in silico* modelling and further *in planta* assays, a potential inhibitor of HAG5 was identified as a promising candidate. This compound is able to mirror multiple *hag5* mutant phenotypes when applied to Col-0 plants. Indeed, treatment with this inhibitor increases root meristem size and improves desiccation tolerance. In addition, inhibitor treatment of Col-0 plants is able to reproduce 74.7% of the transcriptional response to ABA of *hag5* mutants. One of the caveats of the RNA-seq experiment is that the concentration of inhibitor A used for the treatments was extrapolated from the IC value calculated for the human inhibitor used as control in other physiological assays As a consequence, a dose-response assay with inhibitor A and Col-0 seedlings would have helped determine the optimal concentration of inhibitor A and the best timing for the strongest transcriptional response prior sequencing. Nonetheless, we have identified a compound with potential agrochemical properties to enhance plant performance without the use of genetic modification. However, further characterisation of the effects of the inhibitor treatment, as well as *in vitro* binding assays to test the

specificity of the compound are required to discard off-target events. Currently, Dr. Veselina Uzunova is performing *in vitro* biding measurements calculating the association and dissociation curves between HAG5, HAG4 and the inhibitor by using SPR and purified proteins. This experiment will provide information about whether the inhibitor exclusively or preferentially binds to HAG5, a requisite regarding the diversified functions of both enzymes.

The second approach is based on CRISPR edited *Brassica oleracea* lines in order to investigate the effects of mutating HAG5 orthologue in plant performance in a crop plant. We developed these lines in an effort to study the evolutionary conservation of Arabidopsis HAG5-dependent regulation of plant stress and development across plant lineages.

6.8. Conclusions and future outlook

Looking into the findings that have been described throughout this thesis, our contribution to plant biology is reflected through the following achievements:

- We have identified a molecular mechanism that results in bigger plants with increased tolerance to pathogens and drought.
- We have found novel functions of HAG5 and described its role in plant stress responses.
- We discovered new protein-protein interactions between transcription factors and 2 MYST histone acetyltransferases, HAG4 and HAG5 .
- We proved that HAG5 acts through different mechanisms besides H4K5ac.
- We have characterised the first evidence of the evolutionary divergence between *HAG4* and *HAG5*.
- We revealed HAG5 as a novel component of the ABA signalling pathway.
- We described the role of HAG5 in regulating drought tolerance, and got further evidence about its involvement in the timing of senescence through the transcriptional regulation of ROS.
- We identified chemical inhibitors of HAG5 through *in silico* modelling that reproduce *hag5* mutant phenotypes *in planta*.

- We have developed CRISR/Cas9 *B. oleracea* lines that will provide further information about the conservation of the newly characterised roles of *HAG5* in other plant species.
-

6.9. Summary

Reflecting on the presented work and the overall development of this project, there are several alternative strategies that would have made this research period more productive. For instance, when it comes to investigating the function of a protein, and before characterising the phenotypes of the mutant, it is important to investigate the normal patterns of expression of such protein, the tissues in which it gets expressed, its cellular localisation, protein stability and degradation and whether its expression oscillates depending on the circadian clock, cell cycle progression or other external factors. Studying these factors at the beginning of a project are crucial for understanding which processes might this protein of interest be involved on, and would have helped plan future experiments.

Working with plants has a great time limitation, since generating stable homozygous transgenic lines or crossing mutant lines takes several months. Hence, once ARIA was identified as a HAG5 interactor, crossing both *hag5* and *aria* mutant lines to explore whether there is an additive effect on the phenotype of these plants should have been a priority, since presenting genetic evidence is often required to confirm that two proteins have related functions.

Furthermore, given the difficulties finding direct links between the phenotypes of *hag5* mutants and the molecular mechanism of HAG5, having a complemented KO line (*hag5-2*) with a dead version of HAG5 would at least clarify whether its enzymatic activity is required for its hypothesize functions. In addition, including *aria* and *abf2* mutants in the ABA susceptibility assays as controls would have also strengthen the hypothesis of the cooperation between both TFs and HAG5.

Another learnt lesson when working with chromatin-associated proteins is that identifying the regions of the chromatin that the protein of interest binds to is required from a mechanistic point of view. Given that the ChIPseq of H4K5ac did not provide any evidence of HAG5 being a chromatin-remodeller factor, a ChIP-seq with a tagged

version of HAG5 under its native promoter transformed in the KO mutant background remains as a crucial experiment to be performed.

There are several limitations related to the screening of HAG5 inhibitors. To begin with, ensuring that an inhibitor does not have off-targets *in vivo* is hard to assess, yet crucial if it has to be developed into an agrochemical. Also, finding the optimal concentration and time of application is a work that has to be done by external collaborators in industry with more suitable platforms for performing the appropriate trials.

Finally, developing CRISPR/Cas9 *B. oleracea* lines can take even years, specially until the Cas9 is segregated from the progeny and the desired indel is stably inheritable. Hence, generating these lines should take place at the very beginning of a project in order to ensure enough time to perform experiments in the produced lines.

Overall further characterisations of the molecular mechanisms by which HAG5 modulates stress responses in Arabidopsis are needed to fully understand its high level of conservation across plant lineages. Besides the need for further characterisation, the challenge for future research relies on optimising the available tools (HAG5 inhibitors and CRISPR/Cas9 lines) in order to apply the findings of this thesis to agriculture, in an effort to increase plant performance and food production in an incoming unpredictable and rapidly changing environment.

Bibliography

AHUJA, I., KISSEN, R. & BONES, A. M. 2012. Phytoalexins in defense against pathogens. *Trends in Plant Science,* 17**,** 73-90.

AIDA, M., BEIS, D., HEIDSTRA, R., WILLEMSEN, V., BLILOU, I., GALINHA, C., NUSSAUME, L., NOH, Y. S., AMASINO, R. & SCHERES, B. 2004. The PLETHORA genes mediate patterning of the Arabidopsis root stem cell niche. *Cell,* 119**,** 109-20.

ALEXA, A. & RAHNENFUHRER, J. 2007. Gene set enrichment analysis with topGO.

ALFANO, J. R., KLM, H. S., DELANEY, T. P. & COLLMER, A. 1997. Evidence that the Pseudomonas syringae pv. syringae hrp-linked hrmA gene encodes an Avr-like protein that acts in an hrp-dependent manner within tobacco cells. *Mol Plant Microbe Interact,* 10**,** 580-8.

ALONSO, J. M., STEPANOVA, A. N., LEISSE, T. J., KIM, C. J., CHEN, H., SHINN, P., STEVENSON, D. K., ZIMMERMAN, J., BARAJAS, P., CHEUK, R., GADRINAB, C., HELLER, C., JESKE, A., KOESEMA, E., MEYERS, C. C., PARKER, H., PREDNIS, L., ANSARI, Y., CHOY, N., DEEN, H., GERALT, M., HAZARI, N., HOM, E., KARNES, M., MULHOLLAND, C., NDUBAKU, R., SCHMIDT, I., GUZMAN, P., AGUILAR-HENONIN, L., SCHMID, M., WEIGEL, D., CARTER, D. E., MARCHAND, T., RISSEEUW, E., BROGDEN, D., ZEKO, A., CROSBY, W. L., BERRY, C. C. & ECKER, J. R. 2003. Genome-wide insertional mutagenesis of Arabidopsis thaliana. *Science,* 301**,** 653-7.

ALVAREZ, S., SUELA, J., VALENCIA, A., FERNÁNDEZ, A., WUNDERLICH, M., AGIRRE, X., PRÓSPER, F., MARTÍN-SUBERO, J. I., MAIQUES, A., ACQUADRO, F., RODRIGUEZ PERALES, S., CALASANZ, M. J., ROMAN-GÓMEZ, J., SIEBERT, R., MULLOY, J. C., CERVERA, J., SANZ, M. A., ESTELLER, M. & CIGUDOSA, J. C. 2010. DNA Methylation Profiles and Their Relationship with Cytogenetic Status in Adult Acute Myeloid Leukemia. 5.

ANDARGIE, M. & LI, J. 2016. Arabidopsis thaliana: A Model Host Plant to Study Plant-Pathogen Interaction Using Rice False Smut Isolates of Ustilaginoidea virens. *Frontiers in plant science,* 7**,** 192-192.

ANDRADE, M. A., PETOSA, C., O'DONOGHUE, S. I., MULLER, C. W. & BORK, P. 2001. Comparison of ARM and HEAT protein repeats. *J Mol Biol,* 309**,** 1-18.

ANNA DE LEONARDIS, M. P., PASQUALE DE VITA, ANNA MARIA MASTRANGELO 2012. *Genetic and Molecular Aspects of Plant Response to Drought in Annual Crop Species*, IntechOpen.

ARAVIND, L. & KOONIN, E. V. 1998. The HORMA domain: a common structural denominator in mitotic checkpoints, chromosome synapsis and DNA repair. *Trends Biochem Sci,* 23**,** 284-6.

AXTELL, M. J. & STASKAWICZ, B. J. 2003. Initiation of RPS2-specified disease resistance in Arabidopsis is coupled to the AvrRpt2-directed elimination of RIN4. *Cell,* 112**,** 369-77.

BACAICOA, E., MORA, V., ZAMARRENO, A. M., FUENTES, M., CASANOVA, E. & GARCIA-MINA, J. M. 2011. Auxin: a major player in the shoot-to-root

regulation of root Fe-stress physiological responses to Fe deficiency in cucumber plants. *Plant Physiol Biochem,* 49**,** 545-56.
BAI, Y., SUNARTI, S., KISSOUDIS, C., VISSER, R. G. F. & VAN DER LINDEN, C. G. 2018. The Role of Tomato WRKY Genes in Plant Responses to Combined Abiotic and Biotic Stresses. *Frontiers in plant science,* 9**,** 801-801.
BARBARA, D. J. & CLEWES, E. 2003. Plant pathogenic Verticillium species: how many of them are there? *Mol Plant Pathol,* 4**,** 297-305.
BARBARA W PENNYPACKER, R. B. 2004. Verticillium Wilts. By G F Pegg and B L Brady. *The Quarterly Review of Biology,* 79**,** 80-80.
BEBBER, D. P., RAMOTOWSKI, M. A. T. & GURR, S. J. 2013. Crop pests and pathogens move polewards in a warming world. *Nature Climate Change,* 3**,** 985.
BEEMSTER, G. T. & BASKIN, T. I. 1998. Analysis of cell division and elongation underlying the developmental acceleration of root growth in Arabidopsis thaliana. *Plant Physiol,* 116**,** 1515-26.
BERGER, S. L. 2007. The complex language of chromatin regulation during transcription. *Nature,* 447**,** 407-12.
BERTANI G. 1951. Studies on Lysogenesis I: The Mode of Phage Liberation by Lysogenic Escherichia coli. *J Bacteriol, 62, 193-300*
BHATTACHARJEE, S. 2005. Reactive oxygen species and oxidative burst: Roles in stress, senescence and signal transducation in plants. *Current Science,* 89**,** 1113-1121.
BIELUSZEWSKI, T., GALGANSKI, L., SURA, W., BIELUSZEWSKA, A., ABRAM, M., LUDWIKOW, A., ZIOLKOWSKI, P. A. & SADOWSKI, J. 2015. AtEAF1 is a potential platform protein for Arabidopsis NuA4 acetyltransferase complex. *BMC Plant Biol,* 15**,** 75.
BOLLER, T. & FELIX, G. 2009. A renaissance of elicitors: perception of microbe-associated molecular patterns and danger signals by pattern-recognition receptors. *Annu Rev Plant Biol,* 60**,** 379-406.
BOSWELL, R. E. & MAHOWALD, A. P. 1985. tudor, a gene required for assembly of the germ plasm in Drosophila melanogaster. *Cell,* 43**,** 97-104.
BOYCHEVA, I., VASSILEVA, V. & IANTCHEVA, A. 2014. Histone Acetyltransferases in Plant Development and Plasticity. *Curr Genomics.*
BOYKO, A., KATHIRIA, P., ZEMP, F. J., YAO, Y., POGRIBNY, I. & KOVALCHUK, I. 2007. Transgenerational changes in the genome stability and methylation in pathogen-infected plants: (virus-induced plant genome instability). *Nucleic acids research,* 35**,** 1714-1725.
BRASIL, J. N., CABRAL, L. M., ELOY, N. B., PRIMO, L. M. F., BARROSO-NETO, I. L., GRANGEIRO, L. P. P., GONZALEZ, N., INZÉ, D., FERREIRA, P. C. G. & HEMERLY, A. S. 2015. AIP1 is a novel Agenet/Tudor domain protein from Arabidopsis that interacts with regulators of DNA replication, transcription and chromatin remodeling. *BMC plant biology,* 15**,** 270-270.
BRINKMAN, E. K., CHEN, T., AMENDOLA, M. & VAN STEENSEL, B. 2014. Easy quantitative assessment of genome editing by sequence trace decomposition. *Nucleic Acids Research,* 42**,** e168-e168.
BROCCHIERI, L. 2013. Phenotypic and Evolutionary Distances in Phylogenetic Tree Reconstruction. *Journal of Phylogenetics & Evolutionary Biology,* 01.

BRUNETTI, C., FINI, A., SEBASTIANI, F., GORI, A. & TATTINI, M. 2018. Modulation of Phytohormone Signaling: A Primary Function of Flavonoids in Plant–Environment Interactions. *Frontiers in Plant Science,* 9.

BRUSSLAN, J. A., BONORA, G., RUS-CANTERBURY, A. M., TARIQ, F., JAROSZEWICZ, A. & PELLEGRINI, M. 2015. A Genome-Wide Chronological Study of Gene Expression and Two Histone Modifications, H3K4me3 and H3K9ac, during Developmental Leaf Senescence. 168**,** 1246-1261.

CAMPI, M., D'ANDREA, L., EMILIANI, J. & CASATI, P. 2012. Participation of chromatin-remodeling proteins in the repair of ultraviolet-B-damaged DNA. *Plant Physiol,* 158**,** 981-95.

CAMPO, S., BALDRICH, P., MESSEGUER, J., LALANNE, E., COCA, M. & SAN SEGUNDO, B. 2014. Overexpression of a Calcium-Dependent Protein Kinase Confers Salt and Drought Tolerance in Rice by Preventing Membrane Lipid Peroxidation. *Plant Physiology,* 165**,** 688.

CAMPOS, M. L., YOSHIDA, Y., MAJOR, I. T., DE OLIVEIRA FERREIRA, D., WERADUWAGE, S. M., FROEHLICH, J. E., JOHNSON, B. F., KRAMER, D. M., JANDER, G., SHARKEY, T. D. & HOWE, G. A. 2016. Rewiring of jasmonate and phytochrome B signalling uncouples plant growth-defense tradeoffs. *Nature Communications,* 7**,** 12570.

CAO, F. Y., YOSHIOKA, K. & DESVEAUX, D. 2011. The roles of ABA in plant-pathogen interactions. *J Plant Res,* 124**,** 489-99.

CASATI, P., CAMPI, M., CHU, F., SUZUKI, N., MALTBY, D., GUAN, S., BURLINGAME, A. L. & WALBOT, V. 2008. Histone acetylation and chromatin remodeling are required for UV-B-dependent transcriptional activation of regulated genes in maize. *Plant Cell,* 20**,** 827-42.

CESARI, S., BERNOUX, M., MONCUQUET, P., KROJ, T. & DODDS, P. N. 2014. A novel conserved mechanism for plant NLR protein pairs: the integrated decoy hypothesis. *Frontiers in Plant Science,* 5.

CHAKRABORTY, S. & NEWTON, A. C. 2011. Climate change, plant diseases and food security: an overview. *Plant Pathology,* 60**,** 2-14.

CHAVES, M. M., MAROCO, J. P. & PEREIRA, J. S. 2003. Understanding plant responses to drought; from genes to the whole plant. *Functional Plant Biology,* 30**,** 239-264.

CHAVES, M. M. & OLIVEIRA, M. M. 2004. Mechanisms underlying plant resilience to water deficits: prospects for water-saving agriculture. *Journal of Experimental Botany,* 55**,** 2365-2384.

CHEN, C., NOTT, T. J., JIN, J. & PAWSON, T. 2011. Deciphering arginine methylation: Tudor tells the tale. *Nat Rev Mol Cell Biol,* 12**,** 629-42.

CHEN, H. & BOUTROS, P. C. 2011. VennDiagram: a package for the generation of highly-customizable Venn and Euler diagrams in R. *BMC Bioinformatics,* 12**,** 35.

CHEN, L., XIANG, S., CHEN, Y., LI, D. & YU, D. 2017. Arabidopsis WRKY45 Interacts with the DELLA Protein RGL1 to Positively Regulate Age-Triggered Leaf Senescence. *Mol Plant,* 10**,** 1174-1189.

CHEN, X., LU, L., MAYER, K. S., SCALF, M., QIAN, S., LOMAX, A., SMITH, L. M. & ZHONG, X. 2016. POWERDRESS interacts with HISTONE DEACETYLASE 9 to promote aging in Arabidopsis. 5.

CHINCHILLA, D., BOLLER, T. & ROBATZEK, S. 2007. Flagellin signalling in plant immunity. *Adv Exp Med Biol,* 598**,** 358-71.

CHOI, S.-M., SONG, H.-R., HAN, S.-K., HAN, M., KIM, C.-Y., PARK, J., LEE, Y.-H., JEON, J.-S., NOH, Y.-S. & NOH, B. 2012. HDA19 is required for the repression of salicylic acid biosynthesis and salicylic acid-mediated defense responses in Arabidopsis. *The Plant Journal,* 71**,** 135-146.

CHOUDHURY, F. K., RIVERO, R. M., BLUMWALD, E. & MITTLER, R. 2017. Reactive oxygen species, abiotic stress and stress combination. *Plant J,* 90**,** 856-867.

CHUNG, H. S., KOO, A. J., GAO, X., JAYANTY, S., THINES, B., JONES, A. D. & HOWE, G. A. 2008. Regulation and function of Arabidopsis JASMONATE ZIM-domain genes in response to wounding and herbivory. *Plant Physiol,* 146**,** 952-64.

COFFEY, K., BLACKBURN, T. J., COOK, S., GOLDING, B. T., GRIFFIN, R. J., HARDCASTLE, I. R., HEWITT, L., HUBERMAN, K., MCNEILL, H. V., NEWELL, D. R., ROCHE, C., RYAN-MUNDEN, C. A., WATSON, A. & ROBSON, C. N. 2012. Characterisation of a Tip60 Specific Inhibitor, NU9056, in Prostate Cancer. 7**,** e45539.

COLCOMBET, J. & HIRT, H. 2008. Arabidopsis MAPKs: a complex signalling network involved in multiple biological processes. *Biochem J,* 413**,** 217-26.

COLLINS, T., STONE, J. R. & WILLIAMS, A. J. 2001. All in the family: the BTB/POZ, KRAB, and SCAN domains. *Mol Cell Biol,* 21**,** 3609-15.

CRICK, F. 1970. Central Dogma of Molecular Biology. *Nature,* 227**,** 561-563.

DANGL, D & JONES, J. 2006. The plant immune system. *Nature,* 444**,** 323-329.

DANGL, J. L. 1996. Death Don't Have No Mercy: Cell Death Programs in Plant-Microbe Interactions. 8**,** 1793-1807.

DANGL, J. L. & JONES, J. D. G. 2001. Plant pathogens and integrated defence responses to infection. *Nature,* 411**,** 826-833.

DANQUAH, A., DE ZELICOURT, A., BOUDSOCQ, M., NEUBAUER, J., FREI DIT FREY, N., LEONHARDT, N., PATEYRON, S., GWINNER, F., TAMBY, J. P., ORTIZ-MASIA, D., MARCOTE, M. J., HIRT, H. & COLCOMBET, J. 2015. Identification and characterization of an ABA-activated MAP kinase cascade in Arabidopsis thaliana. *Plant J,* 82**,** 232-44.

DANQUAH, A., DE ZELICOURT, A., COLCOMBET, J. & HIRT, H. 2014. The role of ABA and MAPK signaling pathways in plant abiotic stress responses. *Biotechnology Advances,* 32**,** 40-52.

DE TORRES-ZABALA, M., TRUMAN, W., BENNETT, M. H., LAFFORGUE, G., MANSFIELD, J. W., RODRIGUEZ EGEA, P., BÖGRE, L. & GRANT, M. 2007. Pseudomonas syringae pv. tomato hijacks the Arabidopsis abscisic acid signalling pathway to cause disease. 26**,** 1434-1443.

DEBENER, T., LEHNACKERS, H., ARNOLD, M. & DANGL, J. L. 1991. Identification and molecular mapping of a single Arabidopsis thaliana locus determining resistance to a phytopathogenic Pseudomonas syringae isolate. *Plant J,* 1**,** 289-302.

DELARUE, D. L., MOUSSA, B., YVES, H., SÉVERINE, D., WANHUI, K., DAO-XIU, Z. & MARIANNE 2008. The MYST histone acetyltransferases are essential for gametophyte development in Arabidopsis. *BMC Plant Biology,* 8**,** 1.

DENOUX, C., GALLETTI, R., MAMMARELLA, N., GOPALAN, S., WERCK, D., DE LORENZO, G., FERRARI, S., AUSUBEL, F. M. & DEWDNEY, J. 2008. Activation of defense response pathways by OGs and Flg22 elicitors in Arabidopsis seedlings. *Molecular plant,* 1**,** 423-445.

DEPUYDT, S. & HARDTKE, CHRISTIAN S. 2011. Hormone Signalling Crosstalk in Plant Growth Regulation. *Current Biology,* 21**,** R365-R373.
DING, B. & WANG, G. L. 2015. Chromatin versus pathogens: the function of epigenetics in plant immunity. *Front Plant Sci,* 6**,** 675.
DING, Y., FROMM, M. & AVRAMOVA, Z. 2012. Multiple exposures to drought 'train' transcriptional responses in Arabidopsis. 3**,** 740.
DOLAN, L., JANMAAT, K., WILLEMSEN, V., LINSTEAD, P., POETHIG, S., ROBERTS, K. & SCHERES, B. 1993. Cellular organisation of the Arabidopsis thaliana root. *Development,* 119**,** 71-84.
DOYON, Y. & COTE, J. 2004. The highly conserved and multifunctional NuA4 HAT complex. *Curr Opin Genet Dev,* 14**,** 147-54.
DREZE, M., MONACHELLO, D., LURIN, C., CUSICK, M. E., HILL, D. E., VIDAL, M. & BRAUN, P. 2010. High-Quality Binary Interactome Mapping. *Guide to Yeast Genetics: Functional Genomics, Proteomics, and Other Systems Analysis.*
DU, Z., ZHOU, X., LING, Y., ZHANG, Z. & SU, Z. 2010. agriGO: a GO analysis toolkit for the agricultural community. *Nucleic acids research,* 38**,** W64-W70.
EARLEY, K. W., SHOOK, M. S., BROWER-TOLAND, B., HICKS, L. & PIKAARD, C. S. 2007. In vitro specificities of Arabidopsis co-activator histone acetyltransferases: implications for histone hyperacetylation in gene activation. *Plant J,* 52**,** 615-26.
EKWURZEL, B., BONEHAM, J., DALTON, M. W., HEEDE, R., MERA, R. J., ALLEN, M. R. & FRUMHOFF, P. C. 2017. The rise in global atmospheric CO2, surface temperature, and sea level from emissions traced to major carbon producers. *Climatic Change,* 144**,** 579-590.
ERFFELINCK, M.-L., RIBEIRO, B., PERASSOLO, M., PAUWELS, L., POLLIER, J., STORME, V. & GOOSSENS, A. 2018. A user-friendly platform for yeast two-hybrid library screening using next generation sequencing. *PLOS ONE,* 13**,** e0201270.
FANG, Y. & XIONG, L. 2015. General mechanisms of drought response and their application in drought resistance improvement in plants. *Cell Mol Life Sci,* 72**,** 673-89.
FARRONA, S., HURTADO, L. & REYES, J. C. 2007. A nucleosome interaction module is required for normal function of Arabidopsis thaliana BRAHMA. *J Mol Biol,* 373**,** 240-50.
FELIX, G., DURAN, J. D., VOLKO, S. & BOLLER, T. 1999. Plants have a sensitive perception system for the most conserved domain of bacterial flagellin. *Plant J,* 18**,** 265-76.
FENG, Z., MAO, Y., XU, N., ZHANG, B., WEI, P., YANG, D.-L., WANG, Z., ZHANG, Z., ZHENG, R., YANG, L., ZENG, L., LIU, X. & ZHU, J.-K. 2014. Multigeneration analysis reveals the inheritance, specificity, and patterns of CRISPR/Cas-induced gene modifications in Arabidopsis. *Proceedings of the National Academy of Sciences of the United States of America,* 111**,** 4632-4637.
FERNÁNDEZ-CALVO, P., CHINI, A., FERNÁNDEZ-BARBERO, G., CHICO, J.-M., GIMENEZ-IBANEZ, S., GEERINCK, J., EECKHOUT, D., SCHWEIZER, F., GODOY, M., FRANCO-ZORRILLA, J. M., PAUWELS, L., WITTERS, E., PUGA, M. I., PAZ-ARES, J., GOOSSENS, A., REYMOND, P., DE JAEGER, G. & SOLANO, R. 2011. TheArabidopsisbHLH Transcription Factors MYC3 and MYC4 Are Targets

of JAZ Repressors and Act Additively with MYC2 in the Activation of Jasmonate Responses. *The Plant Cell,* 23**,** 701-715.

FIELD, C. B., V. R. BARROS, D. J. DOKKEN, K. J. MACH, M. D. MASTRANDREA, T. E. BILIR, M. CHATTERJEE, K. L. EBI, Y. O. ESTRADA, R. C. GENOVA, B. GIRMA, E. S. KISSEL, A. N. LEVY, S. MACCRACKEN, P. R. MASTRANDREA, AND L. L. WHITE 2014. IPCC Climate change 2014: impacts, adaptation and vulnerability. *Cambridge University Press.*

FINKELSTEIN, R. 2013. Abscisic Acid synthesis and response. *Arabidopsis Book,* 11**,** e0166.

FINKELSTEIN, R. R., GAMPALA, S. S. & ROCK, C. D. 2002. Abscisic acid signaling in seeds and seedlings. *Plant Cell,* 14 Suppl**,** S15-45.

FOLEY, J. A., RAMANKUTTY, N., BRAUMAN, K. A., CASSIDY, E. S., GERBER, J. S., JOHNSTON, M., MUELLER, N. D., O'CONNELL, C., RAY, D. K., WEST, P. C., BALZER, C., BENNETT, E. M., CARPENTER, S. R., HILL, J., MONFREDA, C., POLASKY, S., ROCKSTRÖM, J., SHEEHAN, J., SIEBERT, S., TILMAN, D. & ZAKS, D. P. M. 2011. Solutions for a cultivated planet. *Nature,* 478**,** 337.

FRANCO-ZORRILLA, J. M., LÓPEZ-VIDRIERO, I., CARRASCO, J. L., GODOY, M., VERA, P. & SOLANO, R. 2014. DNA-binding specificities of plant transcription factors and their potential to define target genes. *Proceedings of the National Academy of Sciences,* 111**,** 2367.

FU, Z. Q. & DONG, X. 2013. Systemic Acquired Resistance: Turning Local Infection into Global Defense. *Annual Review of Plant Biology,* 64**,** 839-863.

FUCHS, S., GRILL, E., MESKIENE, I. & SCHWEIGHOFER, A. 2013. Type 2C protein phosphatases in plants. 280**,** 681-693.

FUJII, H., VERSLUES, P. E. & ZHU, J.-K. 2007. Identification of two protein kinases required for abscisic acid regulation of seed germination, root growth, and gene expression in Arabidopsis. *The Plant cell,* 19**,** 485-494.

FUJII, H. & ZHU, J.-K. 2009. Arabidopsis mutant deficient in 3 abscisic acid-activated protein kinases reveals critical roles in growth, reproduction, and stress. *Proceedings of the National Academy of Sciences,* 106**,** 8380.

FUJITA, M., FUJITA, Y., NOUTOSHI, Y., TAKAHASHI, F., NARUSAKA, Y., YAMAGUCHI-SHINOZAKI, K. & SHINOZAKI, K. 2006. Crosstalk between abiotic and biotic stress responses: a current view from the points of convergence in the stress signaling networks. *Curr Opin Plant Biol,* 9**,** 436-42.

FUJITA, Y., FUJITA, M., SATOH, R., MARUYAMA, K., PARVEZ, M. M., SEKI, M., HIRATSU, K., OHME-TAKAGI, M., SHINOZAKI, K. & YAMAGUCHI-SHINOZAKI, K. 2005. AREB1 is a transcription activator of novel ABRE-dependent ABA signaling that enhances drought stress tolerance in Arabidopsis. *The Plant cell,* 17**,** 3470-3488.

FUJITA, Y., FUJITA, M., SHINOZAKI, K. & YAMAGUCHI-SHINOZAKI, K. 2011. ABA-mediated transcriptional regulation in response to osmotic stress in plants. *J Plant Res,* 124**,** 509-25.

FUJITA, Y., NAKASHIMA, K., YOSHIDA, T., KATAGIRI, T., KIDOKORO, S., KANAMORI, N., UMEZAWA, T., FUJITA, M., MARUYAMA, K., ISHIYAMA, K., KOBAYASHI, M., NAKASONE, S., YAMADA, K., ITO, T., SHINOZAKI, K. & YAMAGUCHI-SHINOZAKI, K. 2009. Three SnRK2 Protein Kinases are the Main Positive Regulators of Abscisic Acid Signaling

in Response to Water Stress in Arabidopsis. *Plant and Cell Physiology,* 50**,** 2123-2132.
FYODOROV, D. V., ZHOU, B.-R., SKOULTCHI, A. I. & BAI, Y. 2018. Emerging roles of linker histones in regulating chromatin structure and function. *Nature Reviews Molecular Cell Biology,* 19**,** 192-206.
GABALDÓN, T. 2007. Evolution of proteins and proteomes: a phylogenetics approach. *Evolutionary bioinformatics online,* 1**,** 51-61.
GARCIA-CANO, E., HAK, H., MAGORI, S., LAZAROWITZ, S. G. & CITOVSKY, V. 2018. The Agrobacterium F-Box Protein Effector VirF Destabilizes the Arabidopsis GLABROUS1 Enhancer/Binding Protein-Like Transcription Factor VFP4, a Transcriptional Activator of Defense Response Genes. *Mol Plant Microbe Interact,* 31**,** 576-586.
GILROY, S., BIAŁASEK, M., SUZUKI, N., GÓRECKA, M., DEVIREDDY, A. R., KARPIŃSKI, S. & MITTLER, R. 2016. ROS, Calcium, and Electric Signals: Key Mediators of Rapid Systemic Signaling in Plants. *Plant physiology,* 171**,** 1606-1615.
GLAZEBROOK, J. 2005. Contrasting mechanisms of defense against biotrophic and necrotrophic pathogens. *Annu Rev Phytopathol,* 43**,** 205-27.
GÓMEZ-GÓMEZ, L. & BOLLER, T. 2000. FLS2: An LRR Receptor–like Kinase Involved in the Perception of the Bacterial Elicitor Flagellin in Arabidopsis. *Molecular Cell,* 5**,** 1003-1011.
GOODMAN, R. H. & SMOLIK, S. 2000. CBP/p300 in cell growth, transformation, and development. *Genes Dev,* 14**,** 1553-77.
GRASSER, M. & GRASSER, K. D. 2018. The plant RNA polymerase II elongation complex: A hub coordinating transcript elongation and mRNA processing. *Transcription,* 9**,** 117-122.
GREENBERG, J. T. 2003. PROGRAMMED CELL DEATH IN PLANT-PATHOGEN INTERACTIONS. Annual Review of Plant Physiology and Plant Molecular Biology , 48, 525-545.
GUO, Y. & GAN, S. S. 2014. Translational researches on leaf senescence for enhancing plant productivity and quality. 65**,** 3901-3913.
HAN, S.-K., SANG, Y., RODRIGUES, A., BIOL, F., WU, M.-F., RODRIGUEZ, P. L. & WAGNER, D. 2012. The SWI2/SNF2 chromatin remodeling ATPase BRAHMA represses abscisic acid responses in the absence of the stress stimulus in Arabidopsis. *The Plant cell,* 24**,** 4892-4906.
HAN, Z., YU, H., ZHAO, Z., HUNTER, D., LUO, X., DUAN, J. & TIAN, L. 2016. AtHD2D Gene Plays a Role in Plant Growth, Development, and Response to Abiotic Stresses in Arabidopsis thaliana. *Frontiers in plant science,* 7**,** 310-310.
HARPER, J. F., BRETON, G. & HARMON, A. 2004. DECODING Ca2+ SIGNALS THROUGH PLANT PROTEIN KINASES. *Annual Review of Plant Biology,* 55**,** 263-288.
HATTORI, T. 2002. Experimentally Determined Sequence Requirement of ACGT-Containing Abscisic Acid Response Element. 43**,** 136-140.
HAUSER, M. T., AUFSATZ, W., JONAK, C. & LUSCHNIG, C. 2011. Transgenerational epigenetic inheritance in plants. *Biochim Biophys Acta,* 1809**,** 459-68.
HEARD, E. & ROBERT 2014. Transgenerational Epigenetic Inheritance: Myths and Mechanisms. *Cell,* 157**,** 95-109.

HEBBES, T. R., THORNE, A. W. & CRANE-ROBINSON, C. 1988. A direct link between core histone acetylation and transcriptionally active chromatin. *Embo j,* 7**,** 1395-402.
HOFFMANN, M. H. 2002. Biogeography of Arabidopsis thaliana (L.) Heynh. (Brassicaceae). *Journal of Biogeography,* 29.
HSU, P. D., LANDER, E. S. & ZHANG, F. 2014. Development and applications of CRISPR-Cas9 for genome engineering. *Cell,* 157**,** 1262-1278.
HUOT, B., YAO, J., MONTGOMERY, B. L. & HE, S. Y. 2014a. Growth-defense tradeoffs in plants: a balancing act to optimize fitness. *Mol Plant,* 7**,** 1267-87.
HUOT, B., YAO, J., MONTGOMERY, B. L. & HE, S. Y. 2014b. Growth–Defense Tradeoffs in Plants: A Balancing Act to Optimize Fitness. *Molecular Plant,* 7**,** 1267-1287.
IPCC 1990. IPCC first assessment report overview and policymaker summaries. *IPCC supplement.*
JENUWEIN, T. 2001. Translating the Histone Code. *Science,* 293**,** 1074-1080.
JERZMANOWSKI, A. 2007. SWI/SNF chromatin remodeling and linker histones in plants. *Biochim Biophys Acta,* 1769**,** 330-45.
JOHNSON, W. L. & STRAIGHT, A. F. 2017. RNA-mediated regulation of heterochromatin. *Current Opinion in Cell Biology,* 46**,** 102-109.
JONES, J. D. & DANGL, J. L. 2006. The plant immune system. *Nature,* 444**,** 323-9.
KADONAGA, J. T. 1998. Eukaryotic transcription: an interlaced network of transcription factors and chromatin-modifying machines. *Cell,* 92**,** 307-13.
KAGAYA, Y., HOBO, T., MURATA, M., BAN, A. & HATTORI, T. 2002. Abscisic acid-induced transcription is mediated by phosphorylation of an abscisic acid response element binding factor, TRAB1. *Plant Cell,* 14**,** 3177-89.
KERSEY, P. J., ALLEN, J. E., ALLOT, A., BARBA, M., BODDU, S., BOLT, B. J., CARVALHO-SILVA, D., CHRISTENSEN, M., DAVIS, P., GRABMUELLER, C., KUMAR, N., LIU, Z., MAUREL, T., MOORE, B., MCDOWALL, M. D., MAHESWARI, U., NAAMATI, G., NEWMAN, V., ONG, C. K., PAULINI, M., PEDRO, H., PERRY, E., RUSSELL, M., SPARROW, H., TAPANARI, E., TAYLOR, K., VULLO, A., WILLIAMS, G., ZADISSIA, A., OLSON, A., STEIN, J., WEI, S., TELLO-RUIZ, M., WARE, D., LUCIANI, A., POTTER, S., FINN, R. D., URBAN, M., HAMMOND-KOSACK, K. E., BOLSER, D. M., DE SILVA, N., HOWE, K. L., LANGRIDGE, N., MASLEN, G., STAINES, D. M. & YATES, A. 2018. Ensembl Genomes 2018: an integrated omics infrastructure for non-vertebrate species. *Nucleic Acids Res,* 46**,** D802-D808.
KHANNA-CHOPRA, R. 2012. Leaf senescence and abiotic stresses share reactive oxygen species-mediated chloroplast degradation. *Protoplasma,* 249**,** 469-81.
KIM, J.-M., TO, T. K., MATSUI, A., TANOI, K., KOBAYASHI, N. I., MATSUDA, F., HABU, Y., OGAWA, D., SAKAMOTO, T., MATSUNAGA, S., BASHIR, K., RASHEED, S., ANDO, M., TAKEDA, H., KAWAURA, K., KUSANO, M., FUKUSHIMA, A., ENDO, T. A., KUROMORI, T., ISHIDA, J., MOROSAWA, T., TANAKA, M., TORII, C., TAKEBAYASHI, Y., SAKAKIBARA, H., OGIHARA, Y., SAITO, K., SHINOZAKI, K., DEVOTO, A. & SEKI, M. 2017. Acetate-mediated novel survival strategy against drought in plants. *Nature Plants,* 3**,** 17097.
KIM, J. M., TO, T. K., ISHIDA, J., MOROSAWA, T., KAWASHIMA, M., MATSUI, A., TOYODA, T., KIMURA, H., SHINOZAKI, K. & SEKI, M. 2008a.

Alterations of Lysine Modifications on the Histone H3 N-Tail under Drought Stress Conditions in Arabidopsis thaliana. 49**,** 1580-1588.
KIM, K.-C., LAI, Z., FAN, B. & CHEN, Z. 2008b. Arabidopsis WRKY38 and WRKY62 Transcription Factors Interact with Histone Deacetylase 19 in Basal Defense. *The Plant Cell,* 20**,** 2357-2371.
KIM, S., CHOI, H. I., RYU, H. J., PARK, J. H., KIM, M. D. & KIM, S. Y. 2004a. ARIA, an Arabidopsis arm repeat protein interacting with a transcriptional regulator of abscisic acid-responsive gene expression, is a novel abscisic acid signaling component. *Plant Physiol,* 136**,** 3639-48.
KIM, S., KANG, J. Y., CHO, D. I., PARK, J. H. & KIM, S. Y. 2004b. ABF2, an ABRE-binding bZIP factor, is an essential component of glucose signaling and its overexpression affects multiple stress tolerance. *Plant J,* 40**,** 75-87.
KIM, T.-H., BÖHMER, M., HU, H., NISHIMURA, N. & SCHROEDER, J. I. 2010. Guard Cell Signal Transduction Network: Advances in Understanding Abscisic Acid, CO2, and Ca2+Signaling. *Annual Review of Plant Biology,* 61**,** 561-591.
KIM, W., IIZUMI, T. & NISHIMORI, M. 2019. Global Patterns of Crop Production Losses Associated with Droughts from 1983 to 2009. *Journal of Applied Meteorology and Climatology,* 58.
KIM, Y. J., WANG, R., GAO, L., LI, D., XU, C., MANG, H., JEON, J., CHEN, X., ZHONG, X., KWAK, J. M., MO, B., XIAO, L. & CHEN, X. 2016. POWERDRESS and HDA9 interact and promote histone H3 deacetylation at specific genomic sites in Arabidopsis. *Proceedings of the National Academy of Sciences of the United States of America,* 113**,** 14858-14863.
KING E.O. 1954. Media for the demonstration of pyocyanin and fluorescein, J. *Lab. Clin. Med*. 44, 301.
KLEINBOELTING N., HUEP G., KLOETGEN A., VIEHOEVER P., WEISSHAAR B. 2012. GABI-Kat SimpleSearch: new features of the Arabidopsis thaliana T-DNA mutant database. *Nuleic Acids Res,* 40, D1211-D1215.
KOORNNEEF, M. & MEINKE, D. 2010. The development of Arabidopsis as a model plant. *The Plant Journal,* 61**,** 909-921.
KORNBERG, R. D. & LORCH, Y. 1999. Twenty-five years of the nucleosome, fundamental particle of the eukaryote chromosome. *Cell,* 98**,** 285-94.
KOURELIS, J. & VAN DER HOORN, R. A. L. 2018. Defended to the Nines: 25 Years of Resistance Gene Cloning Identifies Nine Mechanisms for R Protein Function. *The Plant Cell,* 30**,** 285-299.
KOUZARIDES, T. 2007. SnapShot: Histone-modifying enzymes. *Cell,* 131**,** 822.
KOVTUN, Y., CHIU, W.-L., TENA, G. & SHEEN, J. 2000. Functional analysis of oxidative stress-activated mitogen-activated protein kinase cascade in plants. *Proceedings of the National Academy of Sciences,* 97**,** 2940.
KRAMER, P. J. A. B., J.S. 1995. Water relations of plants and soils. *Academic Press, San Diego.*
KRYSAN, P. J., YOUNG, J. C. & SUSSMAN, M. R. 1999. T-DNA as an Insertional Mutagen in Arabidopsis. *The Plant Cell,* 11**,** 2283-2290.
KULIK, A., WAWER, I., KRZYWIŃSKA, E., BUCHOLC, M. & DOBROWOLSKA, G. 2011. SnRK2 Protein Kinases—Key Regulators of Plant Response to Abiotic Stresses. 15**,** 859-872.
KUMAR, M. N., HSIEH, Y. F. & VERSLUES, P. E. 2015. At14a-Like1 participates in membrane-associated mechanisms promoting growth during drought in Arabidopsis thaliana. *Proc Natl Acad Sci U S A,* 112**,** 10545-50.

KUMAR, R., SOLANKEY, S. S. & SINGH, M. 2012. Breeding for drought tolerance in vegetables. *Vegetable Science,* 39**,** 1-15.

LAKOWICZ, J. R. 1988. Principles of frequency-domain fluorescence spectroscopy and applications to cell membranes. *Subcell Biochem,* 13**,** 89-126.

LATRASSE, D., JEGU, T., LI, H., DE ZELICOURT, A., RAYNAUD, C., LEGRAS, S., GUST, A., SAMAJOVA, O., VELUCHAMY, A., RAYAPURAM, N., RAMIREZ-PRADO, J. S., KULIKOVA, O., COLCOMBET, J., BIGEARD, J., GENOT, B., BISSELING, T., BENHAMED, M. & HIRT, H. 2017. MAPK-triggered chromatin reprogramming by histone deacetylase in plant innate immunity. *Genome Biol,* 18**,** 131.

LAWRENSON, T., HUNDLEBY, P. & HARWOOD, W. 2019. Creating Targeted Gene Knockouts in Brassica oleracea Using CRISPR/Cas9. *Methods Mol Biol,* 1917**,** 155-170.

LAWRENSON, T., SHORINOLA, O., STACEY, N., LI, C., OSTERGAARD, L., PATRON, N., UAUY, C. & HARWOOD, W. 2015. Induction of targeted, heritable mutations in barley and Brassica oleracea using RNA-guided Cas9 nuclease. *Genome Biol,* 16**,** 258.

LEE, S., SEO, P. J., LEE, H.-J. & PARK, C.-M. 2012. A NAC transcription factor NTL4 promotes reactive oxygen species production during drought-induced leaf senescence in Arabidopsis. *The Plant Journal,* 70**,** 831-844.

LEE, S. J., CHO, D. I., KANG, J. Y., KIM, M. D. & KIM, S. Y. 2010a. AtNEK6 interacts with ARIA and is involved in ABA response during seed germination. *Mol Cells,* 29**,** 559-66.

LEE, S. J., CHO, D. I., KANG, J. Y. & KIM, S. Y. 2009. An ARIA-interacting AP2 domain protein is a novel component of ABA signaling. *Mol Cells,* 27**,** 409-16.

LEE, S. J., KANG, J. Y., PARK, H. J., KIM, M. D., BAE, M. S., CHOI, H. I. & KIM, S. Y. 2010b. DREB2C interacts with ABF2, a bZIP protein regulating abscisic acid-responsive gene expression, and its overexpression affects abscisic acid sensitivity. *Plant Physiol,* 153**,** 716-27.

LEGUBE, G. & TROUCHE, D. 2003. Regulating histone acetyltransferases and deacetylases. *EMBO reports,* 4**,** 944-947.

LENOBLE, M. E., SPOLLEN, W. G. & SHARP, R. E. 2004. Maintenance of shoot growth by endogenous ABA: genetic assessment of the involvement of ethylene suppression. *J Exp Bot,* 55**,** 237-45.

LETUNIC, I. & BORK, P. 2018. 20 years of the SMART protein domain annotation resource. *Nucleic Acids Research,* 46**,** D493-D496.

LEWIS, L. A., POLANSKI, K., DE TORRES-ZABALA, M., JAYARAMAN, S., BOWDEN, L., MOORE, J., PENFOLD, C. A., JENKINS, D. J., HILL, C., BAXTER, L., KULASEKARAN, S., TRUMAN, W., LITTLEJOHN, G., PRUSINSKA, J., MEAD, A., STEINBRENNER, J., HICKMAN, R., RAND, D., WILD, D. L., OTT, S., BUCHANAN-WOLLASTON, V., SMIRNOFF, N., BEYNON, J., DENBY, K. & GRANT, M. 2015. Transcriptional Dynamics Driving MAMP-Triggered Immunity and Pathogen Effector-Mediated Immunosuppression in Arabidopsis Leaves Following Infection with Pseudomonas syringae pv tomato DC3000. 27**,** 3038-3064.

LI, B., MENG, X., SHAN, L. & HE, P. 2016a. Transcriptional Regulation of Pattern-Triggered Immunity in Plants. *Cell Host & Microbe,* 19**,** 641-650.

LI, B., MENG, X., SHAN, L. & HE, P. 2016b. Transcriptional Regulation of Pattern-Triggered Immunity in Plants. *Cell Host Microbe,* 19**,** 641-50.

LI, J.-F., NORVILLE, J. E., AACH, J., MCCORMACK, M., ZHANG, D., BUSH, J., CHURCH, G. M. & SHEEN, J. 2013. Multiplex and homologous recombination–mediated genome editing in Arabidopsis and Nicotiana benthamiana using guide RNA and Cas9. *Nature Biotechnology,* 31**,** 688.

LI, K., YANG, F., ZHANG, G., SONG, S., LI, Y., REN, D., MIAO, Y. & SONG, C. P. 2017a. AIK1, A Mitogen-Activated Protein Kinase, Modulates Abscisic Acid Responses through the MKK5-MPK6 Kinase Cascade. *Plant Physiol,* 173**,** 1391-1408.

LI, S., LIN, Y.-C. J., WANG, P., ZHANG, B., LI, M., CHEN, S., SHI, R., TUNLAYA-ANUKIT, S., LIU, X., WANG, Z., DAI, X., YU, J., ZHOU, C., LIU, B., WANG, J. P., CHIANG, V. L. & LI, W. 2019. The AREB1 Transcription Factor Influences Histone Acetylation to Regulate Drought Responses and Tolerance in Populus trichocarpa. *The Plant Cell,* 31**,** 663-686.

LI, X., CHEN, L., FORDE, B. G. & DAVIES, W. J. 2017b. The Biphasic Root Growth Response to Abscisic Acid in Arabidopsis Involves Interaction with Ethylene and Auxin Signalling Pathways. *Frontiers in Plant Science,* 8.

LI, Y., CAI, H., LIU, P., WANG, C., GAO, H., WU, C., YAN, K., ZHANG, S., HUANG, J. & ZHENG, C. 2017c. Arabidopsis MAPKKK18 positively regulates drought stress resistance via downstream MAPKK3. *Biochem Biophys Res Commun,* 484**,** 292-297.

LI, Z., WOO, H. R. & GUO, H. 2017d. Genetic redundancy of senescence-associated transcription factors in Arabidopsis. *Journal of Experimental Botany*.

LIAN-MEI TAN, ZHANG, C.-J., HOU, X.-M., SHAO, C.-R., LU, Y.-J., ZHOU, J.-X., LI, Y.-Q., LI, L., CHEN, S. & HE, X.-J. 2018. The PEAT protein complexes are required for histone
deacetylation and heterochromatin silencing. *The EMBO Journal*.

LIEW, L. C., SINGH, M. B. & BHALLA, P. L. 2013. An RNA-Seq Transcriptome Analysis of Histone Modifiers and RNA Silencing Genes in Soybean during Floral Initiation Process. 8**,** e77502.

LINDEBERG, M., CUNNAC, S. & COLLMER, A. 2012. Pseudomonas syringae type III effector repertoires: last words in endless arguments. *Trends Microbiol,* 20**,** 199-208.

LIVAK, K. J. & SCHMITTGEN, T. D. 2001. Analysis of relative gene expression data using real-time quantitative PCR and the 2(-Delta Delta C(T)) Method. *Methods,* 25**,** 402-8.

LOUDET, O., CHAILLOU, S., MERIGOUT, P., TALBOTEC, J. & DANIEL-VEDELE, F. 2003. Quantitative trait loci analysis of nitrogen use efficiency in Arabidopsis. *Plant physiology,* 131**,** 345-358.

LOVE, M. I., HUBER, W. & ANDERS, S. 2014. Moderated estimation of fold change and dispersion for RNA-seq data with DESeq2. *Genome Biology,* 15**,** 550.

LU, C., HAN, M. H., GUEVARA-GARCIA, A. & FEDOROFF, N. V. 2002. Mitogen-activated protein kinase signaling in postgermination arrest of development by abscisic acid. *Proceedings of the National Academy of Sciences of the United States of America,* 99**,** 15812-15817.

LUO, M., CHENG, K., XU, Y., YANG, S. & WU, K. 2017. Plant Responses to Abiotic Stress Regulated by Histone Deacetylases. *Frontiers in plant science,* 8**,** 2147-2147.

LUO, M., WANG, Y.-Y., LIU, X., YANG, S., LU, Q., CUI, Y. & WU, K. 2012. HD2C interacts with HDA6 and is involved in ABA and salt stress response in Arabidopsis. *Journal of experimental botany,* 63**,** 3297-3306.

LUO, X., CHEN, Z., GAO, J. & GONG, Z. 2014. Abscisic acid inhibits root growth in Arabidopsis through ethylene biosynthesis. *Plant J,* 79**,** 44-55.

LUSSER, A., KOLLE, D. & LOIDL, P. 2001. Histone acetylation: lessons from the plant kingdom. *Trends Plant Sci,* 6**,** 59-65.

M. PASQUI, E. D. G. 2019. Climate change, future warming, and adaptation in Europe. *Animal Frontiers,* 9**,** 6-11.

MA, C., ZHU, C., ZHENG, M., LIU, M., ZHANG, D., LIU, B., LI, Q., SI, J., REN, X. & SONG, H. 2019. CRISPR/Cas9-mediated multiple gene editing in Brassica oleracea var. capitata using the endogenous tRNA-processing system. *Horticulture Research,* 6**,** 20.

MA-LAUER, Y., SZOSTKIEWICZ, I., KORTE, A., MOES, D., YANG, Y., CHRISTMANN, A. & GRILL, E. 2009. Regulators of PP2C Phosphatase Activity Function as Abscisic Acid Sensors. *Science (New York, N.Y.),* 324**,** 1064-8.

MACHO, A. P. & ZIPFEL, C. 2014. Plant PRRs and the activation of innate immune signaling. *Mol Cell,* 54**,** 263-72.

MAI, S., GATTUSO, H., MONARI, A. & GONZÁLEZ, L. 2018. Novel Molecular-Dynamics-Based Protocols for Phase Space Sampling in Complex Systems. *Frontiers in Chemistry,* 6.

MARK VAN DE, W., CENTRE FOR GENETIC RESOURCES, T. N. W. U., RESEARCH, C., CHRIS, K., CENTRE FOR GENETIC RESOURCES, T. N. W. U., RESEARCH, C., THEO VAN, H., CENTRE FOR GENETIC RESOURCES, T. N. W. U., RESEARCH, C., ROB VAN, T., CENTRE FOR GENETIC RESOURCES, T. N. W. U., RESEARCH, C., BERT, V., CENTRE FOR GENETIC RESOURCES, T. N. W. U. & RESEARCH, C. 2016. Genetic erosion in crops: concept, research results and challenges. *Plant Genetic Resources,* 8**,** 1-15.

MCLEAY, R. C. & BAILEY, T. L. 2010. Motif Enrichment Analysis: a unified framework and an evaluation on ChIP data. *BMC Bioinformatics,* 11**,** 165.

MEHDI, S., DERKACHEVA, M., RAMSTRÖM, M., KRALEMANN, L., BERGQUIST, J. & HENNIG, L. 2015. MSI1 functions in a HDAC complex to fine-tune ABA signaling. *Plant Cell.* 1, 42-54.

MELOTTO, M., UNDERWOOD, W. & HE, S. Y. 2008. Role of stomata in plant innate immunity and foliar bacterial diseases. *Annual review of phytopathology,* 46**,** 101-122.

MELOTTO, M., UNDERWOOD, W., KOCZAN, J., NOMURA, K. & HE, S. Y. 2006. Plant stomata function in innate immunity against bacterial invasion. *Cell,* 126**,** 969-80.

MI, H., DONG, Q., MURUGANUJAN, A., GAUDET, P., LEWIS, S. & THOMAS, P. D. 2009. PANTHER version 7: improved phylogenetic trees, orthologs and collaboration with the Gene Ontology Consortium. *Nucleic Acids Research,* 38**,** D204-D210.

MITTLER, R. 2002. Oxidative stress, antioxidants and stress tolerance. *Trends Plant Sci,* 7**,** 405-10.

MONTILLET, J. L., LEONHARDT, N., MONDY, S., TRANCHIMAND, S., RUMEAU, D., BOUDSOCQ, M., GARCIA, A. V., DOUKI, T., BIGEARD, J., LAURIERE, C., CHEVALIER, A., CASTRESANA, C. & HIRT, H. 2013. An abscisic acid-independent oxylipin pathway controls stomatal closure and immune defense in Arabidopsis. *PLoS Biol,* 11**,** e1001513.

MORI, I. C., MURATA, Y., YANG, Y., MUNEMASA, S., WANG, Y.-F., ANDREOLI, S., TIRIAC, H., ALONSO, J. M., HARPER, J. F., ECKER, J. R., KWAK, J. M. & SCHROEDER, J. I. 2006. CDPKs CPK6 and CPK3 Function in ABA Regulation of Guard Cell S-Type Anion- and Ca2+-Permeable Channels and Stomatal Closure. 4**,** e327.

MUNNÉ-BOSCH, S. & ALEGRE, L. 2004. Die and let live: leaf senescence contributes to plant survival under drought stress. *Functional Plant Biology,* 31**,** 203-216.

NARUSAKA, Y., NAKASHIMA, K., SHINWARI, Z. K., SAKUMA, Y., FURIHATA, T., ABE, H., NARUSAKA, M., SHINOZAKI, K. & YAMAGUCHI-SHINOZAKI, K. 2003. Interaction between two cis-acting elements, ABRE and DRE, in ABA-dependent expression of Arabidopsis rd29A gene in response to dehydration and high-salinity stresses. *The Plant Journal,* 34**,** 137-148.

NARUYA SAITOU, M. N. 1987. The neighbor-joining method: a new method for reconstructing phylogenetic trees. *Molecular Biology and Evolution*.

NEKRASOV, V., STASKAWICZ, B., WEIGEL, D., JONES, J. D. G. & KAMOUN, S. 2013. Targeted mutagenesis in the model plant Nicotiana benthamiana using Cas9 RNA-guided endonuclease. *Nature Biotechnology,* 31**,** 691.

NELLEMAN, C., MCDEVETTE, M., MANDERS, T., EICKHOUT, B., SVIHUS, B,. PRINS A. G., KALTERBORN, B. P. 2009. The environmental food crisis - The environment's role in averting future food crises.

NEMHAUSER, J. L., HONG, F. & CHORY, J. 2006. Different plant hormones regulate similar processes through largely nonoverlapping transcriptional responses. *Cell,* 126**,** 467-75.

NG, L. M., MELCHER, K., TEH, B. T. & XU, H. E. 2014. Abscisic acid perception and signaling: structural mechanisms and applications. *Acta Pharmacologica Sinica,* 35**,** 567-584.

NGUYEN, H. M., SAKO, K., MATSUI, A., UEDA, M., TANAKA, M., ITO, A., NISHINO, N., YOSHIDA, M. & SEKI, M. 2018. Transcriptomic analysis of Arabidopsis thaliana plants treated with the Ky-9 and Ky-72 histone deacetylase inhibitors. *Plant Signal Behav,* 13**,** e1448333.

NIGHTINGALE, K. P., WELLINGER, R. E., SOGO, J. M. & BECKER, P. B. 1998. Histone acetylation facilitates RNA polymerase II transcription of the Drosophila hsp26 gene in chromatin. *The EMBO journal,* 17**,** 2865-2876.

O'MALLEY, R. C., HUANG, S. C., SONG, L., LEWSEY, M. G., BARTLETT, A., NERY, J. R., GALLI, M., GALLAVOTTI, A. & ECKER, J. R. 2016. Cistrome and Epicistrome Features Shape the Regulatory DNA Landscape. *Cell,* 165**,** 1280-1292.

OERKE, E. C. 2006. Crop losses to pests. *The Journal of Agricultural Science,* 144**,** 31-43.

ORESKES, N. 2004. The Scientific Consensus on Climate Change. *Science,* 306**,** 1686-1686.

PANDEY, G., SHARMA, N., PANKAJ SAHU, P. & PRASAD, M. 2016. Chromatin-Based Epigenetic Regulation of Plant Abiotic Stress Response. *Current Genomics,* 17**,** 490-498.

PARK, S. Y., FUNG, P., NISHIMURA, N., JENSEN, D. R., FUJII, H., ZHAO, Y., LUMBA, S., SANTIAGO, J., RODRIGUES, A., CHOW, T. F. F., ALFRED, S. E., BONETTA, D., FINKELSTEIN, R., PROVART, N. J., DESVEAUX, D., RODRIGUEZ, P. L., MCCOURT, P., ZHU, J. K., SCHROEDER, J. I.,

VOLKMAN, B. F. & CUTLER, S. R. 2009. Abscisic Acid Inhibits Type 2C Protein Phosphatases via the PYR/PYL Family of START Proteins. *Science*.
PEK, J. W., ANAND, A. & KAI, T. 2012. Tudor domain proteins in development. *Development,* 139**,** 2255-2266.
PELLETIER, N., CHAMPAGNE, N., STIFANI, S. & YANG, X.-J. 2002. MOZ and MORF histone acetyltransferases interact with the Runt-domain transcription factor Runx2. *Oncogene,* 21**,** 2729-2740.
PERRELLA, G., LOPEZ-VERNAZA, M. A., CARR, C., SANI, E., GOSSELE, V., VERDUYN, C., KELLERMEIER, F., HANNAH, M. A. & AMTMANN, A. 2013. Histone deacetylase complex1 expression level titrates plant growth and abscisic acid sensitivity in Arabidopsis. *Plant Cell,* 25**,** 3491-505.
PETRICKA, J. J. & BENFEY, P. N. 2008. Root layers: complex regulation of developmental patterning. *Curr Opin Genet Dev,* 18**,** 354-61.
POLAKIS, P. 2000. Wnt signaling and cancer. *Genes & Development*.
PONTING, C. P. 1997. Tudor domains in proteins that interact with RNA. *Trends in Biochemical Sciences,* 22**,** 51-52.
POOLE, L. B., KARPLUS, P. A. & CLAIBORNE, A. 2004. Protein sulfenic acids in redox signaling. *Annu Rev Pharmacol Toxicol,* 44**,** 325-47.
POOLE, L. B. & NELSON, K. J. 2008. Discovering mechanisms of signaling-mediated cysteine oxidation. *Current opinion in chemical biology,* 12**,** 18-24.
PRUNEDA-PAZ, J. L., BRETON, G., NAGEL, D. H., KANG, S. E., BONALDI, K., DOHERTY, C. J., RAVELO, S., GALLI, M., ECKER, J. R. & KAY, S. A. 2014. A genome-scale resource for the functional characterization of Arabidopsis transcription factors. *Cell reports,* 8**,** 622-632.
QUIRINO, B. F. & BENT, A. F. 2003. Deciphering host resistance and pathogen virulence: the Arabidopsis / Pseudomonas interaction as a model. 4**,** 517-530.
RAIVO KOLDE. 2019. pheatmap: Pretty Heatmaps. R package version 1.0.12. https://CRAN.R-project.org/package=pheatmap
RATUSHNY, V. & GOLEMIS, E. 2008. Resolving the network of cell signaling pathways using the evolving yeast two-hybrid system. *Biotechniques,* 44**,** 655-62.
RIBONI, M., GALBIATI, M., TONELLI, C. & CONTI, L. 2013. GIGANTEA enables drought escape response via abscisic acid-dependent activation of the florigens and SUPPRESSOR OF OVEREXPRESSION OF CONSTANS. *Plant physiology,* 162**,** 1706-1719.
RICE-EVANS, C., MILLER, N. & PAGANGA, G. 1997. Antioxidant properties of phenolic compounds. *Trends in Plant Science,* 2**,** 152-159.
RIOV, J., DAGAN, E., GOREN, R. & YANG, S. F. 1990. Characterization of abscisic Acid-induced ethylene production in citrus leaf and tomato fruit tissues. *Plant physiology,* 92**,** 48-53.
RITCHIE, M. E., PHIPSON, B., WU, D., HU, Y., LAW, C. W., SHI, W. & SMYTH, G. K. 2015. limma powers differential expression analyses for RNA-sequencing and microarray studies. *Nucleic Acids Res,* 43**,** e47.
RITU PANDEY, A. M., CAROLYN A. NAPOLI, DAVID A. SELINGER, CRAIG S. PIKAARD, ERIC J. RICHARDS, JUDITH BENDER, DAVID W. MOUNT, RICHARD A. JORGENSEN 2002. Analysis of histone acetyltransferase and histone deacetylase families of Arabidopsis thaliana suggests functional diversification of chromatin modification among multicellular eukaryotes. *Nucleic Acids Research,* 30**,** 5036-5055.

RIVERO, R. M., KOJIMA, M., GEPSTEIN, A., SAKAKIBARA, H., MITTLER, R., GEPSTEIN, S. & BLUMWALD, E. 2007. Delayed leaf senescence induces extreme drought tolerance in a flowering plant. 104**,** 19631-19636.

RODRÍGUEZ-GACIO, M. D. C., MATILLA-VÁZQUEZ, M. A. & MATILLA, A. J. 2009. Seed dormancy and ABA signaling

The breakthrough goes on. *Plant Signaling & Behavior,* 4**,** 1035-1048.

ROSA, S., NTOUKAKIS, V., OHMIDO, N., PENDLE, A., ABRANCHES, R. & SHAW, P. 2015. Cell differentiation and development in Arabidopsis are associated with changes in histone dynamics at the single-cell level. *Plant Cell,* 26**,** 4821-33.

ROSAS-DIAZ, T., ZHANG, D., FAN, P., WANG, L., DING, X., JIANG, Y., JIMENEZ-GONGORA, T., MEDINA-PUCHE, L., ZHAO, X., FENG, Z., ZHANG, G., LIU, X., BEJARANO, E. R., TAN, L., ZHANG, H., ZHU, J.-K., XING, W., FAULKNER, C., NAGAWA, S. & LOZANO-DURAN, R. 2018. A virus-targeted plant receptor-like kinase promotes cell-to-cell spread of RNAi. *Proceedings of the National Academy of Sciences,* 115**,** 1388-1393.

ROTH, S. Y., DENU, J. M. & ALLIS, C. D. 2001. Histone Acetyltransferases. *Annual Review of Biochemistry,* 70**,** 81-120.

ROUDIER, F., AHMED, I., BÉRARD, C., SARAZIN, A., MARY-HUARD, T., CORTIJO, S., BOUYER, D., CAILLIEUX, E., DUVERNOIS-BERTHET, E., AL-SHIKHLEY, L., GIRAUT, L., DESPRÉS, B., DREVENSEK, S., BARNECHE, F., DÈROZIER, S., BRUNAUD, V., AUBOURG, S., SCHNITTGER, A., BOWLER, C., MARTIN-MAGNIETTE, M.-L., ROBIN, S., CABOCHE, M. & COLOT, V. 2011. Integrative epigenomic mapping defines four main chromatin states in Arabidopsis. *The EMBO journal,* 30**,** 1928-1938.

RYU, H., CHO, H., BAE, W. & HWANG, I. 2014. Control of early seedling development by BES1/TPL/HDA19-mediated epigenetic regulation of ABI3. *Nature Communications,* 5**,** 4138.

SADE, N., DEL MAR RUBIO-WILHELMI, M., UMNAJKITIKORN, K. & BLUMWALD, E. 2018. Stress-induced senescence and plant tolerance to abiotic stress. *Journal of Experimental Botany,* 69**,** 845-853.

SAH, S. K., REDDY, K. R. & LI, J. 2016. Abscisic Acid and Abiotic Stress Tolerance in Crop Plants. *Frontiers in plant science,* 7**,** 571-571.

SAKAMOTO, H., MARUYAMA, K., SAKUMA, Y., MESHI, T., IWABUCHI, M., SHINOZAKI, K. & YAMAGUCHI-SHINOZAKI, K. 2004. Arabidopsis Cys2/His2-type zinc-finger proteins function as transcription repressors under drought, cold, and high-salinity stress conditions. *Plant Physiol,* 136**,** 2734-46.

SAKURABA, Y., JEONG, J., KANG, M.-Y., KIM, J., PAEK, N.-C. & CHOI, G. 2014. Phytochrome-interacting transcription factors PIF4 and PIF5 induce leaf senescence in Arabidopsis. 5.

SAVCHENKO, T., KOLLA, V. A., WANG, C. Q., NASAFI, Z., HICKS, D. R., PHADUNGCHOB, B., CHEHAB, W. E., BRANDIZZI, F., FROEHLICH, J. & DEHESH, K. 2014. Functional convergence of oxylipin and abscisic acid pathways controls stomatal closure in response to drought. *Plant Physiol,* 164**,** 1151-60.

SCHNEIDER, C. A., RASBAND, W. S. & ELICEIRI, K. W. 2012. NIH Image to ImageJ: 25 years of image analysis. *Nature Methods,* 9**,** 671-675.

SCOTT, R. N. S. & PETER, R. 2005. Plant Disease: A Threat to Global Food Security. *Annual reviews in Phytopathology,* 45, 83-116.

SEKI, M., ISHIDA, J., NARUSAKA, M., FUJITA, M., NANJO, T., UMEZAWA, T., KAMIYA, A., NAKAJIMA, M., ENJU, A., SAKURAI, T., SATOU, M., AKIYAMA, K., YAMAGUCHI-SHINOZAKI, K., CARNINCI, P., KAWAI, J., HAYASHIZAKI, Y. & SHINOZAKI, K. 2002. Monitoring the expression pattern of around 7,000 Arabidopsis genes under ABA treatments using a full-length cDNA microarray. *Funct Integr Genomics,* 2**,** 282-91.

SEKI, M., UMEZAWA, T., URANO, K. & SHINOZAKI, K. 2007. Regulatory metabolic networks in drought stress responses. *Curr Opin Plant Biol,* 10**,** 296-302.

SEO, M., PEETERS, A. J., KOIWAI, H., ORITANI, T., MARION-POLL, A., ZEEVAART, J. A., KOORNNEEF, M., KAMIYA, Y. & KOSHIBA, T. 2000. The Arabidopsis aldehyde oxidase 3 (AAO3) gene product catalyzes the final step in abscisic acid biosynthesis in leaves. *Proc Natl Acad Sci U S A,* 97**,** 12908-13.

SHAN, Q., WANG, Y., LI, J., ZHANG, Y., CHEN, K., LIANG, Z., ZHANG, K., LIU, J., XI, J. J., QIU, J.-L. & GAO, C. 2013. Targeted genome modification of crop plants using a CRISPR-Cas system. *Nature Biotechnology,* 31**,** 686.

SHANNON, P., MARKIEL, A., OZIER, O., BALIGA, N. S., WANG, J. T., RAMAGE, D., AMIN, N., SCHWIKOWSKI, B. & IDEKER, T. 2003. Cytoscape: a software environment for integrated models of biomolecular interaction networks. *Genome research,* 13**,** 2498-2504.

SHARP, R. E. & LENOBLE, M. E. 2002. ABA, ethylene and the control of shoot and root growth under water stress. *Journal of Experimental Botany,* 53**,** 33-37.

SHI, K., LI, X., ZHANG, H., ZHANG, G., LIU, Y., ZHOU, Y., XIA, X., CHEN, Z. & YU, J. 2015. Guard cell hydrogen peroxide and nitric oxide mediate elevated CO2 -induced stomatal movement in tomato. *New Phytol,* 208**,** 342-53.

SHIN, A. S. A. G. 2006. *Discover Biology* (Sixth Edition).

SHIWEI LIU, Z. L., YIHUI LIU, LING LI AND LIDA ZHANG 2018. Network analysis of ABA-dependent and ABA-independent drought responsive genes in Arabidopsis thaliana. *Genetics and Molecular Biology,* 41**,** 624-637.

SHU, K., CHEN, Q., WU, Y., LIU, R., ZHANG, H., WANG, S., TANG, S., YANG, W. & XIE, Q. 2016. ABSCISIC ACID-INSENSITIVE 4 negatively regulates flowering through directly promoting Arabidopsis FLOWERING LOCUS C transcription. *Journal of Experimental Botany,* 67**,** 195-205.

SINGH, P., YEKONDI, S., CHEN, P. W., TSAI, C. H., YU, C. W., WU, K. & ZIMMERLI, L. 2014. Environmental History Modulates Arabidopsis Pattern-Triggered Immunity in a HISTONE ACETYLTRANSFERASE1-Dependent Manner. *Plant Cell,* 26**,** 2676-2688.

SKUBACZ, A., DASZKOWSKA-GOLEC, A. & SZAREJKO, I. 2016. The Role and Regulation of ABI5 (ABA-Insensitive 5) in Plant Development, Abiotic Stress Responses and Phytohormone Crosstalk. *Frontiers in plant science,* 7**,** 1884-1884.

SONG, C.-P., AGARWAL, M., OHTA, M., GUO, Y., HALFTER, U., WANG, P. & ZHU, J.-K. 2005. Role of an Arabidopsis AP2/EREBP-Type Transcriptional Repressor in Abscisic Acid and Drought Stress Responses. *The Plant Cell,* 17**,** 2384-2396.

SONG, L., HUANG, S.-S. C., WISE, A., CASTANON, R., NERY, J. R., CHEN, H., WATANABE, M., THOMAS, J., BAR-JOSEPH, Z. & ECKER, J. R. 2016. A transcription factor hierarchy defines an environmental stress response network. *Science,* 354**,** aag1550.

SPOEL, S. H. & DONG, X. 2012. How do plants achieve immunity? Defence without specialized immune cells. *Nat Rev Immunol,* 12**,** 89-100.

SPOEL, S. H., JOHNSON, J. S. & DONG, X. 2007. Regulation of tradeoffs between plant defenses against pathogens with different lifestyles. *Proceedings of the National Academy of Sciences,* 104**,** 18842-18847.

SPOEL, S. H., KOORNNEEF, A., CLAESSENS, S. M. C., KORZELIUS, J. P., VAN PELT, J. A., MUELLER, M. J., BUCHALA, A. J., MÉTRAUX, J.-P., BROWN, R., KAZAN, K., VAN LOON, L. C., DONG, X. & PIETERSE, C. M. J. 2003. NPR1 Modulates Cross-Talk between Salicylate- and Jasmonate-Dependent Defense Pathways through a Novel Function in the Cytosol. *The Plant Cell,* 15**,** 760-770.

SPRINGMANN, M., MASON-D'CROZ, D., ROBINSON, S., GARNETT, T., GODFRAY, H. C. J., GOLLIN, D., RAYNER, M., BALLON, P. & SCARBOROUGH, P. 2016. Global and regional health effects of future food production under climate change: a modelling study. *The Lancet,* 387**,** 1937-1946.

SQUATRITO, M., GORRINI, C. & AMATI, B. 2006. Tip60 in DNA damage response and growth control: many tricks in one HAT. *Trends Cell Biol,* 16**,** 433-42.

SRIDHA, S. & WU, K. 2006. Identification of AtHD2C as a novel regulator of abscisic acid responses in Arabidopsis. *Plant J,* 46**,** 124-33.

STASKAWICZ, J. L. D., DIANA, M. H. & BRIAN, J. 2013. Pivoting the Plant Immune System from Dissection to Deployment.

STRAHL, B. D. & ALLIS, C. D. 2000. The language of covalent histone modifications. *Nature,* 403**,** 41-5.

STROUD, H., OTERO, S., DESVOYES B., RAMIREZ-PARRA E., JACOBSEN SE., GUTIERREZ, C. 2012. Genome-wide analysis of histone H3.1 and H3.3 variants in Arabidopsis thaliana. *PNAS,* 109, 5370-5375.

TAIYUN WEI, V. S., MICHAEL LEVY, YIHUI XIE, YAN JIN, JEFF ZEMLA 2017. Visualization of a Correlation Matrix. 0.84 ed.

TARDIEU, F. & TUBEROSA, R. 2010. Dissection and modelling of abiotic stress tolerance in plants. *Current Opinion in Plant Biology,* 13**,** 206-212.

TENA, G., BOUDSOCQ, M. & SHEEN, J. 2011. Protein kinase signaling networks in plant innate immunity. *Curr Opin Plant Biol,* 14**,** 519-29.

THALER, J. S., HUMPHREY, P. T. & WHITEMAN, N. K. 2012. Evolution of jasmonate and salicylate signal crosstalk. *Trends in Plant Science,* 17**,** 260-270.

THOMAS, T. & VOSS, A. K. 2007. The diverse biological roles of MYST histone acetyltransferase family proteins. *Cell Cycle,* 6**,** 696-704.

TISNE, S., SERRAND, Y., BACH, L., GILBAULT, E., BEN AMEUR, R., BALASSE, H., VOISIN, R., BOUCHEZ, D., DURAND-TARDIF, M., GUERCHE, P., CHAREYRON, G., DA RUGNA, J., CAMILLERI, C. & LOUDET, O. 2013. Phenoscope: an automated large-scale phenotyping platform offering high spatial homogeneity. *Plant J,* 74**,** 534-44.

TJAMOS, S. E., FLEMETAKIS, E., PAPLOMATAS, E. J. & KATINAKIS, P. 2005. Induction of resistance to Verticillium dahliae in Arabidopsis thaliana by the biocontrol agent K-165 and pathogenesis-related proteins gene expression. *Mol Plant Microbe Interact,* 18**,** 555-61.

TO, T. K. & KIM, J. M. 2014. Epigenetic regulation of gene responsiveness in Arabidopsis. *Frontiers in Plant Science.* 7;4:548.

TSUZUKI, M. & WIERZBICKI, A. T. 2018. Buried in PEAT-discovery of a new silencing complex with opposing activities. *EMBO J,* 37.

UMEZAWA, T., SUGIYAMA, N., MIZOGUCHI, M., HAYASHI, S., MYOUGA, F., YAMAGUCHI-SHINOZAKI, K., ISHIHAMA, Y., HIRAYAMA, T. & SHINOZAKI, K. 2009. Type 2C protein phosphatases directly regulate abscisic acid-activated protein kinases in Arabidopsis. *Proceedings of the National Academy of Sciences,* 106**,** 17588-17593.

VAN DEN HEUVEL, S. 2004. Protein degradation: CUL-3 and BTB--partners in proteolysis. *Curr Biol,* 14**,** R59-61.

VERSLUES, P. E., AGARWAL, M., KATIYAR-AGARWAL, S., ZHU, J. & ZHU, J. K. 2006. Methods and concepts in quantifying resistance to drought, salt and freezing, abiotic stresses that affect plant water status. *Plant J,* 45**,** 523-39.

VIGHI, I. L., CRIZEL, R. L., PERIN, E. C., ROMBALDI, C. V. & GALLI, V. 2019. Crosstalk During Fruit Ripening and Stress Response Among Abscisic Acid, Calcium-Dependent Protein Kinase and Phenylpropanoid. *Critical Reviews in Plant Sciences,* 38**,** 99-116.

VIRLOUVET, L., DING, Y., FUJII, H., AVRAMOVA, Z. & FROMM, M. 2014. ABA signaling is necessary but not sufficient for RD29B transcriptional memory during successive dehydration stresses in Arabidopsis thaliana. *The Plant Journal,* 79**,** 150-161.

VISHWAKARMA, K., UPADHYAY, N., KUMAR, N., YADAV, G., SINGH, J., MISHRA, R. K., KUMAR, V., VERMA, R., UPADHYAY, R. G., PANDEY, M. & SHARMA, S. 2017. Abscisic Acid Signaling and Abiotic Stress Tolerance in Plants: A Review on Current Knowledge and Future Prospects. *Front Plant Sci,* 8**,** 161.

VOUSDEN KH., LANE DP.2007. p53 in health an disease. *Nat Rev Mol Cell Biol*, 4, 275-83.

VOYTAS, D. F. & GAO, C. 2014. Precision Genome Engineering and Agriculture: Opportunities and Regulatory Challenges. *PLoS Biology,* 12**,** e1001877.

WANG, C., GAO, F., WU, J., DAI, J., WEI, C. & LI, Y. 2010. Arabidopsis putative deacetylase AtSRT2 regulates basal defense by suppressing PAD4, EDS5 and SID2 expression. *Plant Cell Physiol,* 51**,** 1291-9.

WANG, H., QI, Q., SCHORR, P., CUTLER, A. J., CROSBY, W. L. & FOWKE, L. C. 1998. ICK1, a cyclin-dependent protein kinase inhibitor from Arabidopsis thaliana interacts with both Cdc2a and CycD3, and its expression is induced by abscisic acid. *Plant J,* 15**,** 501-10.

WANG, J., HU, M., WANG, J., QI, J., HAN, Z., WANG, G., QI, Y., WANG, H.-W., ZHOU, J.-M. & CHAI, J. 2019a. Reconstitution and structure of a plant NLR resistosome conferring immunity. *Science,* 364**,** eaav5870.

WANG, P., BAO, H., ZHANG, X. P., LIU, F. & WANG, W. 2018. Regulation of Tip60-dependent p53 acetylation in cell fate decision. *FEBS Lett*.

WANG, P., XUE, L., BATELLI, G., LEE, S., HOU, Y.-J., VAN OOSTEN, M. J., ZHANG, H., TAO, W. A. & ZHU, J.-K. 2013a. Quantitative phosphoproteomics identifies SnRK2 protein kinase substrates and reveals the effectors of abscisic acid action. *Proceedings of the National Academy of Sciences of the United States of America,* 110**,** 11205-11210.

WANG, X., CHANG, P., DING, J. & CHEN, J. 2013b. Distinct and redundant roles of the two MYST histone acetyltransferases Esa1 and Sas2 in cell growth and morphogenesis of Candida albicans. *Eukaryot Cell,* 12**,** 438-49.

WANG, X., GUO, C., PENG, J., LI, C., WAN, F., ZHANG, S., ZHOU, Y., YAN, Y., QI, L., SUN, K., YANG, S., GONG, Z. & LI, J. 2019b. ABRE-BINDING FACTORS play a role in the feedback regulation of ABA signaling by mediating rapid ABA induction of ABA co-receptor genes. *New Phytologist,* 221**,** 341-355.

WANG, Y., LI, L., YE, T., LU, Y., CHEN, X. & WU, Y. 2013c. The inhibitory effect of ABA on floral transition is mediated by ABI5 in Arabidopsis. *Journal of experimental botany,* 64**,** 675-684.

WANG, Z., CAO, H., SUN, Y., LI, X., CHEN, F., CARLES, A., LI, Y., DING, M., ZHANG, C., DENG, X., SOPPE, W. J. J. & LIU, Y.-X. 2013d. Arabidopsis Paired Amphipathic Helix Proteins SNL1 and SNL2 Redundantly Regulate Primary Seed Dormancy via Abscisic Acid–Ethylene Antagonism Mediated by Histone Deacetylation. 25**,** 149-166.

WATKINS, J. M., CHAPMAN, J. M. & MUDAY, G. K. 2017. Abscisic Acid-Induced Reactive Oxygen Species Are Modulated by Flavonols to Control Stomata Aperture. *Plant physiology,* 175**,** 1807-1825.

WEIGEL, D. & GLAZEBROOK, J. 2008. Genetic analysis of Arabidopsis mutants. *CHS Protocols.*

WENG, J.-K., YE, M., LI, B. & NOEL, J. P. 2016. Co-evolution of Hormone Metabolism and Signaling Networks Expands Plant Adaptive Plasticity. *Cell,* 166**,** 881-893.

WHALEN, M. C., INNES, R. W., BENT, A. F. & STASKAWICZ, B. J. 1991. Identification of Pseudomonas syringae pathogens of Arabidopsis and a bacterial locus determining avirulence on both Arabidopsis and soybean. *Plant Cell,* 3**,** 49-59.

WILKINS, M. R., GASTEIGER, E., BAIROCH, A., SANCHEZ, J. C., WILLIAMS, K. L., APPEL, R. D. & HOCHSTRASSER, D. F. 1999. Protein identification and analysis tools in the ExPASy server. *Methods Mol Biol,* 112**,** 531-52.

WOODCOCK, C. L., SKOULTCHI, A.S., & FAN, Y. 2005. Role of linker histone in chromatin structure and function: H1 stoichiometry and nucleosome repeat length. *Chromosome Research,* 14**,** 7-25.

WU, K., ZHANG, L., ZHOU, C., YU, C. W. & CHAIKAM, V. 2008. HDA6 is required for jasmonate response, senescence and flowering in Arabidopsis. *J Exp Bot,* 59**,** 225-34.

XIAOA, J., ZHANGA, H., XINGA, L., XUA, S., LIUA, H., CHONGA, K. & XUA, Y. 2013. Requirement of histone acetyltransferases HAM1 and HAM2 for epigenetic modification of FLC in regulating flowering in Arabidopsis. 170**,** 444–451.

XING, Y., JIA, W. & ZHANG, J. 2008. AtMKK1 mediates ABA-induced CAT1 expression and H2O2 production via AtMPK6-coupled signaling in Arabidopsis. *Plant J,* 54**,** 440-51.

XU, Z. Y., KIM, S. Y., HYEON, D. Y., KIM, D. H., DONG, T., PARK, Y., JIN, J. B., JOO, S. H., KIM, S. K., HONG, J. C., HWANG, D. & HWANG, I. 2013. The Arabidopsis NAC Transcription Factor ANAC096 Cooperates with bZIP-Type Transcription Factors in Dehydration and Osmotic Stress Responses. *The Plant Cell,* 25**,** 4708-4724.

Y. BASHAN, Y. O., Y. HENIS 1978. Infection studies of Pseudomonas Tomato, causal agent of Bacterial speck of Tomato. *Phytoparasitica,* 6.

YANG, W., ZHANG, W. & WANG, X. 2017. Post-translational control of ABA signalling: the roles of protein phosphorylation and ubiquitination. *Plant Biotechnology Journal,* 15**,** 4-14.

YOSHIDA, R., HOBO, T., ICHIMURA, K., MIZOGUCHI, T., TAKAHASHI, F., ARONSO, J., ECKER, J. R. & SHINOZAKI, K. 2002. ABA-activated SnRK2 protein kinase is required for dehydration stress signaling in Arabidopsis. *Plant Cell Physiol,* 43**,** 1473-83.

YOSHIDA, T., FUJITA, Y., MARUYAMA, K., MOGAMI, J., TODAKA, D., SHINOZAKI, K. & YAMAGUCHI-SHINOZAKI, K. 2015. Four A rabidopsis AREB/ABF transcription factors function predominantly in gene expression downstream of SnRK2 kinases in abscisic acid signalling in response to osmotic stress. 38**,** 35-49.

YOSHIDA, T., OBATA, T., FEIL, R., LUNN, J. E., FUJITA, Y., YAMAGUCHI-SHINOZAKI, K. & FERNIE, A. R. 2019. The Role of Abscisic Acid Signaling in Maintaining the Metabolic Balance Required for Arabidopsis Growth under Nonstress Conditions. *Plant Cell,* 31**,** 84-105.

ZHANG, H., HAN, W., DE SMET, I., TALBOYS, P., LOYA, R., HASSAN, A., RONG, H., JÜRGENS, G., PAUL KNOX, J. & WANG, M.-H. 2010. ABA promotes quiescence of the quiescent centre and suppresses stem cell differentiation in the Arabidopsis primary root meristem. 64**,** 764-774.

ZHANG, W., SUN, Y., TIMOFEJEVA, L., CHEN, C., GROSSNIKLAUS, U. & MA, H. 2006. Regulation of Arabidopsis tapetum development and function by DYSFUNCTIONAL TAPETUM1 (DYT1) encoding a putative bHLH transcription factor. *Development,* 133**,** 3085-95.

ZHAO, Y., CHAN, Z., GAO, J., XING, L., CAO, M., YU, C., HU, Y., YOU, J., SHI, H., ZHU, Y., GONG, Y., MU, Z., WANG, H., DENG, X., WANG, P., BRESSAN, R. A. & ZHU, J.-K. 2016. ABA receptor PYL9 promotes drought resistance and leaf senescence. *Proceedings of the National Academy of Sciences,* 113**,** 1949-1954.

ZHAO, Y., THILMONY, R., BENDER, C. L., SCHALLER, A., HE, S. Y. & HOWE, G. A. 2003. Virulence systems of Pseudomonas syringae pv. tomato promote bacterial speck disease in tomato by targeting the jasmonate signaling pathway. *Plant J,* 36**,** 485-99.

ZHAO, Y.-Q., JORDAN, K. & LUNYAK, V. 2013. Epigenetics Components of Aging in the Central Nervous System. *Neurotherapeutics : the journal of the American Society for Experimental NeuroTherapeutics,* 10.

ZHOU, C., ZHANG, L., DUAN, J., MIKI, B. & WU, K. 2005. HISTONE DEACETYLASE19 Is Involved in Jasmonic Acid and Ethylene Signaling of Pathogen Response in Arabidopsis. *The Plant Cell,* 17**,** 1196-1204.

ZHU, E., YOU, C., WANG, S., CUI, J., NIU, B., WANG, Y., QI, J., MA, H. & CHANG, F. 2015. The DYT1-interacting proteins bHLH010, bHLH089 and bHLH091 are redundantly required for Arabidopsis anther development and transcriptome. *Plant J,* 83**,** 976-90.

ZHU, J. K. 2002. Salt and drought stress signal transduction in plants. *Annu Rev Plant Biol,* 53**,** 247-73.

ZIPFEL, C., ROBATZEK, S., NAVARRO, L., OAKELEY, E. J., JONES, J. D., FELIX, G. & BOLLER, T. 2004. Bacterial disease resistance in Arabidopsis through flagellin perception. *Nature,* 428**,** 764-7.